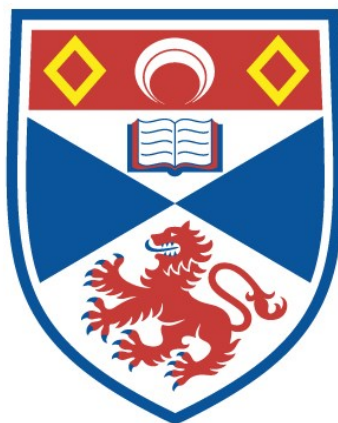


SOME ASPECTS OF THE MOLECULAR STRUCTURE
OF HETEROCYCLIC AND ORGANOMETALLIC
COMPOUNDS

Alastair Fraser Cuthbertson

A Thesis Submitted for the Degree of PhD
at the
University of St Andrews



1983

Full metadata for this item is available in
St Andrews Research Repository
at:

<http://research-repository.st-andrews.ac.uk/>

Please use this identifier to cite or link to this item:

<http://hdl.handle.net/10023/15289>

This item is protected by original copyright

Some Aspects of the Molecular Structure

of Heterocyclic and Organometallic Compounds.

being a thesis

presented by

Alastair Fraser Cuthbertson, B.Sc.

to the

University of St. Andrews

in application for

the degree of Doctor of Philosophy.

St. Andrews

September 1982



ProQuest Number: 10170826

All rights reserved

INFORMATION TO ALL USERS

The quality of this reproduction is dependent upon the quality of the copy submitted.

In the unlikely event that the author did not send a complete manuscript and there are missing pages, these will be noted. Also, if material had to be removed, a note will indicate the deletion.



ProQuest 10170826

Published by ProQuest LLC (2017). Copyright of the Dissertation is held by the Author.

All rights reserved.

This work is protected against unauthorized copying under Title 17, United States Code
Microform Edition © ProQuest LLC.

ProQuest LLC.
789 East Eisenhower Parkway
P.O. Box 1346
Ann Arbor, MI 48106 – 1346

Declaration.

I declare that this thesis is a record of my own experiments, that it is of my own composition, and that it has not previously been presented in application for a higher degree.

The work was carried out in the Department of Chemistry of the University of St. Andrews under the direction of Dr. C. Glidewell.

2819182

Certificate.

I hereby certify that Mr Alastair Fraser Cuthbertson, B.Sc., has spent eleven terms at research work under my supervision, has fulfilled the conditions of the resolution of the University Court 1967, No. 1, and is qualified to submit the accompanying thesis in application for the degree of Doctor of Philosophy.

Research Supervisor

Acknowledgements.

Firstly to my father who instilled my interest in chemistry at an early age and to my mother who encouraged this development.

I am extremely grateful to Professor P.A.H. Wyatt for providing my research grant from the Chemistry Department's Purdie Fund, and for the excellent laboratory facilities available. The department librarian, Mrs. S. Johnson has always been most helpful.

Professor D.H. Reid and his group Peter Pogorzelec, Robin Nicol and Andy McRoberts for helpful discussions related to practical work and heterocyclic chemistry.

The other two members of the research group, Dave Liles, who wrote some of the crystallographic programs used, and Diane Holden were always ready and willing to discuss topics of interest.

I thank the Computing Laboratory staff and computer operators for their help. I am especially grateful to Jim Bews for the implementation of the quantum mechanical programs on the various computers, and for his help with other computational problems.

Lastly my greatest word of thanks goes to my supervisor Dr. C. Glidewell for his patience, encouragement and enthusiasm. I thank him most sincerely.

Abstract.

Various rules which have been used to rationalise molecular geometries are discussed. After this the results from MNDO calculations on simple carbenes, ethers and amines are presented, and these were designed to test the hypothesis that in the presence of ligands of low electronegativity lone pairs would not fulfill their stereochemical role assigned to them in the VSEPR model.

Following on are MNDO calculations on cyclic molecules: the cyclopentadiene ring is planar in silylcyclopentadiene and non-planar in trimethylsilylcyclopentadiene. The calculations attempt to resolve this and in addition the nature of the fluxional exchange. The intermediates which are formed by diazepinium salts when they are protodebrominated are then discussed in the light of MNDO calculations.

Single crystal x-ray work was carried out for four heterocyclic molecules. The compounds reported are: 4-phenyl-3-phenylamino-1,2,4-thiadiazolin-5-one; 5-(N-methylthiocarbamoylimino)-4-phenyl-3-phenylamino-4H-1,2,4-thiadiazoline; N,N'-bis[2-(5-t-butyl-3H-1,2-dithiol-3-ylidene)ethylidene]hydrazine and N,N-dimethyl-N'-[2-(5-t-butyl-3H-1,2-dithiol-3-ylidene)ethylidene]hydrazine.

Details of MNDO calculations which were undertaken on molecules related to the x-ray work are then presented, and in the final chapter a discussion of the heterocyclic crystal structures appears.

The first appendix reports the structure of a macrocyclic ligand, the second provides a list of publications and the third appendix is a list of the structure factors, least-squares planes and anisotropic temperature parameters for the crystal structure determinations.

Contents.

<u>Chapter One.</u>	An Introduction.	1.
<u>Chapter Two.</u>	Rules for Predicting Molecular Structure.	6.
I.	Valence Shell Electron Pair Repulsion.	6.
II.	Walsh's Rules.	10.
III.	Second-Order Jahn Teller Effect.	12.
<u>Chapter Three.</u>	Carbenes, Ethers and Amines.	22.
I.	Introduction.	22.
II.	Symmetry Aspects.	24.
III.	Calculation of Force Constants.	26.
IV.	Method.	29.
V.	Carbenes.	31.
VI.	Ethers.	40.
VII.	Amines.	44.
VIII.	Are MX_3 Groups Really of C_{3v} Symmetry?	48.
IX.	Sixteen Electron Systems.	52.
X.	Conclusions.	53.
<u>Chapter Four.</u>	Silyl Cyclopentadienes.	57.
I.	Introduction.	57.
II.	Method.	58.
III.	Geometries.	59.
IV.	Metallotropic and Prototropic Shifts.	67.

V. Electronic Structure.	71.
<u>Chapter Five. Diazepines.</u>	77.
I. Introduction.	77.
II. Method.	79.
III. Neutral Intermediates - Allenes or Onium Ions?	79.
IV. Charged Intermediates - Carbonium Ions or Allenes?	87.
V. . Complete Delocalisation?	90.
<u>Chapter Six. Four Heterocyclic Crystal Structures.</u>	95.
I. 4-phenyl-3-phenylamino-1,2,4-thiadiazolin-5-one.	95.
II. 5-(N-methylthiocarbamoylimino)-4-phenyl -3-phenylamino-4H-1,2,4-thiadiazoline.	99.
III. N,N'-bis[2-(5-t-butyl-3H-1,2-dithiol-3-ylidene)- ethylidene]hydrazine.	103.
IV. N,N-dimethyl-N'-[2-(5-t-butyl-3H-1,2-dithiol-3-ylidene) ethylidene]hydrazine.	106.
<u>Chapter Seven. Calculations on Heterocycles.</u>	110.
I. Introduction.	110.
II. Hector's Base and Related Molecules.	111.
III. Prototropy.	112.
IV. Adduct Formation : Equilibrium Structures.	115.
V. Adduct Formation : Mechanism.	118.
VI. Hegerschoff Base Formation.	120.
VII. Desulphurisation.	122.
VIII. Triheterapentalenes : General Information.	125.

IX.	Method	129.
X.	Triheterapentalenes : Results.	130.
XI.	Triheterapentalenes : Discussion.	133.
 <u>Chapter Eight. Discussion of Heterocyclic Crystal Structures.</u>		142.
I.	Dost's Keto Compound and the 1:1 Adducts of Hector's Base.	142.
II.	λ^4 Triheterapentalenes.	146.
 <u>Appendix A. A Macrocyclic Ligand.</u>		151.
 <u>Appendix B. Publications.</u>		155.
 <u>Appendix C. Structure Factors, Anisotropic Temperature Factors and Least-Squares Planes.</u>		

Some Aspects of the Molecular Structure

of Heterocyclic and Organometallic Compounds.

Chapter One.

An Introduction.

With the advent of faster and more sophisticated computers and computer programs the study of molecular structure through quantum mechanics has blossomed in the past couple of decades. Gaining an insight to the structure and bonding of molecules is fundamental to chemistry and via the medium of quantum mechanical calculations this goal can be attained. Such calculations using the MNDO program [1] form the basic core of the work presented here.

MNDO stands for Modified Neglect of Diatomic Overlap: this acronym is slightly misleading in that the method is a modified version of the NDDO approach (Neglect of Differential Diatomic Overlap). However MNDDO/2 as it would have been called was considered by the authors Dewar and Thiel to be too cumbersome, and hence MNDO [1].

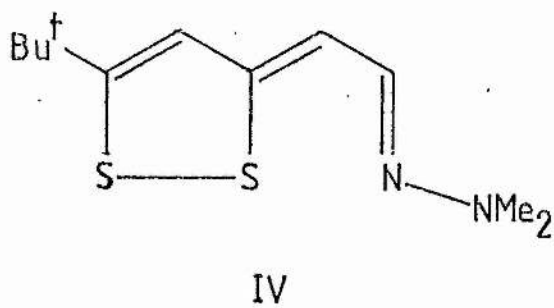
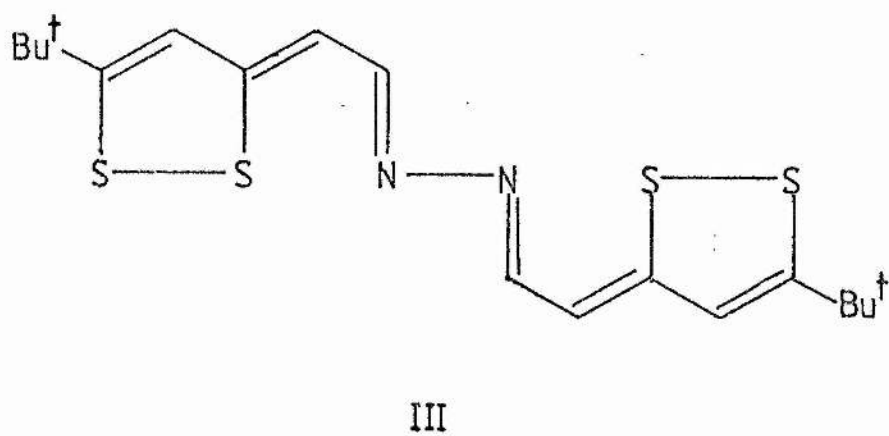
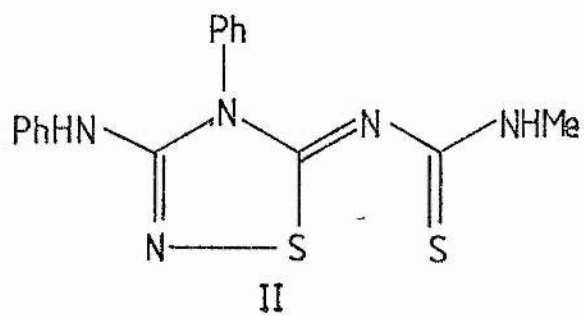
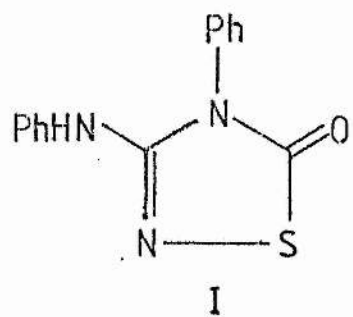
This thesis can be split conveniently into three main sections, those of Chapters Two and Three, Chapters Four and Five and finally Chapters Six to Eight.

Chapter Two provides a review of some of the many rules which are used to describe molecular geometry: attention is drawn to the VSEPR model [2], Walsh's Rules [3] and the Second-Order Jahn Teller effect [4]. Chapter Three builds upon this foundation and describes the

results from MNDO calculations [1] on simple carbenes, ethers and amines, which were designed to test the model that stated that in the presence of ligands of low electronegativity, lone pairs on the central atom would be stereochemically inactive [5]. The results from the calculations show that as the electronegativity of the ligand increases so the skeletal angle decreases. At the same time the skeletal bending force constant becomes more negative and the inversion barrier, which is the energy difference between the linear and bent geometry, increases. These observations are in full accord with the previous model [5] based on the Second-Order Jahn Teller effect, and show that conceptual artefacts such as $p\pi-d\pi$ bonding are not required in explaining these systems.

The next two chapters are concerned with cyclic molecules and the problems of ring conformation and how best to represent them.

Chapter Four again describes MNDO calculations [1] and deals with the controversy surrounding the structure of the cyclopentadiene ring in $(h-C_5H_5)SiH_3$ and $(h-C_5H_5)SiMe_3$, since the ring is planar in the silyl derivative [6] and non-planar with an envelope angle of $158 \pm 4^\circ$ in the trimethylsilyl case [7]. The fluxional behaviour of $(h-C_5H_5)SiH_3$ was also investigated for both the metallotropic and prototropic migrations, which are of a degenerate and non-degenerate nature respectively, to ascertain whether the shifts occurred via a 1,2 or 1,3 shift mechanism. IUPAC nomenclature has been followed in this chapter and so the atom labelling scheme assigns C5 to the unique carbon σ bonded to the silyl group. In addition h has been used instead of η when the formulae are written [8].



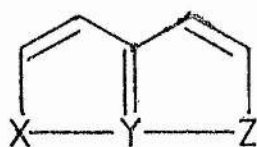
Interest in the intermediates formed when 2,3-dihydro 1,4-diazepinium salts are protodebrominated provoked the MNDO study presented in Chapter Five. Onium ions were postulated as the neutral intermediates involved [9]: the calculations reveal that the molecule is in fact an allene.

The last section comprises of three chapters which are concerned with the structures of heterocyclic compounds.

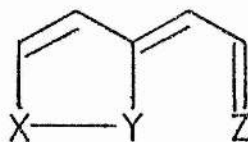
Chapter Six reports the x-ray structure determinations of four heterocyclic molecules. Prior to this definitive structures could not be drawn for any of them. The structures reported are: 4-phenyl-3-phenylamino-1,2,4-thiadiazolin-5-one, I; 5-(N-methyl thiocarbamoylimino)- 4-phenyl-3-phenylamino-4H-1,2,4-thiadiazoline, II; N,N'-bis-[2-(5-t-butyl-3H-1,2-dithiol-3-ylidene)-ethylidene] hydrazine, III; and N,N-dimethyl-N'-[2-(5-t-butyl-3H-1,2-dithiol-3-ylidene)-ethylidene] hydrazine, IV.

Chapter Seven is split into two parts and deals with MNDO calculations [1] carried out on various heterocyclic molecules. The first part of the chapter considers the Hector's Base family of molecules with emphasis on the thermodynamic stability of the two protomeric forms of Hector's Base, Dost's Base and Dost's Keto Compound, and the 1:1 adduct formation. The second half of the chapter looks at the structure of triheterapentalenes with special reference on the thermodynamic stability of the bicyclic and monocyclic forms, to see whether the calculations predict correctly

the experimentally observed isomer.



bicyclic



monocyclic

Chapter Eight then goes on to discuss the four heterocyclic crystal structure determinations described in Chapter Six in light of some of the findings outlined in Chapter Seven.

Appendix A reports MNDO work undertaken on a macrocyclic ligand, and the resulting geometry optimisation of the structure showed that the molecule is a rare example of the point group S_4 . A list of publications is contained in Appendix B.

The references for this thesis, which are in square brackets, [], in the text, can be found at the end of each chapter, and therefore disposes of the need for cross-referencing.

For the sake of clarity each crystal structure determination has been described separately and following each one are a drawing of the molecule and the unit cell, fractional atomic coordinates, equivalent isotropic thermal parameters and the molecular geometry. Appendix C supplies the calculated and observed structure factors, anisotropic temperature factors and the least squares planes.

Chapter One.

Bibliography.

1. M.J.S. Dewar and W. Thiel. J.A.C.S. 99 4899 (1977).
2. R.J. Gillespie and R.S. Nyholm. Quart Rev Chem Soc 11 339 (1957).
3. A.D. Walsh. JCS 2260 (1953).
4. U. Öpik and M.H.L. Pryce. Proc Roy Soc 238 425 (1957).
5. C. Glidewell. Inorg Chim Acta 13 L11 (1975).
6. J.E. Bentham and D.W.H. Rankin. J Organomet Chem 30 C54 (1971).
7. N.N. Veniaminov, Yu.A. Ustynyuk, N.V. Alekseev, I.A. Ronova and Yu.T. Struchkov. J Organomet Chem 22 551 (1970).
8. M. Orchin, F. Kaplan, R.S. Malomber, R.M. Wilson and H. Zimmer. "The Vocabulary of Organic Chemistry" p435. Wiley-Interscience (1980).
9. D. Lloyd and D.R. Marshall. Chem Ind (London) 335 (1972).

Chapter Two.

Rules For Predicting Molecular Structure.

Over the years numerous articles have appeared which try to rationalise and account for the stereochemistry of main group compounds. Two excellent textbooks one, by Burdett [1] and the other by Pearson [2], give lucid accounts of many of the various rules and I have selected three of these which are relevant to this thesis and present a brief outline of each below. For a more detailed approach I refer the reader to the textbooks [1,2].

I. Valence Shell Electron Pair Repulsion.

The Valence Shell Electron Pair Repulsion model, hereafter called VSEPR, was developed by Gillespie and Nyholm [3,4]. Their approach to main group stereochemistry based on equiangular polyhedra was to assign a given structure to a molecule depending on the number of valence electrons present and these assignments are listed in Table 2.1.1.

<u>Number of Electron Pairs</u>	<u>Polyhedron</u>	<u>Point Group</u>
2	linear	$D_{\infty h}$
3	equilateral triangle	D_{3h}
4	tetrahedron	T_d
5	trigonal bipyramid	D_{3h}
6	octahedron	O_h
7	monocapped octahedron	C_{3v}
8	dodecahedron	D_{2d}
	square antiprism	D_{2d}
9	tricapped trigonal prism	D_{3h}
10	bicapped square antiprism	D_{4d}
11	icosahedron minus an apex	C_{5v}
12	icosahedron	I_h

Table 2.1.1.

These arrangements arise from the rules listed below, namely that:

1. Electron pairs in the valence shell adopt an arrangement that maximises their distance apart i.e. they repel each other;
2. Lone pairs take up more room than bonding pairs. This is because there is not another atom present at the distal end of the lone pair which would tend to localise the electrons between the two nuclei and hence reduce the angular volume. Therefore the ordering of repulsive energies is lone pair-lone pair > lone pair-bonding pair > bonding pair-bonding pair;
3. The size of a bonding pair of electrons decreases with the

increasing electronegativity of the ligand;

4. Two electron pairs of a double bond and three electron pairs of a triple bond take up more room than the solitary electron pair of a single bond.

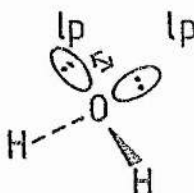


Figure 2.1.1.

This model successfully accounts for the structure of molecules such as CH_4 , H_2O and NH_3 and suggests why the $\angle\text{HOH}$ angle in water and the $\angle\text{HNNH}$ angle in ammonia are less than the tetrahedral angle of 109.47° observed in methane. Methane is predicted to be tetrahedral and is a member of the family of AB_4 molecules. Water is according to the rules predicted to be tetrahedral with two lone pairs i.e. bent and is an example of the AB_2E_2 system where E represents a lone pair of electrons. Ammonia on the other hand is tetrahedral with one lone pair i.e. pyramidal and is representative of the AB_3E systems. The fact that the observed angles are less than the tetrahedral angle is accounted for by Rule 2 above, see Figure 2.1.1. The effect of the number of lone pairs present can be seen from the above description since in the series CH_4 , NH_3 and OH_2 the $\angle\text{HMH}$ bond angle decreases with the increasing steric requirements of the lone pairs. The values are 109.47 [5], 107.3 [6] and 104.5° [7] respectively.

However when an isoelectronic series is considered it is found that the same structure is predicted for all the members of the series. A good example of this is that of ammonia, NH_3 , and its isoelectronic counterparts trimethylamine, $\text{N}(\text{CH}_3)_3$, and trisilylamine, $\text{N}(\text{SiH}_3)_3$. All are predicted to be pyraminal AB_3E systems i.e. tetrahedral with one lone pair which is correct for NH_3 and $\text{N}(\text{CH}_3)_3$ but is awry for $\text{N}(\text{SiH}_3)_3$ which is known from experimental evidence to be planar [8a,b]. In this case the lone pair appears to be stereochemically inactive. One explanation [9] for this is that p-d π back-bonding is employed and that the lone pair in the nitrogen p orbital is delocalised into the vacant 3d orbitals on silicon. However ab-initio calculations [10a] indicate that this may not be the case and that d orbitals on the nitrogen and not silicon may be important. Also MNDO [11] with its limited basis set of s and p orbitals calculates trisilylamine to be planar [10b].

An exactly analogous situation occurs for the series H_2O , $(\text{CH}_3)_2\text{O}$ and $(\text{SiH}_3)_2\text{O}$. Both water and dimethyl ether are bent but disilyl ether is not as bent as expected with a bond angle of 144.1° in the gas phase [12] and 142.2° in the solid [13]. Once more the lone pairs are stereochemically inactive. Ab-initio calculations [14] point out that only d orbitals on the central atom are important and act as polarisation functions: recourse to d orbitals on silicon is not necessary.

II. Walsh's Rules.

Walsh in a classic series of papers [15] expounded the idea that the structure of simple molecules such as AH_2 , AB_2 and AB_3 could be predicted by the construction of a qualitative molecular orbital sequence. Then by considering the way in which the orbital energies changed as the geometry was varied, and by correlating the symmetry classes of the orbitals in one structure with those for the perturbed geometry, he was able to predict observed geometries. The main basis for the change in orbital energies is the increase or decrease in orbital overlap and the increase or decrease of the s and p mixing of the orbitals on the central atom.

Walsh diagrams for AH_2 and AH_3 systems are presented in Figure 2.2.1. and Figure 2.2.2. respectively. In addition the molecular orbitals are displayed in a pictorial fashion alongside their respective symmetry labels. The predictions for AH_2 molecules are set out in Table 2.2.1. and those for AH_3 molecules in Table 2.2.2..

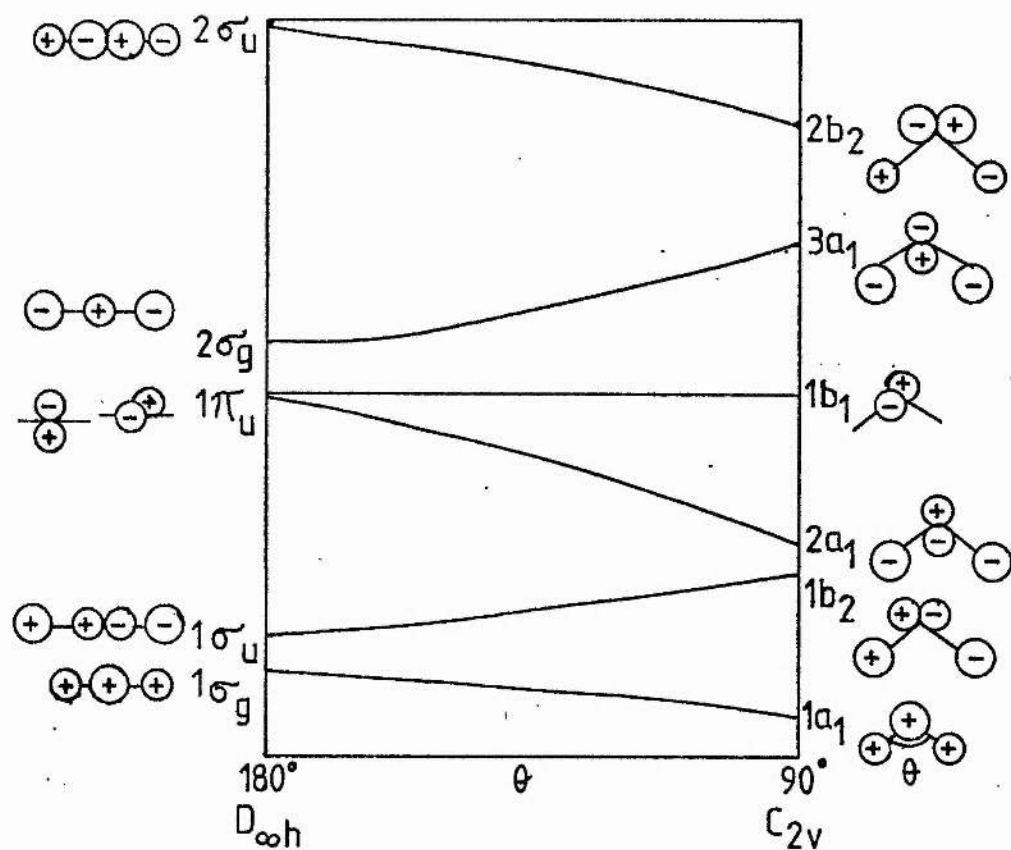


Figure 2.2.1. Walsh Diagram for AH_2 systems.

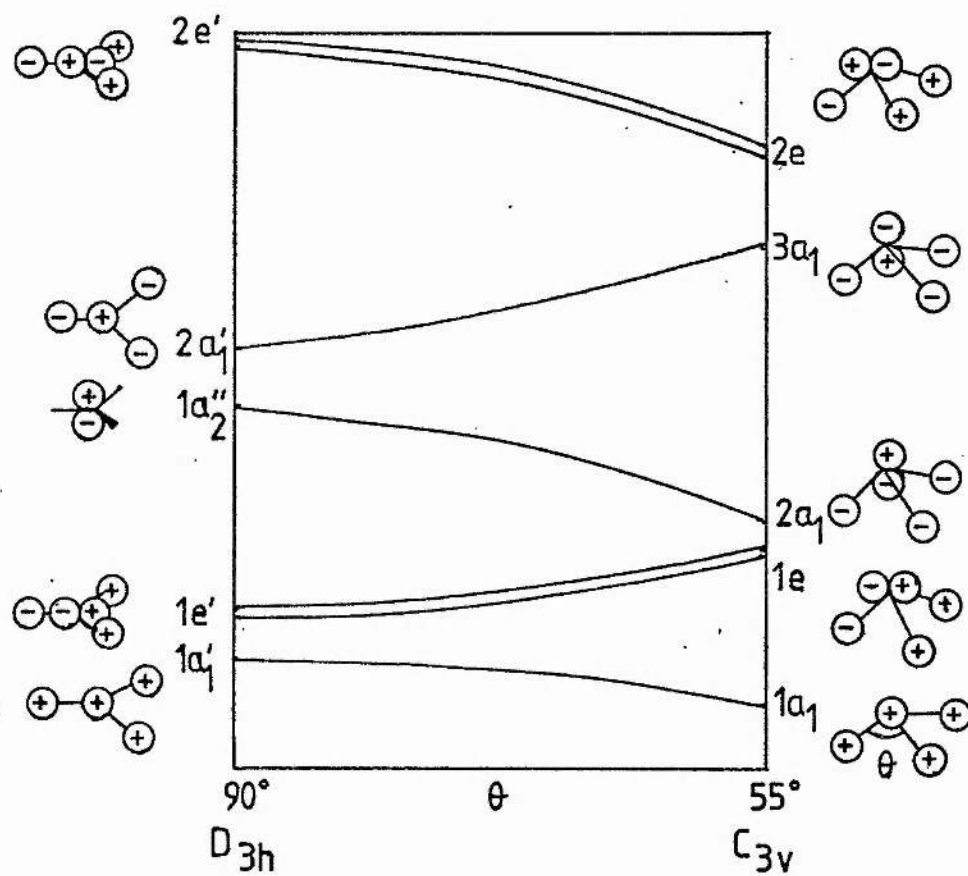


Figure 2.2.2. Walsh Diagram for AH_3 systems.

<u>Electrons</u>	<u>Example</u>	<u>Prediction</u>
4	BeH ₂	linear
5	BH ₂	bent
6	CH ₂	bent
7	NH ₂	bent
8	OH ₂	bent

Table 2.2.1. Walsh's Rules predictions for AH₂ species.

<u>Electrons</u>	<u>Example</u>	<u>Prediction</u>
6	BH ₃	planar
7	CF ₃	bent
8	NH ₃	bent

Table 2.2.2. Walsh's Rules predictions for AH₃ species.

From Table and Figure 2.2.1. we can see that molecules with four electrons are predicted to be linear since the $1\sigma_u$ orbital in $D_{\infty h}$ becomes less stable than the $1b_2$ orbital in C_{2v} .

Molecules containing five, six, seven or eight electrons will be bent since the degenerate π_u orbital in $D_{\infty h}$ is split into the $2a_1$ and $1b_1$ orbitals in C_{2v} . The latter is a lone pair orbital on the central atom and its energy does not change much from $D_{\infty h}$ to C_{2v} . The $2a_1$ orbital on the other hand becomes more stable during the transition from linear to bent and so five and six electron systems are bent as the $2a$ orbital is stabilised on becoming occupied and since there is

no preference for linearity when the $1b_1$ orbital is filled this explains why seven and eight electron systems are also bent. Ten electron systems however should be linear as the $2\sigma_g$ is destabilised on bending.

In the AH_3 molecules, see Table and Figure 2.2.2., the molecules are predicted to be planar with six electrons as the degenerate $1e'$ orbital in D_{3h} is destabilised when it transforms as the $1e$ orbital in C_{3v} . Seven and eight electron systems, though, will be non-planar as the relevant orbital $1a_2''$ is stabilised as the $2a_1$ orbital in C_{3v} . Addition of a further two electrons results in the system reverting once more to planarity.

The key idea in Walsh's approach which allows the geometry predictions to be made is the behaviour of the HOMO and it belongs to the family of treatments which use the angular overlap method [1]. Figure 2.2.1. also shows quite clearly the consequence of the non-crossing symmetry rule which says that states of the same symmetry will not cross but be pushed apart as can be seen with the $2a_1$ and $3a_1$ orbitals.

III. Second-Order Jahn Teller Effect.

The First-Order Jahn Teller (FOJT) effect was first deduced in 1937 by Jahn and Teller [16] and their brute force technique of testing all possible point groups for stability was subsequently improved on by Ruch and Schönhofer [17] who derived a more elegant

proof. The next stage in the development was the publication by Opik and Pryce [18] of the Second-Order Jahn Teller (SOJT) effect but the important link did not arise until Bader tried to predict reaction mechanisms from perturbation theory [19].

Structural predictions can be made from the SOJT effect which uses the symmetry properties of the HOMO and LUMO to test a geometry for stability with respect to a non-totally symmetric vibration which is contained in the direct product of the symmetry classes of the HOMO and LUMO. We study only non-totally symmetric displacements as these are the only ones capable of changing the point group.

The SOJT Theorem states that

Any system which has a ground state symmetry of P_0 (HOMO) and a low lying excited electronic state whose symmetry is P_1 (LUMO) will distort along a non totally symmetric normal vibration the symmetry of which is contained in the direct product $P_0 \times P_1$.

This is the necessary but not sufficient condition for distortion to occur. The sufficient condition only arises when consideration of the energy gap between the HOMO and LUMO is taken into account.

This is in essence identical to the FOJT effect which deals with electronically degenerate systems and has the vibrational coordinate contained in the direct product $P_0 \times P_0$ i.e. the direct product of the symmetry class of the HOMO with itself.

We can express this in a more mathematical way by the use of perturbation theory. Figure 2.3.1. shows a plot of reaction coordinate (Q) against energy (E) and what we want to do is to find out what symmetry has to say about the curvature of the curve .

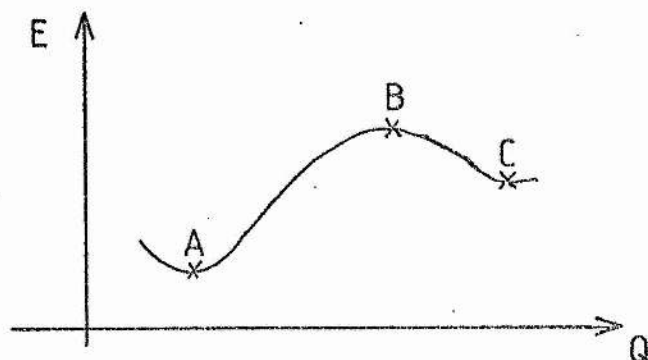


Figure 2.3.1.

We first of all require an expression which relates E to Q and includes terms which are symmetry dependent. The wave equation is solved and this results in a number of eigenvalues $E_0 \dots E_n$ with the corresponding electronic eigenstates $\psi_0 \dots \psi_n$ being obtained. The nuclei are subsequently moved by a small increment Q along the reaction coordinate and the new ground state energy is calculated from second order perturbation theory. A Taylor-Maclaurin expansion is used to write the Hamiltonian after distortion and this shown in eqn. 2.3.1..

$$H = H_0 + (\partial U / \partial Q)Q + (1/2)(\partial^2 U / \partial Q^2)Q^2 \quad \text{eqn 2.3.1.}$$

where H_0 is the original Hamiltonian, U the nuclear-nuclear and nuclear-electronic potential energy and Q the small displacement along

the reaction coordinate. The series is truncated at Q^2 and since the Hamiltonian must be totally symmetric $(\partial U / \partial Q)$ must have the same symmetry as Q , and $(\partial^2 U / \partial Q^2)$ the same symmetry as Q^2 .

The energy thus becomes

$$E = E_0 + \langle \psi_0 | \partial U / \partial Q | \psi_0 \rangle Q + \langle \psi_0 | (\partial^2 U / \partial Q^2) | \psi_0 \rangle Q^2 / 2 + \sum_n \frac{[\langle \psi_0 | (\partial U / \partial Q) | \psi_n \rangle Q]^2}{(E_0 - E_n)} \quad \text{eqn 2.3.2.}$$

where E_0 is the original energy at the point Q_0 . The next two terms are the first order perturbation energy and the first of these, the one linear in Q , is the FOJT term and the second one is the classical restoring energy and is always positive. The last term is an energy decreasing term and is the 'relaxability' [20] along coordinate Q or the second order perturbation energy. The sum of the two terms quadratic in Q after twice differentiating expression 2.3.2. is the force constant, since in classical mechanics the energy V of a simple harmonic oscillator with displacement x is governed by equation 2.3.3..

$$V = 1/2(kx^2) \quad \text{eqn 2.3.3.}$$

The first derivative of V with respect to x is the force and is thus

$$(dV/dx) = kx \quad \text{eqn 2.3.4.}$$

Further differentiation of 2.3.4. yields 2.3.5.

$$(d^2V/dx^2) = k \quad \text{eqn 2.3.5.}$$

and here k is the force constant and this is just Hooke's Law in a different form. The force constant k above is therefore analogous to the sum of the quadratic terms of eqn 2.3.2.

By starting with the molecule at its equilibrium position we can rewrite eqn 2.3.2. as

$$E = E_0 + 1/2(f_{00}Q^2) + 1/2(f_{0n}Q^2) \quad \text{eqn 2.3.6.}$$

and since we started at the equilibrium position the linear term in Q is zero. The experimental force constant is thus the sum of f_{00} and f_{0n} and is shown pictorially in Figure 2.3.2.

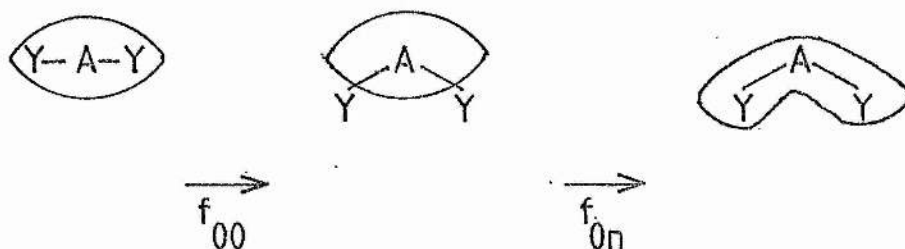


Figure 2.3.2.

The force constant f_{00} shows the nuclear motion with respect to a static electronic distribution and the relaxation term f_{0n} shows the energy change as the electronic distribution moves to follow the nuclei.

Meanwhile the original wavefunction ψ_0 has been changed by perturbation to ψ by the mixing in of various excited state wavefunctions

$$\psi = \psi_0 + \sum_n \frac{\langle \psi_0 | (\partial U / \partial Q) | \psi_n \rangle}{(E_0 - E_n)} \psi_n \quad \text{eqn 2.3.7.}$$

Hence the HOMO is stabilised and the LUMO destabilised by the mixing and this is shown pictorially in Figure 2.3.3.

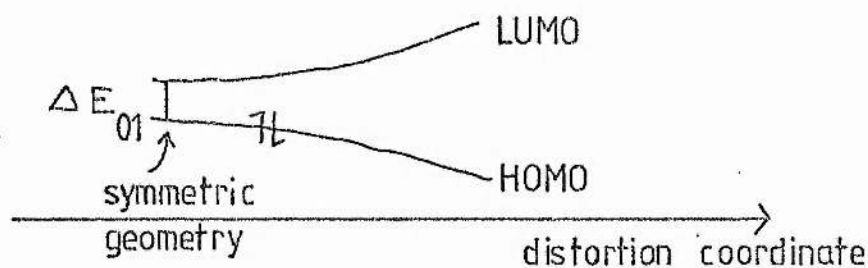


Figure 2.3.3.

This is therefore similar to Walsh's approach which was described in the last section.

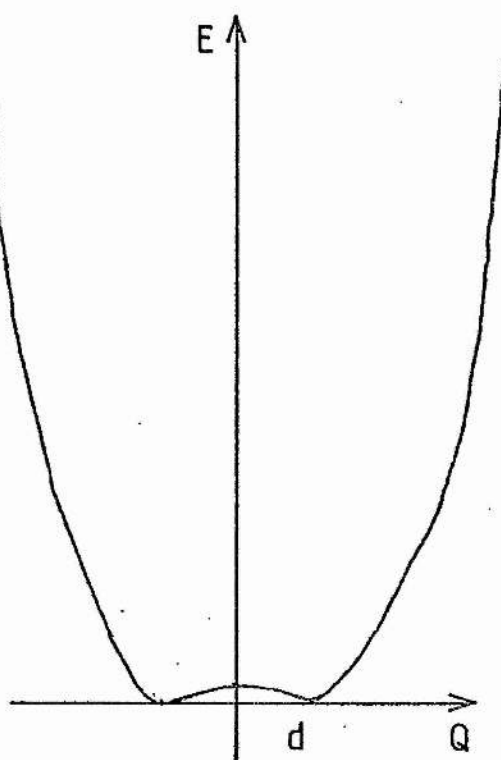
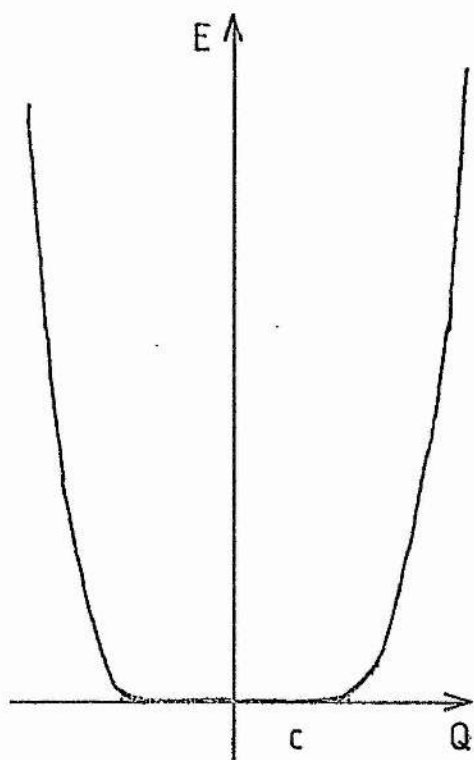
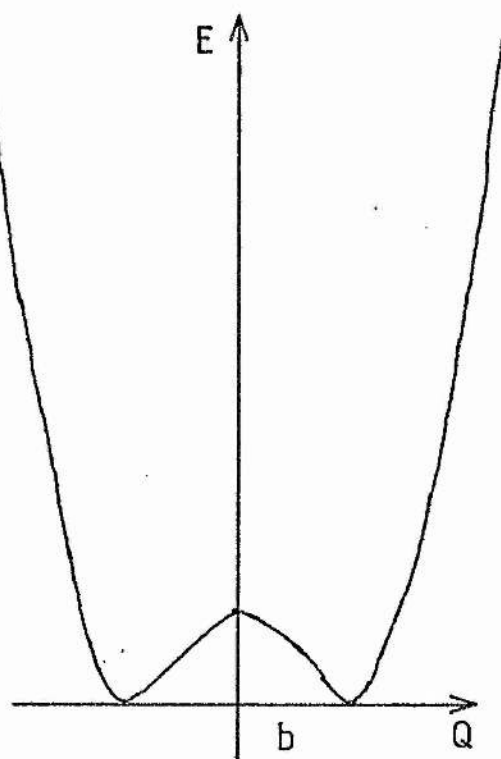
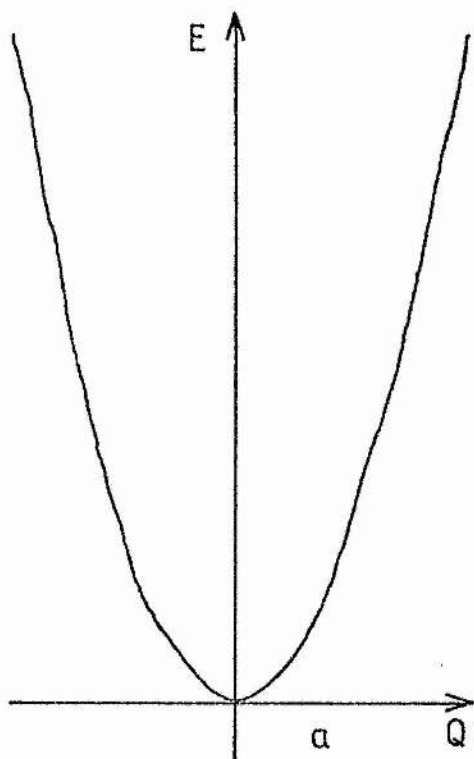


Figure 2.3.4.

Figure 2.3.4. displays four possible potential energy curves. Remembering that the first quadratic term in eqn 2.3.6. is always positive and the second quadratic term always negative we can see that for E to be a minimum as in Figure 2.3.4a then f_{00} must be bigger than f_{0n} . For E to be a maximum as in Figure 2.3.4b then f_{0n} must be greater than f_{00} and this leads to a negative force constant and the molecule will distort along a symmetry coordinate so as to find a position on the curve which yields a positive curvature or in other words a minimum since in the equilibrium position the system is at an energy maximum. Figures 2.3.4c and 2.3.4d show the result when both f_{00} and f_{0n} are of the same magnitude and here the molecule may be stable as in Figure 2.3.4c or it may be unstable as in Figure 2.3.4d. However it may undergo large changes in structure for little or no expenditure of energy.

The reason why the force constant can be positive or negative lies in the denominator of the second quadratic term in eqn 2.3.2. i.e. $(E_0 - E_n)$. The first quadratic term is always positive and so it is the second term which decides the sign of the force constant. The part $(E_0 - E_n)$ is always negative as are E_0 and E_n themselves with E_0 having the greater magnitude. If $(E_0 - E_n)$ is large then the second term in eqn 2.3.2. will be smaller than the first and no distortion occurs (Figure 2.3.4a) but if $(E_0 - E_n)$ is small then the second term is larger than the first and so the sign of the force constant becomes negative and hence distortion results (Figure 2.3.4b).

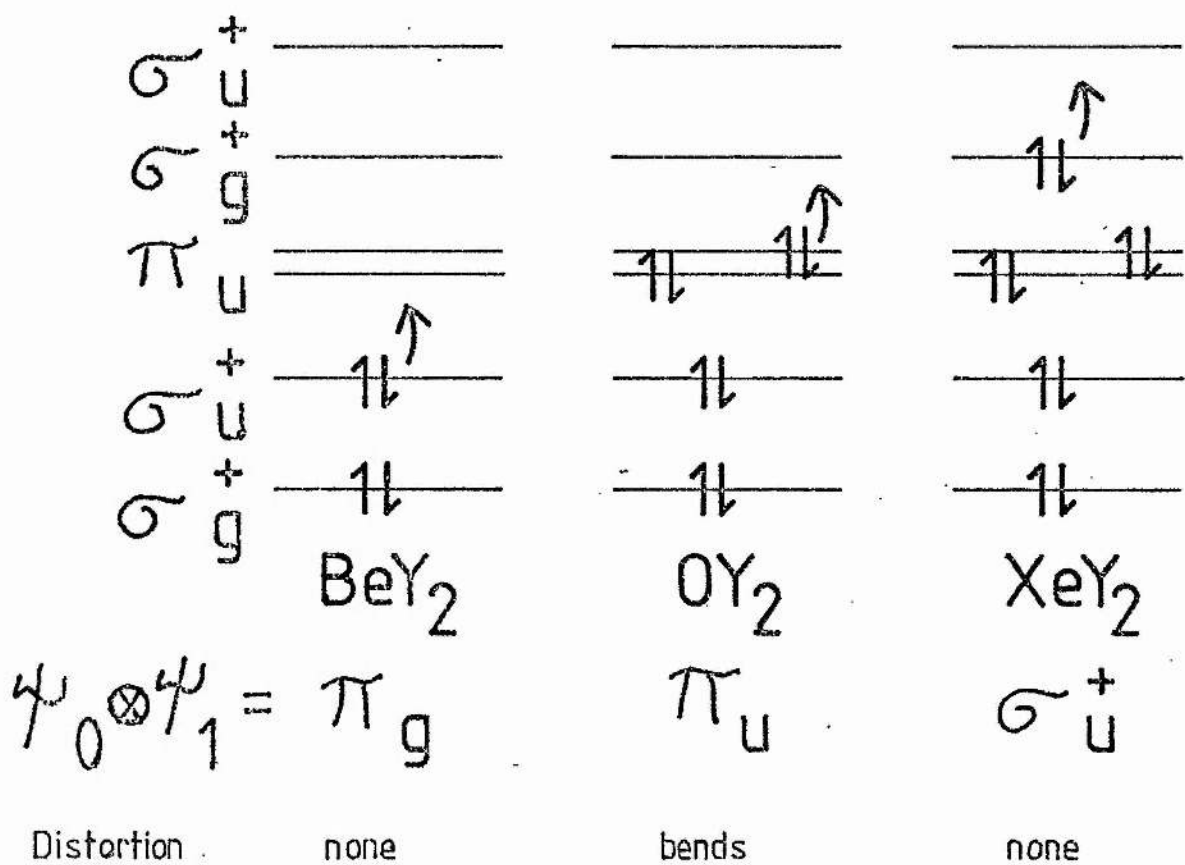


Figure 2.3.5.

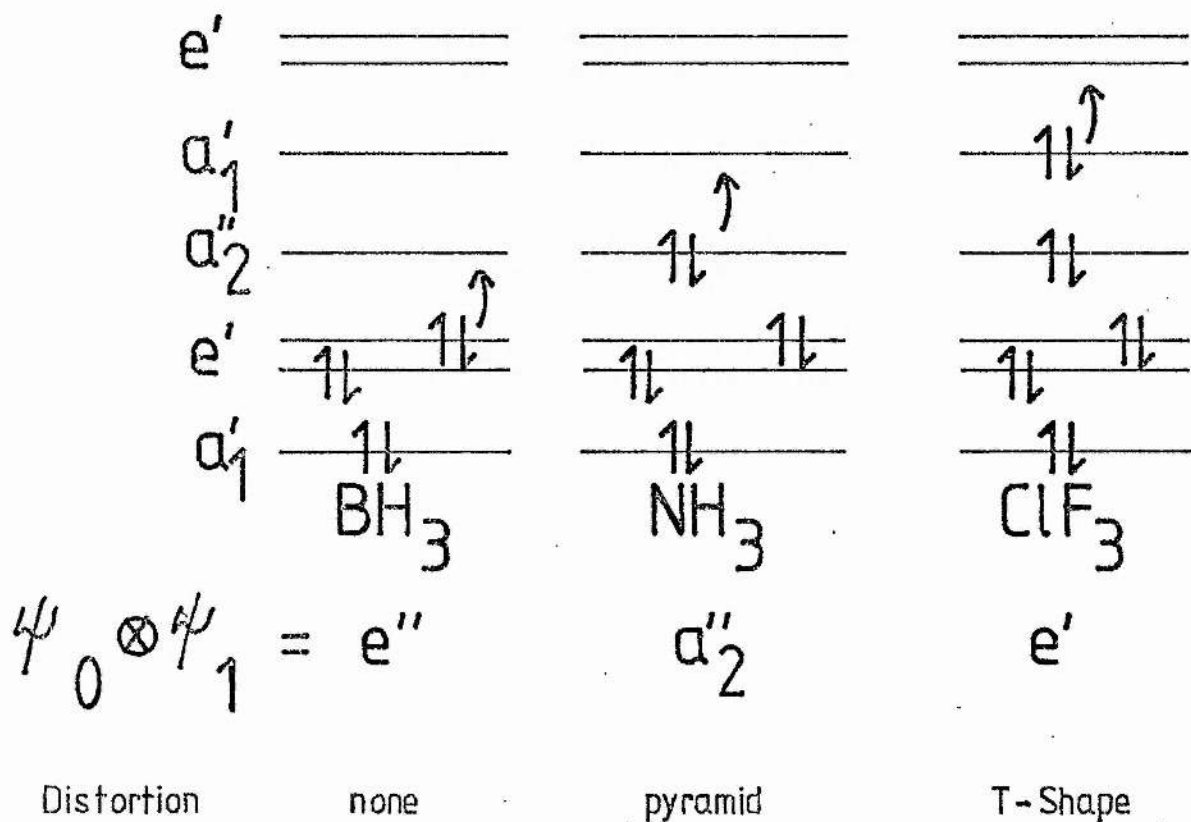


Figure 2.3.6.

In order to illustrate the SOJT effect Figures 2.3.5 and 2.3.6 show the tests undertaken for structural instability of linear AY_2 and trigonal planar AY_3 molecules respectively. The results from these tests will be used in Chapter Three when MNDO calculations on the distortions of linear carbenes and ethers and planar amines are discussed.

Chapter Two

Bibliography

1. J.K. Burdett. 'Molecular Shapes' Wiley-Interscience (1980).
2. R.G. Pearson. 'Symmetry Rules For Chemical Reactions' Wiley-Interscience (1976).
3. R.J. Gillespie and R.S. Nyholm. Quart Rev Chem Soc 11 339 (1957).
4. R.J. Gillespie. 'Molecular Geometry' van Nostrand-Reinhold (1972).
5. H.C. Allen Jnr. and E.K. Plyler. J Chem Phys 26 972 (1957).
6. G.D. Palik and E.E. Bell. J Chem Phys 26 1093 (1957).
7. W.S. Benedict, N. Gailar and E.K. Plyler. J Chem Phys 24 1139 (1956).
- 8a. B. Beagley and A.R. Conrad. Trans Farad Soc 66 2740 (1970).
- 8b. K. Hedberg. J.A.C.S. 77 6491 (1955).
- 9a. E.A.V. Ebsworth. 'Organometallic Compounds of the Group IV Elements' A.G. MacDonald (Ed), Dekker, New York 1,1 (1968).
- 9b. D.W.J. Cruickshank. JCS 5486 (1961).
- 10a. C. Glidewell and C. Thomson. J Comp Chem in press.
- 10b. A.F. Cuthbertson and C. Glidewell. J Mol Struct in press.
11. M.J.S. Dewar and W. Thiel. J.A.C.S. 99 4899 (1977).
12. A. Almenningen, O. Bastiasen, V. Ewing, K. Hedberg and M. Traetteberg. Acta Chem Scand 17 2455 (1963).
13. M.J. Barrow, E.A.V. Ebsworth and M.M. Harding. Acta Cryst B35 2093 (1979).
14. C.A. Ernst, A.L. Allred, M.A. Ratner, M.D. Newton, G.V. Gibbs, J.W. Moscovitz and S. Topiol. Chem Phys Lett 81 424 (1981).

15. A.D. Walsh. J. Chem. Soc. 2260,2266,2288,2296,2301,2306 (1953).
16. H.A. Jahn and E. Teller. Proc Roy Soc A161 220 (1937).
17. E. Ruch and A. Schönhofer. Theoret Chim Acta 3 291 (1965).
18. U. Öpik and M.H.L. Pryce. Proc Roy Soc A238 425 (1957).
19. R.F.W. Bader. Can J Chem 40 1164 (1962).
20. L. Salem. Chem Phys Lett 3 99 (1969).

Chapter Three.

Carbenes, Ethers and Amines.

I. Introduction.

In the previous chapter various rules for predicting molecular structure were put forward and the first and last of these are pertinent to this chapter which deals with MNDO calculations concerning the structures of singlet carbenes, ethers and their isoelectronic analogues, and amines and their isoelectronic counterparts.

The calculations were undertaken to see whether a previous hypothesis by Glidewell [1] was valid. This stated that in the presence of ligands of low electronegativity lone pairs would not fulfil their stereochemical role assigned to them in the VSEPR model, and was proposed in an attempt to rationalise successfully structures such as $(\text{Ph}_3\text{Si})_2\text{O}$ and $(\text{H}_3\text{Si})_3\text{N}$ which have a linear [2] and planar [3] skeleton respectively, and are in direct conflict with the predictions from VSEPR.

Glidewell showed that these structures, among others, could be interpreted by recourse to the Second-Order Jahn Teller (SOJT) effect [1]; which Pearson had earlier applied to VSEPR in order to justify the model [4,5]; and that the normal description of VSEPR was only one of two possible cases, that in which the lone pairs were

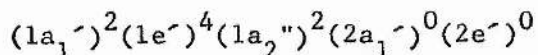
stereochemically active since the ligands had an electronegativity greater than that of the central atom, and that resort to conceptual artefacts like $p\pi \rightarrow d\pi$ bonding [6] were unnecessary in explaining structures such as $(\text{SiH}_3)_3\text{N}$.

The Glidewell argument [1], which is used throughout this chapter, is quoted here for completeness and considers for the sake of simplicity that the atom A, in $(\text{R}_n\text{M})_2\text{A}$, contributes ns and np valence orbitals, and the MR_n substituents each donate a single σ type orbital. Therefore if the MAM skeleton is linear and A carries two lone pairs the electronic configuration is

$$(1\sigma_g^+)^2(1\sigma_u^+)^2(1\pi_u)^4(2\sigma_g^+)^0(2\sigma_u^+)^0$$

The HOMO-LUMO energy gap, $I(1\pi_u) - I(2\sigma_g^+)$, is the determinant of whether the linear arrangement is stable relative to the bending mode and if the gap is large then no distortion occurs, but if this gap is small then the system will be distorted along a symmetry coordinate contained in $\pi_u \times \sum_g^+ = \pi_u$, which is the skeletal bending vibration. The $1\pi_u$ orbital is localised only on the central atom and so the less tightly bound that the ligand orbitals are with respect to those of the central atom, so the larger the energy gap between $1\pi_u$ and $2\sigma_g^+$ will become. Conversely this gap is small if the substituent orbitals are more tightly bound relative to those of the central atom.

Using the same set of orbitals in $(R_nM)_3A$ species yields an electronic configuration of



for a planar AM_3 skeleton with one lone pair formally localised on A.

This time the relevant gap is between $(1a_2'')$ and $(2a_1^-)$ and this is small if the ligand orbitals are tightly bound and a distortion along $1A_2'' \times 2A_1^- = A_2''$ will occur, which is the 'umbrella' out-of-plane bend.

Therefore skeletal linearity and planarity can be understood in terms of electronic arguments provided that MR_n has a low electronegativity. The calculational approach has been vindicated by MINDO/3 calculations [7,8] which indicate that the method which will be described herein has a sound background.

II. Symmetry Aspects.

The carbene and ether species studied were of the form $(X_3M)_2Y^{+n}$, which when linear belong to the point group D_{3h} , and C_{2v} when bent; thus by reference to a set of character tables we see that the vibration that takes linear D_{3h} to bent C_{2v} is E' : this is shown schematically in Figure 3.2.1 along with the reverse vibration which takes C_{2v} to D_{3h} which is A_1 . The microsymmetry of the MYM fragment is $D_{\infty h}$ which bends to C_{2v} .

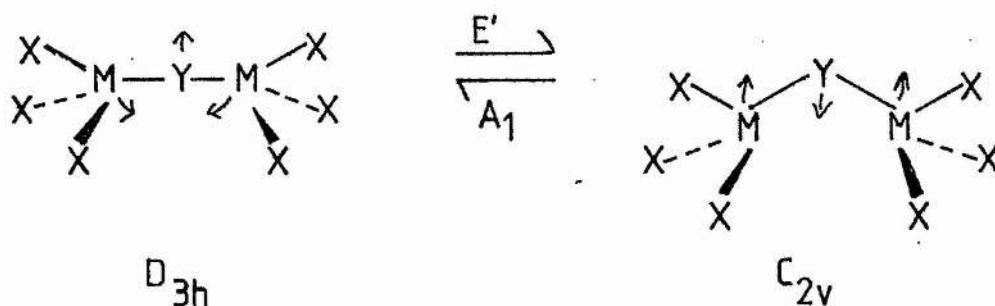


Figure 3.2.1. Vibration of linear D_{3h} species.

For the planar amine species, $(X_3M)_3Y^{+n}$, the point group is once again D_{3h} for the microsymmetry of M_3Y , but this time the bent molecule is in point group C_{3v} , and the relevant vibration is that of A_2'' which is the umbrella bending mode and is shown along with the inverse vibration of A_1' in Figure 3.2.2.

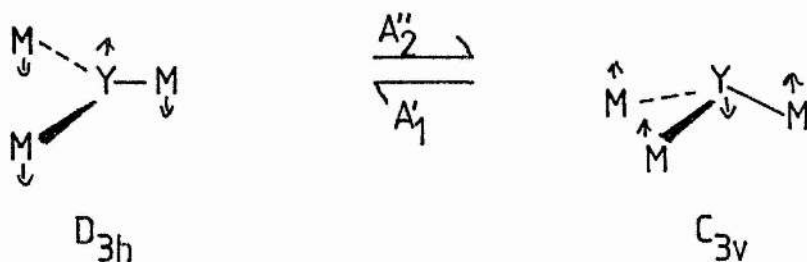


Figure 3.2.2. Vibration of planar D_{3h} species.

If the SOJT effect is to predict correctly the bending mode then the direct product of the symmetry classes of the HOMO and LUMO must contain, for the carbenes and ethers, the E' vibration, and for the amines, the A_2'' vibration. Table 3.2.1 lists all the possible permutations of the direct products, $\Gamma_i \times \Gamma_j$, which generate the relevant modes in D_{3h} [9].

	Γ_i	Γ_j
E'	A'	E'
	A''	E''
	E'	E'
	E''	E''
A_2''	A_1'	A_2''
	A_2'	A_1''

Table 3.2.1. Direct products in D_{3h} which yield E' and A_2'' .

III. Calculation of Force Constants.

We saw in the last chapter that the value and sign of the force constant gave an indication of the equilibrium structure of the molecule. A large positive force constant suggested a stable linear or planar molecule, and a large negative force constant a bent or pyraminal molecule, for the linear and planar D_{3h} species respectively.

Calculation of the force constant is achieved by finding the energy of a system at varying θ values, see Figure 3.3.1.



Figure 3.3.1. Angular bending mode.

The energy differences, ΔV , and angular differences, $\Delta \theta$, between the linear and non-linear geometries are then plotted against each other and the resultant plot is found to be symmetrical about the linear or planar geometry.

This can be represented mathematically by a polynomial of the form

$$V = C + a(\Delta \theta)^2 + b(\Delta \theta)^4 + \dots$$

where $\Delta \theta$ has been converted to radians and C a constant which indicates the point at which the curve cuts the y axis - the smaller the value indicating the better the fit since the curves all pass through the origin, where ΔV and $\Delta \theta$ are both zero. Only even powers of θ are involved because of the symmetrical nature of the curves.

In Chapter Two we saw how the energy of a simple harmonic oscillator was repeatedly differentiated until the force constant, k , was obtained. In a similar fashion our expression

$$V = C + a(\Delta \theta)^2 + b(\Delta \theta)^4 + \dots$$

when differentiated with respect to $\Delta \theta$ yields firstly

$$\frac{\partial (\Delta V)}{\partial (\Delta \theta)} = 2a(\Delta \theta) + 4b(\Delta \theta)^3 + \dots$$

and subsequently

$$\frac{\partial^2(\Delta V)}{\partial (\Delta \theta)^2} = 2a + 12b(\Delta \theta)^2 + \dots$$

Since the linear or planar geometry is where the interest lies for the bending the above becomes

$$\left(\frac{\partial^2(\Delta V)}{\partial (\Delta \theta)^2} \right)_{\Delta \theta = 0} = 2a$$

as all the $\Delta \theta$ terms vanish.

As a result twice the calculated polynomial co-efficient 'a' gives the curvature of the energy well at the linear or planar geometry and the force constant in Nm^{-1} [10] can be found from the following expression

$$f = \frac{2a}{l_1 l_2 L}$$

where l_1 and l_2 are the bond lengths which subtend the force constant angle θ and in all cases in this chapter $l_1 = l_2$. L is Avogadro's constant.

The polynomial coefficients C, a, b etc. are calculated in practice by a program based on the NAG library routine E02ACF [11] which uses the ΔV and $(\Delta \theta)^2$ values as its input data. The degree of polynomial calculated in each case was of degree 5. The results from these calculations are presented in sections V-VII of this chapter.

IV. Method.

All the calculations were carried out with MNDO [12,13] implemented on the University's VAX 11/780 computer. The species studied were for -

Carbenes :

$(X_nM)_2C$, $X=H$: $n=1$, $M=Be, O$; $n=2$, $M=Be^-, B, C^+, C^-$, N, O^+ ; $n=3$, $M=Be^{-2}, B^-, C, N^+, Si$. $X=F$: $n=1$, $M=Be$; $n=2$, $M=Be^-, B, C^+, C^-$; $n=3$, $M=Be^{-2}, B^-, C, Si$ and X_2C : $X=H, F, Cl$. When $X=F$, $n=3$, $M=N^+$ the optimisations failed to achieve self-consistence.

The MCM fragment is formally a six electron fragment and if $g(X)$ is the group number of element X then

$$2g(M) + g(C) - n = 12 \text{ for class A carbenes. (1)}$$

$$2g(M) + g(C) - n = 10 \text{ for class B carbenes. (2)}$$

$$2g(M) + g(C) - n = 14 \text{ for class C carbenes. (3)}$$

$$2g(M) + g(C) - n = 16 \text{ for } (HO)_2C$$

$$2g(M) + g(C) - n = 18 \text{ for } F_2C$$

The class A,B and C refer to later sections in this chapter as the carbenes fall into three distinct classes each with its own behaviour.

Ethers :

$(H_3M)_2Y^{+n}$ where M and Y are permutations of the following M= Be,B,C,N,O,Si,P,S ; Y= B,C,N,O,F and n is found from the following equation

$$2g(M) + g(Y) - n = 14 \quad (4)$$

Also eight $(F_3M)_2Y^{+n}$ species M= B,C,N ; Y= B,C,N,O,F and n is found as before from equation (4). The MYM fragment is thus an eight electron fragment.

Amines :

$(H_3M)_3Y^{+n}$ where permutation of M and Y among M= Be,B,C,N, Si,P ; Y= C,N,O,P with n found from

$$3g(M) + g(Y) - n = 17$$

yield an M_3Y fragment which is formally an eight electron fragment. Also $(H_2M)_3N$ for Be^{-3}, B, C^{+3} were studied.

In every case the M-Y bond lengths were tied together and optimised as one. If this is neglected then some of the species may dissociate or the bond lengths may differ and so a fixed point group would not be obtained. The reaction scans were undertaken by fixing

the $\angle MYM$ angles at a series of values and optimising the rest of the structure without further restraints, and so the energy at each point was obtained. The equilibrium geometry and energy was obtained similarly but the $\angle MYM$ angle was allowed to refine in addition.

The carbenes and ethers when bent have C_{2v} geometries with four close X atoms and two distant, which is typical of $(AB_3)_2C$ systems which are remote from linearity. The amines, on the other hand, are more complicated since the way in which the MX_3 groups gear into one another is crucial if the lowest energy for the system is to be obtained. This is effected if three M-X bonds, in separate MX_3 entities, lie in the M_3Y plane (C_{3h} symmetry).

V. Carbenes.

Recently two contrasting views have been proposed concerning the structure of singlet carbenes [14,15]. The first of these, by Schoeller [14], used the results from ab-initio calculations on CX_2 ; X= Li, BeH, BH_2 , CH_3 , NH_2 , OH, OMe, F; and electronegativity arguments to speculate that ligands which had an electronegativity greater than that of carbon would give a bent carbene, and ligands with a lower electronegativity would realise a linear carbene. An opposing view subsequently appeared from Pauling [15], and pointed to the occurrence of vacant valence shell orbitals on the ligands for the species that Schoeller had found to be linear.

Molecule	d(XM)(Å)	d(MC)(Å)	∠MCM(°)	∠XMC(°)	E/kJmol ⁻¹
Class A					
(H ₃ Be) ₂ C ⁻⁴	1.509	1.747	180.0	117.0	2352.0
(H ₃ B) ₂ C ⁻²	1.211(x2)	1.498	150.0	114.9(x2)	397.0
	1.188(x4)			112.5(x4)	
(H ₃ C) ₂ C	1.114(x2)	1.449	133.7	116.1(x2)	291.0
	1.113(x4)			108.7(x4)	
(H ₃ N) ₂ C ⁺²	1.045(x2)	1.493	118.3	106.0(x2)	-288.3
	1.038(x4)			115.5(x4)	
(F ₃ Be) ₂ C ⁻⁴	1.672	1.785	180.0	117.5	-422.1
(F ₃ B) ₂ C ⁻²	1.409(x2)	1.574	156.7	116.4(x2)	-1783.0
	1.405(x4)			111.5(x4)	
(F ₃ C) ₂ C	1.352(x2)	1.565	125.4	110.1(x2)	-801.8
	1.356(x4)			112.7(x4)	
(F ₃ N) ₂ C ⁺²	Failed to achieve self-consistence.				
(H ₃ Si) ₂ C	1.441	1.729	180.0	109.5	316.7
(F ₃ Si) ₂ C	1.633	1.762	180.0	113.5	-2031.1
Class B					
(H ₂ Be) ₂ C ⁻²	1.363	1.598	180.0	122.3	189.4
(H ₂ B) ₂ C	1.160	1.387	180.0	120.9	123.4
(H ₂ C) ₂ C ⁺²	1.116	1.348	180.0	123.0	2554.5
(F ₂ Be) ₂ C ⁻²	1.569	1.642	180.0	125.4	-1534.9
(F ₂ B) ₂ C	1.325	1.466	180.0	122.4	-1193.2
(F ₂ C) ₂ C ⁺²	1.285	1.429	180.0	121.9	2049.8
(HBe) ₂ C	1.277	1.607	180.0	180.0	224.5
(FBe) ₂ C	1.461	1.591	180.0	180.0	-642.5
Class C					
(H ₂ C) ₂ C ⁻²	1.115(x2)	1.325	162.5	125.7(x2)	884.9
	1.120(x2)			128.1(x2)	
(H ₂ N) ₂ C	1.000(x2)	1.353	119.0	127.3(x2)	156.2

	0.994(x2)			117.7(x2)	
$(\text{H}_2\text{O})_2\text{C}^{+2}$	0.980(x2)	1.392	116.0	132.2(x2)	1944.1
	0.990(x2)			115.1(x2)	
$(\text{F}_2\text{C})_2\text{C}^{-2}$	1.359(x2)	1.355	141.3	130.3(x2)	-300.4
	1.353(x2)			124.5(x2)	
$(\text{HO})_2\text{C}$	0.953	1.314	119.6	122.1	-286.5

Table 3.5.1. ΔH_f^θ and geometries for carbene species.

At the end of this section we will see that the Schoeller and Pauling arguments do not cover all the possibilities, as they confined their studies to a limited series.

The carbenes which were studied were listed in Section IV and their equilibrium energies and geometries can be found in Table 3.5.1. As was mentioned previously, the carbenes fall into three classes and these depend on either the presence, or lack, of lone pairs and vacant orbitals. Class A carbenes are those in which M carries neither lone pairs nor vacant orbitals, class B have at least one vacant orbital on M, and finally class C in which M carries at least one lone pair. It is therefore convenient to take each class separately in order to discuss their diversity of behaviour.

a. Class A Carbenes $(X_3M)_2C^{+n}$.

From Table 3.5.1 we see that the MCM skeleton is non-linear, except in the cases when M = Be or Si when it is accurately linear. All the non-linear species are of C_{2v} symmetry with four X atoms close together. Therefore the bending vibration is of linear D_{3h} to bent C_{2v} , rather than linear D_{3d} which would bend to C_s unless a conformational change took place. The linear species found are all of D_{3h} symmetry and not D_{3d} .

Molecule	$f(\text{Nm}^{-1})$	$\Delta\Delta H_f^\theta (\text{kJmol}^{-1})$
Class A		
$(\text{H}_3\text{Be})_2\text{C}^{-4}$	+29.5	0.0
$(\text{H}_3\text{B})_2\text{C}^{-2}$	-4.9	1.3
$(\text{H}_3\text{C})_2$	-40.7	17.1
$(\text{H}_3\text{N})_2^{+2}$	-288.3	180.8
$(\text{F}_3\text{Be})_2\text{C}^{-4}$	+36.8	0.0
$(\text{F}_3\text{B})_2\text{C}^{-2}$	-11.2	1.9
$(\text{F}_3\text{C})_2\text{C}$	-15.6	23.4
$(\text{H}_3\text{Si})_2\text{C}$	+31.3	0.0
$(\text{F}_3\text{Si})_2\text{C}$	+26.3	0.0
Class B		
$(\text{H}_2\text{Be})_2\text{C}^{-2}$	+50.6	
$(\text{H}_2\text{B})_2\text{C}$	+95.4	
$(\text{H}_2\text{C})_2\text{C}^{+2}$	+142.7	
$(\text{F}_2\text{Be})_2\text{C}^{-2}$	+58.8	
$(\text{F}_2\text{B})_2\text{C}$	+97.8	
$(\text{F}_2\text{C})_2\text{C}^{+2}$	+100.0	
$(\text{HBe})_2\text{C}$	+25.6	
$(\text{FBe})_2\text{C}$	+28.0	
Class C		
$(\text{H}_2\text{C})_2\text{C}^{-2}$	-3.3	0.2
$(\text{H}_2\text{N})_2\text{C}$	-2426.4	448.4
$(\text{H}_2\text{O})_2\text{C}^{+2}$	-415.4	247.9
$(\text{F}_2\text{C})_2\text{C}^{-2}$	-21.7	7.2
$(\text{HO})_2\text{C}$	-698.7	237.7

Table 3.5.2. Force constant and energy differences for carbene species.

When $X = H$ or F the equilibrium $\angle MCM$ angle becomes progressively smaller indicating a more bent structure as M traverses across the Periodic Table from $Be^{-2} - B^{-} - C - N^{+}$. In other words, the more electronegative the substituent the more bent the structure. In addition when $M = Si$ and $X = H$ or F , the skeleton is linear, although the respective carbon compounds, $M=C$, are all non-linear. The MC distance, too, is larger for $X=F$ than $X=H$ without exception.

The force constants, which in this case are for the E' skeletal bending vibration, along with the inversion barriers, which are the energy differences between the linear and equilibrium geometries, are laid out in Table 3.5.2. For both $X = H$ and F the value of the force constant becomes steadily more negative as M moves from Be^{-2} to N^{+} , that is becomes more electronegative: at the same time as this, the structure becomes more bent and the inversion barriers increase to reflect these trends.

The molecules which are linear at equilibrium necessarily have positive force constants at linearity, since they are at the local energy minimum. However, molecules that are non-linear at equilibrium have negative force constants, since the linear structure corresponds to a local energy maximum.

Interestingly, perhaps, the electronegativity for $M = Si$ is found to lie between beryllium and boron and hence explains the positive force constant encountered for the silicon carbenes: in addition in the Pauling and Allred-Rochow electronegativity scales, the scales

related most closely to atoms in molecules, the value for silicon is situated between those for beryllium and boron.

Carbenes of class A, therefore, fully conform to the treatment outlined in Section I, namely that when ligands of low electronegativity are present, the lone pairs on the central atom appear to be stereochemically inactive.

b. Class B Carbenes $(X_2M)_2C^{+n}$ and $(XBe)_2C^{+n}$.

These species at equilibrium all carry at least one vacant orbital on M; and as a result we see from Table 3.5.1 that the MCM skeletons are all thoroughly linear and those species, $(X_2M)_2C$, wholly planar with D_{2h} symmetry, whilst $(XBe)_2C$ species are in point group $D_{\infty h}$. Once again, with no exceptions, the MC distance between analogous species is found to be longer when $X = F$ than with $X = H$.

In order to explain the linearity and planarity we need to recourse to the symmetry of the orbitals. When the $(X_2M)_2C$ species are planar each M atom bears a vacant np orbital which is normal to the plane of the molecule and spans the symmetry classes $B_{2g} + B_{3u}$, whilst the central carbon atom carries a lone pair orbital of B_{3u} symmetry again normal to the molecular plane, and an empty orbital of B_{2u} symmetry in the molecular plane.

The planarity of the skeleton is assured by interaction of the B_{3u} orbitals which yield essentially $C \rightarrow M$ $p\pi-p\pi$ bonding. The skeletal linearity at equilibrium is facilitated by the amalgamation of the carbon B_{2u} orbital with the B_{2u} combination which arises from the $O^-(MX)$ orbitals, which is equivalent to $(MX) \rightarrow C$ $p\pi-p\pi$ bonding.

The linearity of the $(XBe)_2C$ species comes about from overlap of the occupied $p\pi$ orbital on carbon, which is of π_u symmetry, with the $p\pi$ orbitals of beryllium, which span symmetry classes $\pi_g + \pi_u$.

They are all linear because of the presence of the vacant orbitals on M, and as M varies across a row so the value of the force constant increases, as does the inversion barrier. The force constants here are all positive since the linear geometry is at the local energy minimum. Most unusually, though, the same force constant was found for both the B_{2u} and B_{3u} vibrational modes, which are the in and out-of-plane bends respectively, to which the force constant refers in these cases. The increase of the force constant can be explained by reference to the π bond orders between the M and the C perpendicular to the plane: they increase from $Be^- < B < C^+$, the values being 0.619, 0.653 and 0.674, and hence $(p-p)\pi$ donation from $C \rightarrow M$ becomes greater as the electronegativity of the ligand increases. An exactly analogous situation occurs for the $(F_2M)_2C$ series, the C-M bond orders being 0.352, 0.457 and 0.523 for Be^- , B, C^+ respectively; their values indicate that there is more $(F \rightarrow M)\pi$ style bonding and as a result the extent of $C \rightarrow M \pi$ bonding is reduced and the variation in π bonding less marked.

c. Class C Carbenes $(X_2M)_2C^{+n}$ and $(HO)_2C$.

The molecules, all of which have a lone pair of electrons formally localised on each M, have wholly planar structures, but with non-linear MCM backbones. The non-linearity is least pronounced for $(X_2C)_2C^{-2}$ species, and for $X=H$ the ΔH_f^θ is very close to the value found at linearity (see Table 3.5.2); and the species when fixed linear optimise to D_{2h} ; whilst in contrast, $(H_2M)_2C$, $M=N, O^+$, when constrained to linearity give D_{2d} structures on optimisation of the other variables.

A rationale for this can be found, and if we look at $(H_2C)_2C^{+n}$ for $n=-2, 0, +2$, we see that for $n=+2$ the structure is D_{2h} , $n=0$, D_{2d} and addition of a further two electrons ($n=-2$) reverts the structure back to D_{2h} .

The π molecular orbitals, of which there are four in D_{2d} , split into two degenerate pairs having E symmetry, and since there are four electrons to occupy them in $(H_2C)_2C$ the lower bonding pair is occupied whilst the upper pair, which is anti-bonding, is vacant. Correlation of the two E pairs in D_{2d} with the π orbitals in D_{2h} , yield for the bonding pair $B_{3u} + B_{2g}$, which are formed by combinations of the out-of-plane $p\pi$ orbitals. The upper E transform as B_{2u} , which is the in-plane $p\pi$ orbital, and B_{3u} , which is the fully out-of-phase amalgamation of the out-of-plane $p\pi$ orbitals. Table 3.5.3 lists the orbital energies in D_{2h} and D_{2d} for $(H_2M)_2C$, $M=C^-, N, O^+$.

	$(\text{H}_2\text{O})_2\text{C}^{+2}/\text{eV}$	$(\text{H}_2\text{N})_2\text{C}/\text{eV}$	$(\text{H}_2\text{C})_2\text{C}^{-2}/\text{eV}$
D_{2h}			
B_{3u}	-13.32	+1.54	+15.92
B_{2u}	-14.00	-0.05	+5.90
A_g	-23.78	-6.39	(+17.46)
B_{2g}	-26.12	-9.13	+5.84
B_{3u}	-27.38	-11.82	+2.31
D_{2d}			
E	-13.35	+1.23	+14.83
			+7.67
A_1	-23.66	-5.95	(+17.44)
E	-26.84	-10.83	+4.28

Table 3.5.3. Eigenvalues for $(\text{H}_2\text{O})_2\text{C}^{+2}$, $(\text{H}_2\text{N})_2\text{C}$, and $(\text{H}_2\text{C})_2\text{C}^{-2}$, D_{2h} and D_{2d} .

Molecule	CH_2	CF_2	CCl_2
$d(\text{CX})(\text{\AA})$	1.091	1.304	1.748
	(1.11)a	(1.300)b	
$\angle \text{XCX}(^{\circ})$	111.1	108.3	113.9
	(102.4)a	(104.9)b	
$\Delta H_f^{\theta}(\text{kJmol}^{-1})$	+449.2	-237.2	+240.3
$f(\text{Nm}^{-1})$	-94.9	-1455.7	-404.6
$\Delta(\Delta H_f^{\theta})(\text{kJmol}^{-1})$	+58.5	+539.7	+233.1

a=[16] , b=[17,18]

Table 3.5.4. ΔH_f^{θ} , geometries, force constants and energy differences for singlet carbenes.

This shows that the electronic configuration in D_{2h} for $(H_2C)_2C^{-2}$ is $(B_{3u})^2(B_{2g})^2(B_{2u})^2(B_{3u})^0$. But, in both $(H_2O)_2C^{+2}$ and $(H_2N)_2C$, there is an additional orbital of A symmetry, which arises from a combination of 2s and axial 2p orbitals, the energy of which is comparable in magnitude to the π orbitals. This extra orbital is not as tightly bound as the π orbitals in $(H_2C)_2C^{-2}$; however it is low enough in energy so that it is occupied in both $(H_2O)_2C^{+2}$ and $(H_2N)_2C$, for both D_{2h} and D_{2d} geometries, and as a result may be pertinent in the geometrical determination of point group at linearity for these species.

The energy differences between D_{2h} and D_{2d} for the species are listed below - values in kJmol^{-1} .

Species.	Energy.	
$(H_2C)_2C^{-2}$	155.6	D_{2h} more stable
$(F_2C)_2C^{-2}$	165.4	D_{2h} more stable
$(H_2O)_2C^{+2}$	9.6	D_{2d} more stable
$(H_2N)_2C$	69.3	D_{2d} more stable

However in spite of this idiosyncrasy when CCC is linear the molecules all adopt C_{2v} structures when bent.

In D_{2h} , the symmetry of the HOMO and LUMO are A_g and B_{2u} (see Table 3.5.3) for $(H_2M)_2C$ $M = N, O^+$, and here $A_g \times B_{2u}$ yields B_{2u} , which is the skeletal bend. However in $(H_2C)_2C^{-2}$ the HOMO and LUMO are B_{2u} and B_{3u} , and $B_{2u} \times B_{3u} = B_{1g}$, but there is an orbital of A_g

symmetry 1.5 eV above B_{3u} and so if this is brought into play we have $B_{2u} \times A_{1g} = B_{2u}$, as before.

The symmetries of the HOMO and LUMO in D_{2d} are A_1 and E , the former being the HOMO for N and O^+ and LUMO for C^- ; the direct product is thus $A_1 \times E = E$, and one of the E components is the doubly degenerate bend.

In spite of the fact that in this case the increasing electronegativity of the ligand does produce a more bent structure, the force constant, however, does not mirror this. The force constant and energy barrier do correlate though, but the $M=N$ species is slightly awry, although the HOMO-LUMO gap does reflect the force constant and energy barrier correlation. See Table below.

M	$f(Nm^{-1})$	$\Delta\Delta H_f^\theta (kJmol^{-1})$	$\langle MCM \rangle^\theta$	HOMO-LUMO (eV)	
				D_{2h}	D_{2d}
C^-	-3.3	0.2	162.5	11.56	-
N	-2426.4	448.4	119.0	6.34	7.18
O^+	-415.4	247.9	116.0	-	10.31

When $M=C^-$ we find an example of a molecule which has an extremely weak SOJT distortion, see Figure 2.3.4d.

d. Singlet Carbenes.

All the data for CX_2 , $X=H,F,Cl$ are collected in Table 3.5.4, and this shows that the CX_2 species are all markedly non-linear at equilibrium, and although the agreement between the experimentally observed [16-18] and calculated bond angles is not good, the bond length agreement is significantly better. Since CF_2 and CCl_2 are isoelectronic with O_3 and SO_2 , Walsh's Rules [19] would predict a similar bond angle and the values found for O_3 and SO_2 from experiment are 116.8 [20] and 119.5 [21] respectively.

The force constants here all become steadily more negative as the electronegativity of the ligand increases in the order $CH_2 > CCl_2 > CF_2$, which is as predicted [1].

The much wider range of carbenes studied here, show that the previous accounts [14,15] are incomplete. When the ligand has vacant orbitals, then the equilibrium structure will have a linear backbone, but the bending force constant will increase with the electronegativity of the ligand, which is paralleled by the π bond order between carbon and its substituents. However, if the ligand has no vacant orbitals or lone pairs, then the equilibrium geometry depends exclusively on the electronegativity of the ligand, and is linear at C when the substituent is an electron donor: the bending force constant steadily becomes more negative and is mirrored by the increasing electronegativity of the ligand and the decrease in the equilibrium skeletal angle. A carbene with one or more lone pairs on the ligand is bent, and again the force constant for bending varies in accord with the SOJT effect.

Ion	Products
$(\text{H}_3\text{O})_2\text{N}^{+3}$	$\text{N}^+ + 2\text{H}_3\text{O}^+$
$(\text{H}_3\text{O})_2\text{C}^{+2}$	$\text{C} + 2\text{H}_3\text{O}^+$
$(\text{H}_3\text{F})_2\text{C}^{+4}$	$\text{C} + 2\text{H}_3\text{F}^{+2}$
$(\text{H}_3\text{O})_2\text{B}^+$	$\text{B}^+ + 2\text{H}_2\text{O} + 2\text{H}^+$
$(\text{H}_3\text{S})_2\text{C}^{+2}$	$\text{C} + \text{SH}_3\text{S}^+$
$(\text{H}_3\text{Si})_2\text{B}^{-3}$	$\text{H}_2\text{SiBH}_2\text{SiH}_3^{-3}$
$(\text{H}_3\text{P})_2\text{B}^-$	$\text{H}_2\text{PBH}_2\text{PH}_2^-$

Table 3.6.1. Fate of unstable ions.

In general, the MNDO results complement those of Schoeller [14] whilst substantially modifying his explanation: and also provides further support for the model which points at the apparent stereochemical inactivity of lone pairs in some molecules being due to the presence of ligands of low electronegativity [1] and not of d orbital involvement[6].

VI. Ethers $(X_3M)_2Y^{+n}$.

Such diversity of behaviour as was seen above in the carbenes is not shown in the ethers, and are, therefore, more simply dealt with. The fate of the unstable ions is catalogued in Table 3.6.1.

The geometries afforded by the ethers, as seen in Table 3.6.2, exhibit a number of structural characteristics already described in the class A carbenes. The MYM backbone for a given Y is linear only for the least electronegative ligands MX_3 , and so for M a first row atom with $Y=F$ the linear skeleton is encountered for $MX_3=BeH_3, BH_3, BF_3$ and CF_3 only. $Y=O$ yields a linear skeleton for just $MX_3=BeH_3$, and $Y=N$ affords skeletons which are linearly remote. The skeletons for $Y=C$ are linear for $MX_3=BH_3, CH_3$ and CF_3 , but non-linear for $MX_3=NH_3$.

M atoms belonging to the second row of the Periodic Table follow a similar pattern of behaviour. The energy difference between D_{3h} (tops eclipsed) and D_{3d} (tops staggered) for a linear MYM backbone is negligible and once more the optimisations produce equilibrium structures of C_{2v} with four close X atoms, except for $(H_3S)_2O^{+4}$ which

M	Y	n	d(M-H)(Å)	d(M-Y)(Å)	<(HMY)(°)	<(MYM)(°)	ΔH_f^\ominus (kJmol ⁻¹)
Be	F	-3	1.434	1.672	110.4	180.0	+189.9
B	F	-1	1.191	1.414	108.7	180.0	-666.9
C	F	+1	1.114(x2)	1.423	106.6(x2)	153.1	+618.7
			1.113(x4)		107.7(x4)		
N	F	+3	1.092(x2)	1.431	103.0(x2)	150.9	+4586.8
			1.077(x4)		107.4(x4)		
Be	O	-4	1.550	1.644	117.0	180.0	+1893.9
B	O	-2	1.220(x2)	1.425	109.1(x2)	126.1	-140.2
			1.217(x4)		115.5(x4)		
C	O	0	1.116(x2)	1.396	107.3(x2)	119.9	-214.3
			1.118(x4)		112.6(x4)		
N	O	+2	1.064(x2)	1.364	104.5(x2)	121.8	+2190.8
			1.051(x4)		114.0(x4)		
O	O	+4	1.179(x2)	1.404	104.4(x2)	128.6	+7254.8
			1.097(x4)		117.0(x4)		
B	N	-3	1.266(x2)	1.439	112.1(x2)	126.9	+1314.2
			1.277(x4)		122.1(x4)		
C	N	-1	1.124(x2)	1.401	109.6(x2)	117.9	+35.6
			1.138(x4)		116.9(x4)		
N	N	+1	1.038(x2)	1.392	104.2(x2)	118.5	+924.5
			1.035(x4)		116.1(x4)		
B	C	-4	1.380	1.401	123.7	180.0	+3189.9
C	C	-2	1.176	1.337	119.2	180.0	+841.6
N	C	0	1.019(x2)	1.405	104.8(x2)	122.4	+517.1
			1.043(x4)		117.9(x4)		
C	B	-3	1.182(x2)	1.412	117.5(x2)	133.3	+1999.2
			1.251(x4)		126.4(x4)		
N	B	-1	1.014(x2)	1.443	105.4(x2)	117.4	+504.3

			1.084(x4)		124.0(x4)		
Si	F	+1	1.440	1.725	102.4	180.0	+190.8
P	F	+3	1.416	1.645	104.5	180.0	+3802.1
Si	O	0	1.445	1.665	107.6	180.0	-334.1
P	O	+2	1.389(x2)	1.597	103.1(x2)	137.9	+1941.4
			1.377(x4)		110.3(x4)		
S	O	+4	1.660(x2)	1.660	99.2(x2)	140.0	+6855.1
			1.463(x2)		109.3(x2)		
			1.474(x2)		114.0(x2)		
Si	N	-1	1.454(x2)	1.712	110.2(x2)	122.4	-18.6
			1.463(x4)		117.5(x4)		
P	N	+1	1.360(x2)	1.637	104.4(x2)	121.1	+983.7
			1.358(x4)		116.6(x4)		
S	N	+3	1.419(x2)	1.742	101.2(x2)	134.8	+4595.5
			1.399(x4)		117.9(x4)		
Si	C	-2	1.501	1.618	120.2	180.0	+602.4
P	C	0	1.360	1.511	115.2	180.0	+621.9
S	B	+1	1.347	1.876	114.2	180.0	+1387.0

Table 3.6.2. ΔH_f^θ and geometries for $(H_3M)_2Y^{+n}$ species.

M\Y	F	O	N	C	B
Be	+37.1	+19.6			
B	+7.5	-90.5	-74.0	+44.6	
C	-12.7	-177.9	-146.2	+37.8	-16.8
N	-32.6	-697.2	-1064.3	-102.3	-1304.1
O		-2564.8	a	a	a

M\Y	F	O	N	C	B
Si	+24.5	+4.7	-4.2	34.1	b
P	+53.9	-33.9	-87.9	56.1	b
S		-218.5	-1332.2	a	+9.1

Table 3.6.3. Force constants in Nm^{-1} for $(\text{H}_3\text{M})_2\text{Y}^{+n}$.

M\Y	F	O	N	C	B
Be	0.0	0.0			
B	0.0	52.2	43.6	0.0	
C	2.0	113.4	108.3	0.0	10.3
N	6.2	257.7	330.9	86.6	360.4
O		447.2	a	a	a

M\Y	F	O	N	C	B
Si	0.0	0.0	10.2	0.0	b
P	0.0	16.8	85.7	0.0	b
S		76.4	267.3	a	0.0

Table 3.6.3. Inversion barriers in kJmol^{-1} for $(\text{H}_3\text{M})_2\text{Y}^{+n}$.

a Dissociates, see Table 3.6.1. b Rearranges, see Table 3.6.1.

has an equilibrium geometry of C_s as the tops are staggered.

The MY distance is again longer for $(F_3M)_2Y$ species than for the respective $(H_3M)_2Y$ systems. The YMX_3 tops have exact C_{3v} symmetry when $MYM=180^\circ$, however when $MYM < 180^\circ$ the tops are at best in point group C_s with their departure from C_{3v} becoming greater as the MYM angle decreases. This will be described more fully in Section VIII.

When MYM is bent the minimum $M \cdots M$ close contact distance decreases as $Be > B > C > N$: however none appear close to the sum of the non-bonded intramolecular atomic radii [22], and so electronic and not steric factors should dominate the detailed structure of these molecules.

The inversion barriers and force constants for the E' skeletal bending vibration have been tabulated together, and can be found in Table 3.6.3. From this we see that a pattern emerges when M (a first row atom) varies with constant Y; namely the more electronegative that MH_3 becomes, the smaller the MYM angle: but when Y varies with constant MH_3 a complex behavioural pattern results. This generalisation holds when M is a second row atom, except for the pairs $(SiH_3)_2F^+$ and $(PH_3)_2F^{+3}$, and $(SiH_3)_2C^{-2}$ and $(PH_3)_2C$, which are all calculated to be linear: although as noted before in the carbenes, the force constant for the silicon species lies between the values for beryllium and boron, and therefore may be correct for silicon and wrong for phosphorous.

The system is straightforward when Y is constant as the HOMO-LUMO gap based on the simple model [1] is between the $1\pi_u$ and $2\sigma_g^+$ orbitals of the linear skeleton. The more electronegative that MH_3 becomes so its orbitals, in particular σ orbitals which contribute to the M_2Y skeleton, become more tightly bound. As a result of this, $2\sigma_g^+$ becomes more tightly bound, but the $1\pi_u$ is essentially unaltered as Y is unaltered, thus the HOMO-LUMO gap decreases and so the Second-Order Jahn Teller effect's perturbative mechanism becomes active. The force constant of π_u symmetry becomes more negative or less positive and as a result distorts the structure.

However with M constant and Y varying, two factors must be taken into consideration. As Y becomes more electronegative its orbitals become more tightly bound relative to those of M. If the sp gap in Y was constant, then as the electronegativity of Y increased the HOMO-LUMO gap would also increase and so lead to a force constant for the bend which was more positive or less negative. But the sp gap is not constant - it does in fact increase moving from B(5.7eV) \rightarrow F(26.7eV) [23]. As this gap increases then for a given mean atomic orbital binding energy (fixed electronegativity), the HOMO-LUMO gap would decrease and lead to an increased tendency for the skeleton to bend. This variation in Y leads to two opposing factors for the force constant and since neither varies uniformly across a row a complex pattern is observed for the behaviour of the force constant. However, in the first row the two factors vary monotonically, and as a result some combinations of M_2Y will have the sp gap predominating, whilst others will have the binding energies of Y with respect to M as the

M	Y	n	d(M-F)(Å)	d(M-Y)(Å)	<(FMY)(°)	<(MYM)(°)	ΔH_f^θ (kJmol ⁻¹)
B	F	-1	1.373	1.462	106.9	180.0	-2862.3
C	F	+1	1.320	1.492	103.9	180.0	-451.0
B	O	-2	1.403(x2)	1.437	107.7(x2)	137.8	-2501.8
			1.399(x4)		113.7(x4)		
C	O	0	1.341(x2)	1.406	106.2(x2)	130.7	-1496.5
			1.345(x4)		110.0(x4)		
N	O	+2	1.322(x2)	1.420	104.2(x2)	127.5	+2891.5
			1.321(x4)		110.7(x4)		
C	N	-1	1.361(x2)	1.420	108.8(x2)	122.7	-1503.5
			1.371(x4)		116.2(x4)		
C	C	-2	1.410	1.357	118.3	180.0	-795.0
C	B	-3	1.400(x2)	1.538	114.3(x2)	117.5	271.4
			1.472(x4)		124.6(x4)		

Table 3.6.4. ΔH_f^θ and geometries for $(F_3M)_2Y^{+n}$ species.

M	Y	n	$\Delta\Delta H_f^\theta$ (kJmol ⁻¹)	f(Nm ⁻¹)
B	F	-1	0.0	30.6
C	F	+1	0.0	17.0
B	O	-2	22.6	-57.7
C	O	0	54.9	-109.3
N	O	+2	162.9	-442.9
C	N	-1	92.4	-117.5
C	C	-2	0.0	39.7
C	B	-3	88.5	-90.2

Table 3.6.5. Energy differences and force constants for $(F_3M)_2Y^{+n}$.

salient feature.

For all $(MH_3)_2Y^{+n}$ systems the inversion barrier inversely reflects the ordering of the force constant, thus for example in $(NH_3)_2Y^{+n}$, the force constants all become more negative in the order of Y: $F > C > O > N > B$, and the inversion barriers increase in the order of Y: $F < C < O < N < B$. Hence the more negative the force constant, within a series, the larger the inversion barrier.

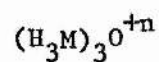
We can see this mathematically, by noting that a classical harmonic-quartic potential function has the form,

$$V(q) = aq^4 - bq^2$$

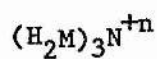
where the force constant is $-2b$ at linearity and leads, subsequently, to an inversion barrier of $b^2/4a$. Therefore, if the coefficient 'a' does not vary drastically, then the inversion barriers will change monotonically in the reverse sense to the change in the force constants.

A limited number of perfluoro species, $(MF_3)_2Y^{+n}$, were studied and the same patterns in force constant behaviour transpire as in the $(MH_3)_2Y^{+n}$ molecules. However, the agreement between the force constants and energy barriers is not quite fully borne out, and Table 3.6.5 shows that in the $(CF_3)_2Y^{+n}$ series the correlation between the force constant and inversion barrier has been reversed for Y = B and O. This is the only reversal found and overall the agreement is very good.

M	n	d(M-Y)/Å	d(M..M)/Å	d(M-H)/Å	<(MYM)/°	<(HMY)/°	$\Delta H_f^\ominus / \text{kJmol}^{-1}$
$(\text{H}_3\text{M})_3\text{N}^{+n}$							
B	-3	1.513	2.583	1.234(x3)	117.2	118.4(x3)	786.3
				1.225(x6)		114.4(x6)	
C	0	1.464	2.484	1.118(x3)	116.1	113.5(x3)	-11.6
				1.114(x6)		110.3(x6)	
N	+3	1.447	2.415	1.054(x3)	113.7	118.1(x3)	3994.9
				1.062(x6)		109.5(x6)	
Si	0	1.757	3.043	1.441(x3)	120.0	109.3(x9)	-131.5
				1.444(x6)			
P	+3	1.681	2.912	1.385(x3)	120.0	110.4(x3)	3720.4
				1.390(x6)		109.4(x6)	
$(\text{H}_3\text{M})_3\text{P}^{+n}$							
Be	-6	2.503	4.335	1.525(x3)	120.0	119.5(x3)	4733.7
				1.534(x3)		118.0(x3)	
				1.532(x3)		118.4(x3)	
B	-3	1.880	3.071	1.199(x3)	109.5	117.1(x3)	583.0
				1.201(x6)		111.2(x6)	
C	0	1.762	2.829	1.104(x3)	106.8	114.2(x3)	-201.7
				1.105(x6)		108.2(x6)	
N	+3	1.768	2.835	1.040(x3)	106.6	114.3(x3)	3310.7
				1.035(x3)		120.0(x3)	
				1.046(x3)		107.3(x3)	
$(\text{H}_3\text{M})_3\text{C}^{+n}$							
B	-4	1.522	2.688	1.248(x3)	120.0	119.8(x3)	2384.1
				1.284(x6)		120.5(x6)	
C	-1	1.465	2.537	1.117(x3)	120.0	113.6(x3)	-50.4
				1.126(x6)		114.2(x6)	
N	+2	1.444	2.501	1.030(x3)	120.0	112.3(x3)	1930.9



Be	-5	1.787	3.095	1.034(x6)	111.7(x6)
				1.571(x3) 120.0	119.2(x3) 2820.7
				1.521(x6)	116.4(x6)
B	-2	1.484	2.570	1.197(x3) 120.0	111.8(x3) -337.8
				1.202(x6)	110.9(x6)
C	+1	1.467	2.541	1.112(x3) 120.0	109.0(x3) 618.1
				1.113(x6)	101.2(x6)



Be	-3	1.640	2.841	1.407(x6) 120.0	126.4(x6) 570.8
B	0	1.436	2.487	1.167(x6) 120.0	120.5(x6) -184.9
C	+3	1.438	2.491	1.114(x6) 120.0	120.1(x6) 4271.2

Table 3.7.1. ΔH_f^θ and geometries for $(\text{H}_n\text{M})_3\text{Y}^{+n}$ species.

The results presented in this section, once more, provide solid support for the model, concerning the stereochemical inactivity of lone pairs in the presence of electron donor ligands and is a consequence of a positive force constant rather than of (p-d) π bonding.

VII. Amines $(H_3M)_3Y^{+n}$, $(H_2M)_3Y^{+n}$, $H_2NMH_3^{+n}$ and $HN(MH_3)_2^{+n}$.

The equilibrium energies and structures for the $(H_3M)_3Y^{+n}$ and $(H_2M)_3Y^{+n}$ species are listed in Table 3.7.1 and the fate of the unbound ions can be found in Table 3.7.2. As with the carbenes and ethers, the amines show the same structural trends: namely that for a constant Y in $(H_3M)_3Y^{+n}$, the M_3Y moiety is planar only for the least electronegative substituents MH_3 .

For first row MH_3 there is no skeletal planarity when $Y = N$, but only for second row $MH_3 = SiH_3$ and PH_3^+ . Planarity when $Y = P$ occurs for only $MH_3 = BeH_3^{-2}$, and when $Y = C$ or O , all the skeletons studied were found to be planar. As a consequence, systematic trends can be found when M varies with constant Y, but not conversely. The reason for this was explained in the last section, and here, an exactly analogous argument applies.

The M_3Y part of the $(H_3M)_3Y$ molecules when planar have local D_{3h} symmetry, whereas the whole molecule has C_{3h} symmetry. Non-planar M_3Y has C_{3v} symmetry with the overall molecular symmetry reduced to C_3 . Species which agree to the formula $(H_2M)_3Y^{+n}$, $M = Be^-$, B , C^+ , have totally planar structures at equilibrium with D_{3h} symmetry: the

Ion.	Products.
$(\text{H}_3\text{Be})_3\text{N}^{-6}$	$(\text{H}_2\text{Be})_3\text{N}^{-3} + 3\text{H}^-$
$(\text{H}_3\text{O})_3\text{N}^{+6}$	$(\text{H}_2\text{O})_3\text{N}^{+3} + 3\text{H}^+$
$(\text{H}_3\text{S})_3\text{N}^{+6}$	$(\text{H}_2\text{S})_3\text{N}^{+3} + 3\text{H}^+$
$(\text{H}_3\text{O})_3\text{P}^{+6}$	$\text{P}^{+3} + 3\text{H}_3\text{O}^+$

Table 3.7.2. Fate of unstable ions.

vibration studied for the M_3Y portion when the overall symmetry is D_{3h} was a_2'' , and when C_{3h} , a'' . Planar $(H_3M)_3Y^{+n}$, $Y = C, N, O$; $(H_2M)_3N^{+n}$ and non-planar $(H_3M)_3N^{+n}$, in addition, all have non-bonded distances close to their limiting values [22].

The local symmetry of the $H_2NMH_3^{+n}$ species is C_{2v} when planar and C_s when bent, and hence the Glidewell approach [1] has to be modified to take into account this lowering of symmetry. For nitrogen two orbitals, one of a_1 symmetry, which comprises 2s and 2p combinations and is directed along M-N, and a b_1 orbital which is the pure $2p_x$ orbital normal to the H_2NM plane are used. The former a_1 interacts in and out-of-phase with the single σ orbital localised on M and points along M-N, to give rise to a bonding and anti-bonding combination, $1a_1$ and $2a_1$ respectively: hence the electronic configuration for M-N is $(1a_1)^2(1b_1)^2(2a_1)^0$. The HOMO is $1b_1$, which was formally the nitrogen lone pair, and the LUMO, $2a_1$ - anti-bonding M-N σ orbital. The critical gap becomes smaller as the M σ orbital becomes more tightly bound in relation to the nitrogen orbitals, and so a distortion occurs for ligands of low electronegativity as expected [1].

Unfortunately, however, this is not borne out in the series $H_2NMH_3^{+n}$, $M = Be^{-2}, B^-, C, N^+$, where the sums of the angles at nitrogen are respectively: 311.3, 316.9, 325.1 and 325.4°; whilst the corresponding inversion barriers are: 39.5, 109.8, 330.8 and 41.6 $kJmol^{-1}$.

$MH_3 \backslash Y$	$CH_2 / ^\circ$	$NH / ^\circ$	$O / ^\circ$
BeH_3^{-2}	143.8	155.6	180.0
BH_3^-	124.7	121.6	126.1
CH_3	116.8	117.6	119.9
NH_3^+	114.3	117.9	121.8
OH_3^{+2}	a	125.8	128.6
AlH_3^-	125.7	135.9	180.0
SiH_3	116.4	127.4	180.0
PH_3^+	117.8	129.5	137.9
SH_3^{+2}	a	130.1	140.0

a = Dissociates to CH_2^{+2} and $2MH_3^+$.

Table 3.7.3. Bond angles for CH_2 , NH and O bridged MH_3 species.

The species $\text{HN}(\text{MH}_3)_2^{+n}$ behave as expected and the MNM angle and the sum of the valence angles at nitrogen (Table 3.7.3.) both decrease as the MH_3 electronegativity increases. For second row M the skeletons are all planar except for $\text{M} = \text{S}$, and with M an atom of the first row, planarity is observed only when $\text{M} = \text{Be}$.

The force constants for the out-of-plane 'umbrella' bending mode along with the inversion barriers for the amines are laid out in Table 3.7.4. For $(\text{MH}_3)_3\text{Y}^{+n}$ species, two generalisations can be made. Firstly; that for constant Y, and M a first row atom, the force constant steadily becomes more negative or less positive as the electronegativity of MH_3 increases. However when $\text{M} = \text{Si}$ and P ; this pair are found to be anomalous, in that the anticipated decrease in the force constant because the electronegativity has increased is not fulfilled, and may be, as mentioned earlier for the ethers, due to an inadequate parameterisation for these elements.

Secondly, with M constant and Y varying, the force constants behave in an unpredictable manner. This, again, has been discussed previously, and both patterns can be explained within the framework of the SOJT effect.

The $(\text{H}_2\text{M})_3\text{Y}^{+n}$ species each carry a vacant $p\pi$ orbital formally localised on each M and is normal to the molecular plane. As a consequence of this they are similar to the class B carbenes discussed in Section V. The more electronegative that MH_2 becomes so the greater the extent of the $p\pi - p\pi$ delocalisation, and this results in

	M	n	f/Nm^{-1}	$\langle(MYM)/^\circ$	$(\Delta H_f^\ominus)/kJmol^{-1}$
$(H_3M)_3N^{+n}$	B	-3	-160.7	117.2	2.0
	C	0	-578.6	116.1	7.0
	N	+3	-2145.0	113.7	8.4
	Si	0	584.5	120.0	0.0
	P	+3	1127.6	120.0	0.0
$(H_3M)_3P^{+n}$	Be	-6	146.5	120.0	0.0
	B	-3	-776.1	109.5	39.2
	C	0	-899.8	106.8	47.2
	N	+3	-5637.0	106.6	176.7
$(H_3M)_3C^{+n}$	B	-4	1414.6	120.0	0.0
	C	-1	1226.2	120.0	0.0
	N	+2	482.5	120.0	0.0
$(H_3M)_3O^{+n}$	Be	-5	941.6	120.0	0.0
	B	-2	278.5	120.0	0.0
	C	+1	210.8	120.0	0.0
$(H_2M)_3N^{+n}$	Be	-3	405.5	120.0	0.0
	B	0	1268.1	120.0	0.0
	C	+3	3417.6	120.0	0.0

Table 3.7.4. Force constants and energy barriers for MH_3 species.

two features. Firstly the M-Y bond order increases with the increasing electronegativity of the ligand and secondly the a_2'' force constant becomes more positive. Consistent with this is the shorter M-N bond length found in $(MH_2)_3N^{+n}$ species than in $(MH_3)_3N^{+n}$ when M= B or C.

The inversion barriers, again within a series, reflect the magnitude of the force constant, and are necessarily zero for species which have a positive force constant.

The species, $HN(MH_3)_2^{+n}$, complete the series $Y(MH_3)_2^{+n}$ where Y= CH_2 , NH and O; and lie between $O(MH_3)_2^{+n}$ and $H_2C(MH_3)_2^{+n}$, whose structures, in the case of the former, were presented in the last section, and in the latter, in a publication by Glidewell and Liles [24]. Table 3.7.3 lists the $\langle MYM \rangle$ angles for the species $(MH_3)_2Y^{+n}$, Y= O, NH, CH_2 and shows that generally for a constant MH_3 ligand the $\langle MYM \rangle$ angles follow the order: $CH_2 < NH < O$, for which, there is experimental evidence when M= Si [24]. When the ligand electronegativity increases with constant Y, a decrease in the $\langle MYM \rangle$ angle is observed.

There exists experimental data for the $Y(MH_3)_2^{+n}$ systems when M= C and Si for all Y= CH_2 , NH and O, and their values are presented below with their respective references in square brackets.

M\Y	$CH_2/^o$	NH/ o	O/ o
C	112.4(2) [25]	111.8(6) [26]	111.5(15) [27]
Si	114.4 [28]	127.7 [29]	142.2 [30]

By comparing the experimentally observed and calculated values we find that when $M = C$, the MYM angles are, in each case, calculated to be a bit too large. However when $M = Si$, the angles compare very well, except when $Y = O$. This is due though, to a minute bump in the bending potential function at linearity [31] and can be reproduced by computational techniques only by including d-orbitals on oxygen which act as polarisation functions [32,33]: silicon d-orbitals are not required. Similarly the planarity of the Si_3N skeleton in some molecules requires d-orbitals on the nitrogen in order to reproduce the observed behaviour [33]: once more recourse to d-orbitals on silicon is not necessary.

VIII. Are MX_3 Groups Really of C_{3v} Symmetry?

When molecular structures are determined by either electron diffraction or microwave techniques it is usual, if MX_3 groups are present, to fix them in a rigid C_{3v} framework alleviated only by a tilt variable, which is the angle between the MX_3 principal axis and the M-Y vector.

X_3MYZ species, for example, will only have exact C_{3v} symmetry if the YZ fragment also belongs to this group, or a higher group of which C_{3v} is a sub-group. If YZ has less than three symmetry planes then the MX_3 moiety will be reduced to C_s , and if YZ has none then the symmetry is reduced still further to C_1 . In addition if YZ has only C_3 symmetry then that is the symmetry of MX_3 too. This results because in most cases the M-X distances are all different -- see Table

3.6.2 for example.

There always exists a vector from any point P on which the substituents X are equidistant, and with which the PX vectors make equal angles. However this vector may not pass through the atom M, and only when MX_3 has C_{3v} symmetry is the vector coincident with the M-Y bond. If MX_3 has only C_s symmetry this vector does not pass through M but cuts the MY vector at some other point. With no symmetry for MX_3 the vector is skew to the MY vector and hence does not pass through M or intersect MY.

The number of internal variables required to describe an MX_3 group is eight - a ninth external variable, the tilt angle, defines the MX_3 orientation relative to YZ. We define the internal variables in the following manner. The three ligands X_i ($i = 1, 2, 3$) lie on a circle, the base of which is a right circular cone and the new vector is now the cone axis. The PX_i vectors all lie on the cone's surface; and if M is positioned on the origin with MY taken as the positive x direction and the ligand X_1 , which is chosen to be the unique X in C_s symmetry specified to lie in the xy plane with y positive, then the right handed axis is defined.

Two angular variables, a_1 and a_2 , specify the orientation of the cone axis - in our case these are the angles between the projections of the aforementioned axis onto the xy and xz planes respectively. Furthermore the x axis is positive when looking to the origin from +z or +y respectively and so the rotation from +x is the clockwise projection.

A further pair of variables, d_1 and a_3 , are used to locate the cone axis, the former being the perpendicular distance of the conical axis from M to a point Q, which is defined as positive if the foot of the normal to the cone axis is positive in y; and the latter being the angle between the normal projection onto the yz plane. The +y axis is again positively defined if the projection from +y is clockwise when viewed from +x to the origin. In order to define the position and radius of the cone circle on which the X_1 lie, two more variables are required. The first of these, d_2 , is the distance from the X_1 to Q and is in effect the idealised bond length in the new system, and the other is a_4 , which is the external angle at Q between the axis of the cone and the QX_1 vectors.

To define totally the system a final two angular variables, a_5 and a_6 , are needed and are the angles the centre of the $X_1X_2X_3$ circle subtends by X_1X_2 and X_1X_3 . These are the torsional angles of X_2 and X_3 . Where a plane of symmetry is present the a_2 and a_3 are zero, and $a_5 = -a_6$. Three fold rotational symmetry renders all of a_1, a_2, a_3 and d_1 zero.

The geometric data of Table 3.6.2 - that for the ether geometries - has been put into this alternative description and are listed in Table 3.8.1. The a_2 and a_3 angles are zero unless stated to the contrary, and similarly $a_5 = -a_6$; also the orientation of the two cone axes has been made to be greater than the $\angle MYM$ angle, which has been catalogued alongside for comparison.

Compound	$a_1(^{\circ})$	$a_4(^{\circ})$	$\pm a_5(^{\circ})$	$d_1(\text{\AA})$	$d_2(\text{\AA})$	$\langle \text{MYM} (^{\circ}) \rangle$
$(\text{CH}_3)_2\text{F}^+$	0.74	107.34	119.94	-0.009	1.113	153.1
$(\text{NH}_3)_2\text{F}^-$	3.01	106.01	119.73	-0.042	1.081	150.9
$(\text{BH}_3)_2\text{O}^{-2}$	4.33	113.20	119.74	-0.075	1.216	126.1
$(\text{CH}_3)_2\text{O}$	3.58	110.70	120.10	-0.048	1.116	119.9
$(\text{NH}_3)_2\text{O}^{+2}$	6.34	110.42	119.30	-0.092	1.051	121.8
$(\text{OH}_3)_2\text{O}^{+4}$	6.17	107.17	131.52	+0.437	1.250	128.6
$(\text{BH}_3)_2\text{N}^{-3}$	6.93	118.23	119.88	-0.139	1.266	126.9
$(\text{CH}_3)_2\text{N}^-$	5.03	114.21	120.79	-0.072	1.131	117.9
$(\text{NH}_3)_2\text{N}^+$	8.01	111.46	120.02	-0.110	1.030	118.5
$(\text{NH}_3)_2\text{C}$	9.07	112.74	120.99	-0.112	1.029	122.4
$(\text{CH}_3)_2\text{B}^{-3}$	7.18	122.99	120.88	-0.115	1.222	133.3
$(\text{NH}_3)_2\text{B}^-$	13.07	116.29	123.28	-0.171	1.046	117.4
$(\text{PH}_3)_2\text{O}^{+2}$	4.75	107.68	119.88	-0.077	1.378	137.9
$(\text{SH}_3)_2\text{O}^{+4}$ a	6.73	106.74	a	-0.202	1.506	140.0
$(\text{SiH}_3)_2\text{N}^-$	5.03	114.82	119.81	-0.101	1.457	122.4
$(\text{PH}_3)_2\text{N}^+$	8.22	111.80	120.31	-0.149	1.350	121.1
$(\text{SH}_3)_2\text{N}^{+3}$	11.34	110.97	119.21	-0.223	1.388	134.8
$(\text{BF}_3)_2\text{O}^{-2}$	4.01	111.52	119.79	-0.074	1.398	137.8
$(\text{CF}_3)_2\text{O}$	3.21	109.29	120.04	-0.047	1.343	130.7
$(\text{NF}_3)_2\text{O}^{+2}$	4.36	108.36	120.09	-0.064	1.320	127.5
$(\text{CF}_3)_2\text{N}^-$	5.09	113.49	120.15	-0.091	1.365	122.7
$(\text{CF}_3)_2\text{B}^{-3}$	7.95	120.63	120.95	-0.151	1.440	117.5

Overall symmetry of H_3SO is C_1 : $a_2=0.76^{\circ}$, $a_3=-4.77^{\circ}$, $a_5=-106.76^{\circ}$, $a_6=+139.85^{\circ}$.

Table 3.8.1.

The calculation of the various a_n and d_n was undertaken with a program specially written for the purpose by D.C. Liles [34].

The overall symmetry when MYM is linear for $(X_3M)_2Y$ is D_{3h} or D_{3d} , and in each of the YMX_3 groups, the MX_3 axis is coincident with MY. The MX_3 groups retain their C_s symmetry when MYM is non-linear, except for $(H_3S)_2O^{+4}$. The a_1 angle, which is synonymous to the tilt angle in this symmetry, is small for species having large MYM angles, e.g. $(H_3C)_2F^+$ and $(H_3N)_2F^-$; but can approach a value of 10° for systems which have a small MYM angle. This value represents the torsional repulsion of the four close X atoms in $(X_3M)_2Y$ and hence in some cases may be important in deciding the overall molecular structure.

The d_1 distance only approaches zero for the $(H_3C)_2F^+$ species which has a large $\angle CFC$ angle: other cases show that the cone axis can be as far as 0.44 Å away from M.

The $\pm a_5$ angles are rather surprising in that in most examples they differ only marginally from $\pm 120^\circ$, which indicates that they have almost exact C_{3v} symmetry about the axis displaced from M, although the MX_3 symmetry is no higher than C_s .

IX. Sixteen Electron Systems.

Sixteen electron molecules , CO_2 , CS_2 , CN_2^{-2} , N_3^- , NO_2^+ and BO_2^- have been studied in the Walsh-Mulliken model by Nemes and he obtained a ' casual ' relationship between the electronegativity and the bending force constant with a regression coefficient of 0.846 [35].

As a result of an enquiry [36] we calculated the π_u bending force constant for the above named species with MNDO and found that it was large and positive.

The MNDO calculations deal with isolated molecules in the gas phase and Nemes' data are taken mainly from the solid state and as a result the two are not really comparable. The calculations reveal that the HOMOS are all of π_g symmetry with the LUMOS in all cases π_u , bar BO_2^- where it is σ_g^+ . The direct product of $\pi_g \times \pi_u$ in $D_{\infty h}$ yields \sum_u^+ , \sum_u^- and Δ_u , and $\pi_g \times \sigma_g^+$ gives π_g . There are no Δ vibrations of a linear triatomic molecule and so the only vibration left is of \sum_u^+ and this is the asymmetric stretch and not a bending mode at all. The bending mode as we have seen before has π_u symmetry and since the direct products of the HOMOS and LUMOS do not generate it, the species all remain linear. This is coupled with very large HOMO-LUMO gaps which too would yield an unperturbed skeleton.

X. Conclusions.

The model which was proposed previously [1], and which was outlined in Section I, has therefore been shown to be correct, and only minor modifications are required in order to account for the observations from the calculations.

Recently a paper appeared on the microwave spectrum of 2,5-dihydrothiophen S,S-dioxide [37] and showed that the ring was easily deformed with a vibration of about 1.2 kJmol^{-1} : this too is an example of a weak SOJT distortion, so that the carbenes, ethers and amines are by no means the only species which exhibit this type of behaviour.

Chapter Three.

Bibliography.

1. C. Glidewell. Inorg Chim Acta 29 L283 (1978).
2. C. Glidewell and D.C. Liles. Acta Cryst B34 124 (1978).
- 3a. K. Hedberg. J.A.C.S. 77 6491 (1955).
- 3b. B. Beagley and A.R. Conrad. Trans Farad Soc 66 2740 (1970).
4. R.G. Pearson. Symmetry Rules For Chemical Reactions Wiley-Interscience (1976).
5. R.G. Pearson. J.A.C.S. 91 4947 (1969).
- 6a. E.A.V. Ebsworth. Organometallic Compounds of the Group IV Elements A.G. MacDonald (Ed.) Dekker, New York 1,1 (1968).
- 6b. D.W.J. Cruickshank. J Chem Soc 5486 (1961).
7. C. Glidewell. J Mol Struct 65 231 (1980).
8. C. Glidewell. J Mol Struct 67 121 (1980)..
9. J.A. Salthouse and M.J. Ware. Point Group Character Tables and Related Data. Cambridge University Press (1972).
10. J.C.D. Brand, J.C. Speakman and J.K. Tyler. Molecular Structure - The Physical Approach 2nd. Edition, p338 Edward Arnold (1975).
11. NACFLIB:1279/189:Mk5:OCT75. Adapted from Algorithm 318 by J. Boothroyd (C.A.C.M. 10 810 (1967)).
12. M.J.S. Dewar and W. Thiel. J.A.C.S. 99 4899 (1977).
13. W. Thiel. QCPE 11 353 (1978).
14. W.W. Schoeller. Chem Comm 124 (1980).
15. L. Pauling. Chem Comm 688 (1980).

16. G. Herzberg. Molecular Spectra and Molecular Structure, Electronic Spectra of Polyatomic Molecules. D. Van Nostrand, Princeton, NJ, (1966).
17. F.X. Powell and D.R. Lide Jr. J Chem Phys 45 1067 (1966).
18. C.W. Matthews. Can J Phys 45 2355 (1967).
19. A.D. Walsh. J Chem Soc 2266 (1953).
20. R.H. Hughes. J Chem Phys 24 131 (1956).
21. D. Kivelson. J Chem Phys 22 904 (1954).
22. C. Glidewell. Inorg Chim Acta 12 219 (1975).
23. R.E. Ballard. Photoelectron Spectroscopy and Molecular Orbital Theory. Hiliger, Bristol (1978).
24. C. Glidewell and D.C. Liles. J Orgmet Chem in press.
25. D.R. Lide. J Chem Phys 33 1514 (1960).
26. B. Beagley and T.G. Hewitt. Trans Farad Soc 64 2561 (1968).
27. K. Kimura and M. Kubo. J Chem Phys 30 151 (1959).
28. A. Almennigen, H.M. Seip and R. Seip. Acta Chem Scand 24 1697 (1970).
29. D.W.H. Rankin, A.G. Robiette, G.M. Sheldrick, W.S. Sheldrick, R.J. Aylett, I.A. Ellis and J.J. Monaghan. J Chem Soc (A) 1224 (1969).
30. M.J. Barrow, E.A.V. Ebsworth and M.M. Harding. Acta Cryst B35 2093 (1979).
31. J.R. Durig, M.J. Flanagan and V.F. Kalasinsky. J Chem Phys 66 2775 (1977).
32. C.A. Ernst, A.L. Allred, M.A. Ratner, M.D. Newton, G.V. Gibbs, J.W. Moscovitz and S. Topiol. Chem Phys Lett 81 424 (1981).
33. C. Glidewell and C. Thomson. J Comp Chem in press.
34. D.C. Liles. Personal communication.

35. L. Nemes. J Mol Struct 19 807 (1973).
36. L. Nemes. Personal communication.
37. J.L. Alonso and D.G. Lister. Chem Comm 93 (1982).

Chapter Four.

Silyl Cyclopentadienes.

I. Introduction.

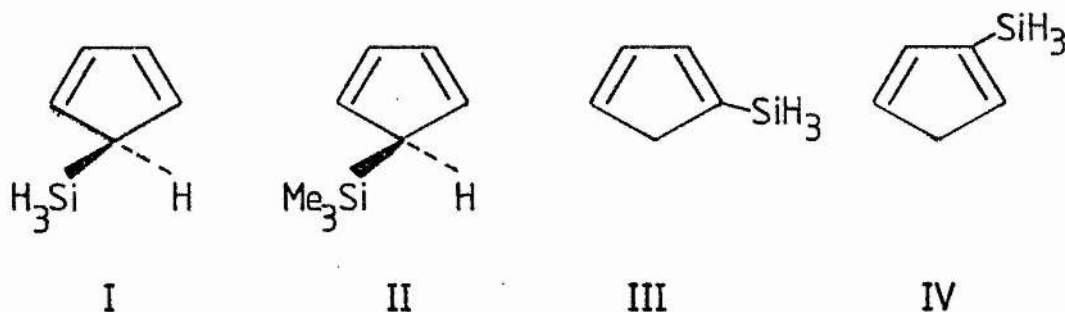
The structure of the cyclopentadiene ring in $(\eta^5\text{-C}_5\text{H}_5)\text{SiH}_3$ (I) and $(\eta^5\text{-C}_5\text{H}_5)\text{SiMe}_3$ (II) is somewhat enigmatic in that in the former Bentham and Rankin [1] found a planar monohapto ring within the assumption of overall C_5 molecular symmetry, but in the latter Veniaminov et al [2] reported a non-planar ring with the carbon bonded to the trimethylsilyl group, relieving the ring planarity by some $22 \pm 4^\circ$ in such a way that the silicon atom is brought closer to the centre of the ring, henceforth designated 'cis'.

This rather surprising discrepancy is mirrored in the structures of $(\eta^5\text{-C}_5\text{H}_5)\text{GeH}_3$ and $(\eta^5\text{-C}_5\text{H}_5)\text{GeMe}_3$ where once again the former has a planar ring in the gas phase [3] and a slightly bent ring with an envelope angle of $4.1 \pm 0.6^\circ$ in the solid [3], where it is of course subject to intermolecular forces, and the latter which has a non-planar ring with a folding angle of 156° in the gas phase [4].

In an attempt to resolve this controversy, ab-initio calculations have appeared concerning the energies of the various conformers of $5\text{-SiH}_3\text{C}_5\text{H}_5$ [5] and showed that the 'cis' conformation was more stable than the planar form [6] which is contrary to the experimental findings [1]. In that study Cradock et al [6] held all the geometric data constant except for the ring fold angle. In contrast however

MNDO calculations using fully optimised geometries to which this chapter refers indicate planar rings for both derivatives.

Silyl and germyl cyclopentadienes belong to a class of molecules which exhibit fluxional behaviour in solution [7-10], that is to say the silyl or germyl group migrates round all the five carbon atoms of the ring, and whilst proton n.m.r. has been unable to distinguish whether the fluxional exchange proceeds via a 1,2 or 1,3 shift mechanism, ^{13}C n.m.r. shows a definite distinction between them and demonstrates clearly that the fluxionality occurs by way of 1,2 shifts [10]. In addition it has been found that rapid prototropic rearrangement takes place in solution for 5- $\text{SiH}_3\text{C}_5\text{H}_5$ (I) to form 1- $\text{SiH}_3\text{C}_5\text{H}_5$ (III) and 2- $\text{SiH}_3\text{C}_5\text{H}_5$ (IV) most likely by a sequence of 1,2 hydrogen shifts [10].



II. Method.

The calculations were all performed with MNDO [11] operating on the University's VAX 11/780 computer. No geometric assumptions or constraints of any sort whatsoever were imposed for the computation of the equilibrium structures of the h^5 species. However local C_{5v} symmetry on the C_5H_5 ring in the h^5 ('piano stool') species was

imposed, and although treated as a rigid entity the overall symmetry of these molecules is no more than C_s the barrier calculated by MNDO for the internal rotation of the two symmetric tops is less than 0.1 kJmol^{-1} : hence these molecules are better represented as non-rigid and as a result belong to a point group of order 30.

When the potential energy curves for the ring folding were studied the unique carbon atom C(5) was fixed in a series of positions in such a way that the ring dihedral angle θ varied by 5° increments on either side of 180° (planarity). The molecular energy was thus optimised with respect to the rest of the variables for each value of θ without further recourse to any other symmetry constraints.

The reaction coordinate for the pathway of the 1,2 and 1,3 shifts was chosen to be that distance between the migrating atom and its destination. All the geometric variables were then optimised with respect to a descending series of values of this coordinate; that is to say the distance between the migrating group and its final point became progressively shorter. However if the scan was approached in the opposite sense then the migrant group was inclined to be lost from the system entirely.

III. Geometries.

When the cyclopentadiene anion $C_5H_5^-$ is reacted with a molecular halide RX the initial products formed are either one of two structures both of which have one hydrogen atom per carbon. The first of these is the pentahapto ($h^5-C_5H_5$)R species in which the R group is bonded

symmetrically to the ring, hence the name 'piano stool'. The second is the monohapto species ($h^5-C_5H_5$)R shown in Figure 4.3.1 which is the experimentally found isomer for R=H, SiH₃ or SiMe₃.

<u>Molecule</u>	<u>Point Group</u>	<u>ΔH_f^θ kJmol⁻¹</u>
C ₅ H ₅	C _{2v}	133.9
1-SiH ₃ C ₅ H ₅	C _s	90.0
2-SiH ₃ C ₅ H ₅	C _s	90.9
5-SiH ₃ C ₅ H ₅	C _s	106.3
1-Me ₃ SiC ₅ H ₅	C _s	-216.3
2-Me ₃ SiC ₅ H ₅	C _s	-216.6
5-Me ₃ SiC ₅ H ₅	C _s	-197.1
1-MeC ₅ H ₅	C _s	90.3
2-MeC ₅ H ₅	C _s	90.4
5-MeC ₅ H ₅	C _s	115.5
($h^5-C_5H_5$)H	C _{5v}	632.2
($h^5-C_5H_5$)SiH ₃	see text	351.7
($h^5-C_5H_5$)SiMe ₃	see text	92.7

Table 4.3.1.

The point groups and molecular energies for C₅H₆; the 1,2 and 5 isomers of R C₅H₅, R=SiH₃, SiMe₃ and CH₃ and the 'piano stool' species ($h^5-C_5H_5$)R, R=H, SiH₃ and SiMe₃ are in Table 4.3.1 and the geometric data for ($h^5-C_5H_5$)SiH₃, ($h^5-C_5H_5$)SiMe₃ and the 'piano stool' molecules ($h^5-C_5H_5$)SiR₃, R=H, Me along with the observed geometries where available are gathered together in Table 4.3.2.

	5-H ₃ SiC ₅ H ₅		5-Me ₃ SiC ₅ H ₅	
	<u>Observed</u>	<u>Calculated</u>	<u>Observed</u>	<u>Calculated</u>
d(C(5)-Si)/Å	1.881(10)	1.845	1.90(1)	1.871
d(C(5)-C(1))/Å	1.500(13)	1.515	1.53(3)	1.515
d(C(1)-C(2))/Å	1.389(13)	1.364	1.40(2)	1.364
d(C(2)-C(3))/Å	1.436 c	1.473	1.40(2)	1.472
d(Si-H)/Å	a	1.438	-	-
d(Si-C)/Å	-	-	1.90(1)	1.859
d(C(5)-H)/Å	mean	1.111	1.11(2)	1.113
d(C(1)-H)/Å	d(C-H)	1.082	1.11(2)	1.082
d(C(2)-H)/Å	1.109(18)	1.082	1.11(2)	1.082
<(C(5)C(1)C(2))/°	112.0(10)	110.0	a	110.3
<(C(1)C(2)C(3))/°	107.9(6)	108.9	a	108.8
<(C(1)C(5)C(4))/°	100.3(15)	102.1	109 c	101.8
<(C(1)C(5)Si))/°	106.6(6)	112.1	109(3)	114.0
<(C(5)SiH)/°	a	111.5(x1) 109.7(x2)	-	-
<(C(5)SiC)/°	-	-	109.5 c	111.8(x1) 109.2(x2)

a=Not reported. b=Assumed equal. c=Fixed.

Table 4.3.2. Observed and calculated geometries for 5-H₃SiC₅H₅ and 5-Me₃SiC₅H₅.

In general the agreement between the observed [1] and calculated structures for (h⁻-C₅H₅)SiH₃ is good (see Table 4.3.2), and the only major discrepancies between them arise in the Si-C distance which is known to be calculated some 2-4% too short by MNDO (here it is 2%) and the C(2)-C(3) distance which was calculated to be 1.473 Å although

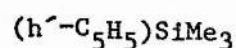
this distance was fixed in the experimental determination at 1.436 Å. However the structural analysis for the analogous ($\text{h}^{\text{'}}\text{-C}_5\text{H}_5$)GeH₃ system [3] is more exhaustive than that for ($\text{h}^{\text{'}}\text{-C}_5\text{H}_5$)SiH₃ and the C(2)-C(3) distance found in the germyl derivative was 1.468(22) Å. This value was not fixed and is essentially identical within experimental error to the calculated value for the silyl derivative.

However in total contrast the agreement between the observed and calculated structures for ($\text{h}^{\text{'}}\text{-C}_5\text{H}_5$)SiMe₃ is rather poor and is due almost certainly to the deductions which were drawn from the experimental electron diffraction data being incorrect because of the unjustified imposition of too many symmetry constraints. There are admittedly a large number of variables for ($\text{h}^{\text{'}}\text{-C}_5\text{H}_5$)SiMe₃, 63 in all, and although the fixing of the ring C-H distances and angles is justifiable the pertinent wrong assumptions made were -

- 1] The silicon atom was assumed to be rigorously tetrahedral;
- 2] The internal angle at C(5) was fixed at 109°, whereas in 5-MH₃C₅H₅, M=Si,Ge it is 100.3(2)°;
- and 3] Two of the three independent bond distances in the cyclopentadiene moiety were assumed to be equal which is certainly incorrect as they can differ by as much as 0.1 Å.

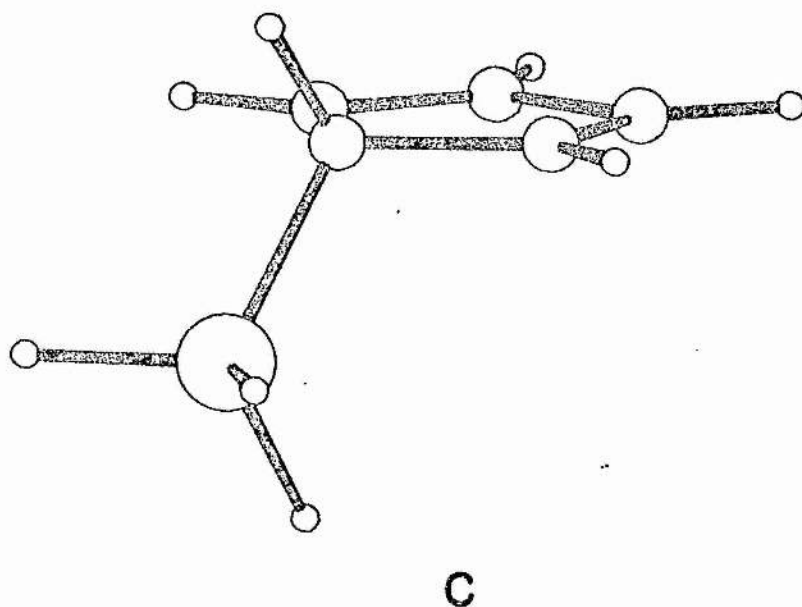
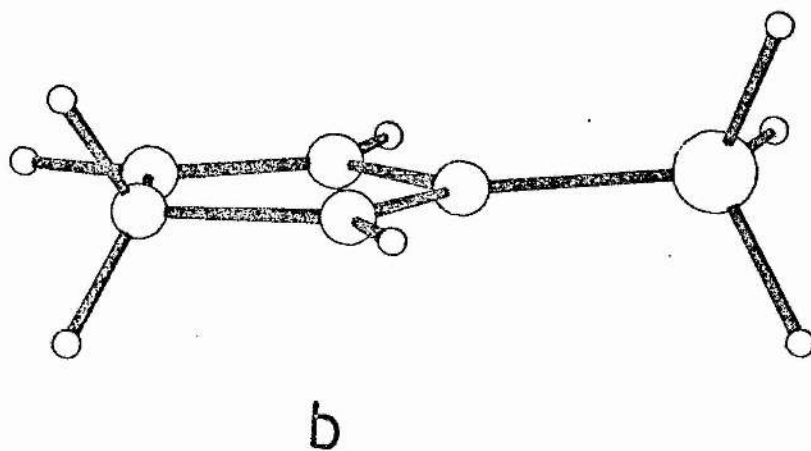
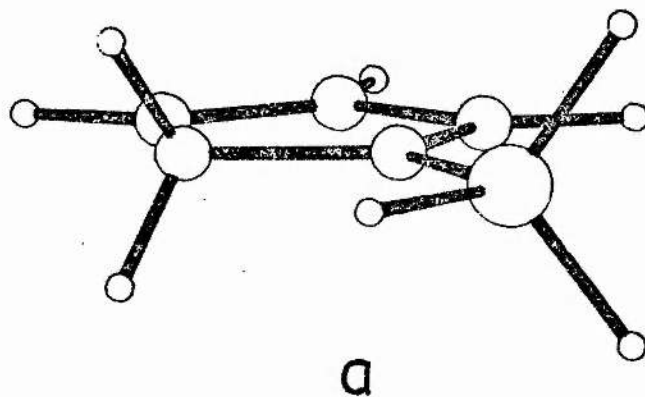
Therefore as a result of these assumptions listed above, and possibly others which were not specified but deal with the internal ring angles, Veniaminov et al [2] deduced that the C₅ ring was non-planar as they did also for the germyl analogue 5-GeH₃C₅H₅ [4].

$(h^{\sim}-C_5H_5)SiH_3$	1- $SiH_3C_5H_5$	2- $SiH_3C_5H_5$	5- $SiH_3C_5H_5$
$d(C(5)-C(1))/\text{\AA}$	1.526	1.522	1.515
$d(C(1)-C(2))/\text{\AA}$	1.365	1.364	1.364
$d(C(2)-C(3))/\text{\AA}$	1.476	1.484	1.473
$d(C(3)-C(4))/\text{\AA}$	1.360	1.360	1.364
$d(C(4)-C(5))/\text{\AA}$	1.520	1.517	1.515
$\angle(C(5)C(1)C(2))/^\circ$	108.2	110.9	110.0
$\angle(C(1)C(2)C(3))/^\circ$	110.3	107.4	108.9
$\angle(C(2)C(3)C(4))/^\circ$	108.7	110.1	108.9
$\angle(C(3)C(4)C(5))/^\circ$	109.7	109.6	110.0
$\angle(C(4)C(5)C(1))/^\circ$	103.1	101.9	102.1
$d(Cn-Si)/\text{\AA}$	1.791	1.793	1.845
$\angle(SiCnC(n+1))/^\circ$	128.1	123.0	112.1



$d(C(5)-C(1))/\text{\AA}$	1.527	1.520	1.515
$d(C(1)-C(2))/\text{\AA}$	1.366	1.364	1.364
$d(C(2)-C(3))/\text{\AA}$	1.476	1.485	1.472
$d(C(3)-C(4))/\text{\AA}$	1.360	1.360	1.364
$d(C(4)-C(5))/\text{\AA}$	1.519	1.518	1.515
$\angle(C(5)C(1)C(2))/^\circ$	107.9	111.2	110.3
$\angle(C(1)C(2)C(3))/^\circ$	110.6	107.2	108.8
$\angle(C(2)C(3)C(4))/^\circ$	108.5	110.2	108.8
$\angle(C(3)C(4)C(5))/^\circ$	109.6	109.6	110.3
$\angle(C(4)C(5)C(1))/^\circ$	103.4	101.8	101.8
$d(Cn-Si)/\text{\AA}$	1.813	1.814	1.871
$\angle(SiCnC(n+1))/^\circ$	127.2	123.0	114.0

Table 4.3.3. Calculated geometries of 1,2,5- $(h^{\sim}-C_5H_5)SiR_3$, R=H, Me.



$a = 1 \cdot \text{SiH}_3$

$b = 2 \cdot \text{SiH}_3$

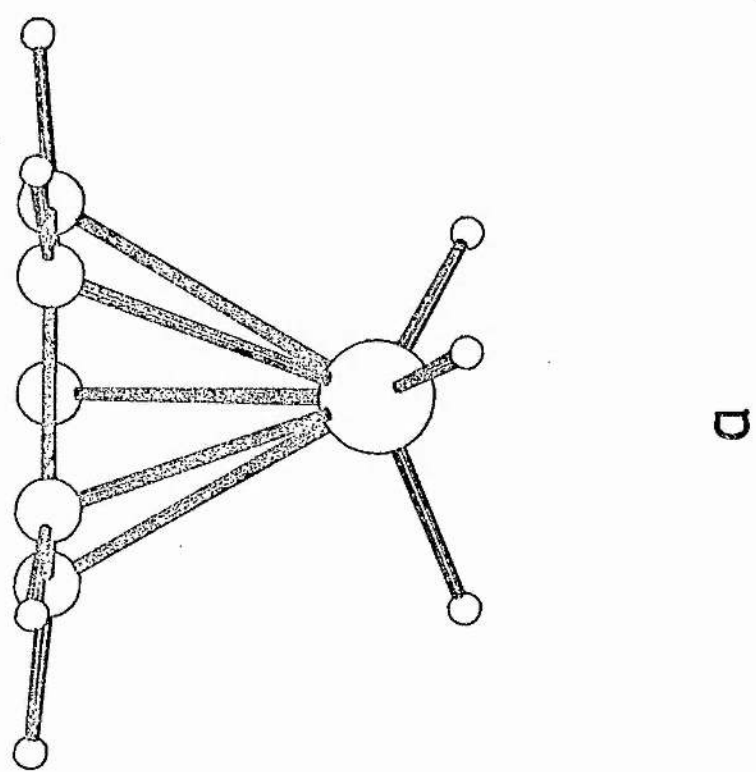
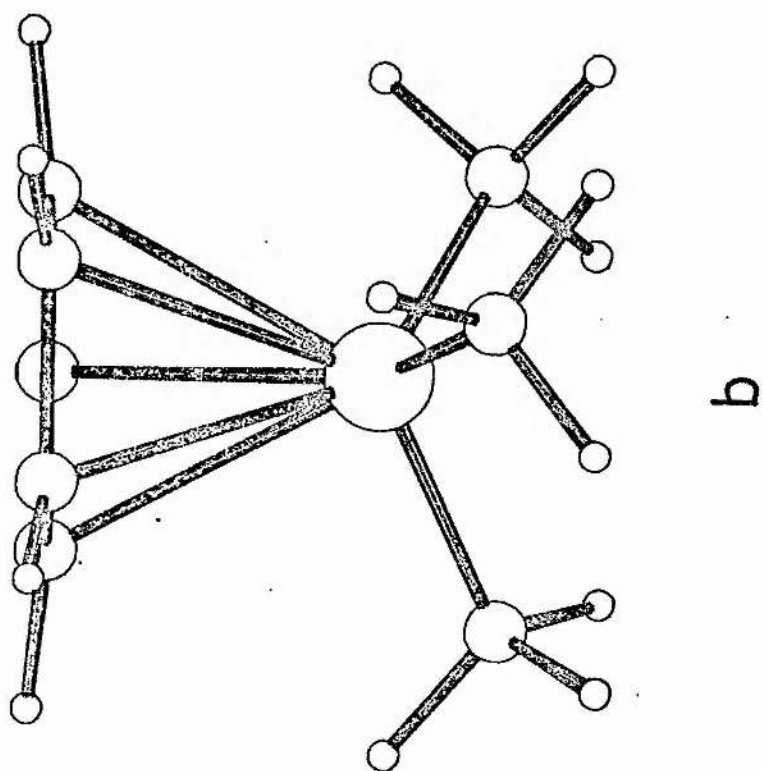
$c = 5 \cdot \text{SiH}_3$

Figure 4.3.1.

The aspect of ring folding will be discussed a little later on but in the meantime we now focus our attention on the hydrogen shifts and the piano stool molecules.

The 1 and 2 isomers formed via hydrogen migration from $5-R_3SiC_5H_5$, $R=H, Me$ [10,12,13] are calculated by MNDO to be thermodynamically more stable than the corresponding 5 isomers: the initial formation of these 5 isomers occurs as noted previously as there is an easy route from the $C_5H_5^-$ anion. The prototropic shifts therefore can only occur after substitution to form the 5 species. Table 4.3.3 collects the geometric data for the h' isomers and Figure 4.3.1 displays the three h' isomers of $C_5H_5SiH_3$. From Figure 4.3.1 and Table 4.3.3 we see that as, with the 5 isomer, the 1 and 2 isomers also have planar cyclopentadiene rings.

Beryllium [14-18], tin and lead [19] form h^5 derivatives although this type of species is as yet unknown for silicon and germanium which only form h' species. It is therefore of considerable interest to look at the results from the MNDO calculations on the 'piano stool' molecules for the silicon species; part of Table 4.3.1 lists the molecular energies for the various derivatives and shows that the energy difference between $5-RC_5H_5$ and the pentahapto species is steadily reduced from 498.3 kJmol^{-1} for $R=H$ through 245.4 kJmol^{-1} for $R=SiH_3$ to just 189.8 kJmol^{-1} for $R=SiMe_3$. Although this is still a fairly large difference it should be possible to obtain a relatively small energy difference by taking a suitably substituted SiX_3 group and C_5Y_5 ring so that the formation of the pentahapto $(h^5-C_5Y_5)SiX_3$



a=SiH₃

b=SiMe₃

Figure 4.3.2.

isomer becomes a definite possibility. We shall return to this point in Section V.

Figure 4.3.2 shows the calculated structures for the pentahapto species $(h^5-C_5H_5)SiR_3$, $R=H, Me$ and a tabulation of the important geometric data for the piano stool molecules can be found in Table 4.3.4.

$(h^5-C_5H_5)R$, $R=$	H	SiH_3	$SiMe_3$	- anion
$d(C-C)/\text{\AA}$	1.4351	1.4344	1.4300	1.4180
$d(C-H)/\text{\AA}$	1.0796	1.0815	1.0816	1.0827
$\angle(CCH)/^\circ$	125.98	125.85	125.80	126.00
$\angle(CCCH)/^\circ$	179.96	174.11	173.19	180.00
$h1\ a/\text{\AA}$	1.1989	1.9640	2.0902	-
$h2\ b/\text{\AA}$	0.0032	0.0900	0.1041	0.0000
$d(C...H, Si)/\text{\AA}$	1.7110	2.3122	2.4184	-
$d(Si-H, C)/\text{\AA}$	-	1.4521	1.8786	-
$\angle(XSiH, C)/^\circ$	-	111.61	112.91	-

a =Distance of H or Si from X. b =Distance of C_5 from H_5 plane.

c =X is point at centre of C_5 ring.

Table 4.3.4.

The data of Table 4.3.4 show that the C-C distances in the ring become progressively shorter at the same time as the C-H distance becomes longer when the axial substituent changes from H to SiH_3 to $SiMe_3$, and approach the values found for the isolated $C_5H_5^-$ anion: this suggests that as far as the pentahapto species considered here are concerned $(h^5-C_5H_5)SiMe_3$ has most ionic character for the bonding

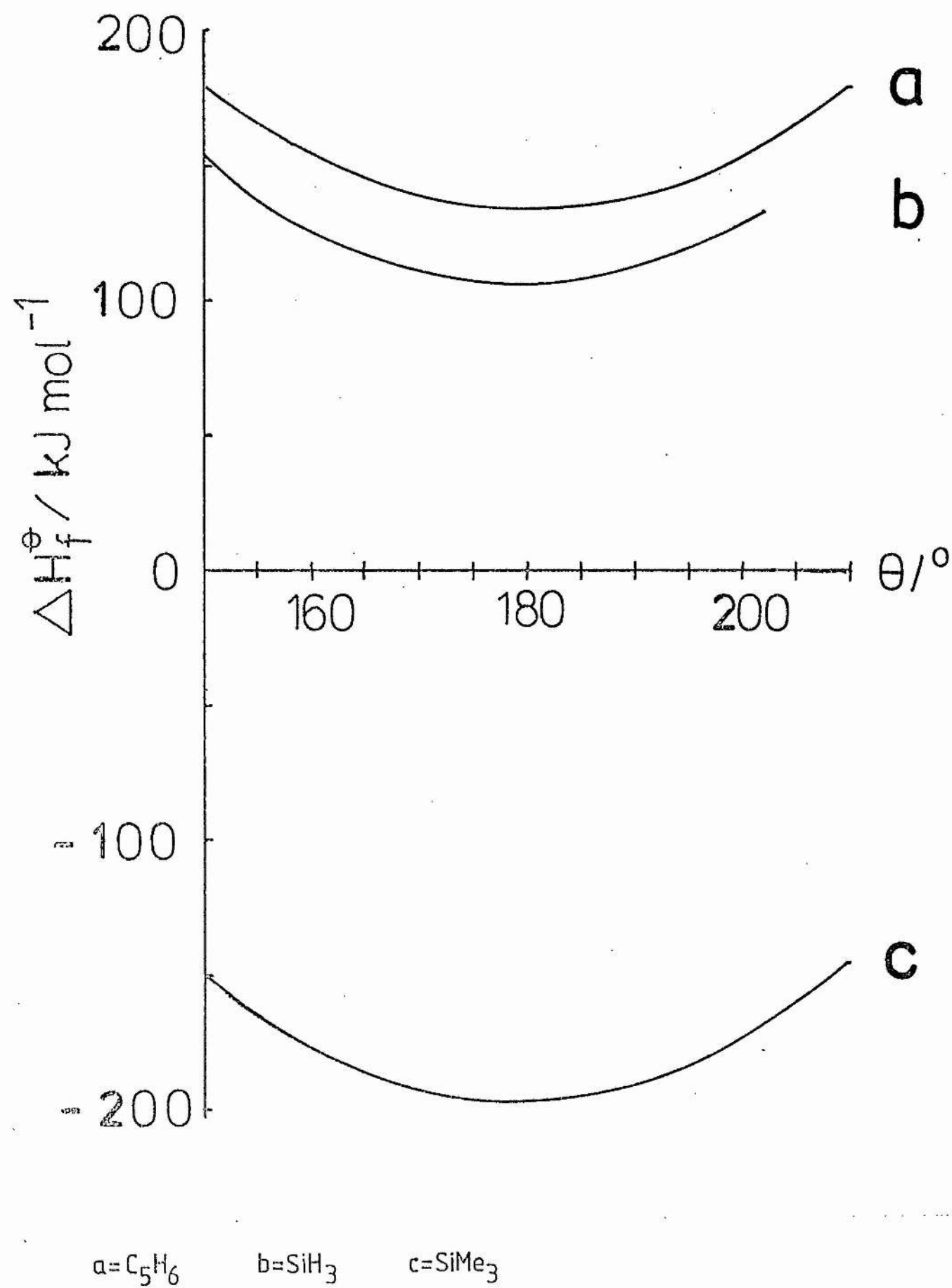


Figure 4.3.3.

of the axial substituent to the ring and $(h^5-C_5H_5)H$ the least. The fact that the species with the least ionic character is also the least stable with respect to its h^5 isomer and the most ionic species the most stable compared to its h^5 isomer may be of some relevance although a much broader range of cyclopentadienides is needed before this principle can be evaluated.

Since the MNDO calculations using fully optimised geometries for $5-SiH_3C_5H_5$, $5-SiMe_3C_5H_5$ and C_5H_6 intimate quite clearly that the rings are accurately planar we now return to the question of ring folding which we left above.

The dihedral angle between the two planes $C(1)C(2)C(3)C(4)$ and $C(4)C(5)C(1)$ was defined above as θ and when $\theta=180^\circ$ the ring is planar; a θ value of less than 180° portrays the cis configuration and a value of θ greater than 180° the trans configuration. This definition is the same as that used by Cradock et al in reference 6.

Figure 4.3.3 displays the potential energy curves for the monohapto species $(h^5-C_5H_5)R$, $R=H, SiH_3$ and $SiMe_3$. The curve for C_5H_6 is necessarily symmetrical about $\theta=180^\circ$ and Figure 4.3.3 shows that all three curves have a single clearly defined minimum at $\theta=180^\circ$ (planarity). They are also very similar in shape and virtually superimposable upon each other which indicates that for the substituents H , SiH_3 and $SiMe_3$ the potential for ring folding is essentially independent of the substituent.

	5tx	5ty	5tz	5px	5py
5ty	107.1				
5tz	274.8	167.7			
5px	51.7	55.4	223.1		
5py	158.3	51.2	116.6	106.6	
5pz	325.2	218.1	50.4	273.5	167.0
5cx	54.3	52.8	220.5	2.6	104.0
5cy	160.4	53.3	114.5	108.7	2.1
5cz	328.1	221.0	53.3	276.4	169.8
	5pz	5cx	5cy		
5cx	270.9				
5cy	164.9	106.1			
5cz	2.9	273.8	167.7		

5t=5-trans $\text{SiH}_3\text{C}_5\text{H}_5$. 5p=5-planar $\text{SiH}_3\text{C}_5\text{H}_5$.

5c=5-cis $\text{SiH}_3\text{C}_5\text{H}_5$.

x= sp basis set. y=sp+s' basis set. z=spd+s' basis set

Table 4.3.5. Energies between and within the basis sets employed in reference 6.

The actual values of the energies expressed in a.u. taken from reference 6 are given in Table 4.3.6.

	5c	5p	5t
x	-481.9748	-481.9738	-481.9541
y	-482.0152	-482.0144	-481.9949
z	-482.0791	-482.0780	-482.0588

Table 4.3.6.

The ring folding potentials required to shift the ring from its planar form to the value of 158° deduced in the experimental study of 5-SiMe₃-C₅H₅ [2] are

C ₅ H ₆	24.1 kJmol ⁻¹
5-SiH ₃ C ₅ H ₅	24.2 kJmol ⁻¹
5-SiMe ₃ C ₅ H ₅	28.2 kJmol ⁻¹

In addition the value for 5-BzHC₅H₅ is 24.5 kJmol⁻¹ and in the light of these findings we can only conclude that the reported structure for 5-SiMe₃C₅H₅ [2] is wrong in its deduction of a non-planar ring and as a consequence of this the folded ring reported for GeMe₃C₅H₅ [4] is therefore most likely to be incorrect also.

The ab-initio study by Cradock and co-workers [6] concluded that the cis conformation was the most stable for 5-SiH₃C₅H₅. In their study a variety of different basis sets were employed; however, the energies produced were total energies and these are not related to ΔH_f^θ . Table 4.3.5 lists the energies which have been converted to kJmol⁻¹ between and within the basis sets used in reference 6. This shows that the energy for a given structure varies with basis set by as much as 275 kJmol⁻¹. However, within a given basis set the relative energies of the different conformations are virtually constant, with cis more stable than planar by some 2.5 kJmol⁻¹, and planar more stable than trans by approximately 51.1 kJmol⁻¹: both much smaller than the variation between basis sets.

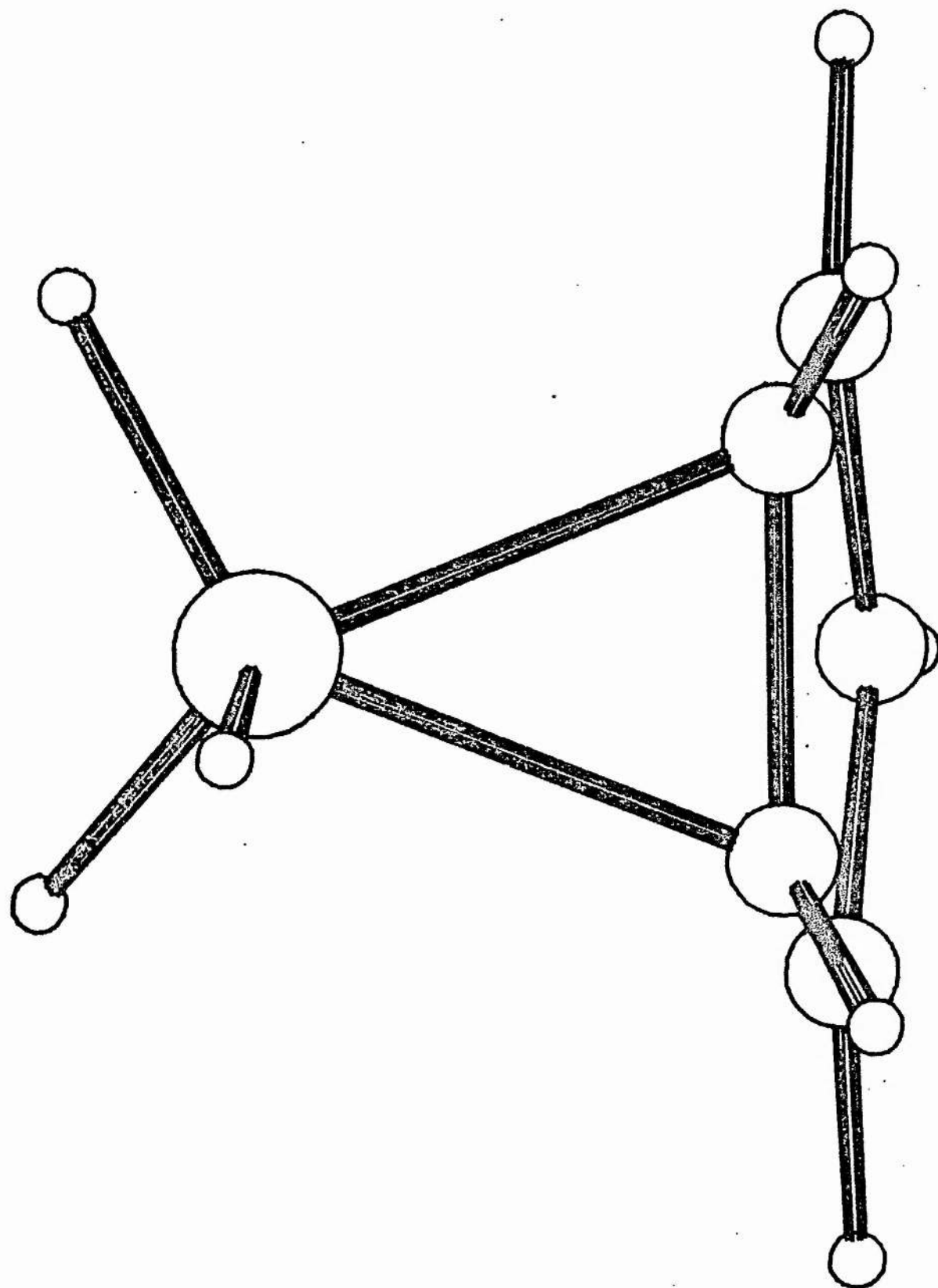


Figure 4.4.1. Geometry of transition state for SiH_3 shift.

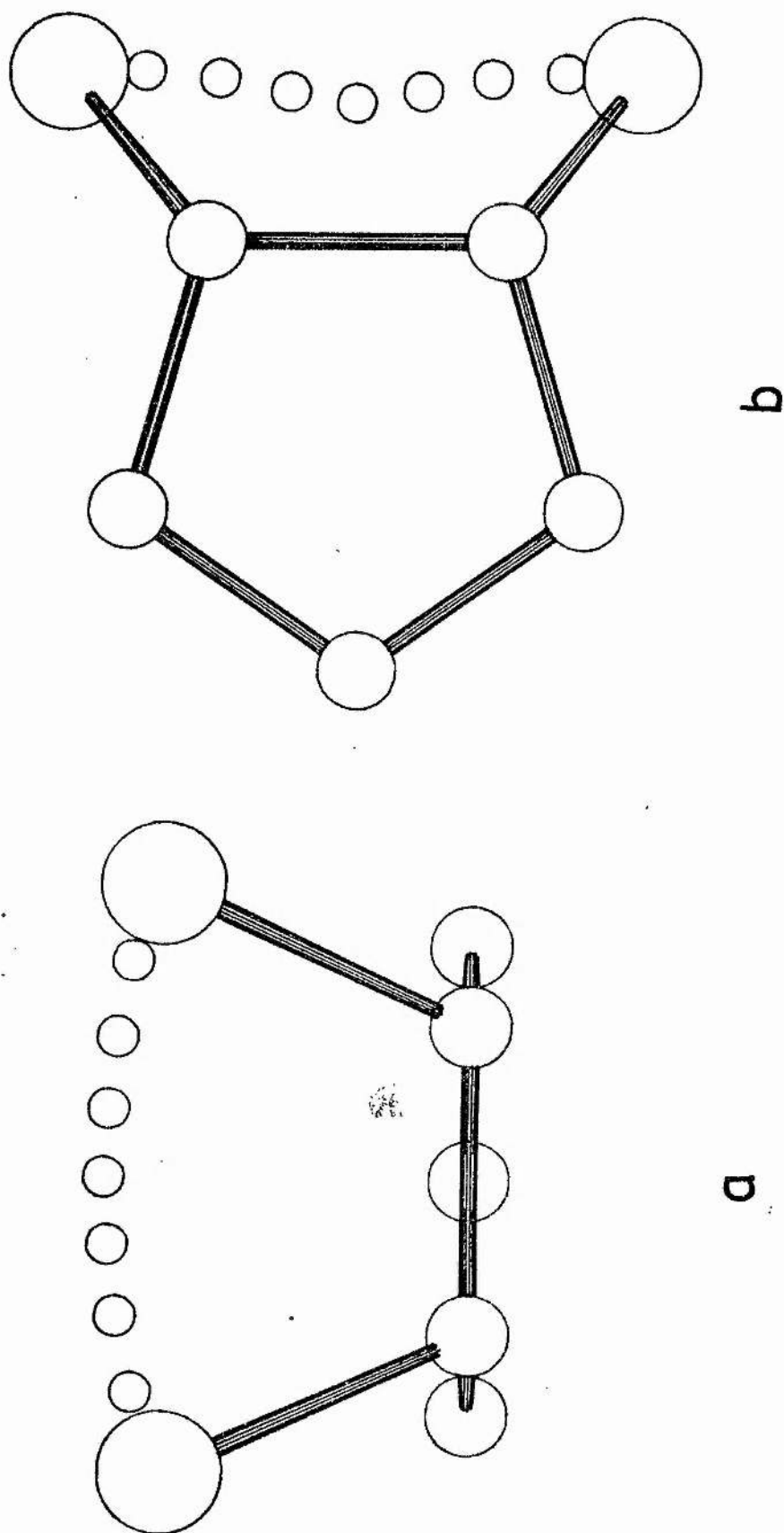


Figure 4.4.1. (a) side and (b) plan view of transition state for SiH_3 shift.

As a consequence of using fixed geometries for all the calculations the energy differences due to the ring folding are highly suspect. Two examples will suffice to prove the point. Firstly if the fully optimised geometry for 5-SiH₃C₅H₅ at $\theta=180^\circ$ is taken and the fold angle θ changed to 158° and the rest of the geometry left unaltered and fixed at the values appropriate for $\theta=180^\circ$ then errors of about 5 kJmol⁻¹ are introduced into the heat of formation. Secondly if random variations of $\pm 0.01 \text{ \AA}$ or $\pm 0.05^\circ$ are implanted into the structure of a fully optimised geometry then once more errors in ΔH_f° of 5 kJmol⁻¹ result. This illustrates that with much larger uncertainties on bond and dihedral angles quite possible when assumed geometries are used, the scope for error therefore is much greater and hence the conclusion arrived at in that work [6], that the cis structure is the most stable, is suspect.

IV. Metallotropic and prototropic shifts.

5-SiR₃C₅H₅ molecules undergo both metallotropic and prototropic migrations. For the metallotropic shifts two mechanisms were investigated namely the 1,2 and 1,3 shifts. Because the structures of the initial and final molecules are identical the 1,2 shift is therefore degenerate and the transition state symmetrical with the silicon atom equidistant from the two carbon atoms between which it is migrating: this transition state is shown in Figure 4.4.1 with the important geometrical parameters collected in Table 4.4.1. The transition state energy of 5-SiH₃C₅H₅ is 99.1 kJmol⁻¹ above that for the equilibrium energy; this cannot be compared to the solution

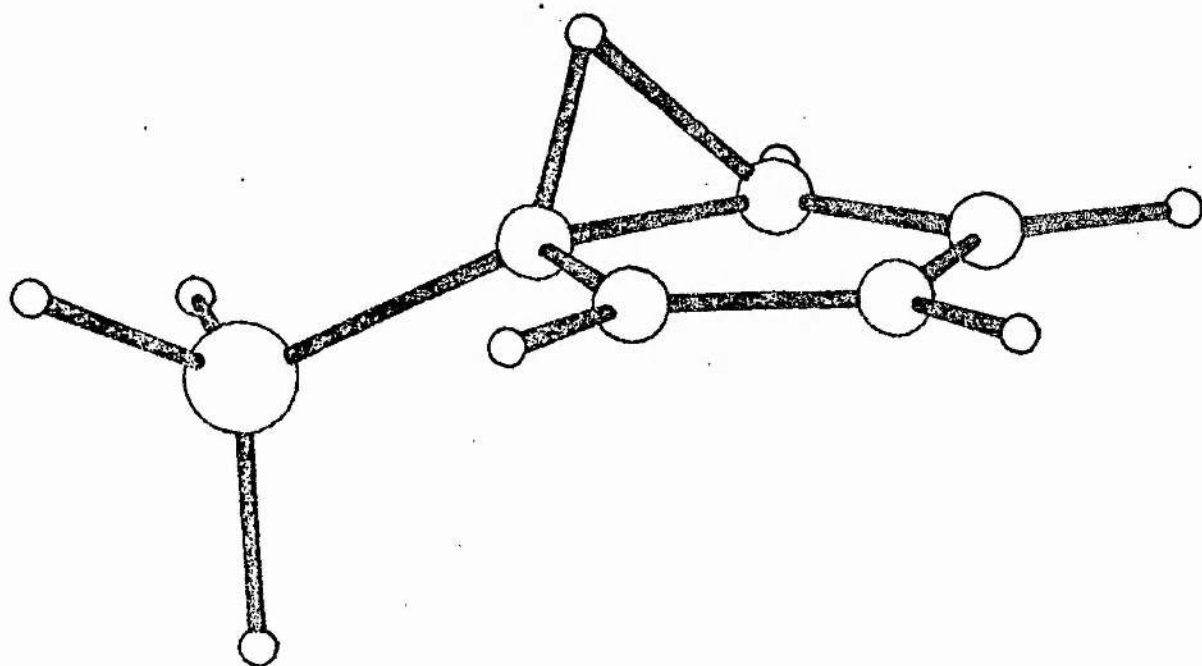
activation energy since the calculation refers to an isolated molecule in the gas phase in the absence of solvation.

$d(C_a-C_a')(x1)/\text{\AA}$	1.506
$d(C_a-C_b)(x2)/\text{\AA}$	1.429
$d(C_b-C_c)(x2)/\text{\AA}$	1.414
$\angle(C_a-C_a'C_b)(x2)/^\circ$	106.3
$\angle(C_aC_bC_c)(x2)/^\circ$	109.0
$\angle(C_bC_cC_b)(x1)/^\circ$	109.4
$d(Si-C_a)(x2)/\text{\AA}$	2.043
$d(Si-C_b)(x2)/\text{\AA}$	2.960
$d(Si-C_c)(x1)/\text{\AA}$	3.391

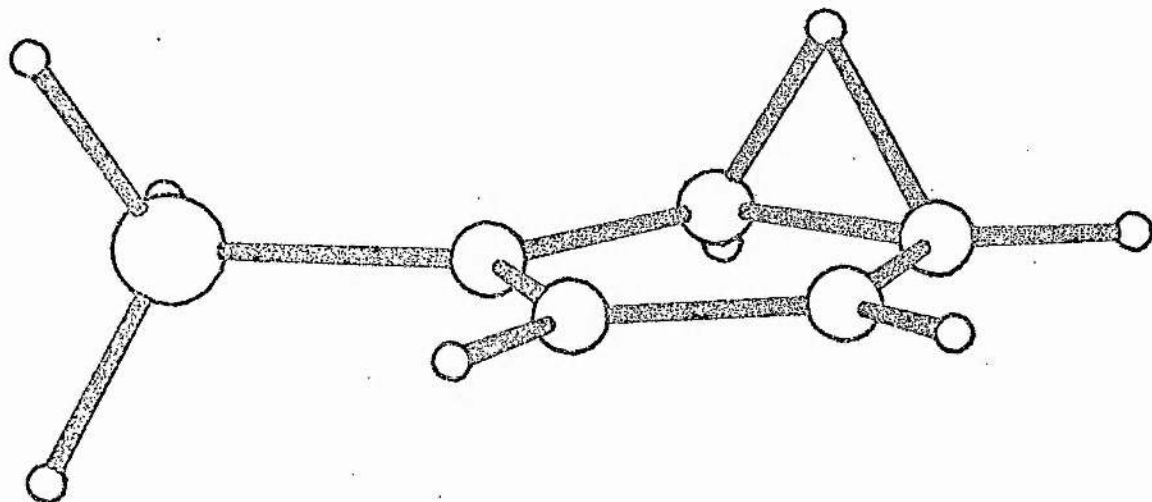
Table 4.4.1.

The 1,3 shift reaction pathway for 5-SiH₃C₅H₅ is also symmetrical since it consists of just two successive 1,2 shifts, and although a direct 1,3 shift pathway may be present the lowest energy pathway is that of the two successive 1,2 shifts: this is in accord with the observations from variable temperature ¹³C n.m.r. [10,20].

Two mechanisms were again studied for the prototropic shifts: firstly the 1,2 shift where the hydrogen moves initially from C(5) to C(1) and then subsequently from C(1) to C(2) and secondly that of the 1,3 shift where the hydrogen migrates directly from C(5) to C(2). Once more n.m.r. evidence supports the stepwise mechanism [10,12]; unlike the metallotropic shifts the prototropic shifts here are non-degenerate in nature and as a result the pathways are not symmetrical.



a



b

Figure 4.4.2.

The transition state energy for the 5→1 hydrogen shift is 282.2 kJmol⁻¹ which is equivalent to a gas phase activation enthalpy of +175.9 kJmol⁻¹ for the forward direction; the corresponding energies for the 1→2 shift are 277.1 kJmol⁻¹ and 187.1 kJmol⁻¹ respectively. The transition states for the 5→1 and 1→2 hydrogen shifts are displayed in Figure 4.4.2 and the relevant structural data in Table 4.4.2.

	(a) 5→1	(b) 1→2
$d(Si-C_a)/\text{\AA}$	1.805	1.787
$d(C_a-C_b)/\text{\AA}$	1.503	1.477
$d(C_b-C_c)/\text{\AA}$	1.390	1.493
$d(C_c-C_d)/\text{\AA}$	1.450	1.390
$d(C_d-C_e)/\text{\AA}$	1.382	1.449
$d(C_e-C_a)/\text{\AA}$	1.477	1.388
$\angle(C_a C_b C_c)/^\circ$	108.9	106.0
$\angle(C_b C_c C_d)/^\circ$	108.4	107.7
$\angle(C_c C_d C_e)/^\circ$	109.3	108.4
$\angle(C_d C_e C_a)/^\circ$	109.6	110.0
$\angle(C_e C_a C_b)/^\circ$	103.8	107.6
$\angle(Si C_a C_b)/^\circ$	126.3	125.1
$\angle(Si C_a C_e)/^\circ$	120.6	127.8
$d(C_a-H^*)/\text{\AA}$	1.182	-
$d(C_b-H^*)/\text{\AA}$	-	1.183

Table 4.4.2.

As in the metallotropic shift the attempts to study the 1,3 shift mechanisms resulted in a pair of successive 1,2 shifts being found: if there is a 1,3 shift then it is of a higher energy than the stepwise path.

Although none of the calculated activation energies can be related to a solution enthalpy it is interesting to note however that the activation energy for the metallotropic migration is much less than that for the prototropic shifts: this is consistent with the n.m.r. data since in solution it is found that SiH_3 migration is rapid [9] whereas the prototropic migration is slow [10]. The rates for $5\text{-SiMe}_3\text{C}_5\text{H}_5$ at 80°C are 10^3 s^{-1} for SiMe_3 [12] and $1.4 \times 10^{-3} \text{ s}^{-1}$ for hydrogen and this margin represents a solution activation energy difference of 39.6 kJmol^{-1} which can be compared favourably with the 76.8 kJmol^{-1} , the value calculated for $\text{SiH}_3\text{C}_5\text{H}_5$ by MNDO, and is of course referring to isolated molecules in the gas phase.

Tables 4.4.1 and 4.4.2 which list the structural data for the transition states for the group and hydrogen shifts show a number of common features, namely that the longest bond and smallest valence angles in the ring in each case are those which span the migrating entity whereas the shortest bond is that directly opposite the migrating fragment.

	Observed/eV	MNDO/eV	Ab-initio/eV
C_5H_6	8.56	9.05	8.88
	10.72	10.84	11.74
	12.2	12.71	13.69
	12.6	12.80	13.38
	13.2	13.35	14.26
	13.8	13.93	15.19
	15.0	14.68	16.63
	16.5	17.14	18.92
	17.5	19.84	19.30
	18.4	20.83	20.15
5-SiH ₃ C ₅ H ₅	8.7	9.03	9.09
	10.2	10.41	11.09
		12.19	12.67
	12.0	12.25	12.72
		12.65	13.18
	12.8	13.09	13.88
	13.9	13.31	14.72
	14.1	13.93	15.56
		14.39	15.65
	16.5	17.06	18.53
	17.0	19.17	19.34
		19.99	19.53

Table 4.5.1. Observed and calculated eigenvalues for C_5H_6 and

5-SiH₃C₅H₅.

V. Electronic Structure.

For the monohapto species there is a fair amount of similarity between the electronic structure calculated by the MNDO and ab-initio techniques [6]. Table 4.5.1 lists some typical values for C_5H_6 and $5-SiH_3C_5H_5$ and the improved fit shown in the Table is also in evidence for the isomers of MeC_5H_5 .

As well as this improved agreement MNDO seems better able at predicting the energy differences between the first two photoelectron bands which has previously [9] been used as a diagnostic tool for fluxional behaviour. A small energy difference of less than 1.5 eV indicates fast fluxional character whilst slow fluxional behaviour is associated with a larger energy difference of the order of 2.1 eV. Table 4.5.2 lists the MNDO calculated energy gaps along with experimental and ab-initio values for C_5H_6 , The 5,1 and 2 isomers of MeC_5H_5 and $5-SiR_3C_5H_5$, $R=H, Me$ and shows that the ab-initio values are further from the experimental data than the MNDO values.

	MNDO(eV)	ab-initio(eV)	experimental(eV)
C_5H_6	1.79	2.86	2.1
$5-MeC_5H_5$	1.80	2.84	unknown
$1-MeC_5H_5$	1.83	3.04	2.2
$2-MeC_5H_5$	1.62	2.50	2.0
$5-SiH_3C_5H_5$	1.38	2.00	1.5
$5-SiMe_3C_5H_5$	1.26	-	-

Table 4.5.2.

There are similarities too in the atomic charges calculated by the ab-initio and MNDO methods for $5\text{-SiH}_3\text{C}_5\text{H}_5$ and it is interesting to note in passing that the silyl group even in the MNDO limited s,p basis is found to be a net electron donor even to the electron rich cyclopentadiene. This fact about net electron donating properties has been noted previously in a number of other silyl containing compounds [21] and is contrary to the electron accepting view described by Ebsworth [22].

The charges in the metallotropic shift transition state in $5\text{-SiH}_3\text{C}_5\text{H}_5$ change somewhat from their values for the equilibrium structure - the silicon for instance becoming more positive by 0.054 e from 0.649 e to 0.703 e with the carbons C(5) and C(1), the atoms involved in the shift, becoming more negative the former going from -0.182 e and the latter from -0.102 e to -0.195 e. In addition C(2) and C(4) become less negative and C(3) more negative and this increased charge separation is mirrored in the dipole moment which increases from 0.172 to 0.303 Debye and as a result the transition state solvation energy will be greater than that for the equilibrium molecule and so will play a major part in the reduction of the high gas phase activation energy to the lower value found in solution. Exactly analogous comments can be made for the prototropic transition states.

Finally in this chapter we consider the pentahapto species and their electronic structure. The bonding of the axial substituent whether it is H, SiH_3 or SiMe_3 is merely a perturbation of the π molecular orbitals of the ring, the symmetries of which in the isolated C_5H_5^- anion are A_2'' , which has σ symmetry with respect to the five-fold axis; E_1'' , which has π symmetry; and E_2'' which has δ symmetry.

Interaction of the A_2'' orbital and the axial hydrogen 1s orbital in $(\text{h}^5\text{-C}_5\text{H}_5)\text{X}$ produces both in and out of phase combinations the former of which is occupied. In the silyl and trimethylsilyl case the relevant silicon orbital involved in the ring bonding is that of the $3p_z$ since the silicon 3s, $3p_x$ and $3p_y$ orbitals are mainly concerned with Si-X bonding (the z axis is coincident with the pseudo five fold axis.)

The $1A_2''$, E_1'' , $2A_2''$ and E_2'' molecular orbital energies, the first two of which are occupied, for the three species mentioned above along with those for C_5H_5^- itself are presented in Table 4.5.3.

$\text{C}_5\text{H}_5^-/\text{eV}$	$(\text{h}^5\text{-C}_5\text{H}_5)\text{H}/\text{eV}$	$(\text{h}^5\text{-C}_5\text{H}_5)\text{SiH}_3/\text{eV}$	$(\text{h}^5\text{-C}_5\text{H}_5)\text{SiMe}_3$
$E_2'' +7.938$	$E_2'' +1.252$	+0.879	+1.339
$E_1'' -2.137$	$2A_2'' -0.962$	-1.680	-1.617
$A_2'' -6.110$	$E_1'' -8.428$	-8.635	-8.272
	$1A_2'' -13.802$	-13.879	-12.278

Table 4.5.3. Eigenvalues for pentahapto species.

Both the doubly degenerate orbital binding energies for $(h^5-C_5H_5)X$ are very sensitive to the overall net ring charges or in other words substituent. However this difference is fairly constant at a value smaller than that found for the $C_5H_5^-$ anion. By way of contrast the energy difference between the two singly degenerate orbitals $1A_2''$ and $2A_2''$ decreases from 12.84 eV for $X=H$ through 12.20 eV when $X=SiH_3$ to just 10.66 eV for $X=SiMe_3$.

In section III we saw how the bonding in $(h^5-C_5H_5)X$ became steadily more ionic as X varied $H - SiH_3 - SiMe_3$ and the axial bonding eigenvalues corroborate this interpretation, which before was based totally on a geometric argument. An entirely ionic interaction would have a $1A_2''-E_2''$ energy gap of 3.97 eV which is the value found for $C_5H_5^-$. This gap is found to be 5.37 eV for $X=H$, 5.24 eV for $X=SiH_3$ and 4.01 eV for $X=SiMe_3$.

Silicon does not form stable 'piano stool' type structures and this is because the π interaction with the ring E_1'' orbital are small. The substituents which do form stable h^5 structures are as mentioned earlier beryllium, tin(II) and lead(II) which use vacant np π orbitals to form strong π interactions and transition elements which make use of their nd π orbitals so if silicon is to form a stable h^5 type structure a strong π interaction is necessary and this can only be achieved if X in SiX_3 is a strong electron sink.

Chapter Four.

Bibliography.

1. J.E. Bentham and D.W.H. Rankin. J. Organomet. Chem. 30 C54 (1971).
2. N.N. Veniaminov, Yu.A. Ustynyuk, N.V. Alekseev, I.A. Ronova and Yu.T. Struchkov. J. Organomet. Chem. 22 551 (1970).
3. M.J. Barrow, E.A.V. Ebsworth, M.M. Harding and D.W.H. Rankin. JCS Dalton 603 (1980).
4. N.N. Veniaminov, Yu.A. Ustynyuk, Yu.T. Struchkov, N.V. Alekseev and I.A. Ronova. Zhur. Strukt. Khim. 11 127 (1970).
5. IUPAC assigns the label 5 to the unique carbon.
6. S. Cradock, R.H. Findlay and M.H. Palmer. JCS Dalton 1650 (1974).
7. A. Davison and P.E. Rakita. Inorg Chem 9 289 (1970).
8. P.C. Angus and S.R. Stobart. JCS Dalton 2374 (1973).
9. S. Cradock, E.A.V. Ebsworth, H. Moretto and D.W.H. Rankin. JCS Dalton 390 (1975).
10. A. Bonny, S.R. Stobart and P.C. Angus. JCS Dalton 938 (1978).
11. M.J.S. Dewar and W. Thiel. JACS 99 4899 (1977).
12. A.J. Ashe. JACS 92 1233 (1970).
13. E.W. Abel and M.O. Dunster. J. Organomet. Chem. 33 161 (1971).
14. A. Haaland and D.P. Novak. Acta Chem Scand A28 153 (1974).
15. T.C. Bartke, A. Bjørseth, A. Haaland, K.M. Marstokk and H. Møllendahl. J. Organomet. Chem. 85 271 (1975).
16. D.A. Drew and A. Haaland. Acta Cryst B28 3671 (1972).
17. A. Haaland. Acta Chem Scand 22 3030 (1968).

18. C.H. Wong, T.Y. Lee, K.J. Chao and S. Lee. Acta Cryst B28 1662 (1972).
19. A. Almenningen, A. Haaland and T. Motzfeld. J. Organomet. Chem. 7 97 (1967).
20. R.D. Holmes-Smith and S.R. Stobart. JACS 102 382 (1980).
21. C. Glidewell. Inorg Chim Acta 13 L11 (1975).
22. E.A.V. Ebsworth. 'Organometallic Compounds of Group IV Elements.' A.G. MacDonald (Ed.). Dekker New York 1,1 (1968).

Chapter Five.

Diazepines.

I. Introduction.

There is a lot of current interest in the intermediates formed by diazepines, which are the nitrogen analogues of push-pull alkenes, when they are protodebrominated since the intermediates could be one of three types, either an allene, carbene or onium ion [1].

The bromodihydrodiazepinium cation, Ia, when heated with triphenylphosphine in the presence of an alcohol, yields the protodebrominated cation, IIa, triphenylphosphine oxide and an alkyl halide [1]. See Figure 5.1.1.

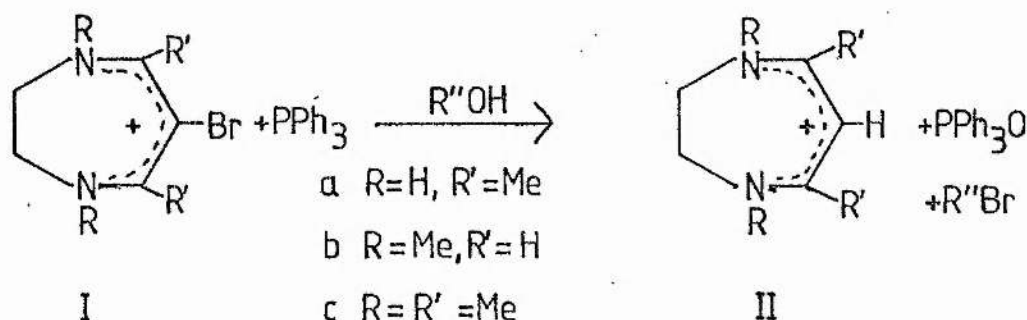
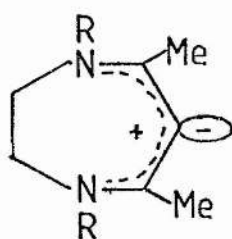


Figure 5.1.1.

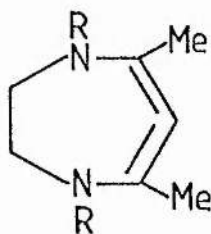
In this protodebromination the bromine is lost essentially as the bromonium ion, Br(I) or Br^+ , and the proposed mechanism is that via an onium ion, III, where a carbanionic lone pair of electrons is orthogonal to a vinamidinium π system. This representation of the intermediate is preferred to the alternative allene type structure,

IV, and carbene type species, V, since formation of both these species involves loss of about 80 kJmol^{-1} of delocalisation energy of the vinamidinium π system [2] and also increases the ring strain in the molecule.

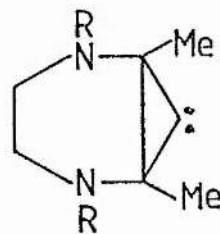
Requiring a higher temperature for reaction, but otherwise under similar conditions, cation Ib affords IIb. If the reaction is carried out in aprotic solvents, Ia still yields IIa, however only intractable material is obtained from Ib. The rationale for this is proton transfer from nitrogen to carbon in the case of IIIa to give VI - this transfer is clearly impossible in the case of IIIb.



III

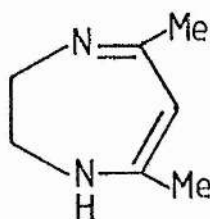


IV



V

The bromine in the protodebromination, as yet, has not been successfully removed as the bromide anion, $\text{Br}(-\text{I})$ or Br^{-1} . If this were to occur, however, the same question could be asked as to the formulation of the doubly positively charged intermediate involved. Is it a carbonium ion, an allene or a carbene?



VI

		Distances / Å.					
	E/kJmol ⁻¹	a	b	c	d	e	H-C
IVa	241.2	1.327	1.433	1.502	1.477	1.567	-
IVc	260.2	1.325	1.438	1.503	1.484	1.561	-
VI	84.3	1.368	1.299	1.520	1.447	1.549	1.096
		1.470	1.405		1.463		
VIIa	194.4	1.326	1.444	1.514	1.468	-	-
VIIb	166.2	1.319	1.445	1.513	1.467	-	-
VIIc	187.5	1.322	1.433	1.517	1.470	-	-
VIII	79.6	1.522	1.289	1.525	1.450	1.544	1.118
XXIV	394.4	1.333	1.430	1.086	1.478	-	-
XXV	272.2	1.315	1.421	1.095	1.471	1.553	-

Table 5.3.1. Geometry and ΔH_f^θ for neutral intermediates.

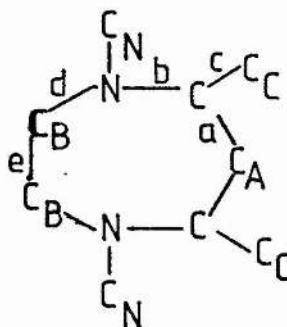
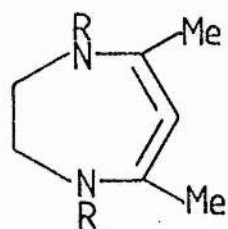


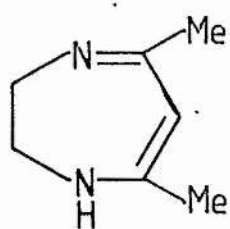
Figure 5.3.2. Atom labelling scheme.

Species	Angles / °					
	aa	ab	ac	bb	cc	dd
IVa	149.0	112.9	126.9	64.0	74.0	68.0
IVc	152.3	114.4	126.2	49.7	77.7	82.5
VI	129.8	125.3	117.1	26.6	34.3	72.4
		127.1	120.4			
VIIa	152.3(f)	123.1	122.9	78.9	83.2	-
VIIb	178.3	122.9	122.9	87.7	88.3	-
VIIc	176.7	122.5	119.3	85.1	-88.4	-
VIII	121.9	130.1	114.9	18.0	11.2	72.6
XXIV	134.2	111.7	130.6	28.7	65.5	-
XXV	161.1	120.6	125.0	50.8	74.6	71.5

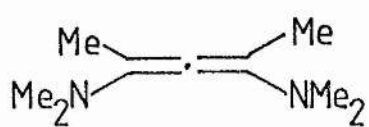
Table 5.3.1.



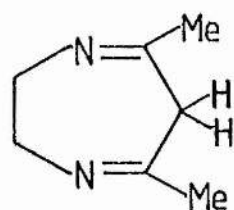
IV



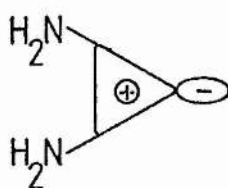
VI



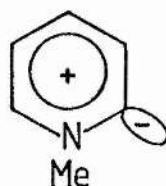
VII



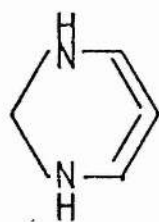
VIII



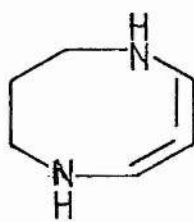
XIX



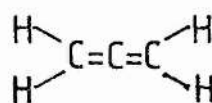
XXI



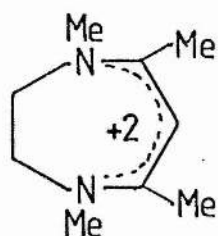
XXIV



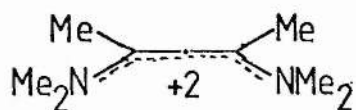
XXV



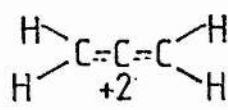
XXVI



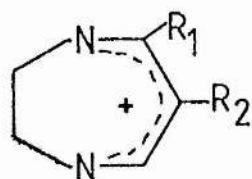
XXVII



XXIX



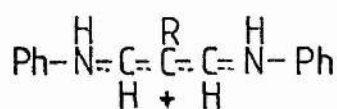
XXXI



XXXIII $R_1=H, R_2=-$

XXXIV $R_1=H, R_2=Ph$

XXXV $R_1=Me, R_2=Ph$



XXXVI $R=H$

XXXVII $R=Ph$

II. Method.

In an attempt to resolve this controversy calculations were undertaken with the semi-empirical SCF program MNDO [4,5] operating on a VAX 11/780 computer. The species studied for the cyclic systems, neutral and charged, were IV, VI, VIII, XIX, XXI, XXIV, XXV, XXVII, XXXIII, XXXIV and XXXV, and for open chain species, charged and uncharged, VII, XXVI, XXIX, XXXI, XXXVI and XXXVII.

III. Neutral Intermediates - Allenes or Onium Ions?

The calculated molecular geometries and energies for the neutral species are presented in Table 5.3.1 and the atom labelling scheme can be found in Figure 5.3.2. In addition Table 5.3.2 lists the net charges of the species studied. These results leave no doubt that, for an isolated molecule to which the calculations refer, structure IV, in which the π system is allenic, is preferred to the onium ion structure, III, and carbene representation, V. The allenic character can be seen from Table 5.3.1 where the bond lengths 'a' are calculated to be equal and also shorter than bond lengths 'b': the difference 'b' - 'a' is 0.113 Å. If structure III resulted from the calculations, then the bond lengths 'a' and 'b' would be very nearly equal, which they clearly are not. The dihedral angles bb' and cc' also support the allene structure IV since they would both be close to zero if the onium ion, III, was correct, and from Table 5.3.1 are seen to be much nearer 90°, which is indicative of an allene.

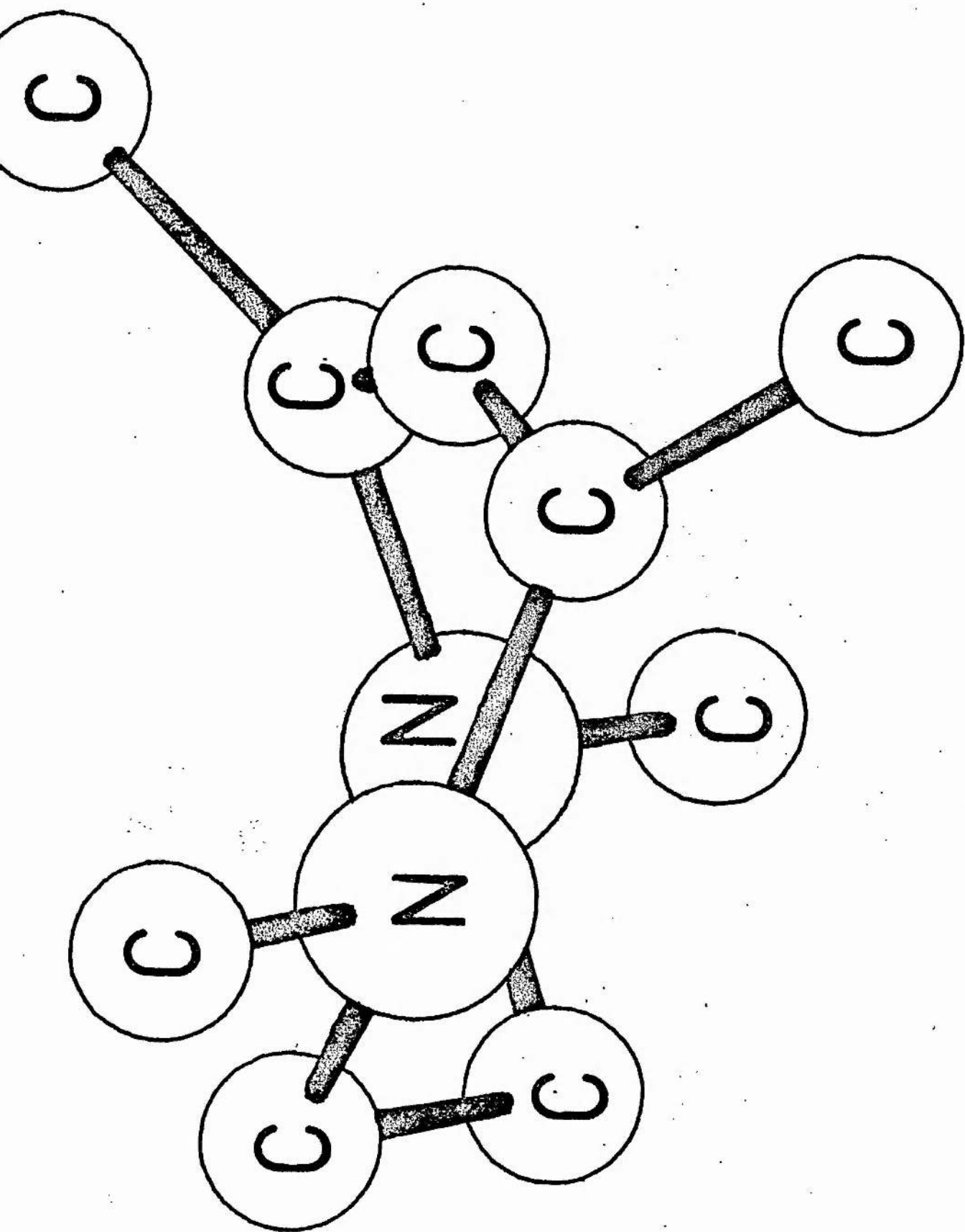


Figure 5.3.3. Molecular configuration of IV_c

The gross molecular configuration of IVc, with the hydrogens omitted for clarity, is shown in Figure 5.3.3 and demonstrates quite nicely the calculated allenic type structure. Note particularly bonds b and b', and c and c', which are far from being coplanar, and also the high degree of puckering in the saturated portion of the molecule.

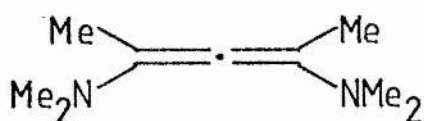
Further proof of the allene structure arises from the similarities which can be seen between the detailed geometries of IVa and IVc, when compared with that for the closely related open chain diaminoallene, VII.

The allenic CCC bond angle in IVa and IVc is calculated to be about 150° and when this angle in the related diaminoallene, VII, is changed from its optimised value of about 180° to the calculated diazepine angle of approximately 150° virtually no change is noticed in the rest of the geometry (see Table 5.3.1.) and, furthermore, the increase in ΔH_f^θ is found to be only 28 kJmol^{-1} . The $C_N NCC_A$ fragments of VIIa and VIIb are non-planar and when fixed to be so as in VIIc, the result is a very modest increase of 21 kJmol^{-1} in ΔH_f^θ . In addition, the charge on the central atom in VIIc is more negative than that in both VIIa and VIIb, the values being $-0.35e$, $-0.24e$ and $-0.24e$ respectively. In all three neutral allene cases, VII(a-c) the CN bonds are nearly orthogonal to each other.

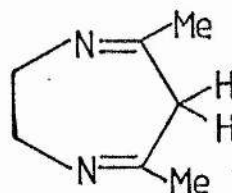
Species	N(x2)	C(x2)	C _A	C _B (x2)	C _N (x2)	C _C (x2)	H _{CA}	H(x4) /e
IVa	-0.32	0.11	-0.30	0.12	0.14	0.08	-	-
IVc	-0.38	0.12	-0.31	0.15	0.19	0.09	-	-
VI	-0.29	0.09	-0.21	0.07	0.15(H)	0.06	0.06	-
	-0.33	0.10		0.13		0.07		
VIIa	-0.39	0.11	-0.23	0.19	0.19	0.08	-	-
VIIb	-0.40	0.12	-0.24	0.19	0.19	0.08	-	-
VIIc	-0.38	0.15	-0.35	0.19	0.19	0.07	-	-
VIII	-0.27	0.03	0.00	0.07	-	0.06	0.03	-
XXIV	-0.36	0.14	-0.33	0.26(x1)	0.15(H)	0.10(H)	-	-
XXV	-0.33	0.16	-0.37	0.14	0.14(H)	0.08(H)	-	-
XXVII	-0.26	0.29	0.08	0.08	0.18	0.02	-	-
XXIX	-0.21	0.25	0.02	0.16	0.16	0.02	-	-
XXIXa	-0.22	0.26	0.05	0.16	0.16	0.00	-	-
XXIXb	-0.24	0.26	0.06	0.16	0.16	0.02	-	-
XXVIa	-	0.00	-0.20	-	-	-	-	0.05
XXVIb	-	0.00	-0.20	-	-	-	-	0.05
XXVIc	-	-0.50	0.50	-	-	-	-	0.13
XXVIId	-	0.46	-0.82	-	-	-	-	0.00(x2)
								-0.05(x2)
XXXIa	-	0.41	0.16	-	-	-	-	0.25
XXXIb	-	0.41	0.17	-	-	-	-	0.25
XXXIc	-	0.41	0.17	-	-	-	-	0.25

Table 5.3.2. Atomic charges for the neutral and charged intermediates.

Figure 5.3.3 shows the rather extreme nature of the ring puckering - especially in the saturated NCCN moiety, the dihedral angle of which is very close to 90° . This arises from the NCCCN fragment being largely allenic. The corresponding ring strain caused by this, however, is remarkably modest, and can be found by locking the NCCN dihedral angle of IVc at zero and optimising the rest of the structure. This results in an increase of 35 kJmol^{-1} in ΔH_f^θ and an essentially unchanged geometry for the allenic fragment. On the other hand, fixing the NCCCN fragment in IVc to be coplanar increases the ΔH_f^θ value by some 85 kJmol^{-1} : the dihedral angles cc' and dd' in this structure are approximately 41 and 87° respectively. However on no occasion during the ring fixing was there any tendency for bonds 'a' and 'b' to equalise and thus attempt to attain an onium ion type structure.



VII

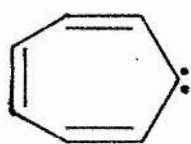


VIII

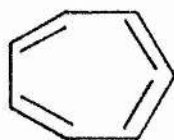
The diaminoallene system in IVa, IVc and VII exhibits a considerable degree of charge separation, with the central carbon atom in IVa and IVc having a net charge of $-0.30e$ and $-0.31e$ respectively. The two outer allenic carbon atoms have respective positive charges of $+0.11e$ and $+0.10e$, whereas the nitrogen atoms carry a negative charge of $-0.33e$ in IVa and $-0.37e$ in IVc. A tautomer of IVa, namely

structure VI, has been invoked as the proton acceptor in the reaction scheme for the conversion of Ia to IIa, and the net charges of VI are found to be similar to those of IVa and VII. However, a further tautomer of IVa is VIII, and this tautomer shows no appreciable separation of charge and all of the carbons are essentially neutral with a charge of $< 0.03e$. The most stable of these tautomers, IVa, VI and VIII, taken as an isolated molecule, is VIII - see Table 5.3.1, but due to its lack of significant charge separation its free energy of solvation in polar solvents, like alcohols for instance, will be much less than that for IVa and VI. Of the two latter species, structure VI, as an isolated molecule, has the much lower ΔH_f^θ and coupled with the strong charge separation means that it will be the more stable in polar solvents, which is consistent with its formation from I in aprotic solvents [1]. The ΔH_f^θ of VI being considerably less than that for IVa means that the proton transfer is exothermic and may occur spontaneously.

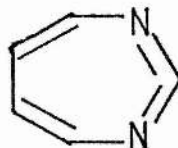
MINDO/3 calculations on cyclic allenes, which are related to IV, have appeared and show that singlet cycloheptatrienylide, IX, is perhaps better described in the form of an allenic tetraene, X [6], and in addition the i.r. spectra of the 1,3 diaza analogue of IX shows that it is better portrayed as the carbodiimide, XI, rather than the carbene, XII [7].



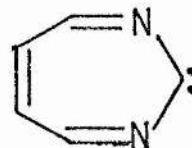
IX



X

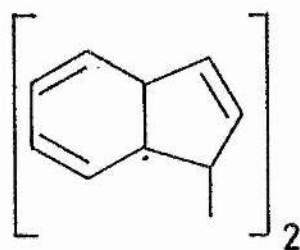


XI

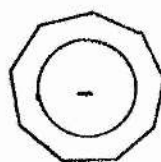


XII

A pathway for the formation of XIII from the cyclononatetraenide anion, XIV, when it reacts with 4-nitrobenzenesulphonyl azide, postulates an intermediate which can be either XV(a-c); namely carbene, allene or tetraenide cation respectively [8].



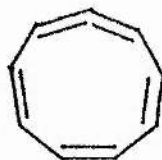
XIII



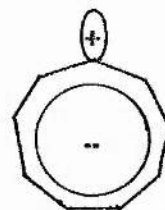
XIV



XVa

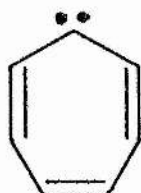


XVb

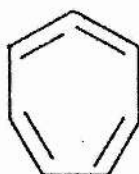


XVc

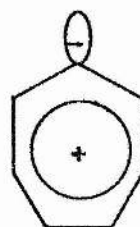
MNDO calculations reveal that structure XVb, the allene, is the preferred geometry [9]. The species C_7H_6 , XVI(a-c), has also been studied by MNDO [10] and reinvestigated with the same system [9], and the latter study shows that the freely optimised C_7H_6 species is best represented as the allene XVIb, and when fixed planar, as the onium ion XVIc.



XVIa

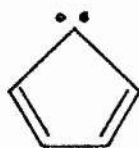


XVIb



XVIc

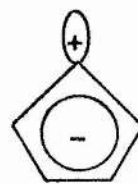
The C_5H_4 system, XVII(a-c), must be planar, but has no allenic character, XVIIb, because the ring would be very strained. However it would appear to show a contribution of a dipolar carbanion cation system, XVIIc, to the overall molecular geometry.



XVIIa



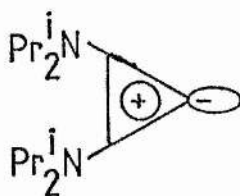
XVIIb



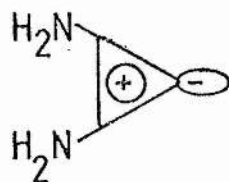
XVIIc

It is therefore interesting that the contributions from the delocalised sextet of electrons for the C_7 and C_5 systems, XVI and XVII, are quite substantial in contrast to the C_9 system with ten delocalised electrons, the contribution of which appears to be small [11].

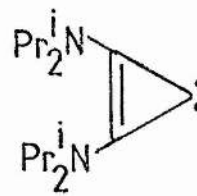
This is not to say that genuine onium ions do not exist as intermediates in other systems. As a model for a proposed intermediate XVIII [12,13]; structure XIX was fully optimised. This shows that the three-membered ring has two electrons delocalised over the carbons, with a lone pair lying along the C_2 axis perpendicular to the π system, and as a result is better represented as XVIII rather than the carbene, XX.



XVIII

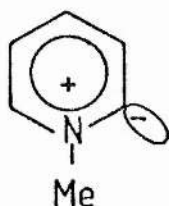


XIX

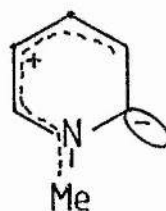


XX

In the onium ion XXI [14,15,16], the calculations reveal that the ring remains perfectly planar and although the six π electrons are delocalised there is a slight complication since the N-methyl group has a π population of 0.81e. Therefore, as a consequence of this, the π population at the carbanionic centre is only 0.40e, which suggests that there is a contribution from a form XXII to the overall structure of this onium ion.



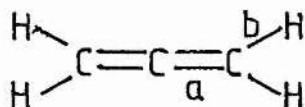
XXI



XXII

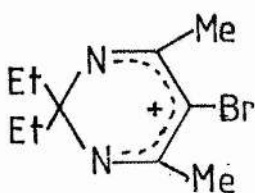
Protodebromination also occurs when a six-membered ring analogue of a bromodihydrodiazepinium salt, XXIII, is heated with thiourea, which reacts similarly to triphenylphosphine with bromodihydrodiazepinium salts [17], in the presence of ethanol [18]. Once again, an onium ion can be invoked as the intermediate, but the calculations on a related species, XXIV, suggest that the intermediate is largely allenic, although the more constrained geometry of the smaller ring means that the allenic character is not as pronounced as in the seven-membered ring, IV.

Species	E/kJmol ⁻¹	Point Group	Distances/Å		Angles/°		
			a	b	aa'	ab	bb'
XXVIa	182.1	D _{2d}	1.306	1.090	180.0	122.9	90.0
XXVIb	215.6	C _s (3)	1.312	1.091	152.3(f)	122.9	-
XXVIc	434.1	D _{2h}	1.320	1.086	180.0(f)	122.5	0.0(f)
XXVIId	489.9	C _s (1)	1.323	1.101	140.0(f)	124.6	0.0(f)
XXXIa	2554.5	D _{2h}	1.348	1.116	180.0	123.0	0.0(f)
XXXIb	2568.4	C _{2v}	1.350	1.114	164.7(f)	121.6	0.0(f)
				1.118		124.5	
XXXIc	2564.5	C _s	1.350	1.116	164.7(f)	123.0	0.0
XIX	579.5	-	1.457	1.373	56.6	151.2	-

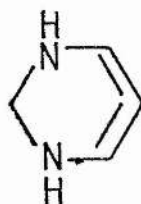


f = fixed

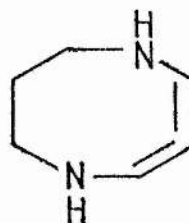
Table 5.3.3. ΔH_f^θ and geometries for C₃H₄ species.



XXIII

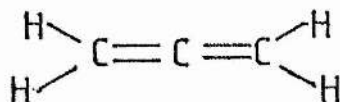


XXIV



XXV

Conversely in the eight-membered ring analogue, XXV, the calculations show that the allenic character is more easily attained than in the six-membered ring, which is as expected, since the ring is less strained. However it would appear that the allenic character is most marked and most easily attained in the seven-membered ring diazepine because the dihedral angle between the $\text{NC}_{\text{C}}\text{A}$ fragments is closest to 90° which is one of the criteria for an allene.



XXVI

A free optimisation of the C_3H_4 species, XXVI, yields a D_{2d} geometry, XXVIa, with a CCC angle of 180° (Table 5.3.3.). When this angle is fixed at the 'diazepine' angle found for the seven-membered ring compound, but with no further constraints, a C_s structure containing three carbon atoms, XXVIb, is found and furthermore ΔH_f^\ominus is increased by 34 kJmol^{-1} on XXVIa. A constrained D_{2h} structure for C_3H_4 , XXVIc, is some 250 kJmol^{-1} less stable than the D_{2d} counterpart, and with the CCC angle locked to give a C_s structure containing one

		Distances / Å.					
	E/kJmol ⁻¹	a	b	c	d	e	
XXVII	2178.9	1.392	1.356	1.519	1.504	1.560	
XXIX	2109.3	1.395	1.341	1.543	1.520	—	
XXIXa	2150.3	1.398	1.345	1.534	1.506	—	
XXIXb	2110.7	1.395	1.343	1.541	1.505	—	
		Angles / °.					
		aa'	ab	ac	bb'	cc'	dd'
XXVII		164.7	111.4	121.8	12.8	15.3	80.2
XXIX		168.4	124.5	112.7	53.5	43.5	—
XXIXa		164.7(f)	123.9	113.5	47.6	51.0	—
XXIXb		169.1	124.8	114.1	0.0(f)	3.3	—

f = fixed

Table 5.4.1. Geometries and ΔH_f^θ for charged intermediates.

carbon atom, as in XXVIId; the result is a further increase of 55 kJmol^{-1} on the D_{2h} species.

The charge distributions calculated for all four C_3H_4 species are interesting. XXVIa, D_{2d} , and XXVIb, C_s , have the same charge distribution - see Table 5.3.2. In contrast however, the pair XXVIc, D_{2h} , and XXVIId, C_s , have the same magnitude but opposite sign for the charge on the outer carbons, and in XXVIId the central carbon carries a charge of $-0.82e$ compared with the $+0.50e$ for the similar carbon in XXVIc. As a result, the hydrogens in XXVIc have a fair amount of charge associated with them, whereas in the rest, XXVIa,b,d, the hydrogens bear little or no charge.

IV. Charged Intermediates. Carbonium Ions or Allenes?

The doubly positively charged species, XXVII, was studied because if the bromine could be removed as Br^- in the protodebromination, then the question arises as to the nature of the intermediate involved. In this section classical organic type structures cannot be drawn for the species, and hence a difficulty arises in how best to represent them.

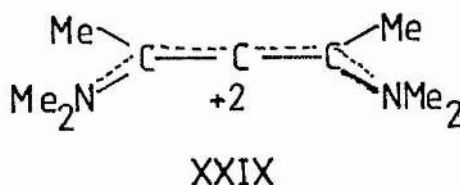
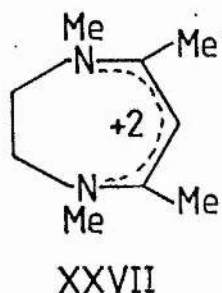
The optimised energies and structural parameters for the doubly positively charged intermediate species studied are presented in Table 5.4.1 and the respective atomic charges can be found in Table 5.3.2. The atom labelling scheme is identical to that in Figure 5.3.1.

The calculations on the species indicate that structure XXVII is a carbonium ion: there are not enough electrons present to draw an allene structure. The bond lengths 'a' and 'b' in XXVII are very nearly equal and the difference 'b' - 'a' is 0.036 Å; cf. 0.113 Å for IVc. The central carbon atom in XXVII is essentially neutral with a charge of 0.08e, which is considerably different from the charge on the respective carbon in IVc which is -0.31e. The nitrogens in XXVII are less negative than in IVc, the difference being 0.12e, and further evidence for the carbonium ion structure can be found in the dihedral angle cc' which is 15.3° in XXVII and also the near planarity of the NCCCN fragment, the dihedral angle bb' having the value 12.8°. Fixing the NCCCN fragment planar increases ΔH_f^θ by 5 kJmol⁻¹. This system is analogous to the 6 π system in C₆H₅⁺ [19].

In the previous section it was seen that there were a number of structural similarities between the diazepine IVc and the related diaminoallene VII. Optimisation of the corresponding +2 open chain species, XXIX, was undertaken and it was found to exhibit structural characteristics akin to those of species XXVII. Tables 5.4.1 and 5.3.2 show that the related bond lengths are very similar as are the net atomic charges. The free optimisation of XXIX has a trans type structure for the Me₂N groups, which is in contrast to structure XXIXa, which fixes the CC_AC angle at the diazepine angle found for XXVII, and affords a cis conformation for the Me₂N groups. The ΔH_f^θ , in addition, is increased by 40 kJmol⁻¹ on XXIX. By forcing the NCC_ACN fragment to become coplanar, as in XXIXb, the molecule adopts a nearly planar structure with the N-methyl groups deviating slightly

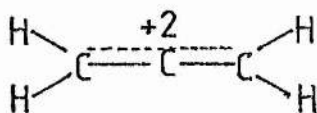
from the plane. Comparison of XXIX with XXIXb indicates that the barrier to rotation of the MeCNMe_2 groups is negligible.

This open chain system is not a diaminoallene because of the lack of electrons. Therefore with the similarity between the bond lengths 'a' and 'b' in species XXIX, and coupled with the nearly identical charge distribution to XXVII, this shows that this molecule is better described as an open chain carbonium ion. In all +2 open chain species the CCC backbone is non-linear.



Species related to C_3H_4 , XXVI, but with two electrons removed to yield $\text{C}_3\text{H}_4^{+2}$, XXXI, were also studied by MNDO. With the total skeleton fixed flat and the CCC angle allowed to refine, as in XXXIa, the optimisations converge to a linear D_{2h} conformation. This structure differs from XXXIb, which has CCC fixed at 164.7° yielding a C_{2v} structure, by being more stable by 14 kJmol^{-1} . However, when the dihedral angles on the hydrogens in XXXIb are allowed to refine the result is a C structure, XXXIc, which is more stable than XXXIa by

only 4 kJmol^{-1} . The charge distribution in all molecules XXXI(a-c) is identical and a free optimisation from the D_{2h} structure affords an identical geometry. The charges on the outer carbons are $0.41e$ and the central carbon carries a charge of $0.25e$. In addition, every hydrogen has a charge of $0.16e$ associated with it, and since all charges are positive, delocalisation of charge is very likely, as in the +2 diazepine and +2 open chain carbonium ion, and so $C_3H_4^{+2}$ is best represented as a delocalised carbonium ion, XXXI.

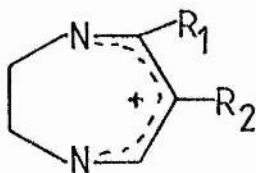


XXXI

The questions posed in the last two section headings are now in a position to be answered. The neutral species appear to have allenic character, whilst the +2 species seem to be like carbonium ions.

V. Complete Delocalisation?

This final section deals with MNDO calculations [4,20] on 2,3 dihydro -1,4-diazepine derivatives XXXIII to XXXV, and the open chain analogues XXXVI and XXXVII.



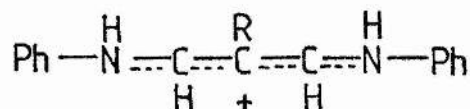
XXXIII $R_1 = H, R_2 = -$

XXXIV $R_1 = H, R_2 = Ph$

XXXV $R_1 = Me, R_2 = Ph$

a = fix parallel

b = fix perpendicular



XXXVI R=H

XXXVII R=Ph

For the phenyl derivatives, XXXIVa and XXXVa, the cations had the phenyl group fixed planar, but all other geometric variables were allowed to refine. In addition, the phenyl groups were started in the perpendicular position, XXXIVb and XXXVb, and allowed to refine, which resulted in no change in the dihedral angle i.e. they stay perpendicular. When starting the phenyl group parallel and allowing the dihedral angle to optimise, the molecule hits a part of the curve which has a very shallow curvature and this gradient is less than the default convergence criterion. Therefore the dihedral angle can change about 15° for only 5 kJmol^{-1} of energy.

The energies for XXXIII, XXXIVa,b and XXXVa,b are listed below along with the energy difference, ΔE , for the pairs.

	E (kJmol ⁻¹)	ΔE (kJmol ⁻¹)
XXXIII	773.9	
XXXIVa	930.5	53.5
XXXIVb	877.0	
XXXVa	970.1	108.5
XXXVb	861.6	

	Charges/e				
	XXXIII	XXXIVa	XXXIVb	XXXVa	XXXVb
N1	-0.29	-0.30	-0.30	-0.30	-0.30
C2	0.14	0.14	0.14	0.14	0.14
C3	0.13	0.13	0.13	0.15	0.15
N4	-0.29	-0.29	-0.29	-0.31	-0.30
C5	0.32	0.32	0.33	0.30	0.31
C6	-0.33	-0.25	-0.28	-0.22	-0.27
C7	0.32	0.32	0.33	0.30	0.32
C8	-	-	-	0.01	0.01
C9	-	-0.05	-0.10	-0.04	-0.10
C10	-	-0.06	-0.03	-0.05	-0.04
C11	-	-0.04	-0.05	-0.04	-0.05
C12	-	-0.03	-0.02	-0.02	-0.02
C13	-	-0.04	-0.05	-0.04	-0.05
C14	-	-0.06	-0.03	-0.07	-0.04

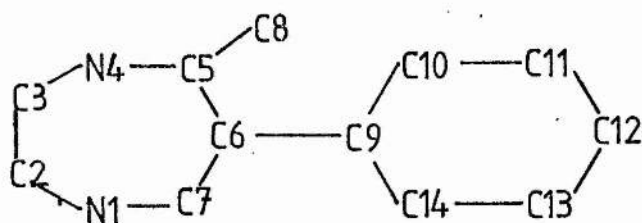


Table 5.5.1.

	Bond Orders				
	XXXIII	XXXIVa	XXXIVb	XXXVa	XXXVb
N1C2	0.903	0.905	0.909	0.907	0.910
C2C3	0.960	0.961	0.960	0.962	0.960
C3N4	0.906	0.910	0.908	0.900	0.903
N4C5	1.346	1.325	1.339	1.306	1.320
C5C6	1.351	1.331	1.338	1.300	1.308
C6C7	1.353	1.333	1.343	1.345	1.359
C7N1	1.344	1.332	1.333	1.321	1.323
C6C9	-	0.983	0.964	0.986	0.965
C9C10	-	1.373	1.385	1.401	1.389
C10C11	-	1.426	1.422	1.396	1.418
C11C12	-	1.399	1.405	1.429	1.407
C12C13	-	1.413	1.406	1.384	1.404
C13C14	-	1.413	1.419	1.445	1.421
C14C9	-	1.385	1.388	1.350	1.386

Table 5.5.1.

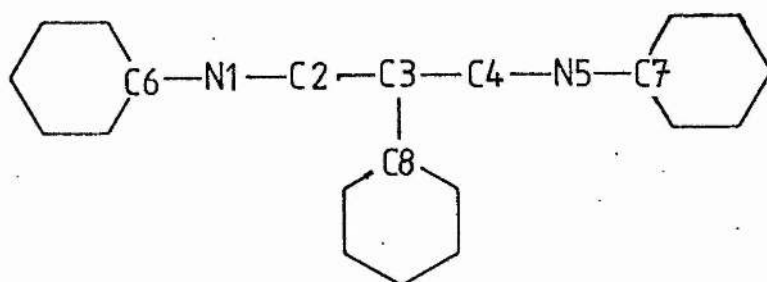
	Charges/e	
	XXXVI	XXXVII
N1	-0.19	-0.19
C2	0.30	0.30
C3	-0.37	-0.31
C4	0.30	0.31
N5	-0.20	-0.20
C6	0.02	0.02
C7	0.02	0.02
C8	0.09(a)	-0.11

	Bond Orders	
	XXXVI	XXXVII
N1C2	1.380	1.381
C2C3	1.324	1.307
C3C4	1.325	1.308
C4N5	1.380	1.381
N1C6	0.949	0.950
N5C7	0.947	0.947
C3C8	0.959(a)	0.980

Energy of XXXVI = 970.2 kJmol^{-1} , XXXVII = $1077.4 \text{ kJmol}^{-1}$.

(a) C8 = H

Table 5.5.1.



The barrier to rotation for the phenyl group when R1=Me is twice that when R1=H, which is as expected, as the methyl group adds extra steric hindrance.

The charges and bond orders for the species XXXIII - XXXVII are tabulated in Table 5.5.1. These indicate that the diazepine part and phenyl part in XXXIV and XXXV are isolated 6π islands. There is, therefore, not total delocalisation of the electrons across the whole molecule; but rather that they exist in two isolated groups. In XXXVI there are three 6π islands and replacement of R=H to R=Ph leads to four 6π islands. Once more there is not total delocalisation of charge.

Chapter Five.

Bibliography.

1. D. Lloyd, R.K. Mackie, G. Richardson and D.R. Marshall. Angew Chem 93 193 (1981); Angew Chem Int Ed Eng 20 190 (1981).
2. D. Lloyd and D.R. Marshall. Chem Ind (London) 335 (1972).
3. D. Lloyd, C. Nyns, C.A. Vincent and D.J. Walton. JCS Perkin II 1441 (1980).
4. M.J.S. Dewar and W. Thiel. J.A.C.S. 99 4899 (1977).
5. W. Thiel. QCPE 353 (1978).
6. M.J.S. Dewar and D. Landman. J.A.C.S. 99 6179 (1977).
7. W. Wentrup and H-W. Winter. J.A.C.S. 102 6159 (1980).
8. E.E. Waali and C.W. Wright. J Org Chem 46 2201 (1981).
9. C. Glidewell and D. Lloyd. Personal Communication.
10. E.E. Waali. J.A.C.S. 103 3604 (1981).
11. L.J. Schaad and B.A. Hess Jnr. J Chem Educ 51 640 (1974).
12. R. Weiss, C. Preisner and H. Wolf. Angew Chem 91 505 (1979); Angew Chem Int Ed Eng 18 472 (1979).
13. R. Weiss, M. Hertel and H. Wolf. Angew Chem 91 506 (1979); Angew Chem Int Ed Eng 18 473 (1979).
14. H. Quast and E. Frankenfeld. Angew Chem 77 680 (1965); Angew Chem Int Ed Eng 4 691 (1965).
15. K.W. Ratts, R.K. Howe and W.G. Phillips. J.A.C.S. 91 6115 (1969).
16. H. Quast and E. Schmitt. Liebigs Ann Chem 732 43 (1970).
17. E.M. Grant, D. Lloyd and D.R. Marshall. Chem Ind (London) 525 (1974).

18. D. Lloyd and H. McNab. JCS Perkin I 1784 (1976).
19. J.D. Dill, P. von R. Schleyer, J.S. Binkley, R. Seeger, J.A. Pople and E. Haselbach. J.A.C.S. 98 5428 (1976).
20. W. Thiel, P. Wiener, J. Stewart and M.J.S. Dewar. QCPE 428 (1982).

Chapter Six.

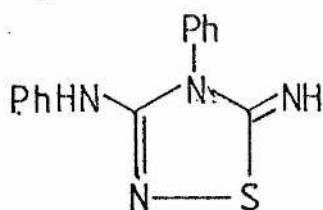
Four Heterocyclic Crystal Structures.

I. 4-PHENYL-3-PHENYLAMINO-1,2,4-THIADIAZOLIN-5-ONE.

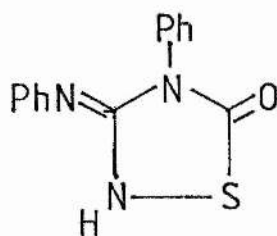
Preparation.

The oxidation of 1-phenylthiourea by H_2O_2 yields a basic compound $C_{14}H_{12}N_4S$ which is known as Hector's Base [1] and whose constitution in the solid state [2], solution [3] and calculationaly [4] is I. Treatment of Hector's Base with concentrated HCl results in a non-basic keto compound, $C_{14}H_{11}N_3OS$, usually called Dost's Keto Compound being obtained. Structure II has been proposed for the structure of Dost's keto Compound, however our x-ray analysis shows it to be III, 4-phenyl-3-phenylamino-1,2,4-thiadiazolin-5-one.

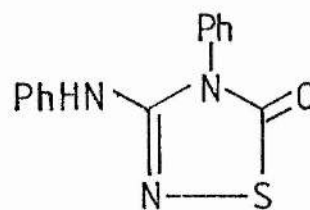
The compound was prepared thus from Hector's Base and repeatedly recrystallised from ethanol to give massive needles about 15mm in length. A fragment cut from one such crystal was used for data collection.



I



II



III

Crystal Data.

$C_{14}H_{11}N_3OS$ (III) is orthorhombic, space group $P2_12_12_1$ (D_2^4 , No. 19) $a=12.252(9)$, $b=11.283(8)$, $c=9.297(10)\text{\AA}$, $U=1285.2\text{\AA}^3$, $Mr=269.32$, $D_c=1.392\text{kg.dm}^{-3}$ for $Z=8$. $F(000)=560.00$. Mo- K_{α} radiation, $\lambda=0.71069\text{\AA}$, $\mu(\text{Mo-}K_{\alpha})=2.01\text{cm}^{-1}$.

Data Collection and Structure Solution.

A Stoe STADI-2 two-circle diffractometer with graphite monochromatised Mo- K_{α} radiation was used in the ω - 2θ scan mode (scan speed $0.0133^\circ\text{s}^{-1}$ in ω , scan width 1.2° in ω) to measure the intensities of 1231 unique reflections with $0^\circ \leq \theta \leq 30.0^\circ$ in the octant $+h,+k,+l$ (layers $h0l$ to $h14l$, $0.000^\circ \leq \mu \leq 26.162^\circ$). Backgrounds were measured at each end of the scan range for a time of (scan time / 2). A standard reflection was measured after every fifty reflections and showed only small random deviations about the mean. Lorentz and polarisation corrections were effected but no correction for absorption was made.

The systematic absences were : in $h00$, $h \neq 2n$; in $0k0$, $k \neq 2n$; in $00l$, $l \neq 2n$. So the space group was determined uniquely as $P2_12_12_1$. All atoms occupy four-fold general positions and the asymmetric unit consists of only one molecule.

Since Dost's Keto Compound crystallises in the same space group as Hector's Base, namely $P2_12_12_1$, and the cell dimensions are very similar it was thought reasonable that the two compounds were isomorphous and so initial coordinates were taken from those of Hector's Base with the imino nitrogen replaced by oxygen.

Six cycles of refinement using SHELX-76 [5] with individual isotropic thermal parameters and 1231 data gave $R=0.166$ and $R_g=0.179$. Introduction of anisotropic thermal parameters for all non-hydrogen atoms and using 1076 data with $F_0 > 6\sigma F_0$ further reduced R_g to 0.139.

The difference map at this point showed both the position of the unique hydrogen, H3, bonded to the exocyclic phenylamino nitrogen N3 and the position of the majority of phenyl hydrogens. Starting with the coordinates from the difference map for H3 and calculated positions for the phenyl hydrogens constraining the carbon-hydrogen distances in the range $0.96 \pm 0.05 \text{ \AA}$ the hydrogen atom coordinates were thus refined. A further six cycles of full-matrix least-squares refinement with all hydrogen atoms given a common isotropic temperature factor converged R to 0.0964 and R_g to 0.1001. The reduction in R_g was significant at the 99.5% level [6] at all stages of refinement. Identical refinement of the alternative enantiomorph yielded an R_g value of 0.1006 which was significantly worse at the 95% level [6] and so was rejected.

Non-unit weights of either $\omega^{-1} = (\sigma^2(F) + K|F|^2)$ or $\omega^{-1} = \sigma^2(F)$ were introduced but they increased the R factors substantially and although the molecular geometry was essentially unchanged the esd's were increased by a factor of two or three. Hence unit weights were used.

Complex neutral atom scattering factors [7,8] were used for all atoms and 206 parameters were varied in the final cycles of refinement and comprised of 90 positional parameters, 114 anisotropic thermal parameters, one isotropic thermal parameter and one overall scale factor. All parameter shifts in the final cycle were less than 0.28 σ .

The equivalent isotropic temperature parameter, U , is defined as the geometric mean of the diagonal components of the diagonalised matrix of U_{ij} .

Fractional Atomic Coordinates ($\times 10^4$; for H $\times 10^3$).
and Equivalent Isotropic Temperature Factors ($\text{\AA}^2, \times 10^4$).

	x	y	z	U
S1	2205(3)	3712(3)	4571(4)	478
N1	1822(8)	2382(9)	5188(4)	366
N2	753(8)	2653(8)	3181(9)	301
N3	521(8)	910(8)	4577(11)	345
O1	1024(8)	4501(8)	2187(10)	458
C1	1047(9)	1938(9)	4368(12)	310
C2	1304(10)	3707(14)	3042(14)	412
C3	627(10)	143(10)	5794(11)	343
C4	1568(11)	121(12)	6643(15)	461
C5	1596(12)	-623(15)	7801(16)	526
C6	778(14)	-1362(14)	8155(14)	461
C7	-184(13)	-1339(13)	7286(15)	522
C8	-237(12)	-579(11)	6127(14)	426
C9	-40(9)	2302(9)	2101(12)	306
C10	294(11)	1604(12)	957(14)	441
C11	-472(15)	1320(13)	-73(14)	524
C12	-1550(13)	1800(15)	50(17)	482
C13	-1847(12)	2450(16)	1178(21)	623
C14	-1067(11)	2786(14)	2215(16)	479
H3	2(11)	37(11)	394(14)	
H4	208(8)	80(7)	650(14)	
H5	210(9)	-27(11)	844(11)	
H6	82(11)	-194(9)	894(9)	
H7	-63(9)	-205(7)	737(15)	
H8	-91(6)	-19(11)	575(14)	
H9	102(7)	120(10)	95(14)	
H11	-33(11)	59(7)	-63(12)	

H12	-215(8)	190(10)	-66(11)
H13	-251(7)	294(10)	113(15)
H14	-128(10)	334(10)	303(9)

Geometry of the Molecule.

Bond Lengths (\AA).

S1-N1	1.673(10)	C9-C14	1.357(16)
S1-C2	1.800(13)	C10-C11	1.378(18)
C1-N1	1.316(14)	C11-C12	1.432(21)
C1-N2	1.414(13)	C12-C13	1.331(22)
C1-N3	1.341(13)	C13-C14	1.409(20)
C2-O1	1.204(17)	N3-H3	1.05(13)
C2-N2	1.374(17)	C4-H4	1.00(5)
C3-N3	1.431(14)	C5-H5	0.94(5)
C3-C4	1.398(16)	C6-H6	0.98(5)
C3-C8	1.371(17)	C7-H7	0.97(5)
C4-C5	1.366(18)	C8-H8	1.00(5)
C5-C6	1.344(21)	C10-H10	1.00(5)
C6-C7	1.429(19)	C11-H11	0.98(5)
C7-C8	1.379(18)	C12-H12	1.00(5)
C9-N2	1.452(13)	C13-H13	0.98(5)
C9-C10	1.385(16)	C14-H14	1.02(5)

Bond Angles ($^{\circ}$).

C1-N1-S1	110.2(8)	N3-C3-C8	117.9(11)
C1-N2-C2	116.3(10)	C4-C3-C8	119.9(11)
C2-S1-N1	95.6(6)	C3-C4-C5	118.5(13)
N1-C1-N2	114.7(10)	C4-C5-C6	123.7(14)
N2-C2-S1	103.3(10)	C5-C6-C7	117.7(12)
O1-C2-S1	125.6(11)	C6-C7-C8	119.5(13)

O1-C2-N2	131.1(12)	C7-C8-C3	120.6(13)
C1-N2-C9	123.7(9)	C9-C10-C11	117.7(13)
C2-N2-C9	120.0(10)	C10-C11-C12	119.0(13)
N1-C1-N3	126.3(11)	C11-C12-C13	121.5(14)
N2-C1-N3	119.0(10)	C12-C13-C14	120.1(15)
N2-C9-C10	119.3(10)	C13-C14-C9	117.5(14)
N2-C9-C14	116.8(11)	C14-C9-C10	123.6(12)
C1-N3-C3	126.5(10)	C1-N3-H3	135(7)
N3-C3-C4	122.2(11)	C3-N3-H3	98(7)

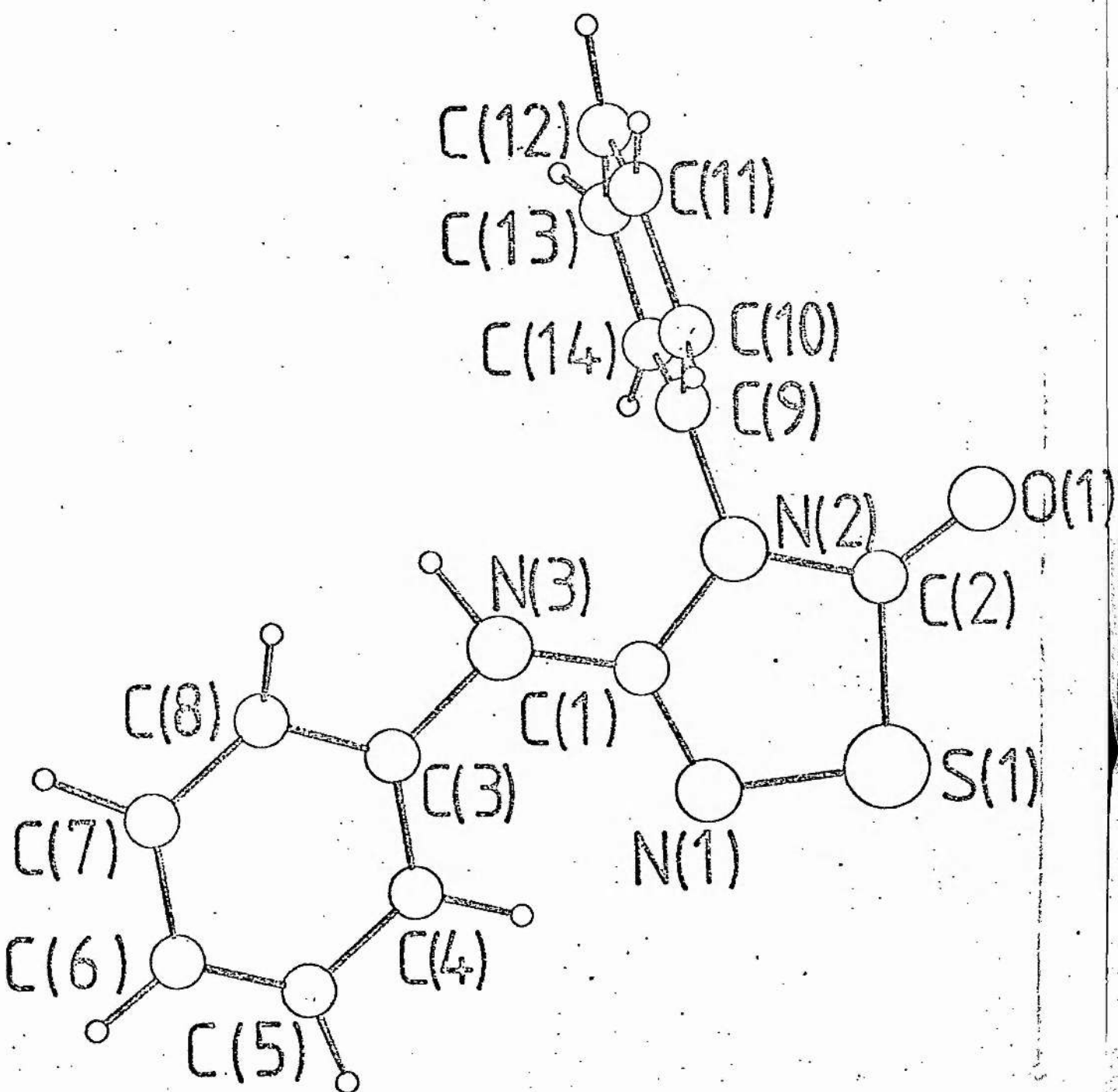


Figure 6.1.1. Geometry and atom labelling scheme.

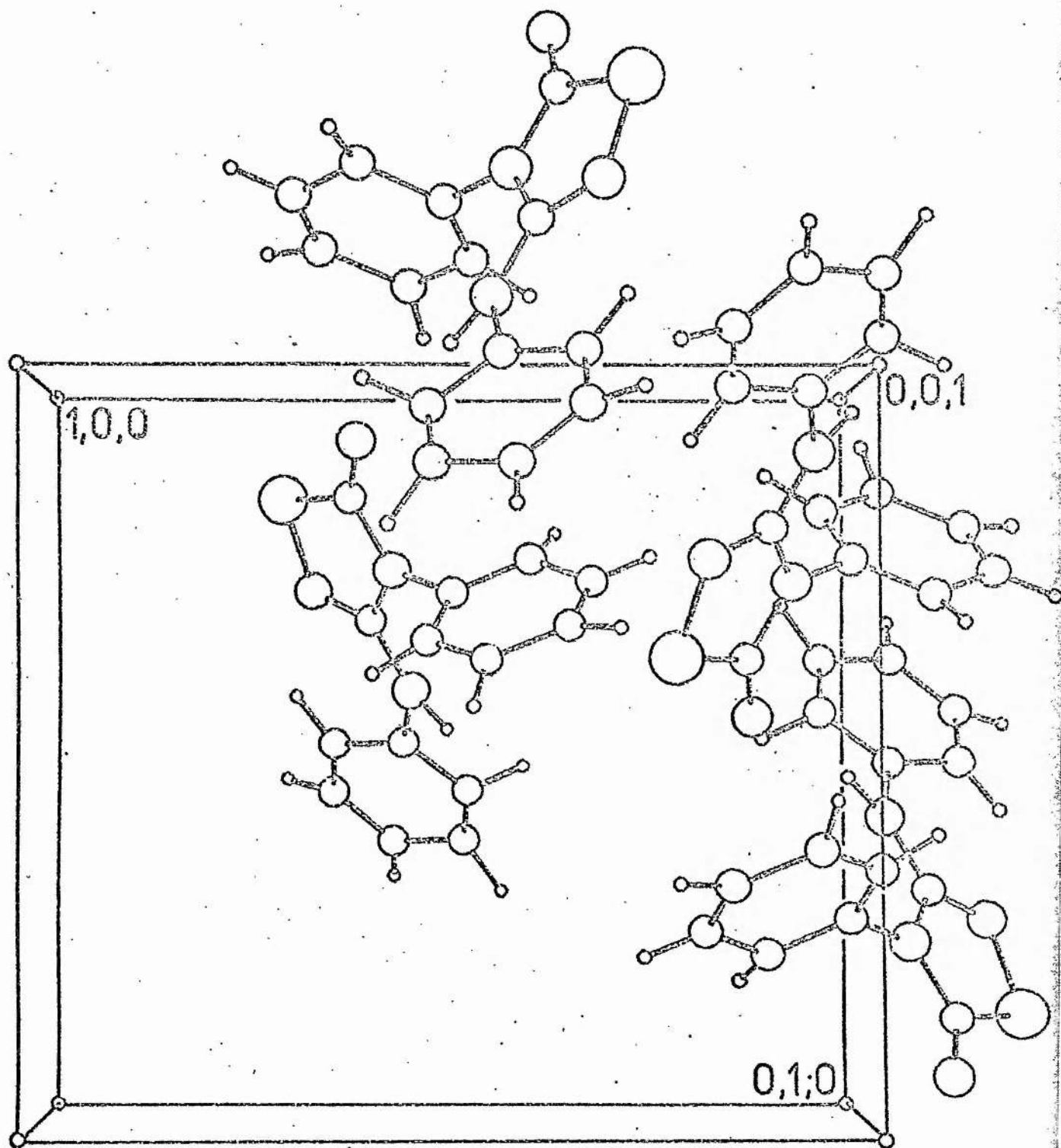
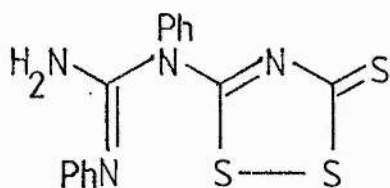


Figure 6.1.2. Unit cell.

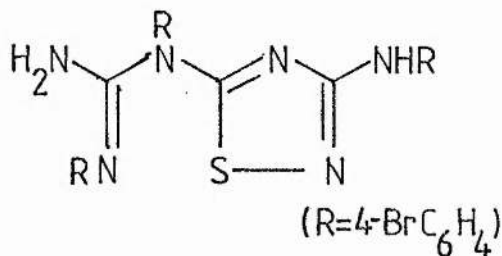
II. 5-(N-METHYLTHIOCARBAMOYLIMINO)-4-PHENYL-3-PHENYLAMINO-4H-1,2,4-THIADIAZOLINE.

Preparation.

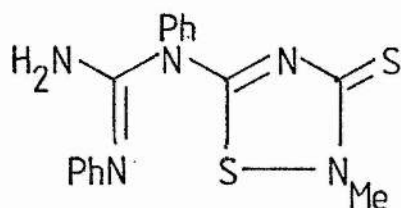
The 1:1 adduct of Hector's Base (I) with CS_2 and 4-bromophenylcyanamide have the structures (IV) and (V) respectively. In each case a heterocyclic rearrangement has occurred and in the light of this plausible structures for the 1:1 adduct of Hector's Base with MeNCS were thought to be (VI) and (VII). However x-ray structure analysis shows the adduct to be (VIII), 5-(N-methylthiocarbamoylimino)-4-phenyl-3-phenylamino-4H-1,2,4-thiadiazoline in which no rearrangement of the heterocyclic system has taken place. The adduct was prepared by reaction of Hector's Base (I) with methylisothiocyanate in ethanol and crystals suitable for x-ray work were obtained from ethanol/acetone solution.



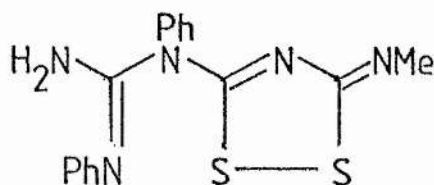
IV



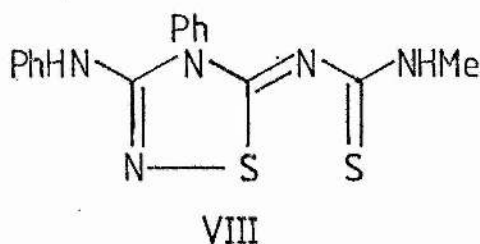
V



VI



VII



Crystal Data.

$C_{16}H_{15}N_5S_2$ (VIII) is monoclinic, space group $P2_1/c$ (C_{2h}^5 , No. 14) $a=9.487(6)$, $b=12.447(9)$, $c=10.063(5)\text{\AA}$, $\beta=103.15(4)^\circ$: $U=1621.9\text{\AA}^3$, $Mr=341.45$, $D_c=1.398\text{kg.dm}^{-3}$ for $Z=4$. $F(000)=712$, Mo- $K\alpha$ radiation, $\lambda=0.71069\text{\AA}$, $\mu(\text{Mo-}K\alpha)=2.85\text{cm}^{-1}$.

Data Collection and Structure Solution.

A Stoe STADI-2 two-circle diffractometer with graphite monochromatised Mo- $K\alpha$ radiation operating in the ω - 2θ scan mode with a scan speed of 0.01°s^{-1} in ω and scan width of 1.0° in ω was used to measure the intensities of 1405 unique reflections having $0^\circ \leq \theta \leq 30^\circ$ in the quadrant $+\underline{h}, +k, +l$ ($h0-201$; $0.000^\circ \leq \mu \leq 24.038^\circ$). Backgrounds were measured at each end of the scan range for a time of (scan time / 2). The intensities of standard reflections for each layer showed only small random deviations about their means. Lorentz and polarisation corrections were applied but no correction for absorption was made.

The systematic absences were : $0k0$, $k=2n$; $h0l$, $l=2n$ and so the space group was uniquely assigned as $P2_1/c$. The asymmetric unit consists of one molecule.

Structure solution and refinement was carried out by the direct methods strategy in SHELX-76 [5]. Starting from a recognisable molecular fragment found in the initial E-map all the heavy atom framework was located using a series of difference maps. Refinement by three cycles of full-matrix least-squares with 1051 data having $F_0 > 6 \sigma F_0$ and anisotropic thermal parameters for sulphur and individual isotropic thermal parameters for carbon and nitrogen gave $R=0.1026$ and $R_g=0.1136$. Anisotropic temperature factors for carbon and nitrogen were then introduced and in a further three cycles reduced R to 0.0882 and R_g to 0.0984. Phenyl hydrogen atoms were then included in calculated positions with a carbon-hydrogen distance of 1.08 Å and common isotropic temperature factor and in another three cycles reduced R to 0.0816 and R_g to 0.0909. This last reduction in R_g was not significant [6].

Throughout the duration of the anisotropic refinement two of the carbon atoms, namely C(5) and C(8), were marginally but persistently non-positive definite and these two atoms were refined isotropically in subsequent cycles.

Inspection of the difference map at this stage revealed clearly the position of H(1) bonded to N(3) and its position was refined with an individual temperature factor, however there was no definitive indication of the position of H(2) which is bonded to N(5). The final R factors were $R=0.0832$ and $R_g=0.0934$. All atoms had complex neutral atom scattering factors [7,8] and in the final cycles of refinement 203 parameters were varied and consisted of 72 positional parameters, 126 anisotropic thermal parameters, four isotropic temperature parameters and one overall scale factor. All the parameter shifts were less than 0.07σ and a final difference map indicated that no electron density greater than 0.50\AA^{-3} was present. No significant trends showed up from the variation of $\sum \omega^2$ with parity group, $\sin \theta$, F_0 and $|h|$, $|k|$ or $|l|$.

The equivalent isotropic temperature parameter, U , is defined as the geometric mean of the diagonal components of the diagonalised matrix of U_{ij} .

Fractional Atomic Coordinates ($\times 10^4$, for H $\times 10^3$)
and Equivalent Isotropic Temperature Factors ($\text{\AA}^2 \times 10^4$).

	x	y	z	U
S1	4738(4)	1141(2)	-1069(3)	256
S2	2890(4)	-66(2)	-2254(3)	313
N1	5729(11)	1844(7)	-141(10)	263
N2	4245(10)	1456(6)	1239(9)	44
N3	5987(12)	2427(7)	2028(12)	237
N4	2714(11)	469(6)	227(10)	217
N5	1218(11)	-481(7)	-592(11)	295
C1	5380(15)	1923(8)	1029(13)	187
C2	3737(13)	938(7)	156(13)	163
C3	2236(13)	-15(9)	-835(13)	273
C4	509(17)	-1091(10)	-1562(16)	334
C5	3726(12)	1423(7)	2482(12)	217 (a)
C6	3900(15)	769(9)	3228(14)	377
C7	3386(15)	744(10)	4434(14)	398
C8	2700(14)	1363(8)	4804(14)	352 (a)
C9	2518(14)	2015(9)	4061(14)	316
C10	3053(14)	2054(8)	2845(13)	332
C11	7162(14)	2919(8)	1881(13)	204
C12	3853(14)	2998(9)	2986(14)	352
C13	9440(15)	3476(9)	2876(15)	399
C14	9392(16)	3888(9)	1691(16)	387
C15	8204(18)	3812(9)	606(15)	457
C16	7035(15)	3351(9)	719(15)	375
H1	572(14)	239(8)	272(14)	306 (a)

(a) Atoms refined isotropically.

Geometry of the Molecule.Bond Lengths (\AA).

S1-N1	1.692(11)	C6-C7	1.407(22)
N1-C1	1.301(18)	C7-C8	1.356(22)
C1-N2	1.404(18)	C8-C9	1.352(21)
N2-C2	1.414(15)	C9-C10	1.429(21)
S1-C2	1.754(14)	C10-C5	1.365(19)
C2-N4	1.283(17)	C1-N3	1.361(17)
N4-C3	1.356(16)	N3-C11	1.441(18)
C3-N5	1.328(18)	C11-C12	1.400(17)
C4-N5	1.497(19)	C12-C13	1.351(22)
C3-S2	1.683(14)	C13-C14	1.385(23)
S1-S2	2.824(5)	C14-C15	1.385(20)
N2-C5	1.446(16)	C15-C16	1.395(23)
C5-C6	1.354(20)	C16-C11	1.373(20)
N3-H1	0.80(15)		

Bond Angles ($^{\circ}$).

S1-N1-C1	110.7(9)	S1-S2-C3	85.2(5)
N1-S1-C2	94.6(6)	N2-C5-C6	119.4(12)
N1-S1-S2	170.9(4)	N2-C5-C10	118.1(11)
N1-C1-N2	115.8(11)	C5-C6-C7	118.8(14)
N1-C1-N3	125.8(13)	C6-C5-C10	122.5(13)
C1-N2-C2	113.2(10)	C6-C7-C8	119.6(15)
C1-N2-C5	125.2(10)	C7-C8-C9	121.8(15)
N2-C1-N3	118.3(12)	C8-C9-C10	119.3(14)
N2-C2-S1	105.6(8)	C9-C10-C5	118.0(13)

N2-C2-N4 119.6(12)
C2-N2-C5 121.2(10)
S1-C2-N4 134.8(10)
C2-S1-S2 76.3(4)
C2-N4-C3 118.3(11)
N4-C3-N5 111.3(12)
S2-C3-N4 125.4(10)
C3-N5-C4 123.6(12)
S2-C3-N5 123.2(10)
H1-N3-C1 116(10)

C1-N3-C11 121.1(12)
N3-C11-C12 118.7(12)
N3-C11-C16 119.6(11)
C11-C12-C13 119.3(13)
C12-C11-C16 121.4(13)
C12-C13-C14 121.0(13)
C13-C14-C15 119.3(15)
C14-C15-C16 120.7(14)
C15-C16-C11 117.9(12)
H1-N3-C11 123(10)

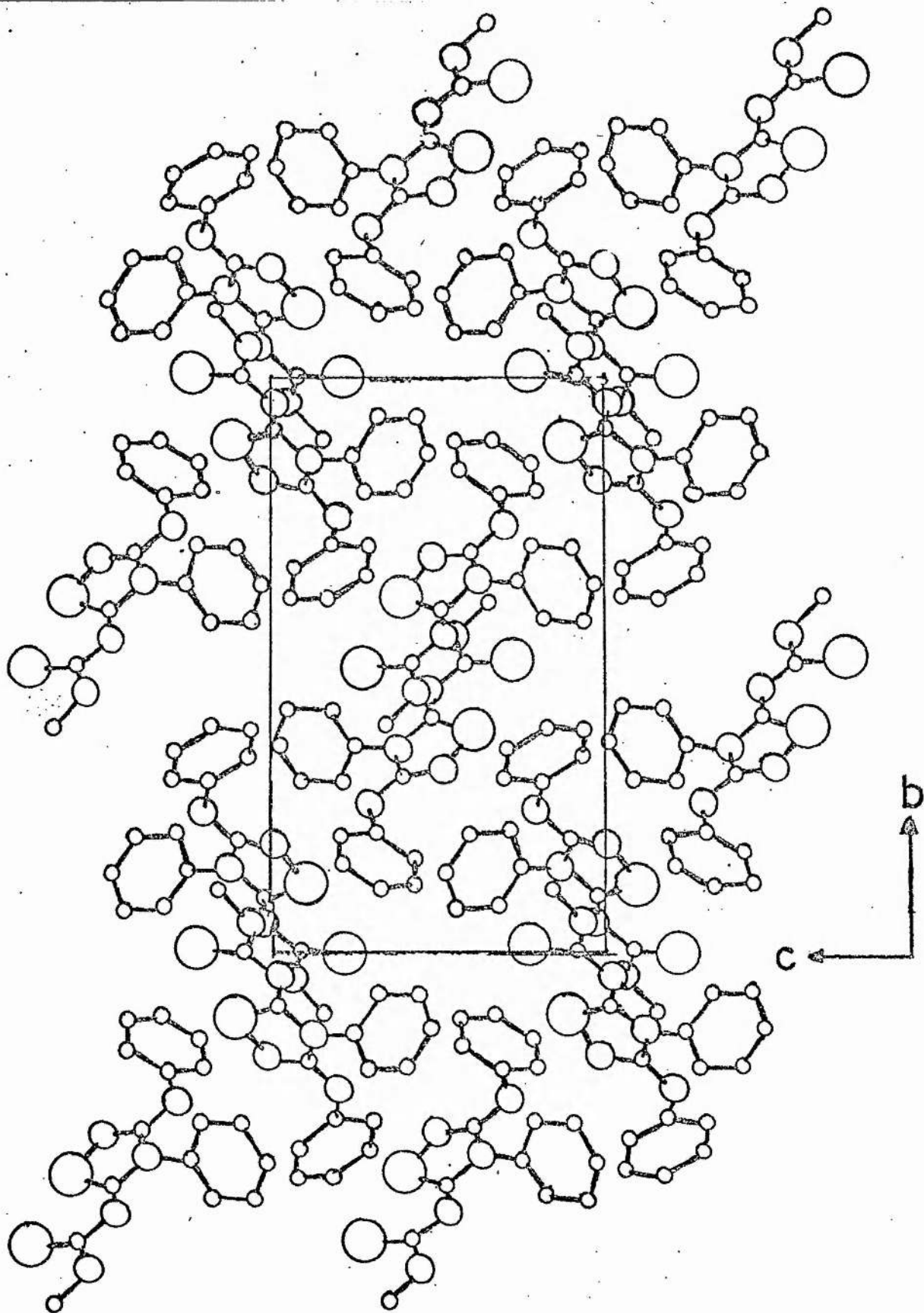
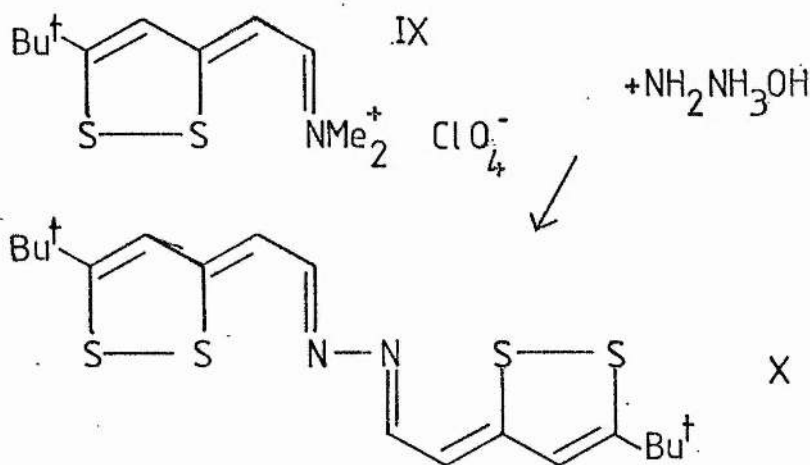


Figure 6.2.2. Unit cell.

III. N,N'-BIS[2-(5-t-BUTYL-3H-1,2-DITHIOL-3-YLIDENE)-ETHYLIDENE]HYDRAZINE.

Preparation.

Crystals suitable for x-ray work were kindly provided by Professor D.H. Reid and Mr. A.M. McRoberts. The title compound (X) was prepared by the treatment of the Vilsmeier salt (IX) with hydrazine hydrate.



Crystal Data.

$C_{18}H_{24}N_2S_4$ (X) is triclinic, space group $P\bar{1}$ (C_1^1 , No. 2) $a=5.929(3)$, $b=8.898(3)$, $c=9.954(2)\text{\AA}$, $\alpha=92.05(3)$, $\beta=102.12(4)$, $\gamma=104.73(4)^\circ$. $U=494.34\text{\AA}^3$, $Mr=396.66$, $D_c=1.332\text{kg.dm}^{-3}$ for $Z=1$. $F(000)=210$, Mo-K α radiation, $\lambda=0.71069\text{\AA}$, $\mu(\text{Mo-K}\alpha)=4.28\text{cm}^{-1}$.

Data Collection and Structure Solution.

The intensities of 1637 reflections in the hemisphere $+h$, $+k$, $+l$ ($2.5^\circ < \theta < 30^\circ$, $h^2 + k^2 + l^2 \leq 28.650^\circ$) were measured in the ω - 2θ scan mode using a Stoe STADI-2 two-circle diffractometer with graphite monochromatised $\text{Mo-K}\alpha$ radiation with a scan speed of 0.01°s^{-1} in ω and a scan width of 2.0° in ω . Backgrounds were measured at each end of the scan for a time of (scan time / 2). A standard reflection was measured every fifty reflections and showed only small random deviations about its mean. Lorentz and polarisation corrections were applied but no absorption corrections were made.

The fast centrosymmetric direct methods strategy in SHELX-76 [5] was used to solve the structure. The best E-map yielded the positions of all the non-hydrogen atoms in the asymmetric unit and a subsequent difference synthesis provided the hydrogen atom positions. Refinement using 1407 data having $F_o > 6\sigma F_o$ by full-matrix least-squares with anisotropic thermal parameters for all non-hydrogen atoms and with separate common isotropic temperature factors for the hydrogen atoms of the main framework and the t-butyl group rendered an R value of 0.0959 and an Rg of 0.0992.

In the final cycles 147 parameters were varied simultaneously and comprised of 72 positional parameters, 72 anisotropic thermal parameters, two common isotropic temperature factors and one overall scale factor. A final difference map revealed no significant residual electron density. Complex neutral atom scattering factors were

employed for all atoms [7,8] and the reduction in R_g at all stages of the refinement was significant at the 99.5% level [6].

The equivalent isotropic temperature parameter, U , is defined as the geometric mean of the diagonal components of the diagonalised matrix of U_{ij} .

Fractional Atomic Coordinates ($\times 10^4$, $\times 10^3$ for H)
 and Equivalent Isotropic Temperature Factors
 (Common Isotropic Temperature Factors for H (\AA^2 , $\times 10^3$))

	x	y	z	U
S1	1560(4)	3458(2)	1135(2)	39(1)
S2	2623(4)	5830(2)	1961(2)	44(1)
N1	812(12)	643(6)	381(6)	30(3)
C1	5453(13)	5823(8)	2869(7)	29(3)
C2	5971(14)	4460(8)	2714(7)	31(3)
C3	4310(13)	3130(8)	1890(7)	29(3)
C4	5659(169)	1686(8)	1703(8)	38(4)
C5	2864(15)	411(8)	921(8)	36(4)
C6	7053(13)	7336(8)	3682(7)	28(3)
C7	8964(16)	6970(9)	4824(8)	37(4)
C8	5619(19)	8194(10)	4350(9)	46(5)
C9	8244(20)	8365(10)	2694(10)	43(5)
H1	748(15)	443(9)	309(8)	46(13)
H2	606(15)	150(9)	211(8)	46(13)
H3	324(15)	-58(9)	67(8)	46(13)
H4	815(18)	629(12)	537(10)	71(10)
H5	1002(18)	799(11)	535(10)	71(10)
H6	1028(18)	670(11)	436(10)	71(10)
H7	429(18)	840(11)	371(10)	71(10)
H8	689(18)	936(11)	497(9)	71(10)
H9	474(18)	775(11)	520(10)	71(10)
H10	916(18)	933(12)	317(10)	71(10)
H11	904(19)	790(12)	232(10)	71(10)
H12	699(19)	863(11)	192(10)	71(10)

Geometry of the Molecule.

Bond Lengths (Å).

S1..N1	2.489(6)	S1-S2	2.124(3)
S1-C3	1.747(7)	S2-C1	1.732(7)
N1-N1 ^I	1.371(10)	N1-C5	1.293(10)
C1-C1	1.335(10)	C1-C6	1.522(9)
C2-C3	1.429(9)	C3-C4	1.365(10)
C4-C5	1.415(10)	C6-C7	1.534(10)
C6-C8	1.510(12)	C6-C9	1.527(11)
C2-H1	0.91(8)	C4-H2	0.90(8)
C5-H3	1.00(8)	C7-H4	0.94(10)
C7-H5	1.02(10)	C7-H6	1.06(10)
C8-H7	0.96(10)	C8-H8	1.18(10)
C8-H9	1.12(10)	C9-H10	0.94(10)
C9-H11	0.84(10)	C9-H12	1.03(10)

Bond Angles (°).

S2-S1-C3	93.5(2)	S1-S2-C1	96.4(2)
S2-C1-C2	113.9(5)	S2-C1-C6	117.9(5)
C2-C1-C6	128.2(7)	C1-C2-C3	122.5(7)
S1-C3-C2	113.6(5)	S1-C3-C4	119.7(6)
C2-C3-C4	126.6(7)	C3-C4-C5	122.7(8)
N1-C5-C4	117.6(7)	N1 ^I -N1-C5	114.0(7)
C1-C6-C7	109.6(6)	C1-C6-C8	111.0(7)
C1-C6-C9	108.6(6)	C7-C6-C8	108.2(7)
C7-C6-C9	110.1(7)	C8-C6-C9	109.3(7)
S2-S1-N1	173.2		

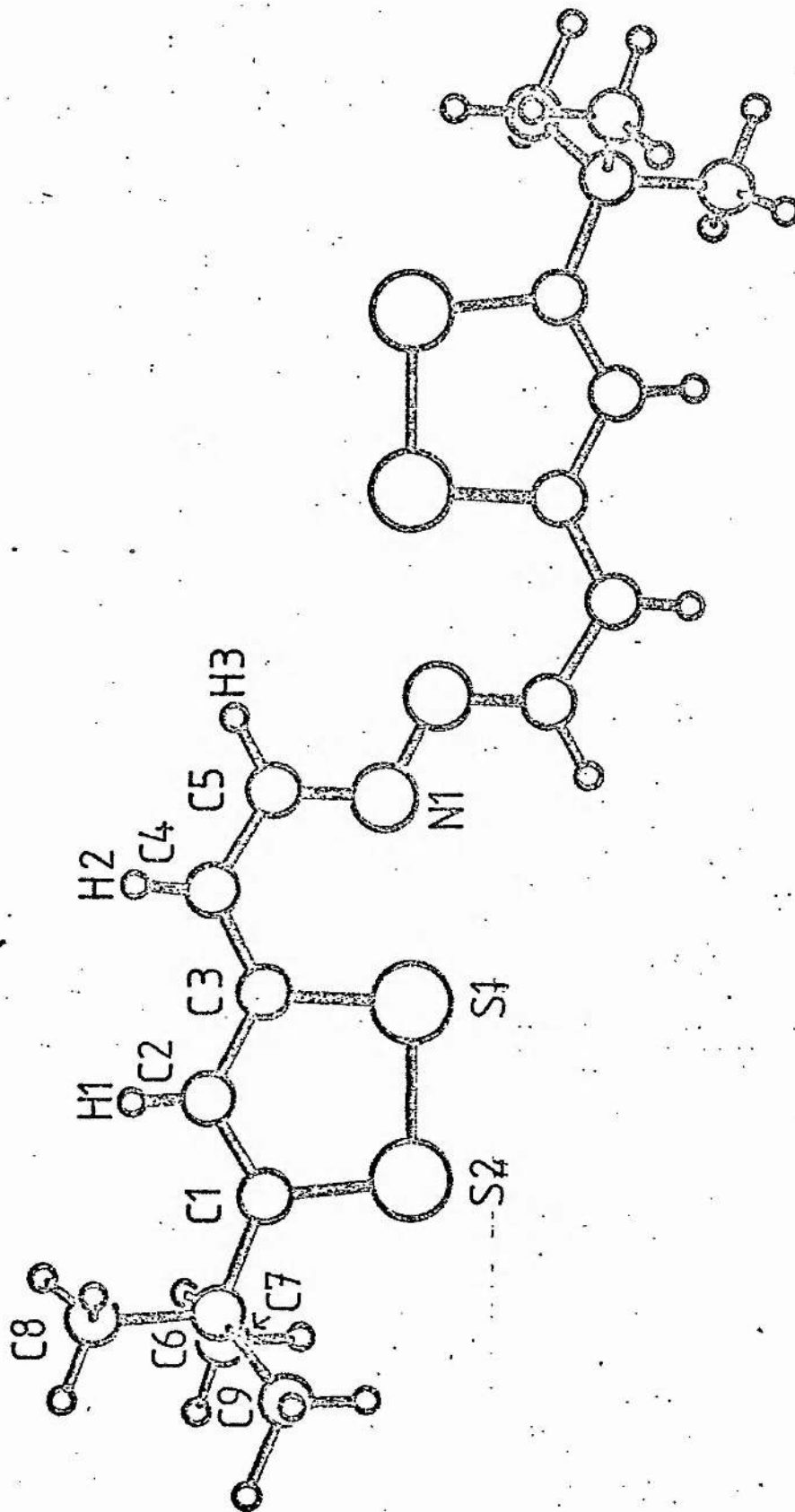


Figure 6.3.1. Geometry and atom labelling scheme.

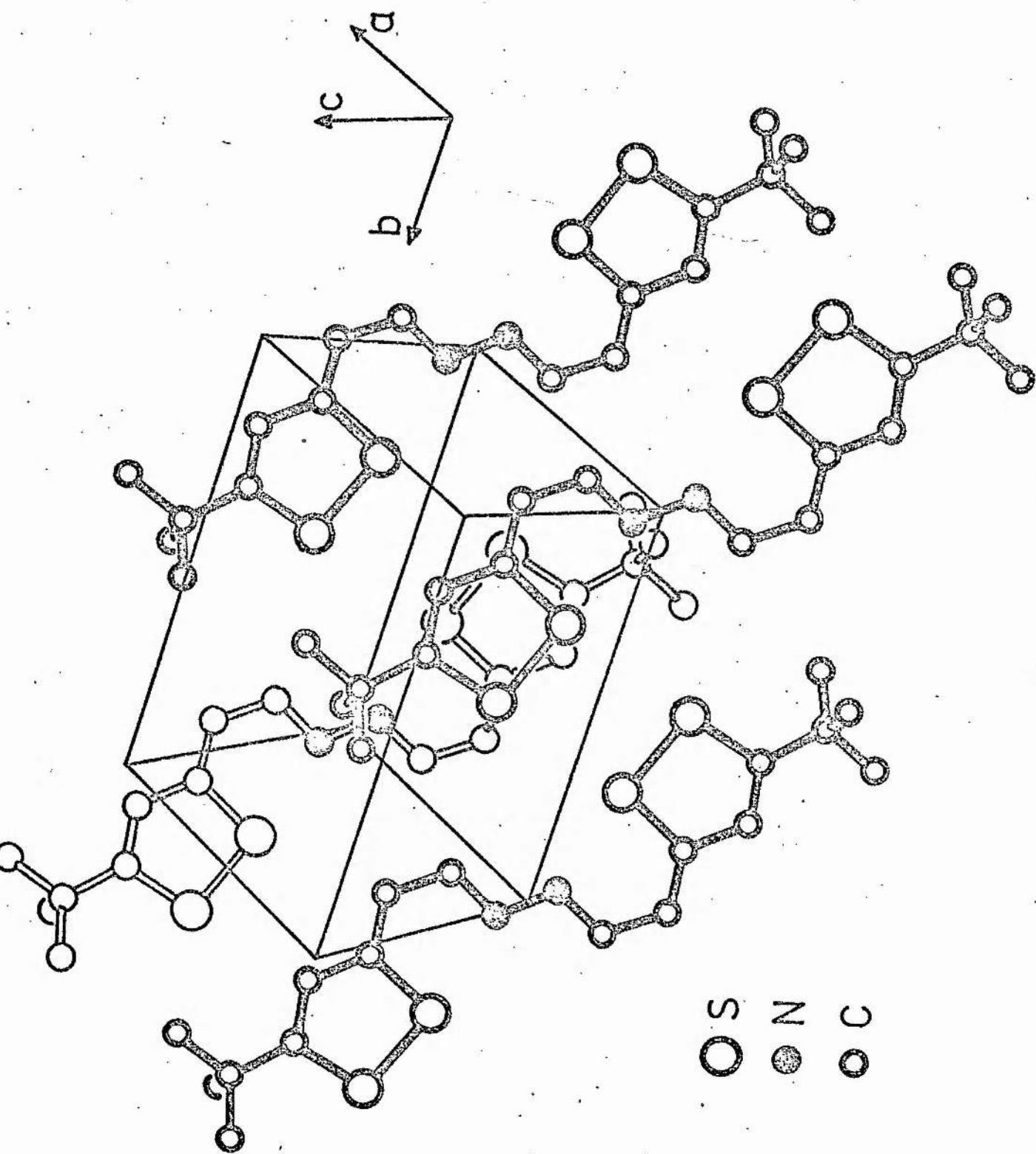
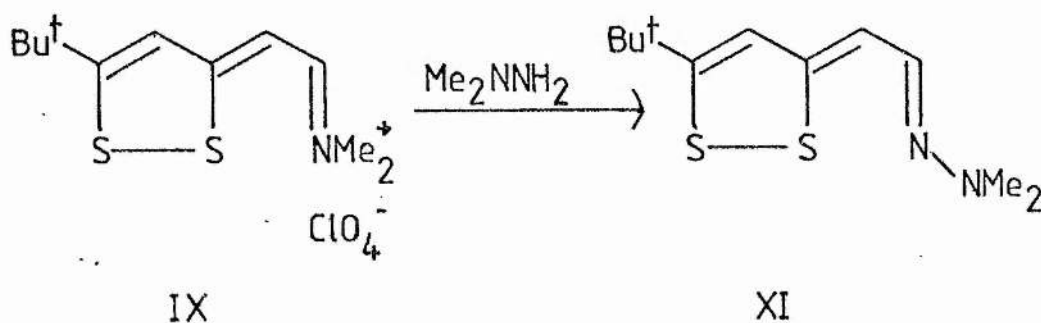


Figure 6.3.2. Unit cell.

IV. N,N-DIMETHYL-N'-[2-(5-t-BUTYL-3H-1,2-DITHIOL-3-YLIDENE)ETHYLIDENE]HYDRAZINE.

Preparation.

Crystals of the title compound (XI) suitable for x-ray investigation were kindly donated by Professor D.H. Reid and Mr. A.M. McRoberts and were prepared from the reaction of the Vilsmeier salt (IX) with N,N-dimethylhydrazine.



Crystal Data.

$\text{C}_{11}\text{H}_{18}\text{N}_2\text{S}_2$ (XI) is triclinic, space group $\text{P}\bar{1}$ (C_1^1 , No. 2).
 $a=5.998(2)$, $b=9.065(2)$, $c=13.078(3)\text{\AA}$, $\alpha=72.04(3)$, $\beta=85.18(4)$,
 $\gamma=73.35(4)^\circ$. $U=648.06\text{\AA}^3$, $M_r=242.41$, $D_c=1.242\text{kg}\cdot\text{dm}^{-3}$ for $Z=2$.
 $F(000)=260$, Mo-K α radiation, $\lambda=0.71069\text{\AA}$, $\mu(\text{Mo-K}\alpha)=3.35\text{cm}^{-1}$.

Data Collection and Structure Solution.

Data were collected using a Stoe STADI-2 two-circle diffractometer with graphite monochromatised Mo-K α radiation. Operating in the ω - 2θ scan mode with a scan speed of 0.01°s^{-1} in ω and scan width of 1.6° in ω , the intensities of 2680 reflections were measured in the hemisphere $+h$, $+k$, $+l$ ($2.5^\circ \leq \theta \leq 30.0^\circ$, $h0-8$ ($0.0^\circ \leq \mu \leq 28.291^\circ$)). Backgrounds were measured at both ends of the scan for a time of (scan time / 2) and standard reflections measured every fifty reflections showed only small random deviations about their means. Implementation of Lorentz and polarisation corrections took place but no correction for absorption was made.

The automatic centrosymmetric direct methods program in SHELX-76 [5] was used to solve the structure. This gave the locations of all the non-hydrogen atoms in the molecule and full-matrix least-squares refinement with anisotropic thermal parameters for this heavy atom framework reduced R from 0.38 to 0.1113 and R_g from 0.37 to 0.1158. A difference Fourier map provided the hydrogen atom positions and these were included in the refinement with separate common isotropic thermal parameters for those in the main skeleton, the t-butyl group and the N-dimethyl group and resulted in final R indices of R=0.0878 and R_g=0.0888 for 2031 data having $F_0 > 6\sigma F_0$.

During the final cycles of refinement 193 parameters were simultaneously varied and these were composed of 99 positional parameters, 90 anisotropic thermal parameters, three common isotropic thermal parameters and one overall scale factor. All the atoms had complex neutral atom scattering factors [7,8] and a final difference map showed no significant residual features. At all stages of refinement the reduction in R_g was significant at the 99.5% level [6].

The equivalent isotropic temperature parameter, U , is defined as the geometric mean of the diagonal components of the diagonalised matrix of U_{ij} .

Fractional Atomic Coordinates ($\times 10^4$, $\times 10^3$ for H) and
 Equivalent Isotropic Temperature Factors ($\times 10^3$)

	x	y	z	U
S1	3732(3)	3038(2)	2302(1)	42(1)
S2	3176(3)	4982(2)	2953(1)	38(1)
N1	3140(9)	7292(6)	3672(4)	38(3)
N2	1841(9)	8037(6)	4385(4)	39(3)
C1	5655(10)	5552(7)	2340(5)	34(3)
C2	6936(11)	4550(7)	1712(5)	37(3)
C3	6309(10)	3289(7)	1621(4)	33(3)
C4	6229(12)	6798(7)	2519(5)	40(4)
C5	4977(12)	7662(7)	3233(5)	41(4)
C6	583(17)	6980(10)	5086(7)	56(5)
C7	3035(16)	8778(10)	4928(7)	54(5)
C8	7609(10)	2051(7)	1072(4)	34(3)
C9	5029(14)	1440(10)	595(6)	51(5)
C10	9085(13)	2810(9)	160(5)	46(4)
C11	9203(13)	633(9)	1897(6)	48(4)
H2	814(11)	471(7)	138(5)	42(10)
H4	780(10)	708(7)	225(5)	42(10)
H5	550(10)	848(7)	338(5)	42(10)
H61	-42(15)	661(10)	461(7)	91(12)
H62	160(16)	611(11)	558(7)	91(12)
H63	-57(16)	755(11)	540(7)	91(12)
H71	453(16)	798(10)	530(7)	91(12)
H72	182(15)	927(10)	542(7)	91(12)
H73	329(15)	987(11)	440(7)	91(12)
H91	495(15)	108(109)	112(7)	81(9)

H92	670(15)	56(10)	46(7)	81(9)
H93	474(14)	238(9)	-22(6)	81(9)
H101	813(14)	372(10)	-49(7)	81(9)
H102	981(15)	209(10)	-22(6)	81(9)
H103	1062(14)	305(9)	51(6)	81(9)
H111	987(14)	-9(10)	146(7)	81(9)
H112	1014(15)	101(10)	211(7)	81(9)
H113	814(15)	15(9)	247(7)	81(9)

Geometry of the Molecule.

Bond Lengths (\AA).

S2..N1	2.541(5)	S1-S2	2.116(2)
S1-C3	1.755(5)	S2-C1	1.762(6)
N1-N2	1.377(6)	N1-C5	1.282(8)
N2-C6	1.444(9)	N2-C7	1.457(9)
C1-C2	1.430(8)	C1-C4	1.359(8)
C2-C3	1.342(8)	C3-C8	1.512(8)
C4-C5	1.431(8)	C8-C9	1.533(9)
C8-C10	1.531(8)	C8-C11	1.531(9)
C2-H2	0.84(6)	C4-H4	1.05(6)
C5-H5	0.96(6)	C6-H61	1.08(9)
C6-H62	0.94(9)	C6-H63	0.89(9)
C7-H71	1.02(9)	C7-H72	1.03(9)
C7-H73	1.06(9)	C9-H91	0.91(8)
C9-H92	0.86(9)	C9-H93	1.26(9)
C10-H101	1.06(8)	C10-H102	0.93(8)
C10-H103	1.16(8)	C11-H111	0.99(9)
C11-H112	0.84(9)	C11-H113	1.02(8)

Bond Angles ($^{\circ}$).

S2-S1-C3	96.2(2)	S1-S2-C1	94.0(2)
S1-S2...N1	171.5(3)	N2-N1-C5	121.7(5)
N1-N2-C6	109.3(5)	N1-N2-C7	116.6(6)
C6-N2-C7	114.9(6)	S2-C1-C2	113.3(4)
S2-C1-C4	120.2(5)	C2-C1-C4	126.4(6)
C1-C2-C3	122.6(5)	S1-C3-C2	113.8(4)
S1-C3-C8	118.1(4)	C2-C3-C8	128.0(5)
C1-C4-C5	123.5(6)	N1-C5-C4	117.5(6)
C3-C8-C9	111.3(5)	C3-C8-C10	109.5(5)
C3-C8-C11	108.7(5)	C9-C8-C10	108.5(6)
C9-C8-C11	109.5(6)	C10-C8-C11	109.3(5)

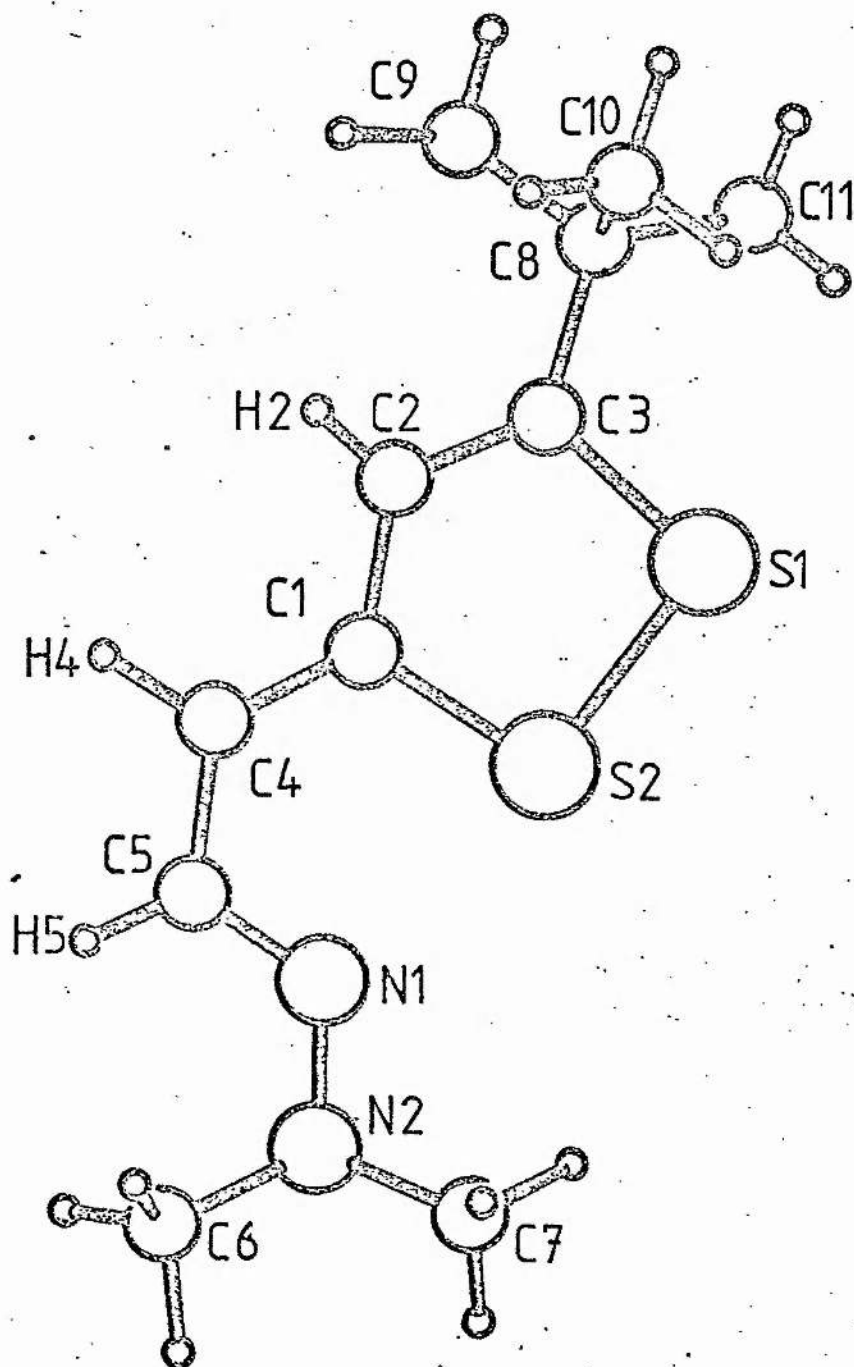


Figure 6.4.1. Geometry and atom labelling scheme.

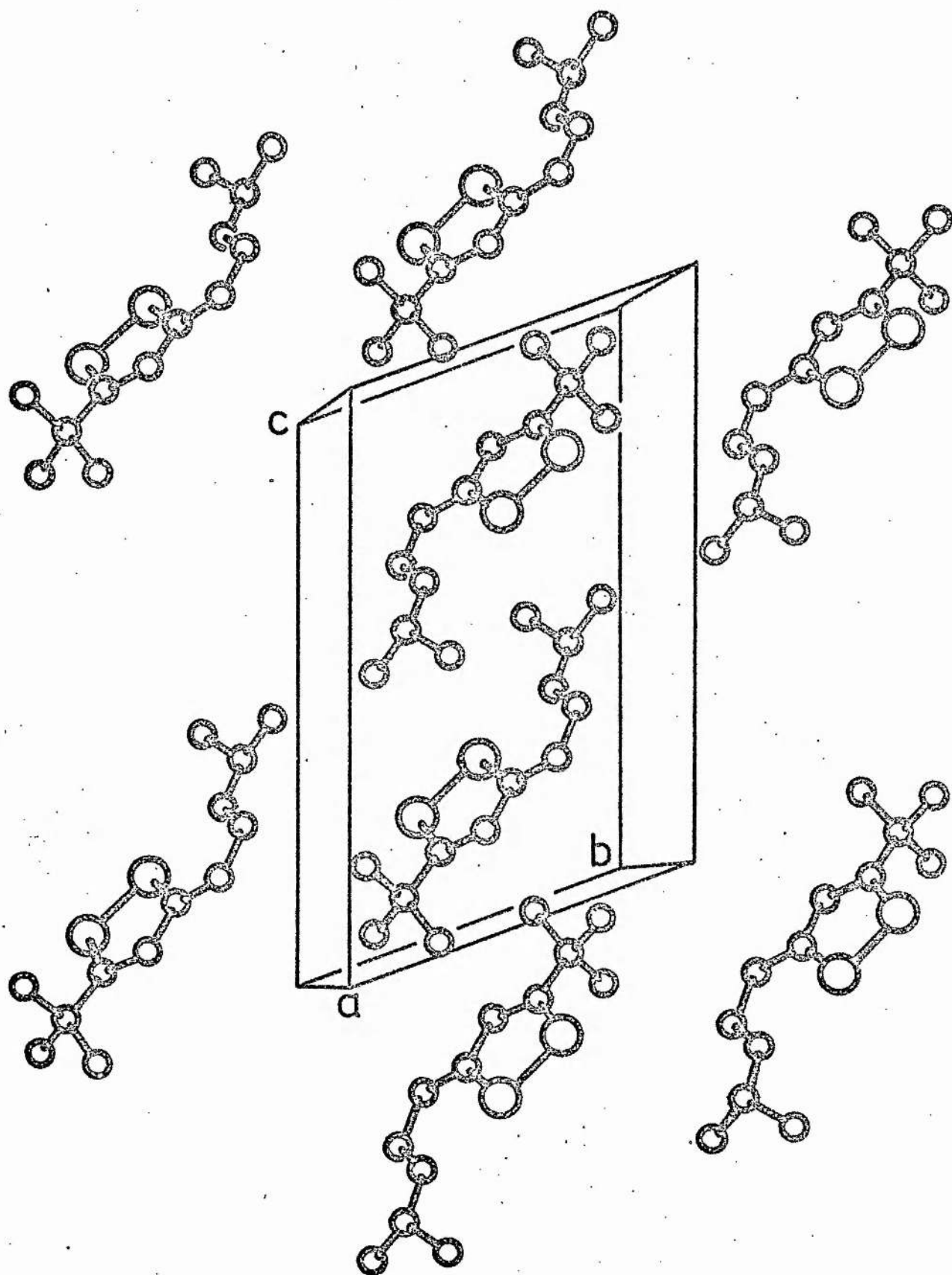


Figure 6.4.2. Unit cell.

Chapter Six.

Bibliography.

1. D.S. Hector. Chem Ber 22 1176 (1889).
2. A.R. Butler, C. Glidewell and D.C. Liles. Acta Cryst B34 3241 (1978).
3. A.R. Butler, C. Glidewell, I. Hussain and P.R. Maw. J Chem Res 114(s),1843(m) (1980).
4. A.F. Cuthbertson and C. Glidewell. J. Mol Struct in press.
5. G.M. Sheldrick. SHELX-76 Program System, University of Cambridge (1976).
6. W.C. Hamilton. Acta Cryst 18 502 (1965).
7. D.T. Cromer and J.B. Mann. Acta Cryst A24 321 (1968).
8. D.T. Cromer and D. Liebermann. J Chem Phys 53 1891 (1970).

Chapter Seven.

Calculations on Heterocycles.

I. Introduction.

Quantum mechanical calculations on heterocycles, in the past, have focused on two techniques, those of ab-initio and CNDO/2 [1]. Both systems allow for the inclusion of d-orbitals, but the latter has a major drawback in that there is no geometry optimisation. This results in x-ray data, which refer to the solid state, being applied in the form of structural parameters to the calculations, which are for isolated molecules in the gas phase. The conformations of most molecules in the solid state are due to intermolecular forces and efficient packing arrangements, and as a consequence of this, the structures cannot really be transferred to the gas phase where intermolecular forces are absent.

This chapter is concerned with MNDO [2] calculations (which allow full geometry optimisation) on various types of heterocyclic systems. Firstly, Hector's Base and its analogues are looked at with respect to their prototropy and adduct formation, and the results can be found in sections II - VII. Sections VIII - XI deal with molecules related to 1,6,6a λ^4 trithiathiophene, with particular attention paid to the point as to which ring, if any, is open. Organic chemistry has been chiefly concerned with mechanistic factors, and so it is of considerable interest to find out if the observed structures, in both the Hector's Base and triheterapentalene series, are the

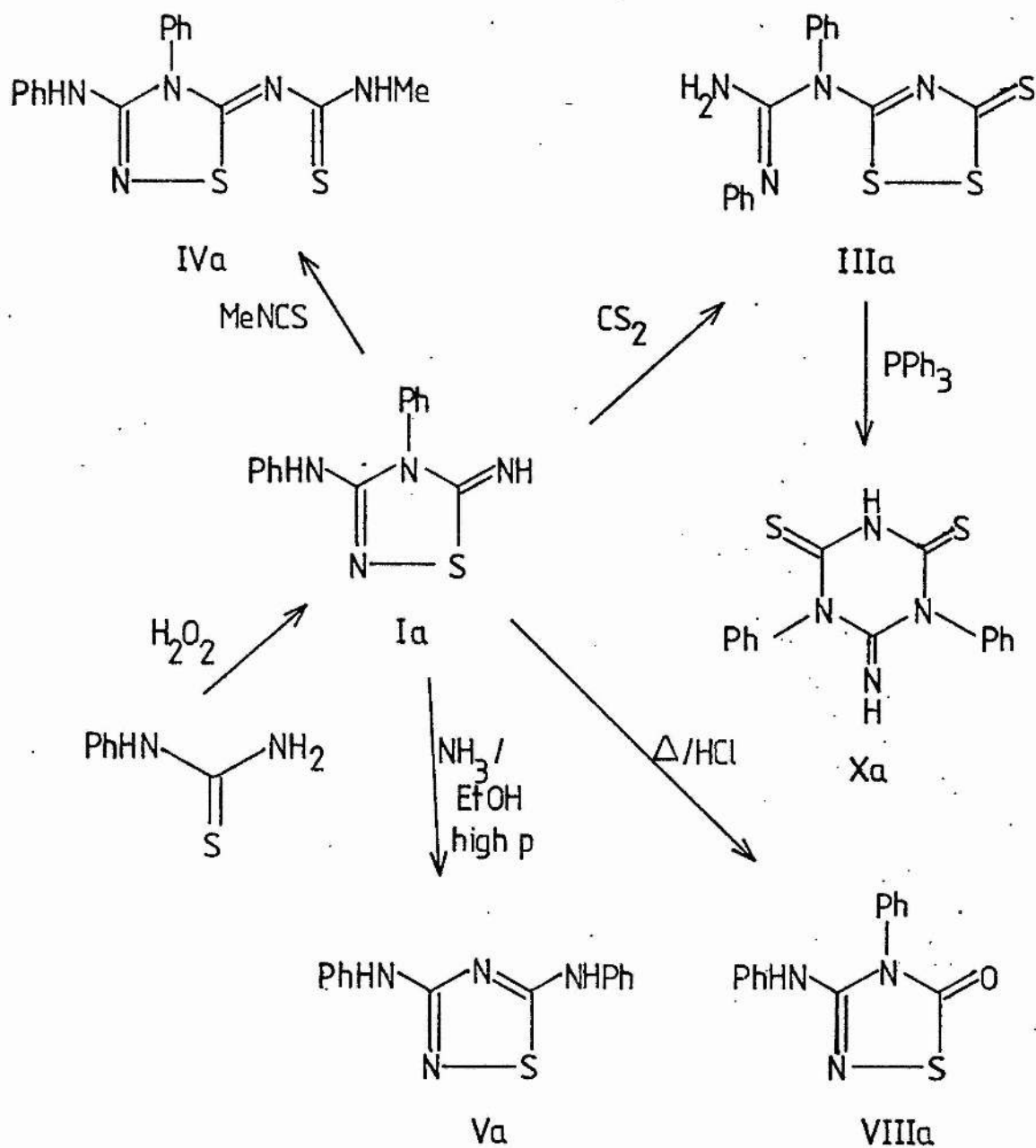


Figure 7.2.1. Reactions and interconversions of Hector's Base.

thermodynamically most stable isomers in each case.

II. Hector's Base and Related Molecules.

Hector's Base is formed from the reaction of 1-phenylthiourea with hydrogen peroxide [3] and its structure has been shown to be Ia rather than IIa, in both the solid state [4] and in solution [5]. In addition Hector's Base forms 1:1 adducts with CS₂ [6] and MeNCS [7] and the solid state structures of these have been found to be IIIa and IVa respectively [8,9]: once more these structures are present in solution [5]. A further three heterocumulenes, MeNCO, PhNCO and PhNCS [10] react likewise with Hector's Base to form adducts IV(b-d), the structures of which were determined by ¹³C and ¹⁵N n.m.r. [5].

Clearly in the CS₂ case a molecular rearrangement has taken place and Akiba et al have described this by the term 'bond-switch' [11]. Similar rearrangements occur for arylcyanamides [11]; however it is by no means apparent from these examples and others [12-14] whether the observed product in each case is the thermodynamically most stable of the possible isomers. Under forcing conditions compounds of type IV rearrange, but this is accompanied by cleavage of the side chain and as a result analogues of IIIa cannot be attained [15].

Treatment of Hector's Base with ethanolic ammonia at high pressure affords Dost's Base [16], the structure of which in solution [5] has been found to be the bis-anilino structure Va as opposed to the bis-imino representation VIa.

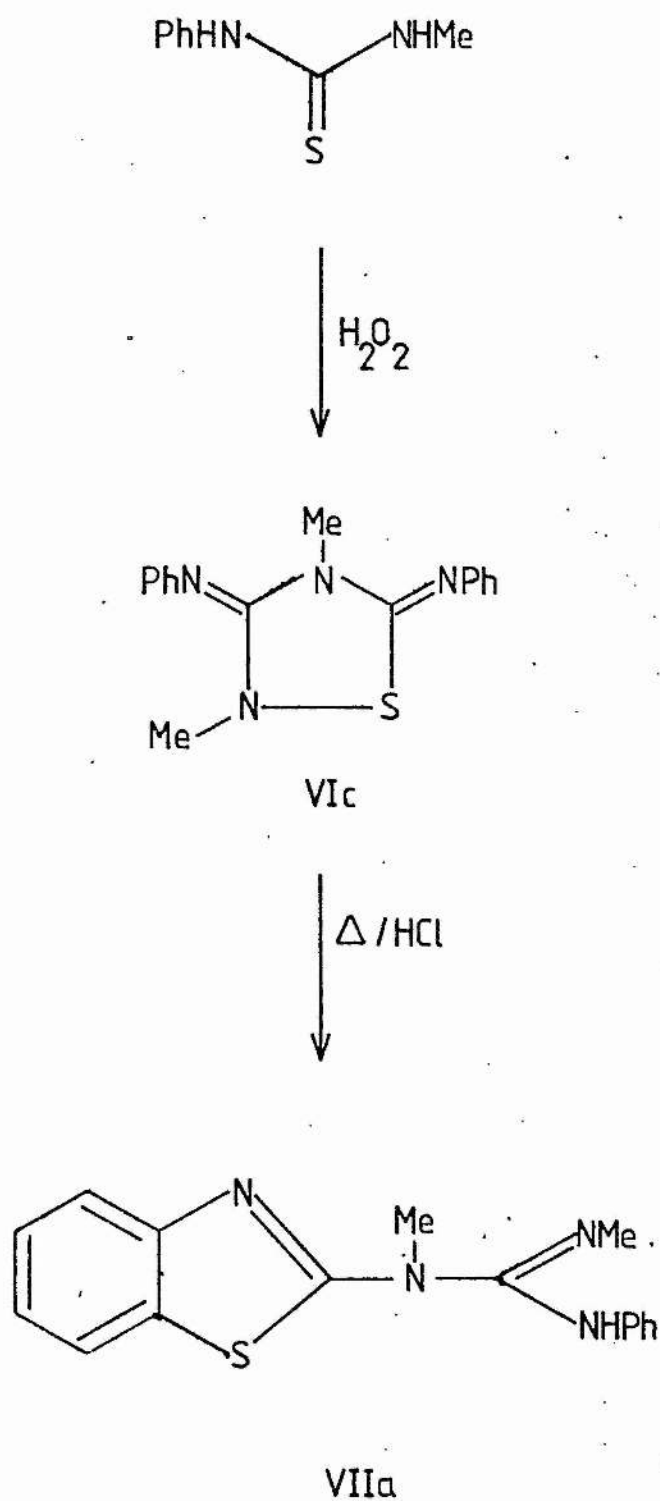


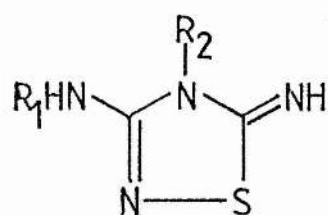
Figure 7.2.2. Reactions of analogues of Hector's Base.

The oxidation of 1-methyl-3-phenylthiourea with hydrogen peroxide gives the bis-imino compound VIc [17], and both VIc and VId, when heated with boiling HCl rearrange to yield the Hegerschaff Bases VIIa and VIIb respectively [17,18]. Hector's Base, Ia, under similar conditions yields Dost's Keto Compound [16], and its structure has been shown to be VIIIa rather than IXa, both by the auspices of x-ray diffraction [19] and ^{13}C and ^{15}N n.m.r. [5]. Dost's Base, on the other hand, does not react with boiling HCl.

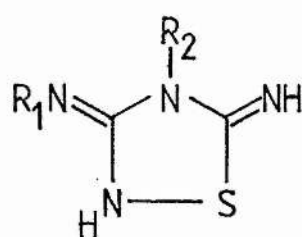
Compound IIIa when it is treated with triphenylphosphine loses one sulphur atom to form X, the structure of which was demonstrated by ^{13}C n.m.r. [20]. The various reactions and interconversions of Hector's Base and its analogues are illustrated in Figures 7.2.1 and 7.2.2.

III. Prototropy.

The question of prototropy arises because although the chemistry of Hector's Base was of considerable interest its structure was unknown, and as a result various authors [21-23] used a number of different representations. There are six possible permutations of two phenyl groups amongst the four distinct nitrogen atoms in the 3,5 diamino -1,2,4-thiadiazoline system and these are shown as structures XI(a-f). On chemical evidence structure XIc was adopted by some workers [23,24], although others preferred XIe [21]. The structure of Hector's Base was subsequently found to be Ia [4], but structure XIc is similar in that the proton R_1 has just migrated to the exocyclic

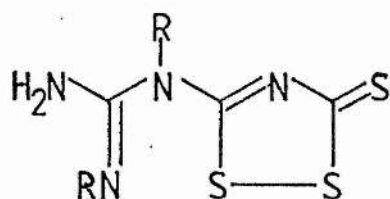


I



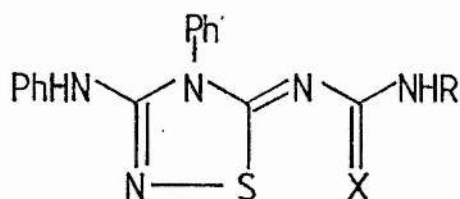
II

- a $R_1=R_2=Ph$
 b $R_1=Ph, R_2=Me$
 c $R_1=Me, R_2=Ph$
 d $R_1=R_2=Me$
-



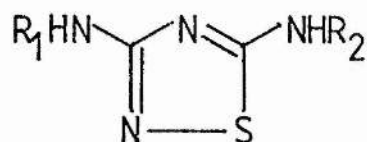
III

- a $R=Ph$
 b $R=Me$



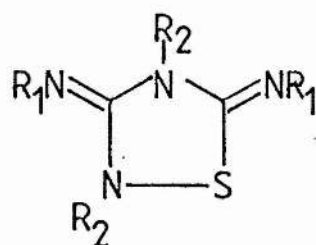
IV

- a $R=Me, X=S$
 b $R=Me, X=O$
 c $R=Ph, X=S$
 d $R=Ph, X=O$
-



V

- a $R_1=R_2=Ph$
 b $R_1=R_2=Me$
 c $R_1=Me, R_2=Ph$



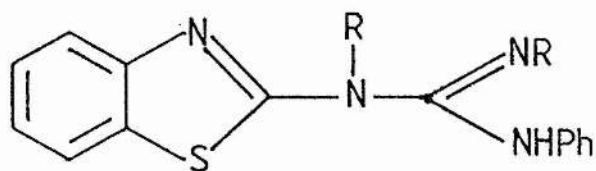
VI

- a $R_1=Ph, R_2=H$
 b $R_1=Me, R_2=H$
 c $R_1=Ph, R_2=Me$
 d $R_1=R_2=Ph$

phenylimino nitrogen. Since XIc was at one time the most accepted form of the six possibilities, MNDO calculations [2,25] were undertaken on I(b-d) and its tautomer II(b-d), IIa = XIc.

Computational problems limited the study of molecules in these series to I(b-d), II(b-d), Vb, VIb, VIII(b-d) and IX(b-d). The reason for this is that the s,p basis set employed by the first release of MNDO is restricted to 75 orbitals and the 'a' structures have at least 87 orbitals in this basis set! Never the less full geometric optimisations were performed on the smaller model pairs amounting to 66 variables for I(b,c), II(b,c), Vb and VIb, and 63 variables for VIII(b,c) and IX(b,c).

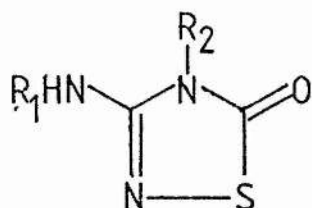
The heats of formation for these molecules are listed in Table 7.3.1, and show that with Hector's Base the structurally observed isomer, I, is always calculated to be more stable than its tautomer, II, for each pair of substituents R_1, R_2 . Therefore, it can be concluded that providing the energy differences between the tautomeric pairs are reasonably large, the substitution of methyl for phenyl will not affect the conclusions and hence structure Ia is probably more stable than IIa and as a result the observed isomer [4,5] is the more stable thermodynamically.



VII

a R=Me

b R=Ph



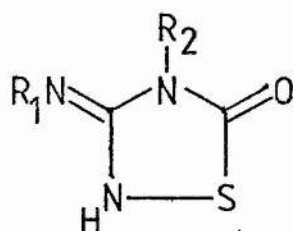
VIII

a $R_1=R_2=Ph$

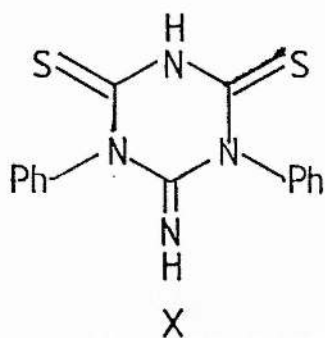
b $R_1=Ph, R_2=Me$

c $R_1=Me, R_2=Ph$

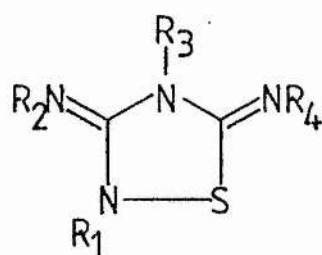
d $R_1=R_2=Me$



IX



X



XI

a $R_1=R_2=H, R_3=R_4=Ph$

b $R_1=R_3=H, R_2=R_4=Ph$

c $R_1=R_4=H, R_2=R_3=Ph$

d $R_2=R_3=H, R_1=R_4=Ph$

e $R_2=R_4=H, R_1=R_3=Ph$

f $R_3=R_4=H, R_1=R_2=Ph$

Species	ΔH_f^θ (kJmol ⁻¹)	Species	ΔH_f^θ (kJmol ⁻¹)
Ib	330.6	IIb	334.9
Ic	327.7	IIc	344.2
Id	199.5	IId	212.8
Vb	157.8	VIb	185.9
VIIIb	92.9	IXb	97.4
VIIIc	88.7	IXc	106.1
VIIId	-39.2	IXd	-24.7

Table 7.3.1. ΔH_f^θ for tautomers.

Continuing with the substitution of methyl for phenyl in Dost's Base, Table 7.3.1 shows that once more the observed isomer V is more stable than protomer VI, and that for Dost's Keto Compound, the structurally observed isomer, either by X-ray diffraction [19] or n.m.r. [5], is always the thermodynamically more stable of the tautomers.

A comparison of the observed and calculated structures for Hector's Base, I, and Dost's Keto Compound, VIII, lends further evidence to the validity of the approach. Both sets of structures can be found in Table 7.3.2 and the similarities between them are quite striking. Admittedly bond lengths to sulphur are calculated 2-4% too short by MNDO [26]. However, the near identity in the structures calculated for I and VIII regardless of substituent show the essential independence of the structure with respect to substituent, and as a result, the model compounds are a valid alternative for Ia and VIIa,

Distances/Å	Ia[4]	Ib	Ic	Id
a	1.691	1.646	1.650	1.647
b	1.761	1.714	1.714	1.713
c	1.402	1.425	1.427	1.425
d	1.386	1.418	1.420	1.421
e	1.294	1.316	1.320	1.318
f	1.264	1.287	1.286	1.287
g	1.365	1.417	1.404	1.408

Angles/°

ab	95.3	96.0	96.4	95.9
bc	104.5	107.2	106.8	107.2
cd	113.7	110.2	110.6	110.3
de	117.6	116.2	116.1	116.0
ea	108.9	110.4	110.1	110.5
bf	131.6	131.2	132.0	131.4
cf	123.9	121.6	121.3	121.4
dg	118.8	119.3	120.0	119.9
eg	123.7	124.5	123.9	124.1

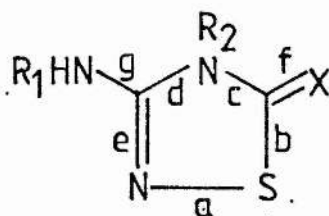
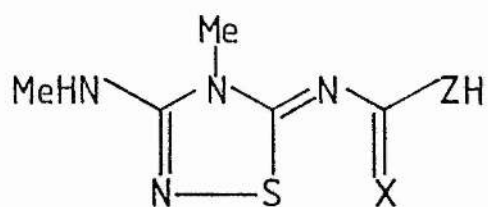


Table 7.3.2. Observed and calculated geometries for Hector's Base.

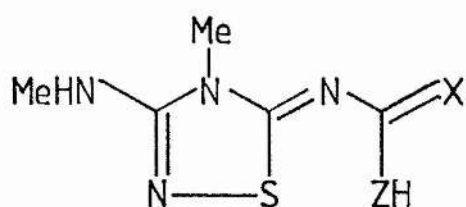
Distances/Å ^o	VIIIta[19]	VIIItb	VIIItc	VIIIt d
a	1.673	1.648	1.648	1.645
b	1.800	1.717	1.714	1.717
c	1.374	1.433	1.437	1.433
d	1.414	1.419	1.419	1.419
e	1.316	1.317	1.320	1.318
f	1.206	1.215	1.214	1.215
g	1.341	1.417	1.401	1.409

Angles/°				
ab	95.5	96.1	96.4	95.9
bc	103.3	106.8	106.5	107.0
cd	116.3	110.3	110.8	110.3
de	114.7	116.2	115.6	115.9
ea	110.2	110.5	110.7	110.9
bf	131.1	128.8	129.6	128.7
cf	125.6	124.3	123.9	124.3
dg	119.0	119.4	120.8	120.0
eg	126.0	124.4	123.6	124.1

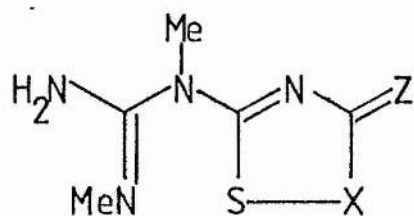
Table 7.3.2. Observed and calculated geometries for Dost's Keto Compound.



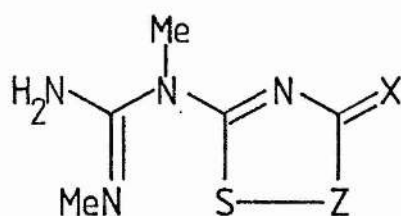
XII



XIII

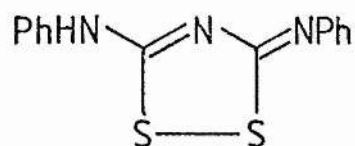


XIV

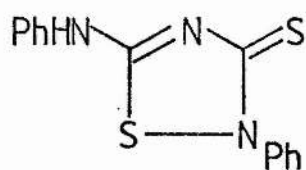


XV

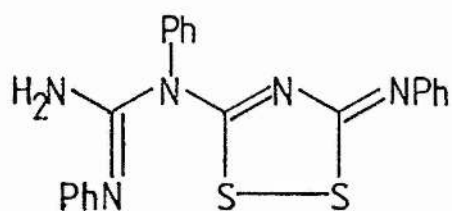
- a $X=Z=S$
 b $X=S, Z=NMe$
 c $X=O, Z=NMe$
-



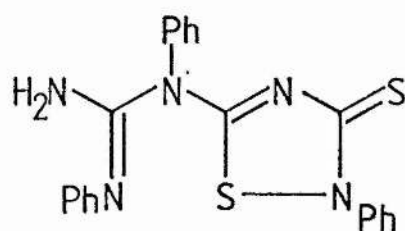
XVI



XVII



XVIII



XIX

which in turn adds weight to the argument that Ia and VIIa are the thermodynamically more stable tautomers. Model compounds with two methyl groups instead of phenyl groups therefore should afford reliable, calculated structures for adducts related to IIIa and IVa, and in addition give dependable results as to the relative stabilities of the prototropic pairs.

IV. Adduct Formation : Equilibrium Structures.

The 1:1 adducts of Hector's Base with heterocumulenes yield either one two structures which are analogues to III or IV. There are two pertinent questions to be answered in this case : firstly are structures III or IV the more stable thermodynamically for a particular isomer, and secondly which route is followed by IV in its formation?

In order to investigate the first of these questions the equilibrium structures and energies of the dimethyl model compounds of XII and XIII were calculated on one hand as opposed to XIV and XV on the other. Structures XII and XIII portray two conformations of the simple adduct, whereas XIV and XV represent two distinct isomers of the bond-switched product. The energies of the various systems studied are catalogued in Table 7.4.1 and this shows very clearly that the bond-switched structure XIVa (=XVa) is the thermodynamically more stable form for the CS₂ adduct. This is in contrast to the MeNCO and MeNCS adducts where the bond-switched structures XIV(b,c) and XV(b,c) are disfavoured on this thermodynamic basis, and as a result structures XII and XIII are the thermodynamically more stable for

these heterocumulene adducts. These data are endorsed by the observed structures of IIIa and IVa [5,8,9].

Species	ΔH_f^θ (kJmol ⁻¹)	Species	ΔH_f^θ (kJmol ⁻¹)
XIIa	285.6	XIIIa	286.6
XIIb	249.2	XIIIb	248.7
XIIc	39.8	XIIIC	38.9
XIVa	268.0	XVa	268.0
XIVb	264.8	XVb	298.4
XIVc	181.9	XVc	79.9

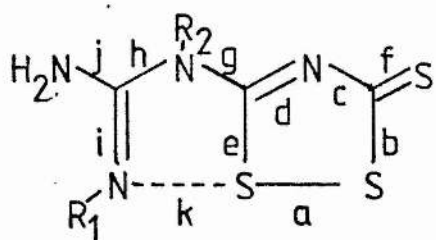
Table 7.4.1. ΔH_f^θ for intermediates.

The energy of XVb is significantly higher than that for XIVb and this is consistent with XVI being formed rather than XVII when IVc is treated with base [15]. It is not surprising, therefore, in the light of the energies in Table 7.4.1 that IVc does not bond-switch to form XVIII or XIX, since the driving force for the reaction of IVc to give XVI is the evolution of ammonia [15] and this must overcome the positive enthalpy change which occurs with the bond-switch in this case.

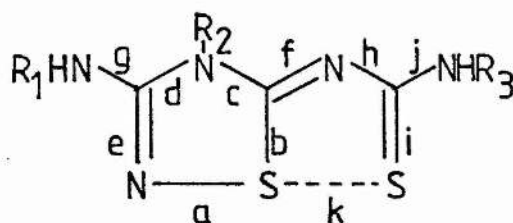
When the observed and calculated geometries for the CS₂ and MeNCS adducts are compared an entirely satisfactory agreement emerges, as with the Hector's Base prototropic pairs, save for the reservation about the bond lengths to sulphur. These structural comparisons have been put together in the form of Table 7.4.2. There is only one major exception and this is bond length 'k' in the CS₂ adduct. Structures

Distances/Å	IIIa[8]	XIVa	XIVa(a)	IVa[9]	XIIb
a	2.121	1.937	1.944	1.697	1.644
b	1.736	1.732	1.722	1.754	1.703
c	1.345	1.388	1.388	1.407	1.415
d	1.309	1.322	1.326	1.403	1.425
e	1.749	1.721	1.712	1.303	1.314
f	1.667	1.548	1.550	1.288	1.303
g	1.379	1.384	1.393	1.361	1.410
h	1.404	1.452	1.434	1.360	1.405
i	1.275	1.285	1.293	1.681	1.590
j	1.331	1.420	1.430	1.323	1.374
k	2.324	3.469	2.535	2.822	3.080

(a) planar structure.



III, XIV



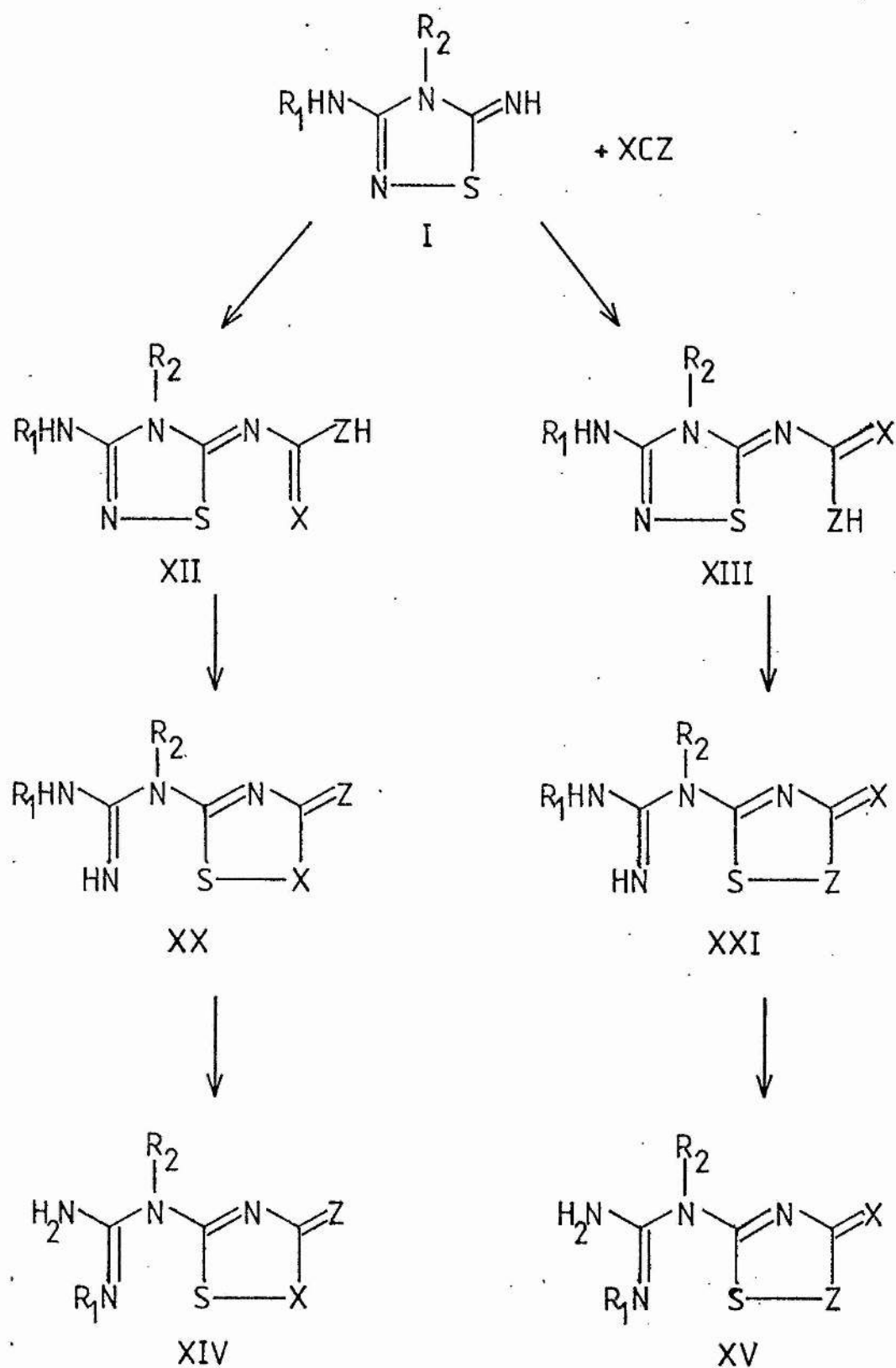
IV, XII

Table 7.4.2. Observed and calculated geometries for Hector's Base adducts.

IIIa and IVa experimentally have planar heavy atom skeletons [8,9]; and the structure calculated for XIIb likewise. However in XIVA the calculations reveal that the guanidino side chain is rotated out of the plane of the hetero ring about bond 'h' by about 67.5° and thus causes a substantial increase in the distance 'k'. Constraining XIVA to have a coplanar heavy atom framework increases the ΔH_f° from 268.0 kJmol^{-1} to 303.8 kJmol^{-1} : the alternative conformation which has the $-\text{NH}_2$ group as opposed to the $=\text{NMe}$ group next to the sulphur yields a ΔH_f° of 307.7 kJmol^{-1} .

This rather unexpected, calculated conformation for XIVA could be due to a computational artefact, regardless of the calculated, observed configuration on the MeNCS adduct. There are, however, three points which suggest otherwise.

- 1] The barrier to planarity is just 35 kJmol^{-1} and this can be easily overcome by the intermolecular forces when the isolated molecule, to which the calculation refers, is combined into the crystal;
- 2] The criterion of parallel $p\pi$ bonds would require the phenyl groups to be coplanar with the hetero ring. There is ample evidence to show that this is not an over-riding factor in the structure determination. The phenyl group attached to N4 in Hector's Base, Ia, for example, has a dihedral angle of 82.8° between it and the hetero ring. The corresponding dihedral angles found experimentally for IIIa, IVa and VIIIa are 84.2 [8], 62.8 [9] and 83.2° [19] respectively and those calculated for Ic and VIIC are 79.1 and 75.0° . The near identity between the calculated and observed dihedral angles in I and VIII indicate that the minimum energy conformers are being calculated correctly;



- a $\text{X}=\text{Z}=\text{S}$
 b $\text{X}=\text{S}, \text{Z}=\text{NMe}$
 c $\text{X}=\text{O}, \text{Z}=\text{NMe}$
- $\text{R}_1, \text{R}_2 = \text{Ph}, \text{Me}$

Figure 7.51.

3] When IIIa is formed from Ia there has to be a 180° rotation about the bond denoted 'd' in I (see Table 7.3.2) and 'h' in III and XIV (see Table 7.4.2). The energy change associated with this rotation from the initial planar configuration to the observed planar representation is -3.9 kJmol^{-1} with an energy minimum as opposed to maximum en route.

Akiba [11-14] has stated that the long N....S distances found in IIIa and related species are within bonding range, and means essentially that any N....S interaction is attractive. This interpretation has been criticised [8] and the calculations indicate that the interactions are far from being attractive, and are, in fact, repulsive. This can be seen from the comparison of the calculated bond angles in the C-guanidino side-chain for the freely optimised and constrained planar geometries of XIVa. The SCN, CNC and NCN angles in the planar form are calculated to be larger than those for the free optimisation by 3.0 , 2.0 and 0.6° respectively.

V. Adduct Formation : Mechanism.

The most realistic pathway for the adduct formation is that shown in Figure 7.5.1 [8] : when $\text{XCZ} = \text{CS}_2$ then the products XIV and XV are identical. Table 7.5.1 lists the energies of the intermediates involved for $\text{R}_1 = \text{R}_2 = \text{Me}$. From this it can be seen that the simple adduct formation of XII or XIII from Id and XCZ is always exothermic and furthermore the conversion of XIIa (=XIIIa) to XIVa (=XVa) is also exothermic at each stage and as a result should proceed smoothly. There is no experimental evidence when $\text{XCZ} = \text{CS}_2$ for the formation of

simple adducts analogous to XII or XIII.

XCZ	CS ₂	MeNCS	MeNCO
Id+XCZ	326.1	327.1	130.1
XII	285.6	249.2	39.8
XX	282.6	327.0	264.8
XIV	268.0	200.8	181.9
OR			
XIII	286.6	248.7	38.9
XXI	282.6	313.1	107.1
XV	268.0	298.4	79.9

All energies in kJmol⁻¹.

Table 7.5.1. ΔH_f^θ for intermediates in the adduct formation.

The formation of the simple adduct when XCZ is MeNCS or MeNCO, is once more exothermic. However the conversions to form the bond-switched structures XIV or XV are endothermic by 15.6 kJmol⁻¹ for XIVb and 41 kJmol⁻¹ for XVc - and by much more for XVb and XIVc - and are all concomitant with large activation energies (see Table 7.5.1). On solvation these activation enthalpies will be reduced, perhaps substantially; however the calculations on the isolated molecules indicate that thermodynamic and kinetic factors are against the bond-switch for XCZ = MeNCS or MeNCO, but that both are favourable in the case of XCZ = CS₂. Accompanied by the bond-switch for XII → XX and XIII → XXI is a proton shift, and it is very likely that this shift is concerted with participation of the solvent. This can be

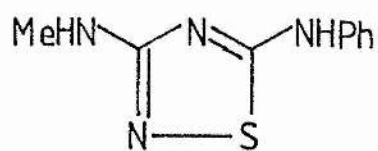
demonstrated by either protonating at nitrogen or deprotonating at X or Z and this causes no bond-switch. However, if the proton is transferred in a concerted fashion from X or Z to nitrogen then a bond-switch always results to give XX or XXI.

VI. Hegerschoff Base Formation.

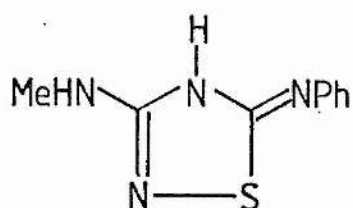
The bis-imino species VIc and VIId when refluxed briefly with aqueous HCl afford VIIa and VIIb respectively, which are Hegerschoff Bases. Neither Hector's Base, Ia, nor Dost's Base, Va, can isomerise in this manner. Both Vc and XXII rearrange to give XXIII and XXIV, R = H, which are model compounds for the Hegerschoff Bases, VII. The calculated heats of formation for these species are shown below

Species.	Energy/ kJmol ⁻¹ .
Vc	290.0
XXII	296.1
XXIII	253.9
XXIV	274.6

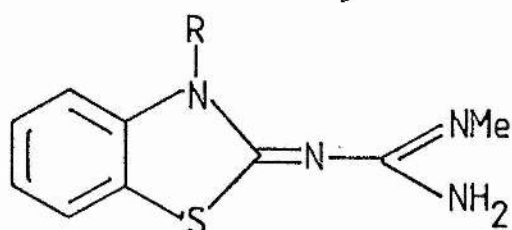
and these data reveal that the rearrangement to form XXIII and XXIV from Vc and XXII respectively is exothermic. The bis-amino structure Vc is more stable than its isomer XXII, and although XXII is more stable than XXIV, Hegerschoff Bases always have R = Me or Ph, and as a result tautomerism of XXIV → XXIII does not usually occur.



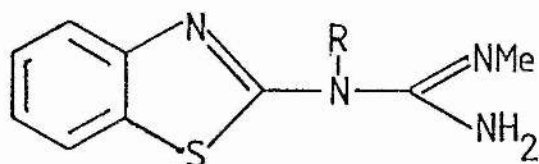
Vc



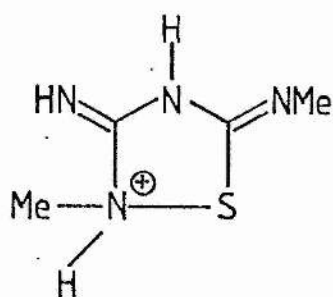
XXII



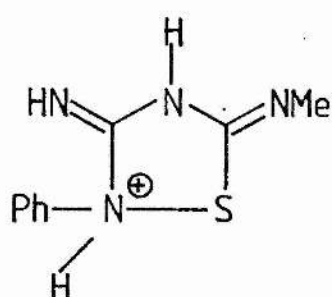
XXIII



XXIV



XXV



XXVI

The proposed mechanism for Hegerschoff Base formation [18] has as its first step a protonation of the heterocycle at N2, which yields a sulphenyl cation on cleavage of the N-S bond. As a consequence of this protonation the calculations on Vc, XXII and the N-protonated derivatives reveal several modifications in the electronic structure which are pertinent to the mechanism. In each case the protonation affords a modest increase in the N-S bond length, and perhaps more striking is the large increases in the charge on the sulphur atom, from +0.154e to +0.319e for Vc and +0.183e to +0.340e for XXII. This increase may be evidence for the start of the formation of the sulphenyl cation. Furthermore the phenyl carbon which is nearest to the sulphur in Vc and XXII carries a small positive charge and after the N-protonation has taken place, this same carbon bears a small negative charge, which will encourage the electrophilic attack by the sulphur. In order to form the benzothiazole system a bond-switch from N-S to S-N has to occur and according to the calculations will only arise after the N-protonated species derived from Vc and XXII have lost a proton from the phenyl carbon which is due to be bonded to the sulphur. When this proton is removed the optimisations converge to either XXIII or XXIV: failure to remove the proton results in no bond-switch from N-S to S-N.

The formation of a Hegerschoff Base from VIId is faster than from VIc and so in order to investigate the effect of substituent at N2 [18] calculations were carried out on the model protonated species XXV and XXVI. These calculations indicate that there are no real discrepancies between them, either in the electronic distribution or

N-S bond length, and especially in the charges on the sulphur and N2 which are essentially identical.

VII. Desulphurisation.

The 1:1 adduct of Hector's Base with CS₂, IIIa, when treated with triphenylphosphine affords a quantitative yield of a pale yellow powder which has the stoichiometry C₁₅H₁₂N₄S₂. Compound Xa has one sulphur atom fewer than its precursor IIIa and its structure was determined by ¹³C n.m.r. Xa only dissolves in strong acids like trifluoroacetic acid and sulphuric acid: the ¹³C n.m.r. spectrum, whether recorded in CF₃COOH or D₂SO₄, shows only six peaks. Four of these peaks are due to the phenyl groups and the remaining two peaks are quaternary resonances. This simple spectrum for a 15 carbon atom molecule suggests a two-fold element of symmetry which would make the two phenyl groups equivalent, and the two C=S groups equivalent. Subtracting these from the formula leaves CH₂N₂. The mass spectrum of Xa, in addition to the parent molecular ion, displays the following daughter ions : (M-HNCS)⁺ and (HNCS)⁺, (M-PhNCN)⁺, (M-PhNCNH)⁺ and (PhNCNH)⁺, (PhNCSCN)⁺ and (PhNCS)⁺, as well as (PhN)⁺ and (Ph)⁺.

A plausible structure which incorporates both the two-fold element of symmetry required by the ¹³C n.m.r. and the mass spectral fragmentations is Xa.

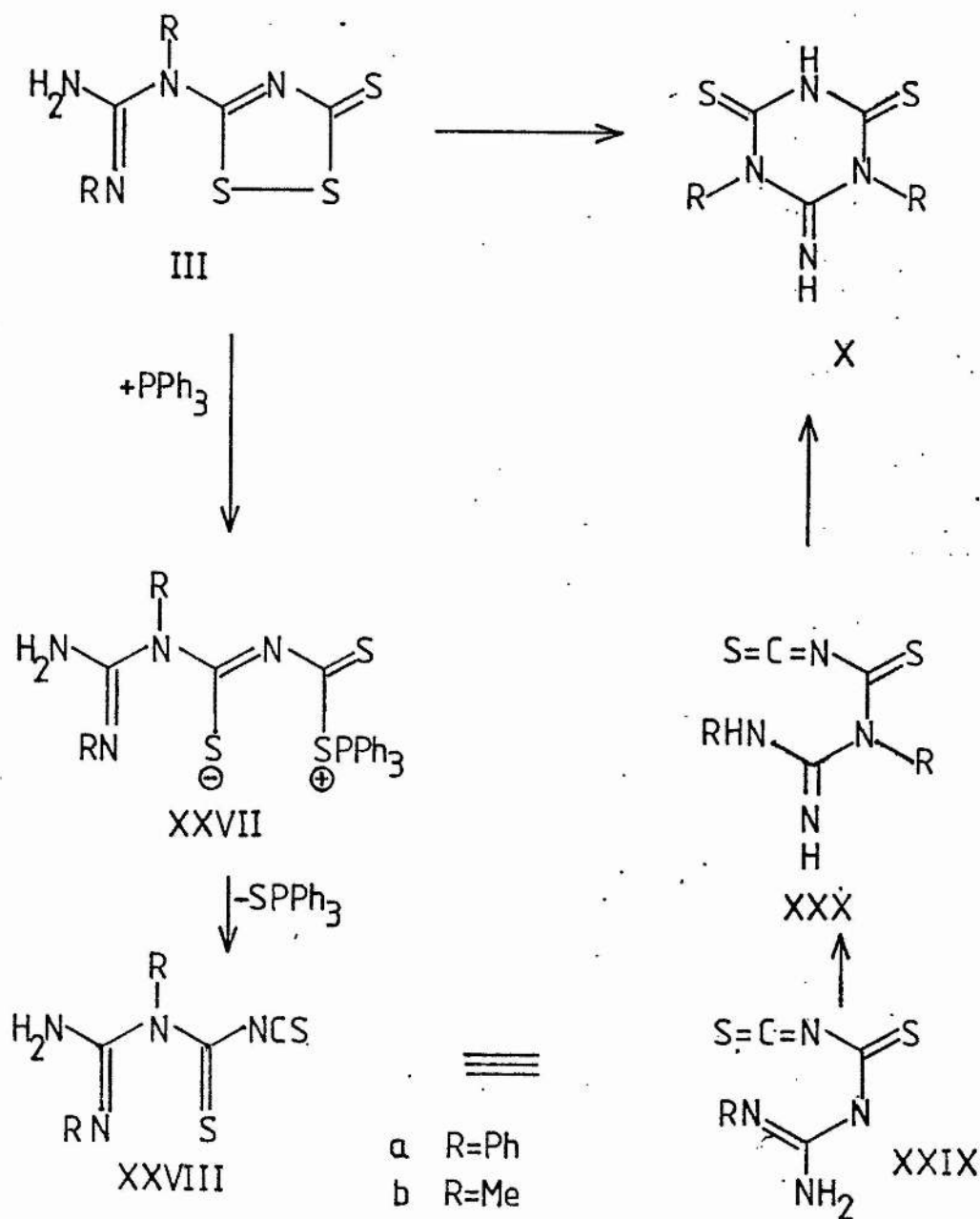
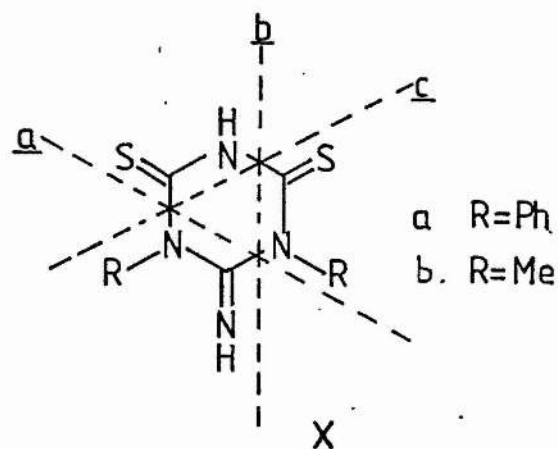


Figure 7.7.1. Reaction scheme for desulphurisation.

Fragmentation at a yields $(\text{PhNCNH})^+$, $(\text{M-PhNCNH})^+$ and $(\text{M-PhNCN})^+$, fragmentation b affords $(\text{PhNCS})^+$, whilst fragmentation c gives $(\text{HNCS})^+$ and $(\text{M-HNCS})^+$, and the formation of $(\text{PhNCSCN})^+$ follows simply from X.

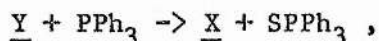
A feasible pathway for the formation of X from III is that in Figure 7.7.1. The desulphurisation of IIIa with triphenylphosphine affords the isothiocyanate XXVIIIa and a conformational change gives XXIXa : a solitary proton shift from XXIXa yields XXXa which has an NH group next to an NCS group and this can condense to afford the thiourea group contained in the final product Xa.

Accordingly MNDO calculations were made in order to test the validity of the mechanism shown in Figure 7.7.1, and the calculated energies for model compounds having R=Me are presented in Table 7.7.1.

<u>X</u>	$\Delta H_f^\theta(\text{X})/\text{kJmol}^{-1}$	$\Delta H_f^\theta(\text{X+SPPPh}_3\text{-PPh}_3)/\text{kJmol}^{-1}$
IIIb	268.0	-
XXVIIIb	308.3	208.3
XXIXb	306.9	206.9
XXXb	326.4	226.4
Xb	242.5	142.5

Table 7.7.1. ΔH_f^θ for intermediates in the desulphurisation.

However this process is actually that of



and as a consequence, the plausibility or otherwise of a certain pathway will be confirmed by comparing the energy of the reactant IIIb, not with the energies of the products X alone, but with the energies of X + SPPh₃ - PPh₃. Because MNDO calculates the energies for compounds which contain P(V) and S(IV) far too high, an experimental value for ($\Delta H_f^\circ(SPPh_3) - \Delta H_f^\circ(PPh_3)$) was sought. This term for simple alkyl and alkoxy derivatives, in condensed phases [27], lies within the range -110 to -115 kJmol⁻¹. The change in the value which would accompany a change in phase should not be more than -10 kJmol⁻¹ [27], and so with no reliable, calculated value for SPPh₃, -100 kJmol⁻¹ seems a reasonable estimate for ($\Delta H_f^\circ(SPPh_3) - \Delta H_f^\circ(PPh_3)$) when applied to isolated molecules. This value of -100 kJmol⁻¹ has been employed in Table 7.7.1 and a comparison of the value in the last column of the Table with the initial value for IIIb gives the overall reaction energies. In total the formation of Xb from IIIb is calculated to be exothermic by about 125 kJmol⁻¹ and only one of the individual steps outlined in Figure 7.7.1 is endothermic. The conversion of XXXb to Xb most probably occurs via a concerted protonation - deprotonation which involves the solvent, as found for the bond-switch in the Hector's Base adduct formation, since protonation or deprotonation of XXXb at the appropriate nitrogen atoms affords no ring closure. However, if the proton in XXXb is shifted from the RNH group to the nitrogen in the NCS group, then the ring closure is spontaneous and affords Xb.

Experimental.

Reaction of triphenylphosphine with IIIa.

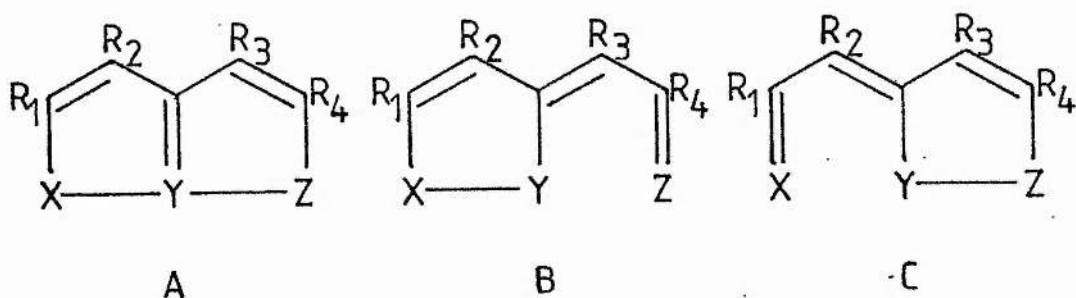
Equimolar quantities (M/1000) of triphenylphosphine and IIIa were dissolved in acetone/ethanol (1:1) and the solutions were mixed and set aside at room temperature. After one hour, the pale yellow precipitate was filtered off, and washed with 5 x 100 ml of methylene chloride to yield the product 5,6-dihydro-6-imino-1,5-diphenyl-s-triazine-2,4 (1H,3H)-dithione in essentially quantitative yield : m.p. 215-217°C; λ_{\max} 3400-3000 (NH), 1620 (C=N), 1550 (C=C) and 720 cm^{-1} (C=S); $\underline{m/e}$ 312 ($\text{C}_{15}\text{H}_{12}\text{N}_4\text{S}_2^+$, 12%), 253 ($\text{C}_{14}\text{H}_{11}\text{N}_3\text{S}^+$, 8.2%), 195 ($\text{C}_8\text{H}_7\text{N}_2\text{S}_2^+$, 16%), 194 ($\text{C}_8\text{H}_6\text{N}_2\text{S}_2^+$, 12%), 161 ($\text{C}_8\text{H}_5\text{N}_2\text{S}^+$, 27%), 135 ($\text{C}_7\text{H}_5\text{NS}^+$, 45%), 118 ($\text{C}_7\text{H}_6\text{N}_2^+$, 51%), 91 ($\text{C}_6\text{H}_5\text{N}^+$, 39%), 77 (C_6H_5^+ , 100%), 59 (CHNS^+ , 20%) (all ions with $\underline{m/e} > 100$ identified by accurate mass measurement); $\delta_{\text{C/p.p.m.}}$ ($[\text{}^2\text{H}_2]$ H_2SO_4) 128.2(d), 131.6(s), 134.4(d), 136.2(d), 152.2(s) and 169.2(s). Found : C, 57.35; H, 3.75; N, 17.85 : $\text{C}_{15}\text{H}_{12}\text{N}_4\text{S}_2$ requires : C, 57.65; H, 3.85; N, 17.95%. Evaporation of the combined filtrate and washings yielded triphenylphosphinesulphide, identified by mass spectrometry.

VIII. Triheterapentalenes : General Information.

The first evidence for the thiathiophthene type system appeared in 1958 with the crystal structure of 2,5-dimethylthiathiophthene [28]. This showed that the two S-S bonds were of equal length, and this work was subsequently repeated in 1969 when the same conclusions were reached [29]. The crystal structure of thiathiophthene itself did not appear until later [30,31], but the equal bond lengths between

the sulphurs, and the fact that the central sulphur was bonded to a carbon as well, prompted much discussion as to the nature of the bonding in these molecules.

The main difficulty lies in deciding from the spectroscopic and chemical evidence whether a given compound is best portrayed in a bicyclic, A, or monocyclic form, B and C, and if the latter which isomer of B or C is the more stable.



The answer to this problem, for a specific compound, has usually been tackled by a structural analysis, either by x-ray or electron diffraction: although both valence shell [32,33] and ESCA [34-39] photoelectron spectroscopy and lately liquid crystal n.m.r. [40] have been applied. All of these techniques can show, for the case of $X=Z$, whether the monocyclic or bicyclic structure is the best representation, that is if a double or single minimum potential well is the more appropriate in describing the oscillation of Y between X and Z. However when $X \neq Z$ there is no straightforward technique in deciding upon the stability of B with respect to C, since fairly small changes in structure can amount to the manifestation of B instead of C, and vice versa. As a result, inferences concerning thermodynamic stability which are based entirely on the nature of an observed

product have to be treated with caution [5,20].

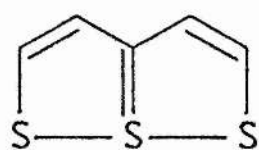
The purpose of the MNDO calculations that will be outlined in the following sections was to ascertain which of the structures A,B or C was the thermodynamically most stable, and in addition, to see if this agreed with the observed structure found from x-ray diffraction. If such a correlation between the observed and calculated structures exists, then this calculational technique should be a fairly useful tool in assigning an unambiguous structure should an x-ray analysis prove not to be feasible.

Some workers have stated that d-orbitals are important in explaining the bonding in the thiathiophthene system and many calculations have appeared at varying levels of sophistication to back up this argument. A PPP study [41] showed that definite π bonding existed within the S-S-S moiety, and a CNDO/2 study [42] indicated that d-orbitals were important: however a proviso was added to the effect that although CNDO/2 overestimates the effect of d-orbitals, it appeared nevertheless that d-orbitals on the central sulphur had a greater effect than those on the terminal sulphurs. Similarly ab-initio calculations have overestimated the effect of d-orbitals [43].

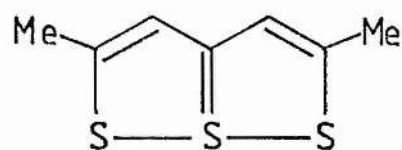
The ab-initio calculations use a series of basis sets of increasing complexity; usually sp, spd and spds: these demonstrate that the energy is subsequently lowered for each basis set, and this is taken as the proof for the necessity of d-orbitals. This, however, is a misconception and is a consequence of the variation theorem,

since all that is observed is the greater variational degree of freedom afforded by taking a larger basis set: the energy is bound to be lowered by this procedure. Analogous results would be obtained if, for instance, the s-orbital basis was increased [1,44,45,46]. Ideally what is required is for the basis set to be increased by the addition of further s and p orbitals until essentially no change is detected in the calculated geometry, that is until an asymptote is reached; then to go back a step and add the d-orbitals, so that the size of the basis set is essentially unaltered. Only by this procedure can the effect of the d-orbitals be seen, and it is found that they act only as polarisation functions: their effect is to improve but not alter the character of the occupied molecular orbitals, which they do by virtue of their higher angular functions and only move some of the electron density off the internuclear axes [45,46]. This effect has been seen already in Chapters Two and Three, and Table 4.3.6 in Chapter Four, in addition, demonstrates rather well the pitfalls inherent with this procedure. Furthermore the energy minima calculated by ab-initio, CNDO/2 or MNDO will all be different and will not necessarily correspond to the experimental minimum.

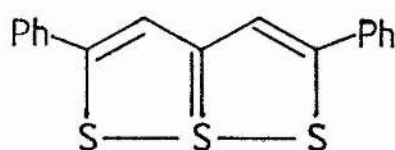
Another set of CNDO/2 calculations [47] have shown that substituents have an effect on the S-S-S bonding and as a result perturb the system from A to B or C. However, in this study the geometry of the molecule was fixed at experimental values, and the energy of the system was observed as a function of the displacement of the central sulphur atom between the two terminal sulphurs. This not only changes the S-S distances but the C(3a)-S(6a) distance and S(1),S(6),-S(6a)-S(6) bond angle as well, and so the observations are



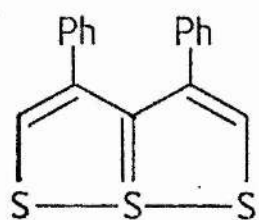
4-726
[30,31]



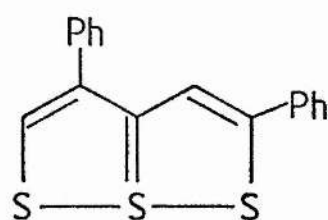
4-716
[28,29]



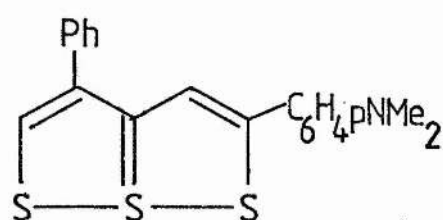
4-666
[48]



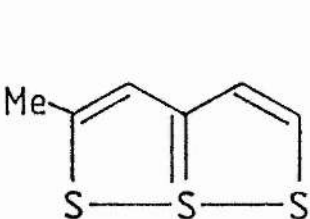
4-666
[49]



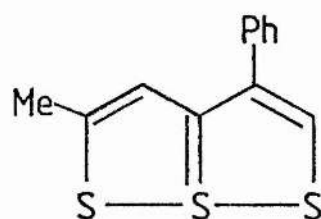
4-717
[50]



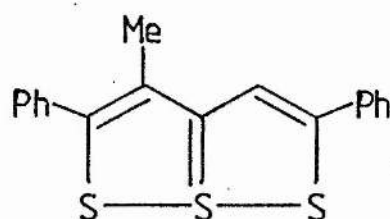
4-698
[51]



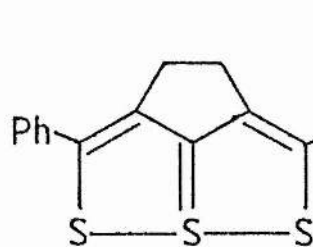
4-739
[52]



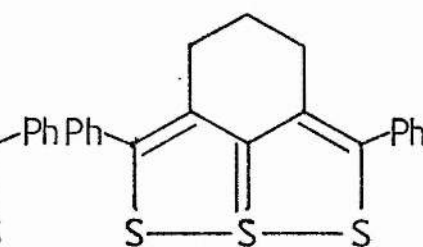
4-723
[53]



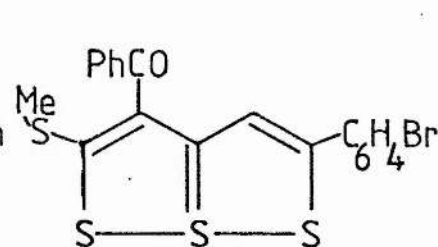
4-653
[54]



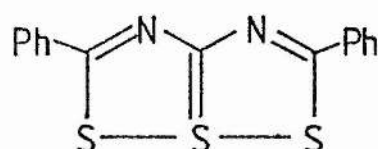
4-694
[55]



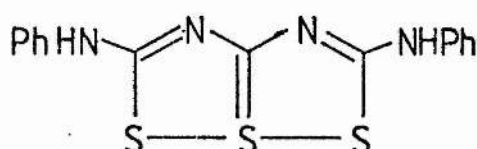
4-617
[56]



4-67
[57,58]

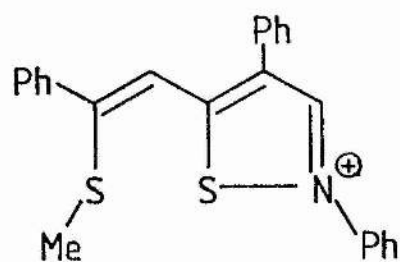


4-547
[59]

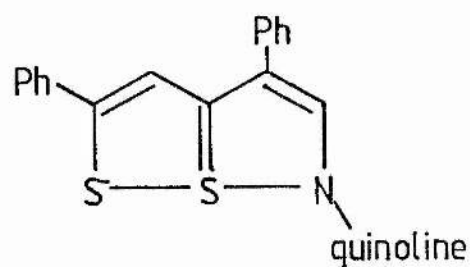


4-454
[60]

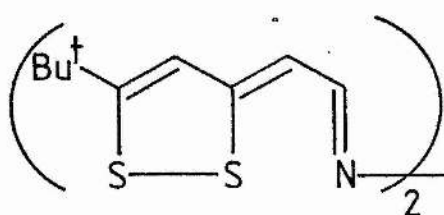
XXXII



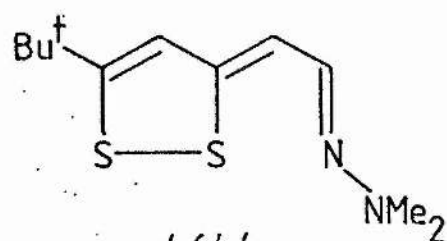
4-531
[61]



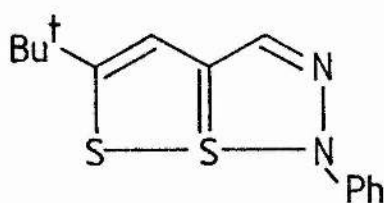
4-246
[61]



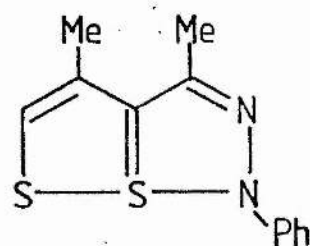
4-605
[62]



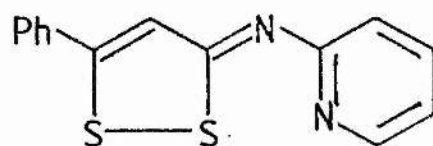
4-644
[63]



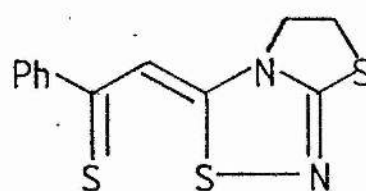
4-284
[64]



4-272
[65]



4-415
[66]

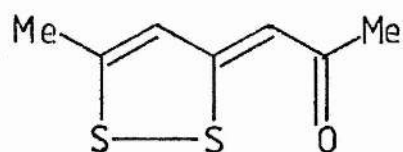


4-471
[67]

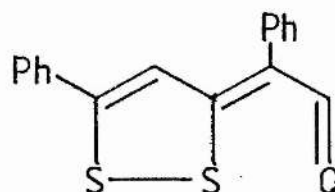
Figure 7.8.1. Geometries of triheterapentalenes.

XXXIII

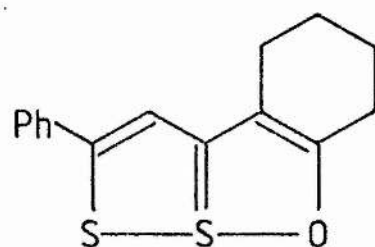
Figure 7.8.1.



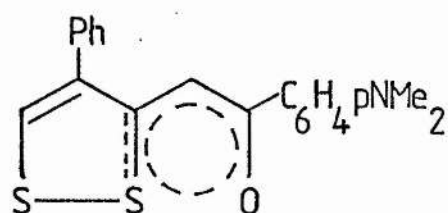
4-522
[72]



4-483
[73]

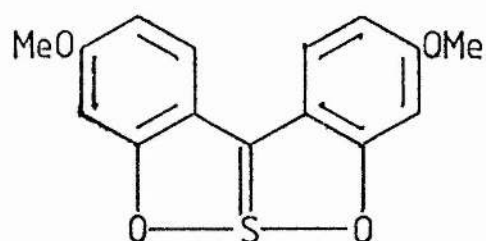


4-576
[74]

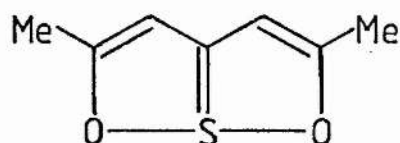


4-544, 4-395
[75,76]

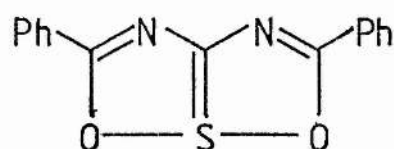
XXXIV



3-758
[80]

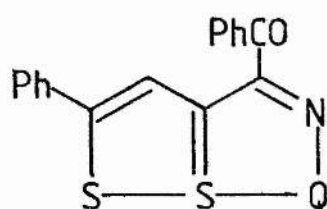


3-741
[81]



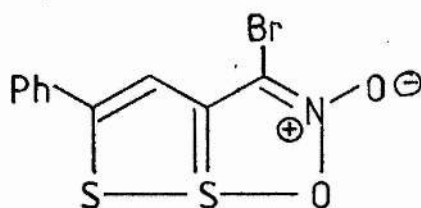
3-749
[81]

XXXV



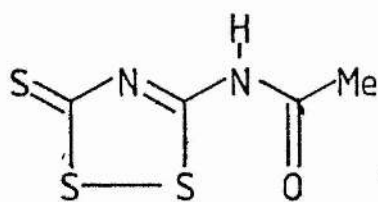
4·206
[78]

XXXVI



4·438
[77]

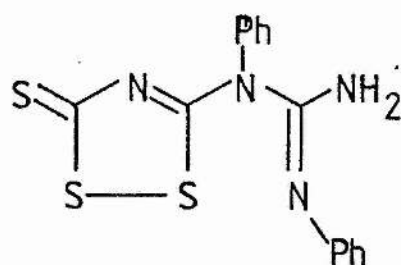
XXXVII



4·541, 4·630
[79]

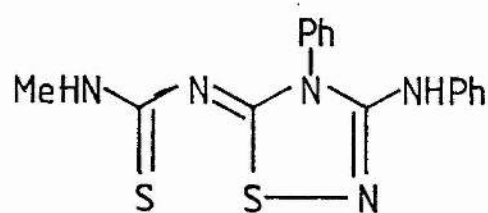
Figure 7.8.1. Geometries of triheterapentalenes.

XXXVIII



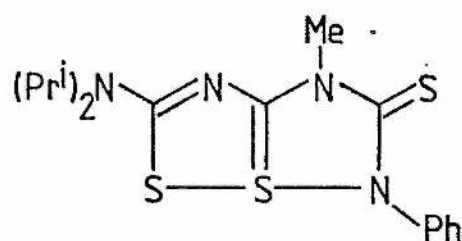
4-345

[8]



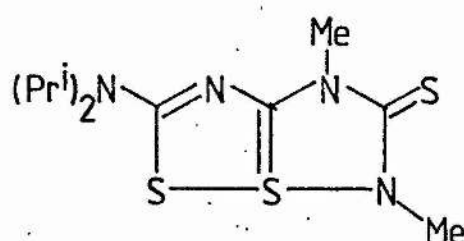
4-505

[9]



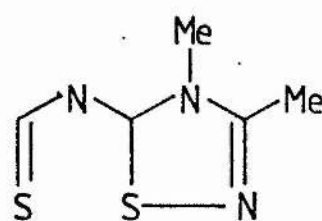
4-291

[68]



4-288

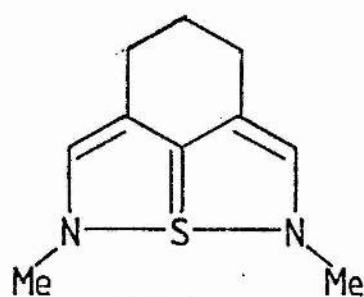
[69]



4-471

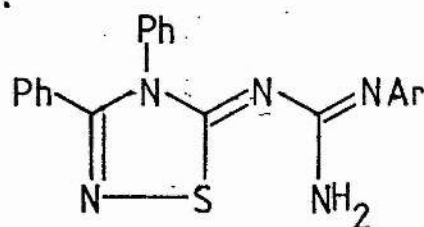
[70]

XXXIX



3-830

[71]



[11]

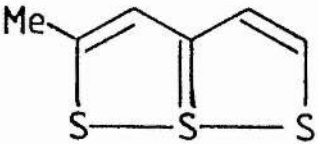
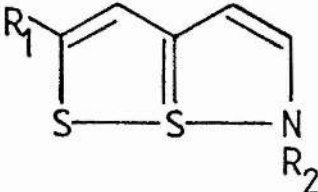
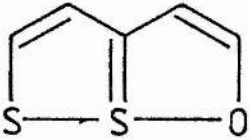
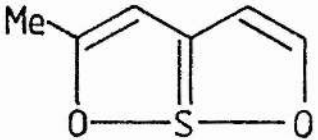
Figure 7.8.1. Geometries of triheteropentalenes.

not only reliant on the different S-S distance but the other dependent variables inherent in this assumption. This study by Hordvik et al [47] concluded that a 2 substituted methyl or twisted phenyl group caused the S(1)-S(6a) bond length to increase; and that a 3 substituted methyl or phenyl group caused a shortening in the S(1)-S(6a) bond length. Furthermore they found a flat, broad potential energy minimum of 0.3 Å for the parent thiathiophthene, which corresponds to system A.

Since the first of these structures were reported many more structures of thiathiophthenes and related molecules have appeared in the literature and a large selection of these are shown in Figure 7.8.1. Underneath each structure is its literature reference, which will be used in the text if the molecule is mentioned specifically, and the distance between the terminal atoms.

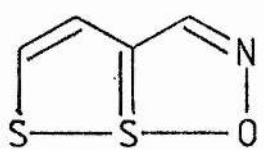
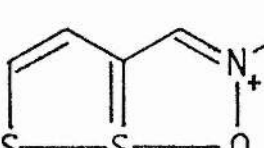
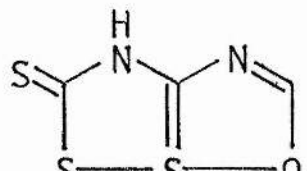
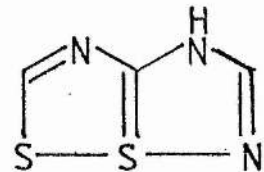
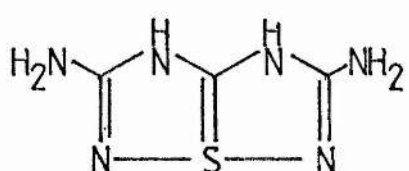
IX. Method.

The calculations on the relative stabilities of A,B and C for a wide range of model systems where Y=S and X and Z can be N,O or S were made using the MNDO method [2,82] using published parameters for sulphur [83]. Model compounds having $R_1-R_4 = H$ were used, although in a few cases, more realistic examples were chosen, in which one of the R groups was a methyl. The molecules were all fixed planar but apart from that no geometric assumptions of any kind were made.

Skeleton	A	B	C	Observed isomer	References
XXXI 	172.4	186.8	(a)	A	[28,31] [48-58]
XXXII (d) 	260.4	220.0	283.3	A B C	[61] [62,63] [61]
XXXIII 	(b)	8.6	146.0	A B	[74-76] [72,73]
XXXIV 	(b)	-113.2	-97.5	A	[80,81]

(a) Optimises to A. (b) Optimises to B. (c) Optimises to C. (d) Data for $R_1=R_2=H$: if $R_1=Bu^t$; $A=219.0$, $B=179.0$, $C=(b)$; if $R_2=NH_2$; $A=(b)$, $B=270.7$, $C=(b)$; if $R_2=NMe_2$; $A=(b)$, $B=293.9$, $C=402.0$. (e) No isomer C without H shift from N to S. (f) No isomer B without H shift from N4 to N6, see text. (g) Require shift of H from N4 to N6. (h) Require shift of H from N4 to N1. All values in kJmol^{-1} .

Table 7.10.1. ΔH_f^\ominus for model systems studied.

XXXV 	(b)	171.9	267.3	A	[78]
XXXVI 	(b)	213.5	347.9	A	[77]
XXXVII 	(b)	42.5	(e)	B	[79]
XXXVIII 	(c)	(f)	274.1	A B C	[68,69] [8] [9,70]
XXXIX 	501.6	261.5	274.5	A B	[71] [11]
		(g)	(h)		

X. Results.

The equilibrium energies for the bicyclic, A, and monocyclic forms, B and C, studied for the model systems, XXXI-XXXIX, are listed in Table 7.10.1. Table 7.10.2 presents the calculated distances and charges for the X-Y-Z moiety.

Table 7.10.1 lends further support to the argument that d-orbitals are unnecessary in these systems, since even MNDO with its limited basis set of s and p-orbitals calculates that the bicyclic form, A, is the thermodynamically most stable isomer for the model system XXXI: this is in accord with the experimental observation [28-31,48-58].

The calculated distances between the terminal sulphur atoms in XXXI are not good (Table 7.10.2). When sulphur is bonded to any other element X, MNDO calculates the S-X bond some 2-4% too short. However this error appears to be additive, in that, when S-S is considered it is calculated to be 6-8% too short. Subsequently the error in S-S-S is rather large and is of the order of 15%. This discrepancy must be due to the inadequate parameterisation for sulphur. However it must be stressed that these calculations refer to isolated molecules in the gas phase and the calculated minimum, be it MNDO or another calculational technique, will not correspond to the experimental value. In addition, the geometry was fully optimised, and therefore corresponds to the true MNDO minimum for the system: it does not lie part-way up the side of a valley wall, as a fixed geometry calculation

	Distances/Å			Charges (/e)		
	X-Y	Y-Z	X-Z	X	Y	Z
XXXIA	2.065	2.056	4.106	0.35	-0.21	-0.20
XXXIB	1.955	3.009	4.963	0.02	0.12	-0.18
XXXIIA	2.053	1.804	3.854	-0.30	0.39	-0.35
XXXIIB	1.956	3.034	4.979	0.01	0.10	-0.22
XXXIIC	2.994	1.652	4.642	-0.27	0.31	-0.42
XXXIIIB	1.954	3.129	5.069	0.03	0.08	-0.28
XXXIIIC	3.101	1.634	4.729	-0.21	0.30	-0.25
XXXIVB	1.631	3.164	4.769	-0.25	0.26	-0.30
XXXIVC	3.080	1.633	4.688	-0.30	0.27	-0.25
XXXVB	1.953	3.035	4.968	0.04	0.07	-0.16
XXXVC	3.169	1.654	4.807	-0.16	0.26	-0.16
XXXVIB	1.957	2.947	4.891	0.04	0.12	-0.34
XXXVIC	3.028	1.642	4.666	-0.19	0.32	-0.22
XXXVIIIB	1.942	3.012	4.924	0.00	0.08	-0.29
XXXVIIIC	3.242	1.651	4.863	-0.27	0.25	-0.27
XXXIXA	1.793	1.775	3.567	-0.47	0.60	-0.48
XXXIXB	1.650	3.084	4.682	-0.32	0.24	-0.29
XXXIXC	2.920	1.638	4.520	-0.32	0.27	-0.34

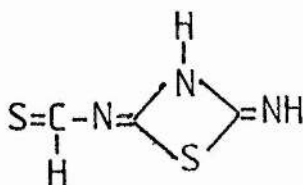
Table 7.10.2. Geometries and charges for model systems studied.

must do.

Both the bicyclic and monocyclic system for the model compound XXXII are observed experimentally, and MNDO calculates the monocyclic form, B, to be the thermodynamically more stable. Surprisingly though, the distance between the terminal atoms is calculated to be longer than the experimental, which is contrary to the concept that the bonds to sulphur are calculated too short.

This anomaly is seen in model system XXXIII, where once more the S..O distance is calculated to be longer than the experimentally found values. System B is calculated to be the most stable for model XXXIII and agrees with some of the experimental data. Experimentally, models XXXIV-XXXVI are all observed as skeleton A. However MNDO calculates that skeleton B is the most stable, and in all cases attempts to optimise structure A, results in skeleton B being found: this is the system in which the oxygen atom is not in the ring. Model XXXVII is predicted to be most stable as skeleton B, and this is the experimentally found isomer also. Once more the terminal distance is calculated somewhat too long.

For model XXXVIII only skeleton C can be calculated and when optimisation of the B system was attempted, a molecular rearrangement took place. (see below).



However skeleton C has been observed in some cases described in the literature.

The bicyclic form, A, for model XXXIX is calculated to be the least stable, although it has been observed [71]. System B is calculated to be the most stable, and this skeleton, likewise, has been observed experimentally [11]. In all model systems XXXII-XXXIX the terminal distance is calculated to be longer than the mean values calculated from the experimental data: for system XXXI the converse holds. It is interesting to note in passing that when a substituent is present, the thermodynamically most stable isomer is that in which the substituent is bonded to the ring. From Table 7.10.1 it is noteworthy that MNDO has a > 60% success rate in predicting an observed structure: this percentage may be able to be increased if the actual observed system is studied in place of a model.

A number of generalisations can be made about the charges on the X-Y-Z fragment (Table 7.10.2). Regardless of skeleton, the central atom Y is always calculated to be positive, except for model XXXI. Likewise the charges on X and Z are in the main negative or very slightly positive: once more model XXXI is anomalous. Furthermore, in models XXXIII-XXXVI, the charge on the single hetero atom present, in these cases oxygen, does not differ much between the isomers B or C. The charges on the sulphur, however, do vary quite substantially.

XI. Discussion.

Two rather interesting non-calculational approaches which have attempted to explain the bonding in the thiathiophthene system have appeared [84,85]. In the first of these by van der Hende and Klingsberg [84], and reviewed by Hordvik and Saethre [86], the X-Y-Z fragment was considered. Both X and Y were sulphurs and Z was selenium, and by subtracting the difference in the covalent radii of sulphur and selenium, Klingsberg showed that a pseudo S-S distance of 2.21 Å resulted [84]. This is close to the S-S distance found in reference 50, and shows that the S-S-Se system is similar to that in thiathiophthene.

The second approach is due to Leung and Nyburg [85], where the differing electronegativities of the atoms in the X-Y-Z fragment were considered. Once more X and Y are sulphurs and as Z changes from S to N to O, so the X...Z distance decreases. However in these studies only a carbon backbone (the rest of the molecule less the X-Y-Z fragment) was used, and if different backbones with nitrogens present (n = number of nitrogens) are studied, two more trends result.

If the mean values, \bar{x} , for the X...Z distances for a given X-Y-Z fragment and backbone are worked out from the experimental data, then it is found that the distances all lie well within two standard deviations of their respective means. These values are to be found in Table 7.11.1.

n\backbone	S-S-S(Å)	S-S-N(Å)	S-S-O(Å)
0	4.690	4.507	4.464
1	-	4.443	4.322
2	4.501	4.380	4.636 a

a only one datum.

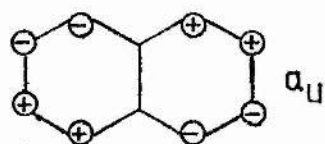
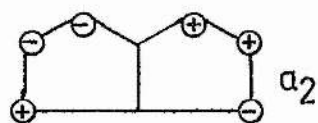
Table 7.11.1. Mean values for the terminal distances in triheterapentalenes.

For a fixed X-Y-Z fragment, as the number of nitrogens in the backbone is increased from zero to two, so the X...Z distance decreases (except S-S-O, n=2). Furthermore for a fixed backbone of either zero, one or two nitrogens, and with X=Y=S, as Z varies from S to N to O (increasing electronegativity), so the X...Z distance becomes smaller (excepting S-S-O, n=2).

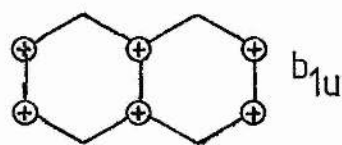
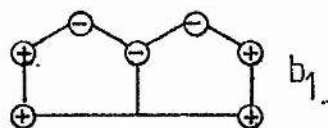
The bond orders calculated by MNDO for the bicyclic and monocyclic skeletons fall into three distinct classes. In the monocyclic forms B and C, the bonds are between X-Y and Y-Z respectively, and here the bond orders are approximately 1.0. For the non-bonded distances Y-Z and X-Y respectively for forms B and C, the bond order is small, < 0.04. However in the bicyclic form A, both X-Y and Y-Z are within bonding range and here the bond orders have an intermediate value of about 0.5. The S(6a) atom in thiathiophthene therefore is calculated as S(II) and not S(IV) by MNDO.

$C_{2v}(y)$ D_{2h}

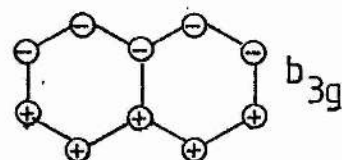
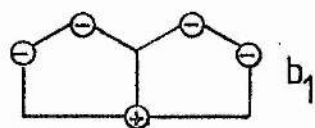
HOMO -9.11



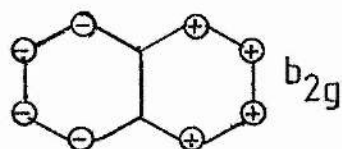
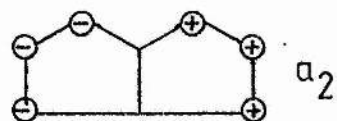
-10.63



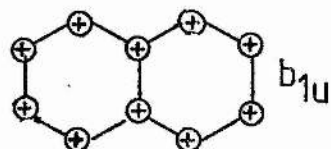
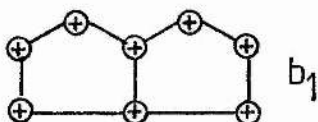
-11.16



-12.43

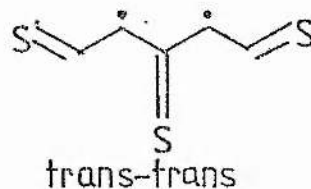
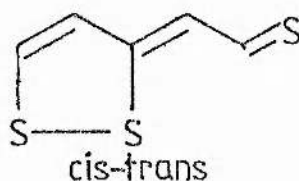
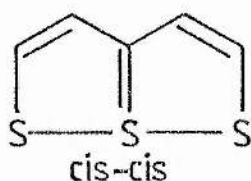


-14.49



A curious feature in the experimental determination of the thiathiophthene structure [30,31] is that the C(3a)-S(6a) distance is longer than that for the S(1),S(6)-C(2) distance. The former distance is for a notional double bond and the latter relates to a single bond, therefore one might expect the opposite. MNDO calculates the C(3a)-S(6a) distance to be longer than the S(1),S(6)-C(2) distance, and so agrees with the experimental findings.

The thiathiophthene system can be expressed as a cis-cis skeleton, a cis-trans or trans-trans formulation.



One question of interest is why is the cis-cis the experimentally observed structure, since this has the greatest nuclear repulsion. The question is best answered by reversing it and asking why the cis-trans and trans-trans are not observed. The trans-trans structure can be disregarded straightaway since it would have to be written as a diradical. The cis-trans structure disrupts the 10 π system in thiathiophthene and hence is less stable. Therefore the only formulation left is cis-cis.

The five occupied π molecular orbitals in thiathiophthene have been likened to those of naphthalene, and these appear in schematic form opposite. These are adapted from reference 89. The numbers refer to the orbital energies in eV calculated by MNDO.

MNDO calculations on thiathiofthene itself fully agree with the ordering and type of orbitals which were calculated by ab-initio methods by Nyburg et al [87]. In addition this study calculated the potential energy surface for thiathiofthene and this showed that the barrier to rotation from cis-cis to cis-trans was 140.4 kJmol^{-1} . The comparable value calculated by MNDO is just 21.6 kJmol^{-1} .

Chapter Seven.

Bibliography.

1. D.T. Clark. Int J Sulfur Chem 7C 11 (1972).
2. M.J.S. Dewar and W. Thiel. J.A.C.S. 99 4899 (1977).
3. D.S. Hector. Chem Ber 22 1176 (1889).
4. A.R. Butler, C. Glidewell and D.C. Liles. Acta Cryst B34 3241 (1978).
5. A.R. Butler, C. Glidewell, I. Hussain and P.R. Maw. J Chem Res 114(S), 1843(M) (1980).
6. E. Fromm and R. Heyder. Chem Ber 42 3804 (1909).
7. I. Hussain. Ph.D. Thesis, University of St. Andrews (1980).
8. A.R. Butler, C. Glidewell and D.C. Liles. Acta Cryst B34 2570 (1978).
9. A.F. Cuthbertson and C. Glidewell. Acta Cryst B37 1419 (1981).
10. A.R. Butler. Personal Communication.
11. K. Akiba, T. Tsuchiya, N. Inamoto, K. Onuma, N. Nagashima and A. Nakamura. Chem Lett 723 (1976).
12. K. Akiba, T. Tsuchiya, N. Inamoto, K. Yamada, H. Tanaka and H. Kawazura. Tet Lett 3819 (1976).
13. K. Akiba, S. Arai and F. Iwasaki. Tet Lett 4117 (1978).
14. K. Akiba, S. Arai, T. Tsuchiya, Y. Yamamoto and F. Iwasaki. Angew Chem 18 166 (1979).
15. A.R. Butler and I. Hussain. J Chem Res 266(S) (1980).
16. K. Dost. Chem Ber 39 863 (1906).

17. C. Christophersen, T Øttersen, K. Seft and S. Treppendahl. J.A.C.S. 97 5237 (1975).
18. A.R. Butler and I. Hussain. J Chem Res 407(S), 4954(M) (1980).
19. A.F. Cuthbertson, C. Glidewell, H.D. Holden and D.C. Liles. J Chem Res 316(S), 3714(M) (1979).
20. A.F. Cuthbertson and C. Glidewell. J Mol Struct in press.
21. F. Kurzer. Adv Heterocyclic Chem 5 126 (1965).
22. K. Akiba, T. Tsuchiya and N. Inamoto. Tet Lett 1877 (1976).
23. A.R. Butler. J. Chem Res 50(S), 855(M) (1978).
24. K. Akiba, T. Tsuchiya, M. Ochiumi and N. Inamoto. Tet Lett 455 (1975).
25. W. Thiel. QCPE 11 353 (1978).
26. J.R. Bews and C. Glidewell. J Mol Struct in press.
27. C.L. Chernick, J.B. Pedley and H.A. Skinner. JCS 1851 (1957).
28. S. Bezzi, M. Mammì and C. Garbuglio. Nature 182 247 (1958).
29. F. Leung and S.C. Nyberg. Chem Comm 137 (1969).
30. L.K.Hansen and A. Hordvik. Acta Chem Scand 24 2246 (1970).
31. L.K. Hansen and A. Hordvik. Acta Chem Scand 27 411 (1973).
32. R. Gleiter, V. Hornung, B. Lindberg, S. Hogberg and N. Lozac'h. Chem Phys Lett 11 401 (1971).
33. R. Gleiter, R. Gygax and D.H. Reid. Helv Chim Acta 58 1591 (1975).
34. D.T. Clark, D. Kilcast and D.H. Reid. Chem Comm 683 (1970).
35. B. Lindberg, S. Hogberg, G. Malmsten, J. Bergmark, O. Nilsson, S.E. Karlson, A. Fahlman, U. Gelius, R. Pinel, M. Stavaux, Y. Mollier and N. Lozac'h. Chem Scripta 1 183 (1971).
36. M.D. Coffey. Thesis, Purdue University (1972).
37. L.J. Saethre, N. Mårtensson, S. Svensson, P.Å. Malmquist, U.

- Gelius and K. Siegbahn. J.A.C.S. 102 1783 (1980).
38. L.J. Saethre, P.Å. Malmquist, N. Mårtensson, S. Svensson, U. Gelius and K. Siegbahn. Inorg Chem 20 431 (1977).
39. L.J. Saethre, S. Svensson, N. Mårtensson, U. Gelius, P.Å. Malmquist, E. Basilier and K. Siegbahn. Chem Phys 20 431 (1977).
40. J.P. Jacobsen, J. Hansen, C.Th. Pedersen and T. Pedersen. JCS Perkin II 1521 (1979).
41. R.A.W. Johnstone and S.D. Ward. Theo Chim Acta 14 420 (1969).
42. D.T. Clark and D. Kilcast. Tetrahedron 27 4367 (1971).
43. J.M. Howell, I. Absar and J.R. Van Wazer. J Chem Phys 59 5895 (1973).
44. M.H. Palmer and R.H. Findlay. Tet Lett 4165 (1972).
45. M.H. Palmer and R.H. Findlay. JCS Perkin II 1885 (1974).
46. M.H. Palmer and R.H. Findlay. J Mol Struct 37 229 (1977).
47. L.K. Hansen, A. Hordvik and L.J. Saethre. Chem Comm 222 (1972).
48. A. Hordvik. Acta Chem Scand 25 1583 (1973).
49. P.L. Johnson and I.C. Paul. Chem Comm 1014 (1969).
50. A. Hordvik, E. Sletten and J. Sletten. Acta Chem Scand 23 1852 (1969).
51. A. Hordvik and L.J. Saethre. Acta Chem Scand 26 3114 (1972).
52. A. Hordvik and L.J. Saethre. Acta Chem Scand 26 1729 (1972).
53. A. Hordvik and K. Juhlshamn. Acta Chem Scand 25 1835 (1971).
54. A. Hordvik, O. Sjølset and L.J. Saethre. Acta Chem Scand 26 1297 (1972).
55. B. Birknes, A. Hordvik and L.J. Saethre. Acta Chem Scand 27 382 (1973).
56. B. Birknes, A. Hordvik and L.J. Saethre. Acta Chem Scand A29 195 (1975).

57. S.M. Johnson, M.G. Newton, I.C. Paul, R.J.S. Beer and D. Cartwright. Chem Comm 1170 (1967).
58. S.M. Johnson, M.G. Newton and I.C. Paul. JCS(B) 986 (1969).
59. A. Hordvik and L. Milje. Chem Comm 182 (1972).
60. A. Hordvik and P. Oftedal. Acta Chem Scand A35 663 (1981).
61. F. Leung and S.C. Nyburg. Chem Comm 707 (1970).
62. A.F. Cuthbertson, C. Glidewell and D.C. Liles. Acta Cryst in press.
63. A.F. Cuthbertson, C. Glidewell and D.C. Liles. Acta Cryst submitted.
64. L.K. Hansen and K. Tomren. Acta Chem Scand A31 292 (1977).
65. L.P. Darro and L.K. Hansen. Acta Chem Scand A31 412 (1977).
66. C. Glidewell and D.C. Liles. Acta Cryst B37 1451 (1981).
67. C. Glidewell, H.D. Holden and D.C. Liles. Acta Cryst B36 1244 (1980).
68. L.K. Hansen. Acta Chem Scand A31 855 (1977).
69. L.K. Hansen. Acta Chem Scand A35 61 (1981).
70. C. Glidewell and D.C. Liles. Acta Cryst B37 1449 (1981).
71. A. Hordvik and K. Juhlshamn. Acta Chem Scand 26 343 (1972).
72. R. Bardi, S. Bezzi, M. Mammi and G. Traverso. Nature 192 1282 (1961).
73. A. Hordvik, E. Sletten and J. Sletten. Acta Chem Scand 23 1377 (1969).
74. R. Pinel, Y. Mollier, E.C. Llaguno and I.C. Paul. Chem Comm 1352 (1971).
75. A. Hordvik and L.J. Saethre. Acta Chem Scand 26 849 (1972).
76. L.J. Saethre and A. Hordvik. Acta Cryst B31 30 (1975).
77. K.I.G. Reid and I.C. Paul. JCS(B) 952 (1971).

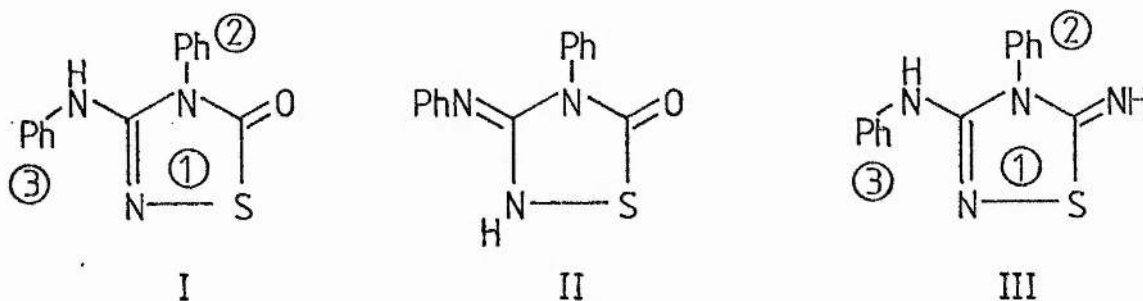
78. P.L. Johnson, K.I.G. Reid and I.C. Paul. JCS(B) 946 (1971).
79. B. Birknes, A. Hordvik and L.J. Saethre. Acta Chem Scand 26 2140 (1972).
80. R.D. Gilardi and I.C. Karle. Acta Cryst B27 1073 (1971).
81. M. Dalseng, L.K. Hansen and A. Hordvik. Acta Chem Scand A35 645 (1981).
82. W. Thiel, P. Wiener, J. Stewart and M.J.S. Dewar. QCPE 428 (1982).
83. M.J.S. Dewar, M.L.McKee and H.S. Rzepa. J.A.C.S. 100 3607 (1978).
84. J.H. van der Hende and E. Klingsberg. J.A.C.S. 88 5045 (1966).
85. F. Leung and S.C. Nyburg. Can J Chem 49 167 (1971).
86. A. Hordvik and L.J. Saethre. Israel J Chem 10 239 (1972).
87. S.C. Nyburg, G. Theodorakopoulous and I.G. Csizmadia. Theo Chim Acta 45 21 (1977).

Chapter Eight.

Discussion of the Heterocyclic Crystal Structures.

I. Dost's Keto Compound and the 1:1 Adducts of Hector's Base.

The x-ray structure of Dost's Keto Compound shows conclusively that it should be represented as the phenylamino compound, I, and not the phenylimino compound, II, due to the successful refinement of H3 bonded to N3, and the corresponding bond distances in the ring.



The molecule is isomorphous and isostructural with Hector's Base, III, [1] and Table 8.1.1 presents a comparison of the cell dimensions for both Hector's Base and Dost's Keto Compound.

	Hector's Base [1]	Dost's Keto Compound
Stoichiometry	$C_{14}H_{12}N_4S$	$C_{14}H_{11}N_3OS$
Space Group	$P2_12_12_1$	$P2_12_12_1$
a	12.196(2)	12.252(9)
b	11.027(2)	11.283(8)
c	9.519(2)	9.297(10)
Z	4	4

Table 8.1.1

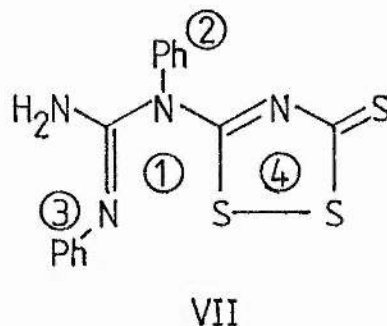
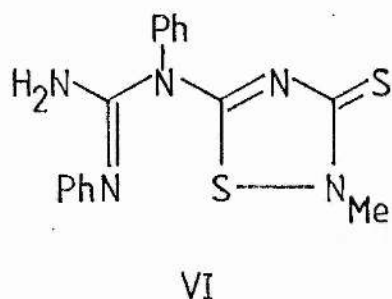
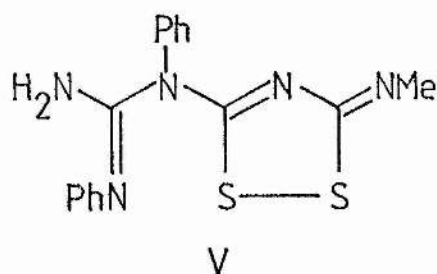
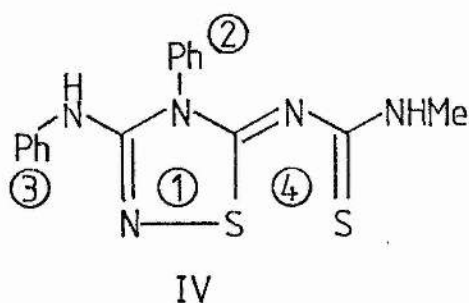
The comparison can be taken further, and the least squares planes between the three rings, presented in Appendix C and in abbreviated form in Table 8.1.2, are virtually identical for Hector's Base and Dost's Keto Compound. The plane numbers referred to are enclosed by circles in the drawings of structures I, III, IV and VII.

There is only one short intermolecular distance and that is between .O1 and N3ⁱ (the superscript i refers to the symmetry position 0.5+x, 0.5-y, -z) and this may represent a weak hydrogen bond N-H...O: N...O = 3.112 Å, N-H 1.053 Å, H...O 2.071 Å, <N-H...O 169.3°.

	Hector's Base [1]	Dost's Keto	HB:CS ₂	HB:MeNCS
1,2/°	-82.79	-83.17	85.04	62.8
1,3/°	24.41	23.82	-44.92	-47.2
1,4/°	-	-	1.10	1.9
2,3/°	78.53	80.33	67.74	88.4
2,4/°	-	-	84.16	60.9
3,4/°	-	-	-45.96	-48.6

Table 8.1.2.

In Chapter Six the 1:1 adduct of Hector's Base, III, with methylisothiocyanate was shown to be IV, rather than one of the two bond-switched structures V and VI, which are akin to the structure of the adduct formed with CS₂, VII, [2].



With hindsight structure IV should not have been as unexpected as it was because of two pieces of chemical evidence. Firstly the CS_2 adduct reacts with metal ions such as Ni^{+2} and in the past has been used as a spot test for nickel ions [3]. Furthermore it reacts with Co^{+2} , Pb^{+2} , Hg^{+2} and Cd^{+2} to form 2:1 metal complexes. The MeNCS adduct does not react in this way with metal ions and so tends to suggest that the structure is different from the CS_2 adduct. Treatment of the CS_2 adduct with an equimolar amount of triphenylphosphine affords a compound which has a stoichiometry of $\text{C}_{15}\text{H}_{12}\text{N}_4\text{S}_2$: this has one sulphur less than the starting product. The 1:1 adduct of Hector's Base with MeNCS on the other hand does not undergo this desulphurisation: again this is suggestive of a different

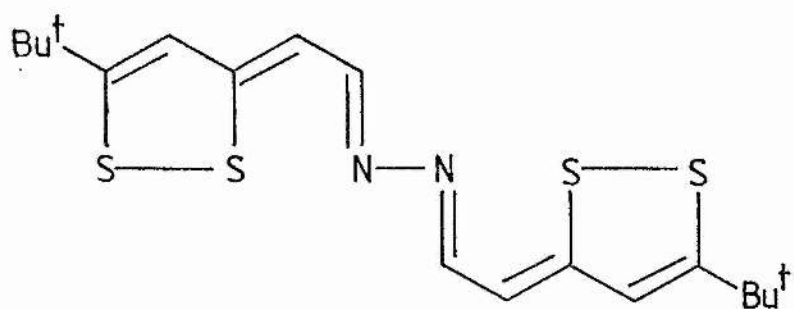
structure.

The dihedral angle between the NC(S)CN side chain and the heterocyclic ring in IV is less than 2° and this near planarity can be ascribed to an extensive π system which encompasses the whole molecule except for the phenyl groups.

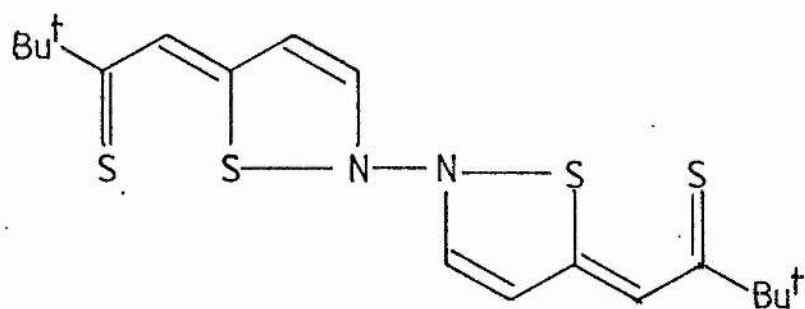
The phenyl ring attached to N3 has a virtually identical orientation to that in the CS₂ adduct (see Table 8.1.2. - dihedral angle 1,3). However the phenyl ring bonded to N2, dihedral angle 1,2 in Table 8.1.2, is rather less twisted with respect to the heterocycle than the analogous ring in the CS₂ adduct. The dihedral angle between the phenyl groups in the MeNCS adduct indicate that they are almost perpendicular to one another: the corresponding angle in the CS₂ adduct is 67.7° .

It is interesting to note however, that although the constitutions of IV and VII are markedly different, the overall molecular shapes are very similar.

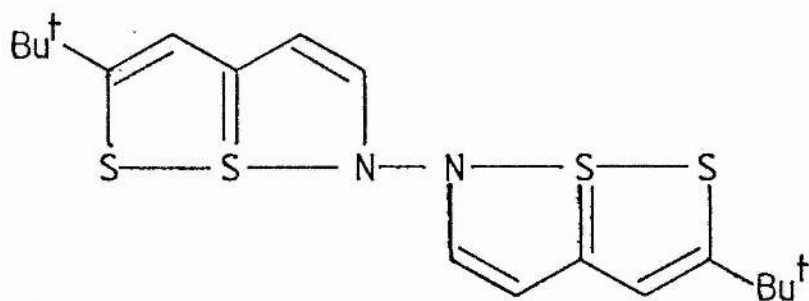
A possible weak hydrogen bond of 2.53 Å between H1 and N1ⁱ (superscript i is the symmetry position x, 0.5-y, 0.5+z) with an angle of N3-H1..N1ⁱ is present and is the only close intermolecular contact.



VIII



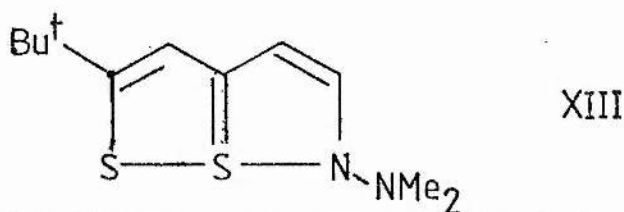
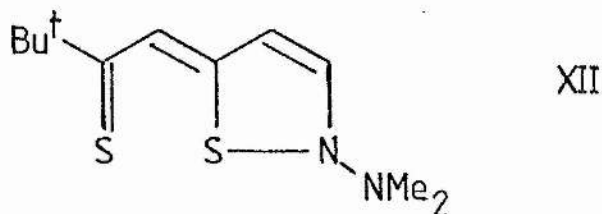
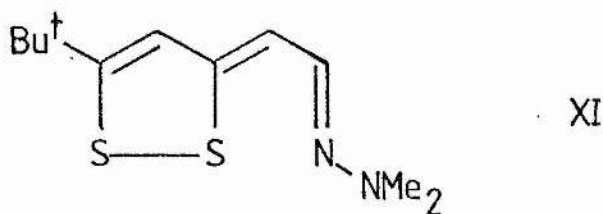
IX



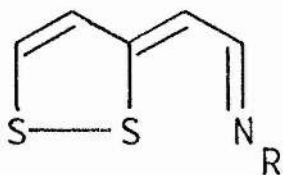
X

II. λ^4 -Triheterapentalenes.

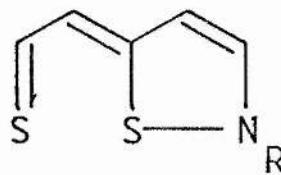
The S-S and S2..N1 distances of 2.124 and 2.489 Å respectively show that N,N'-bis[2-(5-t-butyl-3H-1,2-dithiol-3-ylidene) ethylidene] hydrazine should be portrayed as VIII rather than the other monocyclic form IX, or bicyclic form X. The aforementioned distances are close to those found in a number of other SSN triheterapentalenes: in particular the S-S distance of 2.116 Å and S2..N1 distance of 2.541 Å in N,N-dimethyl-N'-[2-(5-t-butyl-3H-1,2-dithiol-3-ylidene) ethylidene]hydrazine show that this is best represented as the monocyclic structure XI, instead of XII or XIII, which are the monocyclic and bicyclic forms respectively. Despite the fact that the S...N distance is shorter than the sum of the van der Waals' radii of S and N, 3.35 Å [4], it is too long to be regarded as a bond in both VIII and XI.



In section 10 of Chapter Seven, the results of MNDO calculations made on model compounds of these molecules were presented and these showed that the thermodynamically most stable isomer was the experimentally observed structure. In particular for structure XIV and XV, the calculations show that structure XV is steadily destabilised with respect to XIV for the series $R = H, NMe_2, NH_2$ (see Table 7.10.1).



XIV



XV

The acyclic chain in VIII contains three single bonds and this means that both of the main substituents can be either mutually cisoid, c, or transoid, t, and still maintain the skeletal planarity. There are only six possible permutations which preserve the observed configurations about the double bonds, and these are denoted ttt, ttc, ctc, tct, tcc and ccc: thus the observed configuration is designated ctc. Accordingly in order to ascertain the relative stabilities of the six permutations, MNDO calculations were made [5,6] on simpler model compounds where the Bu^t groups were replaced by H. From the calculations the dominant feature appears to be the conformation about the central N-N bond and this conveniently splits the permutations into two sets: the ΔH_f^θ is 40 kJmol^{-1} higher when this is c at N-N than when t. In contrast though a change in conformation from c to t

at either of the other two single bonds affords a decrease of only 1-2 kJmol^{-1} in ΔH_f^θ (see Table 8.2.1.)

Conformation	$\Delta H_f^\theta (\text{kJmol}^{-1})$
ttt	456.6
ttc	458.5
ctc	459.6
tct	494.4
tcc	497.7
ccc	502.6

Table 8.2.1. ΔH_f^θ for conformations of VIII.

From Table 8.2.1 the most stable conformation overall for an isolated molecule is ttt, but the observed conformation is just 3 kJmol^{-1} higher in energy, and this small difference can easily be overcome when the isolated molecule is incorporated into a crystal. The fact that the ttt form is calculated as the most stable is not surprising since this has the least nuclear repulsion of all the possibilities.

The conformations of the Bu^t groups in VIII and XI are different in that in XI the group is rotated through 90° with respect to the heterocyclic plane. MNDO calculations [5,6] indicate, that for isolated molecules, there is free rotation about the C3-C8 bond, and hence the observed configurations are a consequence of packing forces.

In addition the conformation of the -NMe_2 group in IX is of some interest since both methyl groups lie on the same side of the heterocyclic plane. Therefore the three coordinate nitrogen, N2, is pyramidal, and the sum of the bond angles at N2 is 340.8° .

A rather curious molecular stacking arrangement arises in the unit cell of VIII (see Fig 6.3.2). The heterocyclic rings of the molecule centred at (0,0,0) are found to overlap one ring of each of the molecules centred at (1,1,0) and (-1,-1,0), and these overlapping rings are related by the centres of inversion at (0.5,0.5,0) and (-0.5,-0.5,0) respectively. This means that the sulphur atoms from one ring lie over the C=C double bonds associated with the other: one of the sulphurs lying over the endocyclic double bond and the other over the exocyclic double bond. This, when coupled with the rather small interplanar spacing of $4.61(2) \text{ \AA}$, may indicate a significant charge-transfer interaction between the stacked rings; and with the conjugated chain which links the rings in each molecule, suggests that this compound may exhibit interesting electrical properties; maybe even superconductivity!

In contrast however, XI does not have these centrosymmetric ring overlaps: in particular there are no short intermolecular contacts, and as a result the possibility of charge-transfer interactions is greatly reduced.

Chapter Eight.

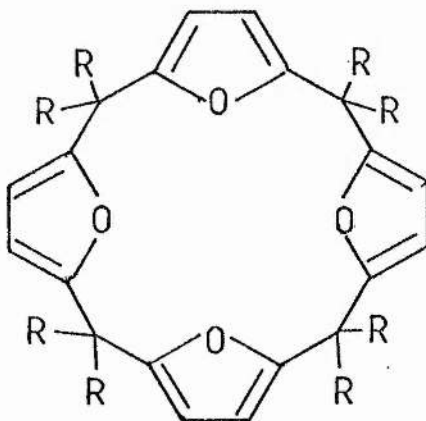
Bibliography.

1. A.R. Butler, C. Glidewell and D.C. Liles. Acta Cryst B34 3241 (1978).
2. A.R. Butler, C. Glidewell and D.C. Liles. Acta Cryst B34 2570 (1978).
3. F. Feigl and K. Weisselberg. Z anal Chem 83 93 (1931).
4. L. Pauling. 'The Nature of the Chemical Bond' 3rd Edn. p. 260 Ithaca: Cornell University Press (1960).
5. M.J.S. Dewar and W. Thiel. J.A.C.S. 99 4899 (1977).
6. W. Thiel. QCPE 11 353 (1978).

Appendix A.

A Macrocyclic Ligand.

Recent interest [1-4] in the macrocyclic tetraoxaquaterenes, I, prompted us to attempt a determination of the structure and conformation of the parent molecule having R=H [5] by means of semi-empirical SCF-MO calculations using the MNDO technique [6-8].



I

The parent macrocycle is a 40 atom molecule, which contains 120 electrons in 112 molecular orbitals, and which requires 114 internal coordinates for the complete specification of its geometry. In order to reduce a very large and expensive geometry optimisation calculation to a practical size, the usual technique of simultaneous optimisation of all variables had to be discarded in favour of a step-wise approach in which rather few variables were optimised at any time.

Firstly the structure of furan and 2,5-dimethylfuran were optimised without any constraints, and the results of these calculations are presented in Table 1, together with the experimental structure for furan, as determined by microwave spectroscopy [9]. The calculated structure of furan agrees well with the experimental structure, and the only significant difference is the magnitude of the C1-C2 bond, calculated to be ca. 0.03 Å too long: despite this, the calculated bond orders, also in Table 1, seem to be reasonably satisfactory for such a weakly aromatic molecule. The differences between the calculated ring geometries for furan and for 2,5-dimethylfuran are minor.

The geometry found for 2,5-dimethylfuran was then transferred, complete, to the macrocycle, and the planarity of the individual furan rings was maintained. The macrocyclic ring structure and conformation are then defined by the eight distances to the bridging methylene carbon atoms, which were constrained to be identical, four angles $\angle(\text{CCC})$ at the methylene carbon atoms, also constrained to be identical, and six dihedral angles, three of type $\angle(\text{CCCO})$ and three of type $\angle(\text{OCCC})$ which define the conformation of the inner ring C_{12}O_4 ring and which were allowed to optimise independently [10]. The optimised values of the CC distances and CCC angle at the bridging carbons are 1.506 Å and 117.2° respectively.

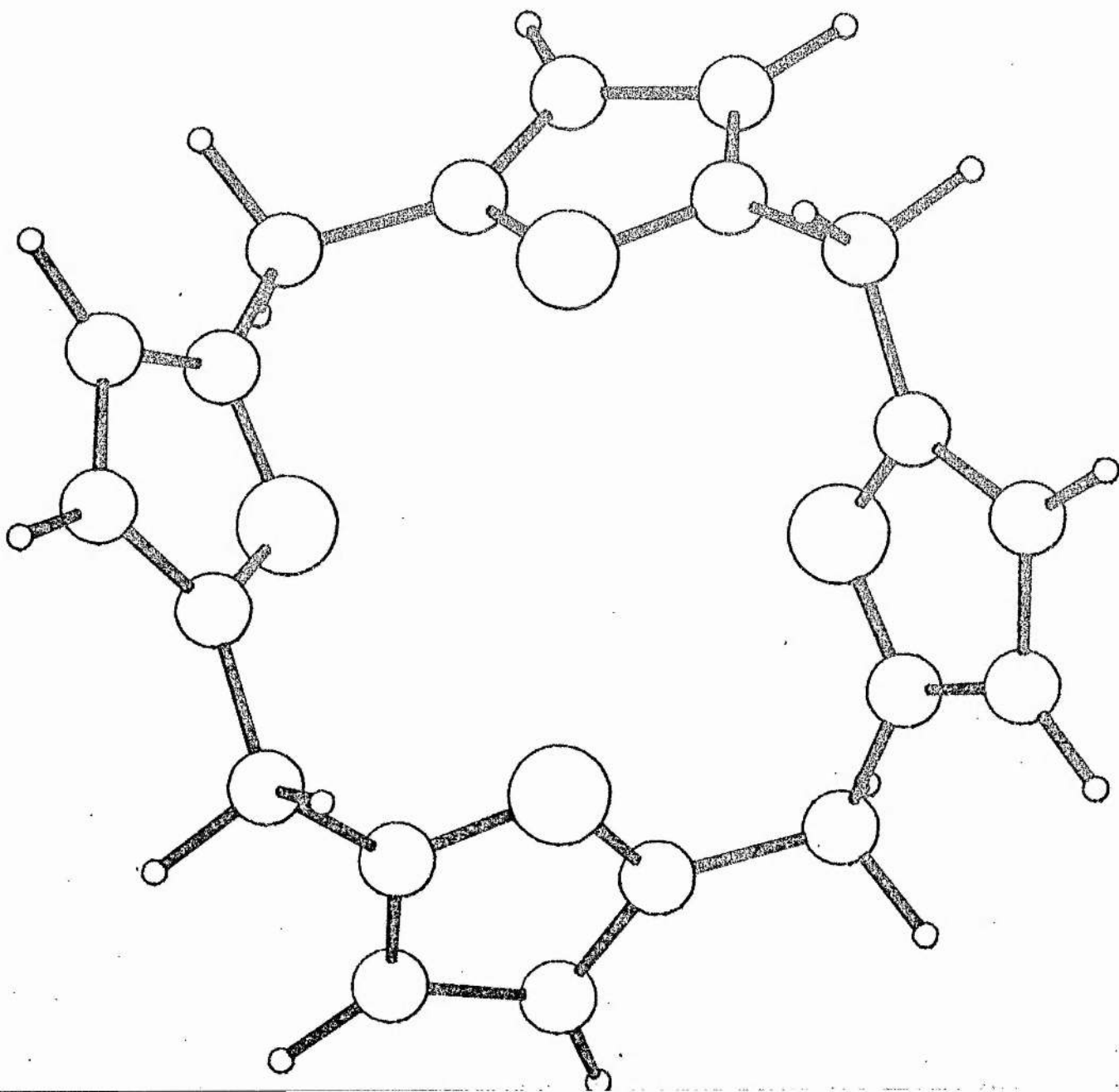
Table 1. Geometrical parameters and bond orders (p) in furan and 2,5-dimethylfuran.

	Furan	Furan	2,5-dimethylfuran
	Calc	Expt a	Calc
d(OC1)/Å	1.363	1.362(1)	1.369
d(C1C2)/Å	1.392	1.361(1)	1.396
d(C2C2')/Å	1.444	1.431(2)	1.436
d(C1H1)/Å	1.083	1.075(2)	(1.495) b
d(C2H2)/Å	1.079	1.077(2)	1.079
<(C1OC1')/°	108.2	106.6(1)	108.4
<(OC1C2)/°	110.0	110.7(1)	109.6
<(OC1C2C2')/°	105.9	106.0(1)	106.2
<(OC1H1)/°	117.3	115.9(1)	(118.0) b
<(C1C2H2)/°	127.5	128.0	127.4
p(OC1)	1.112		1.104
p(C1C2)	1.631		1.604
p(C2C2')	1.216		1.229
p(C1H1)	0.945		(0.969) b
p(C2H2)	0.961		0.961

a. Ref [9]. b. Involve bonds to methyl carbon atoms.

Caption to Figure.

The molecule viewed down the S_4 axis: the distances of the non-hydrogen atoms of the asymmetric unit from the plane defined by the four oxygen atoms are as follows: C2, 0.991 Å; C3, 0.883 Å; C4, 1.611 Å; C5, 1.032 Å; and C6, -0.009 Å: the atom numbering follows that of the systematic name [5].



We had expected at the start of this work that the conformation of the macrocycle might be such that the furan rings were tilted, about the line between the bridging carbons, alternately up and down, yielding an approximately planar set of bridging carbons and a quasi-tetrahedral D_{2d} array of oxygen atoms: in the event we find a quite different puckering mode.

The four oxygen atoms are in an exactly planar array of D_{4h} local symmetry: the overall symmetry of the macrocycle is only S_4 , as the furan rings are not only tilted away from the oxygen plane but skewed also (see Figure). The optimised values of the dihedral angles $\angle(CCCO)$ are alternately $\pm 66.2^\circ$, while the angles $\angle(OCCC)$ all optimise to exactly zero. The dihedral angle between pairs of furan rings related by the S_4 operator is 66.2° , and that between pairs of rings related by the C_2 operator is 78.9° .

The structure and conformation described here represent an isolated molecule, strictly in the gas-phase: however, it also is a good representation of the structure of the isolated ligand in solution in a non-hydroxylic solvent of modest polarity. Structural information of this kind is not easily accessible from x-ray studies on crystalline materials, and it is possible that calculations of this type can be of value in the detailed assessment of ligand conformation in solution.

Appendix A.

Bibliography.

1. A.J. Rest, S.A. Smith and I.D. Tyler. Inorg Chim Acta 16 L1 (1976).
2. M. De Sousa Healy and A.J. Rest. 'Advances in Inorganic Chemistry and Radiochemistry' (Eds. H.J. Emeleus and A.G. Sharpe) Academic Press, New York, Vol 26 (1978).
3. K.W. Field, A.D. Glover, J.S. Moroz, D.J. Collander and K.E. Kolb. J Chem Educ 56 269 (1979).
4. C. Glidewell. J Chem Educ 57 236 (1980).
5. Systematically: 21,22,23,24-tetraoxapentacyclo-[16.2.1.1^{3,6}.1^{8,11}.1^{13,16}]-tetracos-3,5,8,10,13,15,18,20-octaene.
6. M.J.S. Dewar and W. Thiel. J.A.C.S. 99 4899 (1977).
7. W. Thiel, P. Wiener, J. Stewart and M.J.S. Dewar. QCPE No. 428, Chemistry Department, University of Indiana, Bloomington.
8. Computations were undertaken on a VAX 11/780 computer.
9. B. Bak, D. Christensen, W.B. Dixon, L. Hansen-Nygaard, J. Rastrup-Andersen and M. Schottländer. J Mol Spectroscopy 9 124 (1962).
10. Subject to these constraints, the optimisation required ca. 180 hours of CPU time. Other calculated properties are: ΔH_f^θ , -207 kJmol⁻¹; I(vertical), 8.858eV; net atomic charges: C(2), +0.0154e; C(3), -0.030e; C(4), -0.112e; C(5), -0.111e; C(6), -0.035e; O, -0.092e.

Appendix B.

Publications.

1. A.F. Cuthbertson, C. Glidewell, H.D. Holden and D.C. Liles. The constitution of Dost's Keto Compound : crystal and molecular structure of 4-phenyl-3-phenylamino-1,2,4-thiadiazolin-5-one.

J. Chem Res(S) 316 (1979).

J. Chem Res(M) 3714 (1979).

2. A.F. Cuthbertson and C. Glidewell. MINDO/3 Study of some Tetra-atomic Clusters.

Inorg Chim Acta 49 91 (1981).

3. A.F. Cuthbertson and C. Glidewell. The constitution of the 1:1 adduct of Hector's Base and methylisothiocyanate : the crystal and molecular structure of 5-(N-methylthiocarbamoylimino) -4-phenyl -3-phenylamino -4H-1,2,4-thiadiazoline.

Acta Cryst B37 1419 (1981).

4. A.F. Cuthbertson and C. Glidewell. The Structure of Silylcyclopentadienes.

J Organomet Chem 221 19 (1981).

5. A.F. Cuthbertson, C. Glidewell and D. Lloyd. Onium Ions or Allenes in the protodebromination of 6-bromo-2,3-dihydro-1,4-diazepinium ions and related species?

J Chem Res(S) 80 (1982).

6. A.F. Cuthbertson and C. Glidewell. Ligands of Low Electronegativity in the VSEPR model : The structure of singlet carbenes.

J Mol Struct Theochem 87 71 (1982).

7. A.F. Cuthbertson, C. Glidewell and D.C. Liles. Ligands of Low Electronegativity in the VSEPR model : Isoelectronic molecules and ions $(MX_3)_2YE^{+n}$.

J Mol Struct Theochem 87 273 (1982).

8. A.F. Cuthbertson and C. Glidewell. Isomerism and adduct formation in the Hector's Base series : An MNDO study of model compounds.

J Mol Struct Theochem in press.

9. A.F. Cuthbertson, C. Glidewell and D.C. Liles. The Structure of N,N'-bis-(2-(5-t-butyl-3H-1,2-dithiol-3-ylidene)-ethylidene)hydrazine.

Acta Cryst B38 2281 (1982).

10. A.F. Cuthbertson, G. Glidewell and D.C. Liles. The Structure of N,N-dimethyl-N'-(2-(5-t-butyl-3H-1,2-dithiol-3-ylidene)-ethylidene)hydrazine.

Acta Cryst submitted.

11. A.F. Cuthbertson and C. Glidewell. Ligands of Low Electronegativity in the VSEPR model : Molecules and Ions isoelectronic with primary, secondary and tertiary amines.

J Mol Struct Theochem in press.

Appendix C

Observed and Calculated Structure Factors,

Anisotropic Temperature Parameters

and Least-Squares Planes for

4-phenyl-3-phenylamino-1,2,4-thiadiazolin-5-one.

OBSERVED AND CALCULATED STRUCTURE FACTORS FOR DOST'S KETO COMPOUND

H	K	L	10FO	10FC	H	K	L	10FO	10FC	H	K	L	10FO	10FC
2	0	0	586	612	6	6	0	76	80	1	0	1	386	382
4	0	0	143	129	7	6	0	106	101	2	0	1	1106	1182
6	0	0	74	53	8	6	0	65	79	3	0	1	229	212
1	1	0	156	144	9	6	0	120	146	4	0	1	371	373
2	1	0	373	355	10	6	0	93	83	5	0	1	335	319
3	1	0	367	356	13	6	0	82	80	6	0	1	445	423
4	1	0	122	137	1	7	0	135	204	8	0	1	167	187
6	1	0	328	313	3	7	0	189	186	13	0	1	48	67
7	1	0	188	202	4	7	0	174	161	0	1	1	371	363
8	1	0	152	147	6	7	0	146	143	1	1	1	334	314
9	1	0	132	122	7	7	0	77	93	2	1	1	792	830
10	1	0	167	171	8	7	0	41	41	3	1	1	439	426
12	1	0	45	58	11	7	0	70	72	4	1	1	279	300
1	2	0	127	131	12	7	0	101	98	5	1	1	265	256
2	2	0	77	93	1	8	0	18	41	6	1	1	429	396
3	2	0	503	482	2	8	0	87	98	7	1	1	139	153
5	2	0	91	84	4	8	0	161	169	8	1	1	85	94
7	2	0	91	91	5	8	0	91	100	10	1	1	73	66
11	2	0	99	89	6	8	0	42	40	11	1	1	111	104
12	2	0	77	92	8	8	0	78	90	12	1	1	113	118
14	2	0	48	45	9	8	0	47	63	13	1	1	81	98
1	3	0	422	499	14	8	0	76	65	0	2	1	194	189
2	3	0	345	332	2	9	0	59	77	1	2	1	718	730
3	3	0	387	401	3	9	0	100	99	2	2	1	691	708
4	3	0	32	52	4	9	0	142	145	3	2	1	745	749
6	3	0	127	133	5	9	0	83	83	4	2	1	464	467
7	3	0	144	154	6	9	0	59	50	5	2	1	127	132
9	3	0	61	54	10	9	0	48	37	6	2	1	179	169
13	3	0	109	124	12	9	0	67	57	7	2	1	167	181
15	3	0	65	78	0	10	0	21	120	11	2	1	135	139
0	4	0	20	83	1	10	0	25	44	12	2	1	140	137
1	4	0	216	262	3	10	0	55	81	15	2	1	59	75
2	4	0	24	48	4	10	0	45	57	0	3	1	184	225
3	4	0	236	237	6	10	0	35	33	1	3	1	744	786
4	4	0	410	397	7	10	0	113	115	2	3	1	398	411
5	4	0	108	112	9	10	0	91	87	3	3	1	95	94
6	4	0	189	173	11	10	0	79	51	4	3	1	184	173
8	4	0	116	123	1	11	0	54	124	5	3	1	359	350
9	4	0	71	78	2	11	0	31	54	6	3	1	130	118
10	4	0	90	77	3	11	0	30	51	7	3	1	161	160
11	4	0	57	44	4	11	0	58	41	8	3	1	94	113
1	5	0	243	340	5	11	0	114	114	9	3	1	58	45
2	5	0	213	214	0	12	0	145	76	10	3	1	47	39
4	5	0	371	339	1	12	0	40	90	11	3	1	161	164
6	5	0	91	105	2	12	0	41	43	13	3	1	88	93
7	5	0	79	73	3	12	0	22	29	14	3	1	59	70
8	5	0	70	75	5	12	0	61	63	0	4	1	69	80
10	5	0	227	205	7	12	0	34	28	1	4	1	277	290
11	5	0	125	129	8	12	0	56	55	2	4	1	151	148
0	6	0	26	95	1	13	0	21	38	3	4	1	281	258
1	6	0	29	33	4	13	0	59	64	4	4	1	82	67
2	6	0	29	19	10	13	0	111	70	5	4	1	287	276
3	6	0	185	178	1	14	0	31	54	6	4	1	169	155
5	6	0	266	272	5	14	0	68	65	7	4	1	89	89

0	5	1	14	23
1	5	1	96	120
2	5	1	246	254
3	5	1	245	207
4	5	1	158	155
5	5	1	70	82
6	5	1	170	150
7	5	1	142	139
8	5	1	162	186
9	5	1	158	132
10	5	1	137	119
11	5	1	54	53
0	6	1	60	95
1	6	1	363	455
2	6	1	136	132
3	6	1	163	170
4	6	1	133	151
5	6	1	74	48
6	6	1	190	184
7	6	1	60	60
8	6	1	56	55
10	6	1	57	48
11	6	1	84	76
12	6	1	56	61
0	7	1	148	225
1	7	1	156	176
2	7	1	93	123
3	7	1	56	49
4	7	1	87	94
5	7	1	127	115
7	7	1	115	112
8	7	1	58	76
9	7	1	102	117
11	7	1	121	110
12	7	1	57	54
13	7	1	50	46
1	8	1	28	40
2	8	1	128	132
3	8	1	51	57
4	8	1	102	101
5	8	1	90	94
6	8	1	241	222
8	8	1	53	47
9	8	1	34	45
10	8	1	75	64
0	9	1	58	96
2	9	1	139	183
4	9	1	58	66
5	9	1	61	57
6	9	1	97	81
7	9	1	83	78
9	9	1	82	92
0	10	1	56	87
1	10	1	72	104

2	10	1	47	69
3	10	1	75	84
4	10	1	96	105
5	10	1	40	28
6	10	1	44	55
7	10	1	63	63
0	11	1	62	106
1	11	1	43	86
2	11	1	54	60
3	11	1	38	42
7	11	1	104	95
8	11	1	43	44
11	11	1	75	57
1	12	1	16	39
2	12	1	27	38
3	12	1	53	61
4	12	1	63	65
5	12	1	37	30
6	12	1	64	69
8	12	1	60	48
10	12	1	86	57
1	13	1	27	39
2	13	1	56	78
3	13	1	28	26
5	13	1	55	53
8	13	1	42	38
1	14	1	28	37
0	0	2	165	159
1	0	2	566	580
2	0	2	525	522
3	0	2	100	95
4	0	2	557	556
5	0	2	236	240
6	0	2	120	108
7	0	2	101	95
10	0	2	78	84
11	0	2	55	53
0	1	2	491	484
1	1	2	318	304
2	1	2	215	205
3	1	2	497	484
4	1	2	342	312
5	1	2	168	167
6	1	2	240	224
7	1	2	157	154
10	1	2	87	80
12	1	2	48	54
0	2	2	172	164
1	2	2	1014	1056
2	2	2	694	708
3	2	2	293	244
4	2	2	322	312
5	2	2	355	375
6	2	2	360	334

7	2	2	239	251
11	2	2	73	75
12	2	2	45	41
13	2	2	64	79
14	2	2	84	87
0	3	2	27	33
1	3	2	350	337
2	3	2	193	168
3	3	2	119	119
4	3	2	223	211
5	3	2	408	395
6	3	2	360	313
7	3	2	104	111
8	3	2	121	131
9	3	2	89	77
10	3	2	74	78
13	3	2	76	83
0	4	2	438	434
1	4	2	223	198
2	4	2	39	41
3	4	2	88	85
4	4	2	235	220
5	4	2	53	55
6	4	2	189	169
7	4	2	36	43
8	4	2	40	48
9	4	2	68	58
11	4	2	91	85
12	4	2	60	60
13	4	2	74	78
14	4	2	65	72
0	5	2	104	87
1	5	2	131	128
2	5	2	205	201
3	5	2	412	394
5	5	2	166	160
6	5	2	85	71
7	5	2	38	40
8	5	2	236	266
9	5	2	152	133
10	5	2	127	122
11	5	2	48	47
12	5	2	91	84
0	6	2	156	154
1	6	2	111	101
2	6	2	91	88
3	6	2	420	408
4	6	2	106	99
5	6	2	93	89
6	6	2	75	76
7	6	2	227	233
8	6	2	138	142
9	6	2	141	120
10	6	2	125	99

0	7	2	183	204
1	7	2	188	212
2	7	2	138	147
3	7	2	32	34
4	7	2	188	192
5	7	2	121	126
6	7	2	65	63
8	7	2	56	52
10	7	2	68	61
11	7	2	86	79
12	7	2	51	55
13	7	2	61	61
0	8	2	69	84
1	8	2	85	88
2	8	2	210	217
3	8	2	98	110
4	8	2	93	97
5	8	2	36	44
6	8	2	80	67
7	8	2	94	95
8	8	2	78	92
9	8	2	42	35
12	8	2	59	57
13	8	2	47	37
0	9	2	72	105
1	9	2	60	76
2	9	2	73	73
3	9	2	49	48
4	9	2	159	153
5	9	2	31	34
6	9	2	96	81
7	9	2	78	71
8	9	2	72	70
9	9	2	69	50
11	9	2	92	74
0	10	2	66	83
1	10	2	24	33
2	10	2	117	141
3	10	2	48	53
4	10	2	57	54
5	10	2	104	105
6	10	2	31	25
7	10	2	34	37
9	10	2	53	48
0	11	2	64	74
1	11	2	31	43
2	11	2	20	21
3	11	2	49	34
4	11	2	49	53
5	11	2	103	103
8	11	2	75	76
9	11	2	46	41
1	12	2	42	55
2	12	2	52	61

3	12	2	37	37
1	13	2	27	28
2	13	2	30	36
4	13	2	48	51
5	13	2	43	41
7	13	2	50	44
6	14	2	32	32
7	14	2	69	59
1	0	3	58	50
2	0	3	486	442
3	0	3	96	78
4	0	3	41	37
5	0	3	389	378
6	0	3	373	366
7	0	3	168	189
15	0	3	72	88
0	1	3	242	237
1	1	3	173	162
2	1	3	453	409
3	1	3	203	175
4	1	3	386	385
5	1	3	408	384
6	1	3	260	251
7	1	3	132	115
9	1	3	138	133
11	1	3	134	132
12	1	3	94	97
14	1	3	56	67
1	2	3	246	252
2	2	3	488	427
3	2	3	360	328
4	2	3	464	465
5	2	3	101	91
9	2	3	69	67
11	2	3	75	73
14	2	3	70	92
15	2	3	53	67
0	3	3	73	43
1	3	3	181	184
2	3	3	127	87
3	3	3	348	317
4	3	3	304	288
5	3	3	312	294
6	3	3	231	232
7	3	3	189	205
8	3	3	72	86
10	3	3	102	102
11	3	3	85	85
12	3	3	52	64
13	3	3	46	50
14	3	3	52	74
0	4	3	65	55
2	4	3	371	321
3	4	3	215	188

4	4	3	215	221
5	4	3	241	222
6	4	3	274	260
8	4	3	101	112
12	4	3	78	82
13	4	3	76	68
14	4	3	58	62
0	5	3	208	190
1	5	3	382	361
2	5	3	210	180
3	5	3	80	71
4	5	3	202	194
5	5	3	196	166
6	5	3	127	126
7	5	3	135	146
8	5	3	104	116
9	5	3	143	124
10	5	3	113	106
11	5	3	48	47
0	6	3	338	330
1	6	3	169	167
2	6	3	77	75
3	6	3	174	157
4	6	3	111	101
5	6	3	134	112
6	6	3	112	107
7	6	3	85	106
8	6	3	125	133
9	6	3	234	200
0	7	3	130	133
1	7	3	111	111
2	7	3	198	196
4	7	3	70	60
5	7	3	197	177
6	7	3	184	176
8	7	3	57	57
10	7	3	62	55
13	7	3	64	74
0	8	3	57	50
1	8	3	92	106
2	8	3	79	76
3	8	3	47	50
4	8	3	55	52
5	8	3	132	135
6	8	3	216	202
7	8	3	51	48
8	8	3	96	94
9	8	3	117	88
11	8	3	65	53
1	9	3	76	76
2	9	3	165	185
3	9	3	158	169
4	9	3	103	104
5	9	3	59	44

6	9	3	93	94
7	9	3	46	37
9	9	3	75	69
10	9	3	86	58
0	10	3	144	145
1	10	3	53	66
2	10	3	28	39
3	10	3	81	75
4	10	3	132	133
5	10	3	73	45
1	11	3	55	51
3	11	3	34	31
4	11	3	30	28
6	11	3	74	60
7	11	3	59	54
11	11	3	63	55
3	12	3	26	23
5	12	3	48	36
6	12	3	51	41
7	12	3	41	32
1	13	3	33	45
2	13	3	29	40
3	13	3	35	26
5	13	3	41	45
7	13	3	30	24
4	14	3	41	34
0	0	4	592	593
1	0	4	172	178
2	0	4	102	113
3	0	4	501	445
4	0	4	153	136
6	0	4	29	44
9	0	4	51	48
10	0	4	45	54
11	0	4	69	75
12	0	4	50	43
0	1	4	295	282
1	1	4	319	304
2	1	4	169	176
3	1	4	79	65
4	1	4	324	284
5	1	4	44	49
6	1	4	194	200
7	1	4	96	101
8	1	4	107	111
11	1	4	51	67
13	1	4	49	50
0	2	4	251	226
1	2	4	174	161
2	2	4	181	175
3	2	4	272	239
4	2	4	281	270
5	2	4	93	80
7	2	4	32	36

0	3	4	52	41
1	3	4	283	262
2	3	4	302	290
3	3	4	225	200
4	3	4	280	254
5	3	4	153	162
6	3	4	85	95
7	3	4	229	253
9	3	4	127	123
10	3	4	111	120
11	3	4	87	88
13	3	4	51	56
0	4	4	262	257
1	4	4	217	210
2	4	4	133	142
3	4	4	348	310
4	4	4	171	169
5	4	4	288	286
7	4	4	43	63
8	4	4	178	144
10	4	4	53	54
12	4	4	70	78
0	5	4	123	139
1	5	4	114	99
2	5	4	193	188
3	5	4	119	92
5	5	4	37	41
6	5	4	73	67
7	5	4	301	325
8	5	4	124	104
9	5	4	72	60
10	5	4	119	122
11	5	4	75	82
13	5	4	61	72
0	6	4	100	99
1	6	4	74	61
2	6	4	54	61
3	6	4	91	71
4	6	4	172	150
5	6	4	247	234
6	6	4	106	99
7	6	4	66	86
8	6	4	167	134
13	6	4	54	64
14	6	4	61	64
0	7	4	150	167
1	7	4	158	170
2	7	4	108	112
3	7	4	138	113
4	7	4	229	201
5	7	4	172	166
6	7	4	218	215
7	7	4	131	125
11	7	4	60	52

0	8	4	94	98
1	8	4	75	76
2	8	4	94	99
3	8	4	334	283
4	8	4	230	196
5	8	4	69	58
6	8	4	45	33
10	8	4	64	57
12	8	4	45	46
0	9	4	54	48
1	9	4	82	73
2	9	4	114	116
3	9	4	53	43
4	9	4	143	124
5	9	4	122	109
6	9	4	62	60
7	9	4	48	41
8	9	4	66	54
9	9	4	76	52
0	10	4	46	39
1	10	4	35	42
2	10	4	38	43
3	10	4	75	91
4	10	4	76	61
6	10	4	101	89
7	10	4	38	34
8	10	4	76	57
9	10	4	46	37
0	11	4	71	70
2	11	4	73	85
3	11	4	29	35
5	11	4	59	56
6	11	4	57	56
7	11	4	37	27
0	12	4	47	55
1	12	4	50	53
3	12	4	40	41
5	12	4	42	28
10	12	4	46	35
3	14	4	29	31
6	14	4	38	29
1	0	5	192	192
2	0	5	192	180
3	0	5	148	154
6	0	5	131	158
11	0	5	106	126
15	0	5	56	73
0	1	5	206	196
1	1	5	285	265
2	1	5	158	155
3	1	5	183	177
4	1	5	168	179
5	1	5	106	112
7	1	5	102	93

10	1	5	71	86
11	1	5	60	60
13	1	5	53	69
0	2	5	96	132
1	2	5	107	107
2	2	5	474	435
3	2	5	191	196
4	2	5	168	152
7	2	5	104	107
8	2	5	56	57
10	2	5	61	75
11	2	5	60	56
0	3	5	54	43
1	3	5	332	322
2	3	5	158	152
3	3	5	231	216
4	3	5	316	319
5	3	5	142	138
6	3	5	125	141
7	3	5	57	57
8	3	5	158	151
9	3	5	51	51
10	3	5	44	42
12	3	5	71	76
14	3	5	48	55
0	4	5	54	55
1	4	5	92	87
2	4	5	90	91
3	4	5	101	90
6	4	5	45	57
10	4	5	99	106
11	4	5	65	75
14	4	5	54	63
1	5	5	141	135
2	5	5	99	103
3	5	5	153	156
4	5	5	148	153
5	5	5	116	122
7	5	5	89	66
8	5	5	193	181
10	5	5	99	87
12	5	5	66	75
14	5	5	54	52
0	6	5	163	156
1	6	5	101	78
2	6	5	214	184
3	6	5	215	210
5	6	5	210	216
6	6	5	96	110
8	6	5	69	60
10	6	5	59	54
11	6	5	47	46
0	7	5	142	118
2	7	5	95	90

3	7	5	203	185
4	7	5	148	150
5	7	5	131	117
6	7	5	98	103
12	7	5	55	44
13	7	5	72	75
0	8	5	104	112
1	8	5	91	79
2	8	5	132	115
3	8	5	114	122
4	8	5	45	49
5	8	5	99	96
6	8	5	85	79
7	8	5	80	55
9	8	5	63	56
11	8	5	54	57
0	9	5	93	78
1	9	5	80	78
2	9	5	96	84
3	9	5	180	153
4	9	5	99	97
6	9	5	61	53
8	9	5	60	50
9	9	5	44	42
0	10	5	127	128
1	10	5	70	63
2	10	5	86	72
4	10	5	51	36
6	10	5	71	78
8	10	5	48	20
0	11	5	57	56
1	11	5	63	59
2	11	5	59	60
3	11	5	53	55
4	11	5	54	47
6	11	5	44	31
8	11	5	60	41
0	12	5	41	37
3	12	5	58	57
7	12	5	49	36
1	13	5	40	29
3	13	5	46	45
3	0	6	54	41
7	0	6	81	82
0	1	6	109	104
1	1	6	57	61
8	1	6	51	51
9	1	6	63	67
11	1	6	103	123
14	1	6	54	66
2	2	6	93	110
3	2	6	175	194
10	2	6	74	87
11	2	6	60	71

12	2	6	68	77
0	3	6	218	230
1	3	6	134	142
2	3	6	210	227
3	3	6	108	112
4	3	6	158	178
5	3	6	255	220
6	3	6	141	121
7	3	6	83	77
8	3	6	65	65
9	3	6	96	93
11	3	6	62	76
4	4	6	111	125
5	4	6	115	106
6	4	6	97	90
9	4	6	52	39
0	5	6	32	37
1	5	6	232	235
2	5	6	194	202
3	5	6	109	130
5	5	6	227	179
6	5	6	107	106
7	5	6	122	103
8	5	6	74	74
9	5	6	157	150
10	5	6	81	83
11	5	6	59	66
0	6	6	36	37
1	6	6	55	57
2	6	6	132	146
3	6	6	122	132
4	6	6	69	73
5	6	6	61	33
7	6	6	62	52
8	6	6	111	103
10	6	6	149	146
0	7	6	185	173
1	7	6	71	85
2	7	6	158	147
3	7	6	61	64
5	7	6	59	51
6	7	6	71	60
7	7	6	118	100
8	7	6	69	55
11	7	6	72	79
12	7	6	69	72
0	8	6	125	116
1	8	6	113	107
3	8	6	32	37
4	8	6	64	54
5	8	6	110	88
9	8	6	52	44
11	8	6	49	60
0	9	6	176	175

2	9	6	37	24
3	9	6	64	54
4	9	6	71	73
5	9	6	72	84
6	9	6	62	47
7	9	6	56	37
9	9	6	62	47
2	10	6	105	102
3	10	6	40	47
5	10	6	42	47
6	10	6	101	73
0	11	6	97	81
1	11	6	35	31
3	11	6	35	26
4	11	6	56	64
2	12	6	42	48
3	12	6	49	45
6	14	6	34	33
2	0	7	96	89
3	0	7	60	54
5	0	7	91	90
0	1	7	44	30
4	1	7	159	143
7	1	7	91	91
10	1	7	111	122
13	1	7	53	77
8	2	7	80	86
10	2	7	60	65
12	2	7	57	68
13	2	7	73	74
0	3	7	172	163
1	3	7	148	129
2	3	7	142	115
3	3	7	86	73
4	3	7	97	89
5	3	7	105	88
6	3	7	122	125
7	3	7	91	96
8	3	7	94	91
9	3	7	61	56
11	3	7	62	63
5	4	7	201	197
6	4	7	69	71
9	4	7	70	82
11	4	7	69	78
0	5	7	184	149
1	5	7	174	153
3	5	7	166	155
4	5	7	84	63
5	5	7	121	122
7	5	7	69	69
8	5	7	129	125
9	5	7	46	44
10	5	7	79	84

0	6	7	148	111
1	6	7	176	152
2	6	7	146	126
3	6	7	137	111
4	6	7	72	64
7	6	7	73	63
8	6	7	84	79
12	6	7	53	55
0	7	7	49	33
1	7	7	132	96
2	7	7	91	56
3	7	7	109	96
5	7	7	125	111
6	7	7	75	65
8	7	7	46	42
9	7	7	59	52
10	7	7	54	62
0	8	7	48	52
2	8	7	50	33
3	8	7	46	26
4	8	7	60	50
7	8	7	69	73
9	8	7	82	74
11	8	7	53	54
12	8	7	61	60
1	9	7	73	69
2	9	7	84	55
3	9	7	69	63
6	9	7	59	58
7	9	7	49	47
9	9	7	55	49
0	10	7	89	75
1	10	7	53	53
2	10	7	91	97
0	11	7	49	50
2	11	7	73	66
6	11	7	69	49
0	12	7	63	74
4	12	7	45	33
5	12	7	77	59
1	0	8	72	67
9	0	8	50	38
13	0	8	87	118
1	1	8	159	139
5	1	8	58	50
7	1	8	84	93
8	1	8	62	62
9	1	8	75	81
1	2	8	67	64
2	2	8	95	101
6	2	8	60	69
7	2	8	58	63
8	2	8	145	165
10	2	8	56	61

11	2	8	64	83
1	3	8	47	52
2	3	8	145	143
3	3	8	185	186
4	3	8	94	104
6	3	8	105	111
7	3	8	93	88
8	3	8	56	66
11	3	8	63	54
0	4	8	47	46
1	4	8	189	170
3	4	8	96	104
6	4	8	63	66
9	4	8	81	85
1	5	8	101	97
2	5	8	55	48
3	5	8	44	42
4	5	8	106	118
5	5	8	122	115
7	5	8	102	99
10	5	8	83	95
1	6	8	129	127
2	6	8	52	37
4	6	8	60	60
6	6	8	86	78
7	6	8	49	38
8	6	8	68	66
9	6	8	60	64
2	7	8	87	66
3	7	8	70	70
4	7	8	91	91
5	7	8	70	74
9	7	8	67	61
0	8	8	84	56
3	8	8	63	54
5	8	8	73	79
6	8	8	53	51
1	9	8	72	48
7	9	8	50	29
2	10	8	51	36
6	10	8	72	64
7	10	8	80	79
0	11	8	55	43
2	11	8	63	44
1	12	8	62	54
2	12	8	69	54
5	12	8	51	51
1	0	9	71	60
4	0	9	48	39
6	0	9	57	68
7	0	9	130	147
10	0	9	61	78
3	1	9	111	111

5	1	9	51	55
6	1	9	55	66
8	1	9	62	66
9	1	9	100	118
0	2	9	68	79
1	2	9	176	183
3	2	9	83	97
4	2	9	80	92
8	2	9	61	76
9	2	9	57	64
1	3	9	96	112
4	3	9	86	104
6	3	9	73	93
7	3	9	70	95
9	3	9	66	75
0	4	9	106	107
3	4	9	70	59
4	4	9	73	87
5	4	9	67	76
6	4	9	66	82
7	4	9	86	96
10	4	9	60	75
1	5	9	81	77
2	5	9	86	90
3	5	9	77	72
4	5	9	58	55
9	5	9	59	64
1	6	9	68	58
6	6	9	55	59
7	6	9	58	56
8	6	9	59	65
4	7	9	86	94
7	8	9	79	74
0	9	9	74	69
3	9	9	56	48
4	9	9	86	77
2	10	9	57	38
5	10	9	68	63
1	11	9	69	56
2	11	9	54	33
0	0	10	78	81
2	0	10	135	159
3	0	10	56	56
6	0	10	78	93
7	0	10	96	103
3	1	10	106	126
4	1	10	69	80
5	1	10	69	57
10	1	10	52	72
11	1	10	61	73
0	2	10	65	68
1	2	10	48	57
3	2	10	52	60

4	2	10	54	63
5	2	10	101	132
7	2	10	52	67
11	2	10	58	68
0	3	10	102	119
1	3	10	135	155
3	3	10	77	81
5	3	10	76	81
6	3	10	76	93
7	3	10	52	62
8	3	10	48	54
0	4	10	68	73
1	4	10	65	73
2	4	10	68	71
3	4	10	49	53
4	4	10	88	98
5	4	10	50	55
6	4	10	52	49
1	5	10	104	110
3	5	10	59	75
8	5	10	61	64
5	7	10	73	73
6	7	10	67	78
2	8	10	70	70
4	8	10	47	44
0	10	10	89	71
4	10	10	57	43
1	11	10	46	41
6	0	11	66	79
1	1	11	67	75
4	1	11	61	78
3	2	11	90	101
1	3	11	115	136
2	3	11	61	59
4	3	11	55	54
5	3	11	56	72
6	4	11	71	74
0	5	11	85	109
3	5	11	53	60
2	7	11	49	51
7	7	11	49	57
1	8	11	52	57
4	8	11	69	65
0	0	12	54	71
2	2	12	60	63
2	3	12	57	68
3	3	12	62	88
1	5	12	59	66
3	5	12	55	64
0	6	12	59	74
0	7	12	74	84
0	1	13	63	83

Anisotropic thermal parameters ($\text{\AA}^2 \times 10^3$)

Atom	U_{11}	U_{22}	U_{33}	U_{23}	U_{31}	U_{12}
S(1)	48(2)	62(2)	42(2)	-2(2)	-13(2)	-10(2)
N(1)	38(6)	63(6)	22(5)	-1(4)	-7(4)	-4(5)
N(2)	27(5)	52(5)	23(5)	5(4)	-9(4)	0(4)
N(3)	26(5)	59(6)	30(5)	8(5)	-6(5)	-8(4)
O(1)	51(6)	63(6)	38(5)	22(4)	-3(5)	-5(5)
C(1)	34(6)	37(5)	26(5)	-5(4)	-1(5)	9(5)
C(2)	30(7)	79(9)	42(7)	-29(7)	8(6)	-2(7)
C(3)	35(7)	47(6)	26(6)	0(5)	0(5)	9(5)
C(4)	37(8)	61(8)	51(9)	17(7)	-10(7)	0(6)
C(5)	46(9)	99(12)	41(9)	20(8)	-15(7)	0(8)
C(6)	81(11)	68(8)	28(6)	19(7)	-9(7)	22(9)
C(7)	58(9)	68(8)	41(7)	9(7)	7(7)	-15(8)
C(8)	47(8)	57(7)	30(7)	7(6)	0(6)	-3(6)
C(9)	33(6)	42(5)	23(5)	4(5)	-8(5)	-3(5)
C(10)	41(7)	70(8)	32(6)	-11(6)	-3(6)	-3(6)
C(11)	93(12)	55(7)	34(7)	-9(6)	2(8)	-26(9)
C(12)	57(10)	85(10)	52(10)	36(8)	-33(8)	-21(8)
C(13)	36(9)	103(13)	73(12)	-2(11)	-16(9)	-4(9)
C(14)	31(7)	79(9)	48(8)	2(7)	-2(7)	12(7)

The anisotropic temperature factor takes the form

$$\exp [-2\pi^2 (h^2 \underline{a}^2 U_{11} + k^2 \underline{b}^2 U_{22} + l^2 \underline{c}^2 U_{33} + 2kl \underline{b}^* \underline{c}^* U_{23} + 2lh \underline{c}^* \underline{a}^* U_{31} + 2hk \underline{a}^* \underline{b}^* U_{12})]$$

The common isotropic temperature factor for the hydrogen atoms refined to $63(13) \times 10^{-3} \text{\AA}^2$.

Least Squares planes

Plane	Atoms	A	B	C	Atom Distance from Plane ($\sqrt{A^2 + B^2 + C^2} \times 10^{-3}$)
1	S(1) N(1) N(2) C(1) C(2)	0.3006	-0.1915	-0.2387	S(1), -101; N(1), 99; N(2), -51; C(1), -39; C(2), 95; O(1), -344; N(3), -522; C(9), 497.
2	C(3) C(4) C(5) C(6) C(7) C(8)	0.1308	-0.2409	-0.1969	C(3), 43; C(4), 79; C(5), -141; C(6), 76; C(7), 40; C(8), -95; N(3), -92.
3	C(9) C(10) C(11) C(12) C(13) C(14)	-0.2495	-0.7448	0.4803	C(9), 172; C(10), -36; C(11), 75; C(12), -193; C(13), 310; C(14), -304; N(2), -399.

Least-squares planes are defined in orthogonal coordinates (in Å) by the equation: $Ax + By + Cz + 1 = 0$

Dihedral angles between the planes ($^{\circ}$).

Planes: 1,2 1,3 2,3
Angle: 23.82 -83.17 80.33

Appendix C

Observed and Calculated Structure Factors,

Anisotropic Temperature Parameters

and Least-Squares Planes for

5-(N-methylthiocarbamoylimino)-4-phenyl-

3-phenylamino-4H-1,2,4-thiadiazoline.

OBSERVED AND CALCULATED STRUCTURE FACTORS FOR HRMENCs

PAGE 1

H	K	L	10FO	10FC	H	K	L	10FO	10FC	H	K	L	10FO	10FC	H	K	L	10FO	10FC	L	10FO	10FC
2	0	0	486	-562	3	5	0	314	286	5	12	0	190	202	3	2	1	480	-477	1	325	-330
3	0	0	455	428	4	5	0	395	-402	1	13	0	154	241	-3	5	1	545	568	1	90	-58
4	0	0	372	372	6	5	0	171	-186	2	13	0	213	-236	-1	5	1	322	-318	1	71	69
5	0	0	397	-403	7	5	0	150	-131	4	13	0	114	91	0	5	1	224	238	1	117	133
6	0	0	273	-278	2	6	0	551	-555	5	13	0	221	201	1	5	1	239	-242	1	358	402
7	0	0	371	349	3	6	0	173	168	2	14	0	368	-425	2	5	1	156	119	1	482	-495
9	0	0	349	-367	4	6	0	399	396	3	14	0	273	285	5	5	1	255	-237	1	166	172
1	1	0	69	50	5	6	0	256	-250	7	14	0	103	104	-8	6	1	369	-310	1	222	221
2	1	0	766	775	6	6	0	175	-183	1	16	0	74	-104	-6	6	1	235	-239	1	124	113
3	1	0	467	459	7	6	0	362	330	4	16	0	117	156	-5	6	1	738	712	1	275	268
7	1	0	134	108	8	6	0	206	-214	4	17	0	108	-116	-4	6	1	1180	-1189	1	223	222
8	1	0	229	230	1	7	0	168	184	6	17	0	118	-95	-3	6	1	662	-679	1	572	-516
9	1	0	158	-208	2	7	0	307	-307	4	18	0	171	178	-1	6	1	227	255	1	134	-123
1	2	0	366	379	3	7	0	240	214	5	18	0	186	-155	0	6	1	1895	2003	1	397	-473
2	2	0	413	-454	4	7	0	235	-227	4	19	0	112	129	1	6	1	1434	-1446	1	535	495
3	2	0	232	231	6	7	0	376	-391	-8	1	1	162	139	2	6	1	130	-80	1	228	-253
4	2	0	131	154	7	7	0	223	183	-6	1	1	285	324	3	6	1	656	704	1	687	642
5	2	0	366	-365	-5	7	0	195	-172	-5	1	1	396	-372	4	6	1	156	-173	1	653	-682
1	3	0	527	-595	1	8	0	91	-139	-2	1	1	379	360	6	6	1	209	-236	1	297	293
2	3	0	1370	1469	2	8	0	155	116	-1	1	1	405	-441	8	6	1	449	438	1	174	-178
3	3	0	418	-421	4	8	0	262	277	1	1	1	209	-258	7	6	1	226	-229	1	255	215
4	3	0	534	536	7	8	0	147	-113	2	1	1	574	553	-11	7	1	209	200	1	157	-167
5	3	0	111	-111	4	9	0	319	318	3	1	1	833	-811	-8	7	1	409	373	1	200	-188
6	3	0	128	112	5	9	0	186	-210	4	1	1	254	287	-6	7	1	208	-172	1	296	292
9	3	0	153	-176	1	10	0	142	-176	5	1	1	119	114	-4	7	1	252	-206	1	163	-166
10	3	0	193	226	2	10	0	124	-116	6	1	1	458	-514	-3	7	1	74	86	1	725	675
11	3	0	142	-81	4	10	0	393	402	7	1	1	157	152	-2	7	1	201	-187	1	187	187
1	4	0	117	158	5	10	0	249	-226	-10	2	1	172	-209	-1	7	1	274	-276	1	677	-700
2	4	0	1226	-1257	6	10	0	154	172	-8	2	1	177	-186	0	7	1	546	-542	1	105	95
3	4	0	249	262	1	11	0	117	155	-5	2	1	168	-174	1	7	1	375	367	1	430	407
4	4	0	117	98	2	11	0	93	112	-4	2	1	204	184	1	7	1	363	376	1	77	-43
5	4	0	176	-163	4	11	0	99	100	-3	2	1	411	-370	2	7	1	329	-307	1	519	-511
6	4	0	125	-138	1	12	0	47	-60	-1	2	1	449	536	3	7	1	298	-263	1	301	320
7	4	0	467	416	2	12	0	135	-118	0	2	1	114	-39	4	7	1	313	265	1	334	-368
10	4	0	187	185	3	12	0	331	333	1	2	1	414	445	-2	8	1	165	-160	1	88	-84
2	5	0	155	-161	4	12	0	150	-156	2	2	1	418	434	-1	8	1	283	250	1	196	206

OBSERVED AND CALCULATED STRUCTURE FACTORS FOR HRMENCIS

PAGE 2

H	K	L	10FO	10FC	H	K	L	10FO	10FC	H	K	L	10FO	10FC	H	K	L	10FO	10FC
0	8	1	161	-196	-4	13	1	214	-225	9	0	2	345	398	-10	4	2	346	-382
1	8	1	136	160	-3	13	1	412	435	10	0	2	219	-241	-9	4	2	366	375
2	8	1	196	169	-2	13	1	255	-285	-8	1	2	229	228	-6	4	2	163	-133
3	8	1	404	333	0	13	1	147	-228	-7	1	2	231	-205	-5	4	2	348	340
4	8	1	104	-90	1	13	1	324	383	-6	1	2	288	294	-4	4	2	183	-179
5	9	1	144	124	2	13	1	163	-169	-5	1	2	119	93	0	7	2	131	100
6	9	1	238	-248	3	13	1	207	-220	-4	1	2	354	353	-2	7	2	892	835
7	9	1	278	305	-1	14	1	94	172	-3	1	2	353	-367	-1	7	2	475	433
8	9	1	314	-300	0	14	1	96	-147	-2	1	2	116	157	0	7	2	761	-770
9	9	1	490	506	1	14	1	56	44	-1	1	2	132	166	1	7	2	792	761
0	9	1	510	-599	-4	16	1	87	-73	0	1	2	169	-132	2	7	2	305	307
1	9	1	77	106	-2	16	1	66	55	1	1	2	357	-322	3	8	2	376	-370
2	9	1	146	-118	0	16	1	129	-231	2	1	2	243	-220	5	8	2	185	174
3	9	1	207	202	1	16	1	238	350	3	1	2	166	-167	7	8	2	636	-606
4	9	1	152	162	3	16	1	118	-139	5	1	2	210	-241	8	8	2	218	216
5	9	1	202	-176	4	16	1	84	-56	-8	2	2	186	188	-4	8	2	214	-208
6	10	1	308	284	-5	17	1	206	-171	-7	2	2	241	-209	-2	8	2	765	-761
7	10	1	409	-434	-1	17	1	201	-321	-5	2	2	296	296	-1	8	2	279	277
8	10	1	258	303	0	17	1	79	121	-4	2	2	239	-241	0	8	2	73	-11
9	10	1	254	-242	2	17	1	109	-136	-3	2	2	299	-293	1	8	2	440	-434
0	11	1	285	-384	-2	18	1	159	210	-2	2	2	353	-363	2	8	2	482	470
1	11	1	109	110	0	19	1	41	88	0	2	2	358	357	3	8	2	211	183
2	11	1	107	-132	-12	0	2	209	242	1	2	2	296	271	5	8	2	210	232
3	11	1	146	-139	-8	0	2	443	405	2	2	2	173	213	8	9	2	196	-199
4	11	1	186	198	-7	0	2	382	-326	4	2	2	347	-342	-9	9	2	171	149
5	11	1	255	245	-6	0	2	264	309	-5	3	2	155	140	-5	9	2	355	319
6	12	1	182	193	-5	0	2	340	-314	-4	3	2	569	589	-4	9	2	218	-232
7	12	1	134	-186	-3	0	2	681	-669	-3	3	2	309	-311	-3	9	2	387	392
8	12	1	89	135	-2	0	2	130	156	-2	3	2	100	109	-2	9	2	219	201
9	12	1	200	-248	-1	0	2	1575	-1560	-1	3	2	922	-901	-1	9	2	124	-146
0	12	1	91	82	1	0	2	945	934	1	3	2	1131	-1083	0	9	2	243	-247
1	12	1	144	-140	2	0	2	288	-306	2	3	2	642	638	2	9	2	433	406
2	12	1	158	-186	3	0	2	596	-574	4	3	2	223	-221	3	10	2	752	-730
3	12	1	235	217	4	0	2	242	216	5	3	2	303	-306	4	10	2	146	125
4	12	1	187	160	5	0	2	452	470	6	3	2	192	205	5	10	2	262	268
5	13	1	237	247	6	0	2	257	-323	7	3	2	211	-196	-2	10	2	243	-257

OBSERVED AND CALCULATED STRUCTURE FACTORS FOR HBWENCS

PAGE 3

H	K	L	10FO	10FC	H	K	L	10FO	10FC	H	K	L	10FO	10FC	H	K	L	10FO	10FC
1	10	2	482	-494	-9	1	3	286	-286	7	3	3	356	-305	0	7	3	777	-741
0	10	2	185	-183	-8	1	3	584	539	-7	4	3	277	-206	2	7	3	236	233
2	10	2	315	333	-6	1	3	300	-333	-5	4	3	290	287	4	7	3	255	-250
3	10	2	160	-145	-4	1	3	135	176	-4	4	3	278	287	5	7	3	163	176
4	10	2	261	-251	-3	1	3	502	-486	-3	4	3	385	-363	6	7	3	618	562
5	10	2	744	771	-2	1	3	433	-446	-2	4	3	209	-207	8	7	3	227	-250
6	10	2	126	-107	-1	1	3	406	400	-1	4	3	142	124	9	7	3	233	275
-4	11	2	227	228	0	1	3	163	-164	1	4	3	261	-304	-6	8	3	165	-157
-3	11	2	308	-311	1	1	3	323	-313	2	4	3	706	654	-5	8	3	170	184
-1	11	2	199	-222	2	1	3	337	364	3	4	3	316	-278	-4	8	3	155	183
0	11	2	125	123	3	1	3	631	586	4	4	3	312	312	-2	8	3	226	-224
1	11	2	461	-464	4	1	3	601	-635	8	4	3	164	-170	2	8	3	426	-413
2	11	2	146	156	5	1	3	186	201	-10	5	3	201	-217	3	8	3	471	434
3	11	2	190	-182	-7	2	3	242	-193	-9	5	3	190	199	4	8	3	220	-228
-5	12	2	262	248	-6	2	3	535	577	-6	5	3	328	-326	6	8	3	225	190
-4	12	2	147	-180	-5	2	3	388	-369	-5	5	3	161	177	-7	9	3	333	-265
-2	12	2	131	127	-4	2	3	306	311	-4	5	3	440	462	-4	9	3	98	92
0	12	2	149	-166	-3	2	3	329	-319	-2	5	3	195	-205	-3	9	3	142	103
3	12	2	138	-120	-2	2	3	270	303	1	5	3	214	-243	-2	9	3	134	139
6	12	2	173	206	-1	2	3	386	-388	2	5	3	385	371	-1	9	3	196	198
7	12	2	236	-240	0	2	3	142	150	5	5	3	338	-351	0	9	3	293	-273
1	13	2	95	-80	1	2	3	521	-558	6	5	3	318	283	2	9	3	124	-122
2	13	2	178	186	-11	3	3	162	179	-7	6	3	278	189	3	9	3	213	189
3	13	2	249	-270	-10	3	3	342	-395	-6	6	3	346	-338	4	9	3	281	-299
-5	14	2	253	243	-7	3	3	289	230	-5	6	3	381	353	5	9	3	250	237
-4	14	2	166	-145	-6	3	3	251	-265	-4	6	3	194	-188	8	9	3	198	-216
-3	14	2	167	192	-5	3	3	185	187	-3	6	3	385	373	-6	10	3	163	180
-2	14	2	115	125	-4	3	3	383	390	-2	6	3	225	-245	-5	10	3	190	-157
0	14	2	259	-319	-3	3	3	319	-302	-1	6	3	489	467	-3	10	3	179	-165
1	14	2	181	195	-2	3	3	124	-104	0	6	3	608	-589	-1	10	3	271	-262
3	14	2	361	-347	-1	3	3	343	283	3	6	3	633	550	0	10	3	321	328
4	14	2	142	116	0	3	3	297	281	-8	7	3	328	316	1	10	3	248	-255
1	16	2	119	146	2	3	3	511	482	-6	7	3	243	-225	-6	11	3	203	-211
3	17	2	178	189	3	3	3	346	-285	-5	7	3	201	169	-2	11	3	115	129
1	19	2	118	-150	4	3	3	310	-284	-3	7	3	424	-428	1	11	3	305	-320
2	19	2	177	169	6	3	3	294	-234	-1	7	3	446	447	2	11	3	249	220

OBSERVED AND CALCULATED STRUCTURE FACTORS FOR HBMCNCS

PAGE 4

H'	K	L	10FO	10FC	H	K	L	10FO	10FC	H	K	L	10FO	10FC	H	K	L	10FO	10FC	H	K	L	10FO	10FC	H	K	L	10FO	10FC
-3	1	4	180	-194	1	4	4	643	-689	-1	8	4	189	189	6	14	4	333	277	0	3	5	339	323	0	3	5	339	323
-2	1	4	235	215	2	4	4	630	562	0	8	4	112	-109	-3	16	4	97	94	4	3	5	512	456	4	3	5	512	456
-1	1	4	199	-218	4	4	4	196	196	2	8	4	405	-383	-2	16	4	163	-154	5	3	5	361	-317	5	3	5	361	-317
1	1	4	244	-253	5	4	4	469	-433	3	8	4	242	227	-3	17	4	118	114	-9	4	5	199	-204	4	4	5	199	-204
3	1	4	349	346	6	4	4	323	328	4	8	4	203	-207	-2	19	4	144	168	-8	4	5	185	165	4	4	5	185	165
4	1	4	205	-218	-5	5	4	332	302	-3	9	4	166	-166	-8	1	5	170	-196	-3	4	5	142	134	4	4	5	142	134
5	1	4	224	206	-4	5	4	210	-194	-2	9	4	112	121	-7	1	5	367	356	-1	4	5	230	180	4	4	5	230	180
6	1	4	216	-222	-3	5	4	340	343	1	9	4	214	-205	-6	1	5	165	135	0	4	5	327	-293	4	4	5	327	-293
10	2	4	161	-159	-2	5	4	177	-161	3	9	4	113	140	-4	1	5	115	-122	1	4	5	172	-152	4	4	5	172	-152
-7	2	4	337	299	4	5	4	159	165	-7	10	4	306	265	-3	1	5	530	498	5	4	5	213	203	4	4	5	213	203
-5	2	4	186	-196	-9	6	4	181	-173	-6	10	4	114	-133	-2	1	5	710	-660	-9	5	5	191	-196	5	4	5	191	-196
-4	2	4	424	399	-7	6	4	276	252	-4	10	4	243	250	-1	1	5	229	215	-5	5	5	185	-186	5	4	5	185	-186
-2	2	4	372	-403	-6	6	4	242	-241	-3	10	4	200	201	1	1	5	287	293	-4	5	5	124	104	5	4	5	124	104
0	2	4	240	234	-5	6	4	388	-393	-2	10	4	198	-187	2	2	5	349	-360	-2	5	5	256	245	5	4	5	256	245
1	2	4	97	-131	-4	6	4	292	288	-1	10	4	128	121	3	3	5	299	339	-1	5	5	603	-588	5	4	5	603	-588
2	2	4	376	-352	-1	6	4	149	-127	0	10	4	102	-91	6	6	5	180	-208	0	5	5	484	456	5	4	5	484	456
3	2	4	332	381	0	6	4	284	290	2	10	4	198	-190	-8	2	5	158	-146	3	5	5	261	-275	5	4	5	261	-275
5	2	4	384	-353	3	6	4	259	260	3	10	4	177	165	-7	2	5	184	-143	4	5	5	340	319	5	4	5	340	319
-7	3	4	542	-457	5	6	4	202	-164	4	10	4	498	-521	-6	2	5	129	168	-10	6	6	178	-202	6	4	6	178	-202
-6	3	4	536	570	6	6	4	320	265	7	10	4	167	167	-4	2	5	301	289	-6	6	6	279	-296	6	4	6	279	-296
-5	3	4	407	-374	-8	7	4	229	-194	8	10	4	199	-207	-3	2	5	493	-483	-5	6	6	488	506	6	4	6	488	506
-4	3	4	555	505	-6	7	4	221	-257	-5	11	4	310	-293	-2	2	5	323	315	-4	6	6	153	-126	6	4	6	153	-126
-2	3	4	240	242	-5	7	4	307	313	-4	11	4	302	314	0	2	5	176	-176	-2	6	6	177	145	6	4	6	177	145
-1	3	4	321	267	-4	7	4	270	-227	-3	11	4	203	213	1	2	5	276	276	0	6	6	249	-214	6	4	6	249	-214
0	3	4	151	-131	-2	7	4	323	-343	-2	11	4	136	116	4	2	5	206	-156	1	6	6	316	-309	6	4	6	316	-309
1	3	4	144	-164	0	7	4	481	-457	0	11	4	171	181	5	2	5	346	325	2	6	6	208	219	6	4	6	208	219
2	3	4	290	252	2	7	4	190	-180	4	11	4	105	113	6	2	5	242	-233	5	6	6	249	-219	6	4	6	249	-219
8	3	4	225	-256	4	7	4	109	104	6	11	4	228	-210	7	2	5	210	266	6	6	6	257	233	6	4	6	257	233
-9	4	4	172	-163	6	7	4	216	204	-5	12	4	192	-164	-8	3	5	174	-143	7	6	6	181	-150	6	4	6	181	-150
-7	4	4	458	386	-2	7	4	145	-120	-2	12	4	145	168	-7	3	5	240	208	8	6	6	159	181	6	4	6	159	181
-6	4	4	298	-326	-9	8	4	163	-156	-1	12	4	158	-134	-6	3	5	210	224	-8	7	7	218	-172	6	4	7	218	-172
-5	4	4	341	-335	-8	8	4	171	181	0	12	4	233	253	-5	3	5	481	-510	-6	7	7	215	227	6	4	7	215	227
-4	4	4	503	449	-5	8	4	142	-117	4	12	4	236	219	-4	3	5	187	179	-5	7	7	397	-415	6	4	7	397	-415
-3	4	4	246	-271	-4	8	4	174	146	-4	13	4	138	-142	-3	3	5	278	270	-4	7	7	138	-112	6	4	7	138	-112
-2	4	4	142	-117	-3	8	4	419	458	-5	14	4	271	-246	-2	3	5	142	87	-3	7	7	493	482	6	4	7	493	482
0	4	4	613	620	-2	8	4	378	-395	0	14	4	203	196	-1	3	5	1033	-947	-1	7	7	202	195	6	4	7	202	195

OBSERVED AND CALCULATED STRUCTURE FACTORS FOR HBMCNCS

H	K	L	10FO	10FC	H	K	L	10FO	10FC	H	K	L	10FO	10FC	H	K	L	10FO	10FC	H	K	L	10FO	10FC
2	7	5	249	-252	-4	0	6	589	-633	-7	5	6	313	-318	-3	10	6	479	501	4	3	7	241	-253
7	7	5	156	146	-3	0	6	490	506	-6	5	6	396	359	0	10	6	125	-114	5	3	7	191	173
-8	8	5	244	-259	-2	0	6	458	473	0	5	6	295	-320	-1	10	6	183	187	-2	4	7	122	-135
-5	8	5	113	-94	-1	0	6	203	-204	1	5	6	124	-104	3	10	6	223	-183	-1	4	7	393	404
-4	8	5	167	-169	0	0	6	343	-353	2	5	6	116	119	-4	11	6	191	-195	0	4	7	472	-559
-2	8	5	184	155	1	0	6	504	577	3	5	6	301	-267	0	11	6	212	-213	1	4	7	181	141
-1	8	5	252	-226	6	0	6	222	-271	-9	6	6	147	150	1	11	6	196	209	-9	5	7	164	-140
-7	9	5	187	154	9	0	6	203	-281	-6	6	6	460	409	-7	12	6	168	-153	-8	5	7	204	232
-4	9	5	545	-540	-2	1	6	125	125	-4	6	6	152	-165	-2	12	6	392	380	-6	5	7	193	-189
-3	9	5	488	450	1	1	6	188	201	-2	6	6	369	347	4	12	6	181	-182	-4	5	7	183	144
0	9	5	251	-240	3	1	6	187	165	0	6	6	359	-348	-6	14	6	363	284	-3	5	7	209	-212
1	9	5	348	330	-7	2	6	264	-221	3	6	6	514	-449	-3	14	6	176	-180	-2	5	7	206	207
2	9	5	329	-347	-1	2	6	133	-127	-5	7	6	315	348	-2	14	6	299	301	0	5	7	237	-259
-7	10	5	274	-231	0	2	6	161	-182	-4	7	6	104	110	-1	14	6	221	-213	-5	6	7	348	-329
-6	10	5	231	246	1	2	6	137	161	-3	7	6	171	-173	-4	16	6	158	-160	-4	6	7	553	471
0	10	5	158	-129	2	2	6	178	231	-2	7	6	422	430	1	18	6	107	82	-3	6	7	362	-410
1	10	5	207	212	-8	3	6	212	217	-1	7	6	268	-263	-10	1	7	268	-329	-2	6	7	223	239
-7	11	5	224	187	-7	3	6	308	-256	0	7	6	256	243	-6	1	7	209	-178	0	6	7	219	246
-3	11	5	334	301	-6	3	6	252	-218	1	7	6	330	-335	-5	1	7	530	485	1	6	7	598	-500
-1	11	5	260	-208	-4	3	6	169	-194	2	7	6	229	273	-1	1	7	220	238	-5	7	7	450	379
0	11	5	198	172	-3	3	6	138	140	3	7	6	315	-276	1	1	7	495	-433	-3	7	7	457	-505
2	11	5	127	-97	-2	3	6	168	-168	6	7	6	200	217	2	1	7	386	350	-2	7	7	457	514
-6	12	5	206	213	-1	3	6	344	312	-9	8	6	221	211	-5	2	7	206	226	0	7	7	255	-272
-5	13	5	422	-436	0	3	6	186	-216	-3	8	6	215	209	-4	2	7	175	-138	6	7	7	146	150
-4	13	5	245	239	1	3	6	162	-151	-2	8	6	158	154	-3	2	7	222	254	-5	8	7	240	260
-2	13	5	302	271	3	3	6	438	378	0	8	6	300	-306	-2	2	7	159	-202	-2	8	7	296	336
-1	13	5	342	-314	5	3	6	238	252	1	8	6	384	417	-1	2	7	274	307	-1	8	7	220	-221
0	13	5	256	225	6	3	6	174	-160	-6	9	6	360	-315	0	2	7	139	-170	1	8	7	266	-216
-7	17	5	249	197	-10	4	6	146	165	-5	9	6	167	174	-8	3	7	239	261	-5	9	7	262	202
-4	17	5	182	-162	-7	4	6	227	-189	-3	9	6	196	-202	-7	3	7	511	-500	-4	9	7	233	-171
-3	17	5	236	171	-6	4	6	521	458	-2	9	6	189	166	-6	3	7	265	260	-2	9	7	142	142
-2	17	5	120	-103	-4	4	6	212	-202	-1	9	6	238	245	-3	3	7	295	-343	-1	9	7	274	302
-9	0	6	216	231	-3	4	6	326	-343	0	9	6	219	-218	-2	3	7	167	174	0	9	7	166	-167
-8	0	6	445	-455	-2	4	6	480	463	3	9	6	215	191	-1	3	7	263	281	2	9	7	293	270
-7	0	6	264	264	-1	4	6	471	-475	-5	10	6	166	151	0	3	7	397	-458	6	9	7	170	174
-5	0	6	481	538	3	4	6	157	-136	-4	10	6	723	-764	2	3	7	376	333	-6	10	7	154	-159

OBSERVED AND CALCULATED STRUCTURE FACTORS FOR HERMENS

H	K	L	10FO	10FC	H	K	L	10FO	10FC	H	K	L	10FO	10FC	H	K	L	10FO	10FC	H	K	L	10FO	10FC
-5	10	7	218	185	-4	2	8	337	311	0	7	8	247	226	3	3	9	403	410	-8	4	10	223	-249
-4	10	7	155	-158	-3	2	8	172	-179	1	7	8	263	-173	-3	4	9	152	154	-5	4	10	222	201
-3	10	7	208	215	-1	2	8	190	197	-5	8	8	269	-256	-1	4	9	298	283	-4	4	10	314	-313
-2	10	7	251	-274	3	2	8	285	316	0	8	8	276	240	-8	5	9	179	-164	-3	4	10	162	154
-1	10	7	180	196	-9	3	8	164	156	1	8	8	244	-199	-3	5	9	311	315	1	4	10	243	268
3	10	7	202	182	-5	3	8	176	197	-3	9	8	369	320	1	5	9	223	220	2	4	10	257	-285
-1	11	7	154	166	-4	3	8	256	-227	-2	9	8	490	-418	2	5	9	275	-259	-8	6	10	230	-192
2	11	7	311	245	-3	3	8	281	270	-1	9	8	248	175	-7	6	9	245	-236	-4	6	10	191	-205
-2	12	7	148	-158	-2	3	8	307	-261	0	9	8	154	99	-6	6	9	192	212	1	6	10	231	233
-7	13	7	261	-219	-1	3	8	263	209	1	9	8	161	-111	-2	6	9	362	370	-10	7	10	155	189
-6	13	7	257	201	0	3	8	247	-230	-6	10	8	168	-146	-1	6	9	254	-240	-6	8	10	290	265
-5	13	7	162	-129	2	3	8	308	-287	-1	10	8	186	121	-2	7	9	154	-144	-2	8	10	274	276
-3	13	7	253	-251	-4	4	8	414	373	1	10	8	318	-267	0	7	9	222	210	-1	8	10	299	-300
4	13	7	233	-268	-2	4	8	292	-274	-1	11	8	234	188	-6	8	9	146	108	-7	1	11	319	-387
0	16	7	210	215	-1	4	8	710	632	-1	17	8	181	-137	-6	9	9	213	191	-2	1	11	196	228
1	16	7	209	-211	0	4	8	307	-228	0	17	8	238	200	-5	9	9	237	-253	-2	2	11	188	237
11	0	8	278	316	2	4	8	160	-160	0	1	9	519	546	0	9	9	268	272	-10	3	11	163	-195
10	0	8	180	-203	3	4	8	285	309	1	1	9	400	-400	-3	11	9	169	138	-5	3	11	147	194
-6	0	8	521	-535	-7	5	8	196	-231	4	1	9	187	226	-1	12	9	149	-130	-5	5	11	290	280
-5	0	8	249	265	-2	5	8	379	314	-9	2	9	271	289	-4	13	9	192	-174	-1	5	11	154	166
-4	0	8	155	147	-1	5	8	158	-102	-8	2	9	186	-194	-2	13	9	215	-186	-1	6	11	195	224
-3	0	8	283	-277	-6	6	8	238	-253	-4	2	9	191	-193	-6	0	10	199	208	-3	9	11	269	-277
1	0	8	800	-768	1	6	8	342	-314	0	2	9	245	-247	-1	0	10	231	-270	-8	0	12	244	301
2	0	8	583	587	3	6	8	260	258	2	2	9	171	155	0	0	10	310	350	-4	3	12	151	154
5	0	8	207	-232	4	6	8	213	-202	3	2	9	173	-201	1	0	10	280	-323	-3	3	12	178	-208
6	0	8	202	231	-7	7	8	204	-189	-4	3	9	224	207	3	0	10	250	-329	-6	4	12	208	-257
-6	1	8	178	-185	-5	7	8	278	-284	-3	3	9	170	120	-6	2	10	232	262	-3	4	12	185	-168
-5	1	8	220	240	-4	7	8	367	326	-2	3	9	210	-225	0	2	10	182	-187	-5	2	13	192	-251
-4	1	8	185	-211	-2	7	8	491	411	-1	3	9	198	191	3	3	10	226	-267	-4	6	13	242	-278
1	1	8	301	-306	-1	7	8	238	-208	2	3	9	516	-546	4	4	10	156	191	-3	7	14	263	109
9	2	8	159	-224																				

Anisotropic temperature factors ($\text{\AA}^2 \times 10^4$)

Atom	U_{11}	U_{22}	U_{33}	U_{23}	U_{13}	U_{12}
S(1)	325(19)	408(21)	168(16)	-52(18)	108(14)	-48(19)
S(2)	299(20)	579(27)	207(17)	-107(19)	56(15)	-49(20)
N(1)	373(71)	459(80)	169(58)	59(55)	80(52)	-171(60)
N(2)	209(54)	312(59)	86(53)	33(47)	114(42)	-84(49)
N(3)	358(71)	458(82)	181(63)	-139(60)	162(55)	-163(59)
N(4)	206(59)	406(71)	176(58)	7(54)	18(47)	-156(58)
N(5)	187(58)	484(79)	372(68)	-136(62)	81(52)	-99(58)
C(1)	386(80)	326(84)	180(67)	196(73)	106(61)	108(73)
C(2)	219(73)	133(71)	272(71)	21(59)	-89(58)	88(59)
C(3)	169(65)	453(89)	269(74)	-2(75)	19(56)	-6(75)
C(4)	608(110)	565(110)	561(102)	-372(98)	58(87)	-392(99)
C(6)	394(87)	641(115)	307(80)	-29(78)	191(71)	-42(83)
C(7)	490(100)	719(121)	295(82)	194(80)	187(76)	43(89)
C(9)	335(86)	621(109)	368(87)	-232(80)	194(72)	36(78)
C(10)	356(83)	395(86)	305(78)	-5(71)	121(69)	37(73)
C(11)	319(79)	310(79)	277(75)	9(61)	245(64)	-26(64)
C(12)	256(76)	625(107)	278(79)	63(75)	-6(64)	8(78)
C(13)	344(89)	537(107)	454(101)	-57(85)	-93(75)	-167(82)
C(14)	425(94)	532(102)	625(108)	-81(94)	364(87)	-182(89)
C(15)	708(116)	497(103)	367(87)	-2(84)	250(85)	-91(98)
C(16)	288(83)	502(103)	459(97)	77(77)	-12(72)	-164(77)

The common isotropic temperature factor for the phenyl hydrogens refined to $58(14) \times 10^{-3} \text{\AA}^2$.

Least squares planes

Plane	Atoms	A	B	C	D	Atom distance from plane($\text{\AA} \times 10^{-3}$)	
1	S(1)	-0.598(4)	0.680(9)	-0.423(95)	1.038(20)	S(1)	-1(20)
	N(1)					N(1)	103(23)
	N(2)					N(2)	171(23)
	C(1)					C(1)	-181(25)
	C(2)					C(2)	-93(24)
						N(3)	-392(23)
2	S(2)	-0.612(5)	0.656(2)	-0.441(3)	1.091(12)	S(2)	-41(13)
	N(4)					N(4)	-72(17)
	N(5)					N(5)	-14(18)
	C(3)					C(3)	152(20)
	C(4)					C(4)	-26(22)
						C(2)	-476(18)
3	C(5)	-0.778(1)	-0.339(1)	-0.528(1)	4.434(7)	C(5)	5(15)
	C(6)					C(6)	43(17)
	C(7)					C(7)	-79(18)
	C(8)					C(8)	67(18)
	C(9)					C(9)	-18(17)
	C(10)					C(10)	-18(17)
4	C(11)	0.544(7)	-0.751(8)	-0.373(6)	1.080(28)	C(11)	298(31)
	C(12)					C(12)	-90(32)
	C(13)					C(13)	-89(32)
	C(14)					C(14)	56(32)
	C(15)					C(15)	145(33)
	C(16)					C(16)	-320(32)
						N(3)	-192(30)

Least squares planes are defined in orthogonal coordinates (in \AA) by the following equation:- $Ax + By + Cz + D = 0$

Dihedral angle between planes ($^\circ$)

Planes:	1,2	1,3	1,4	2,3	2,4	3,4
Angle	1.9(25)	62.8(32)	-47.2(36)	60.9(3)	-48.6(23)	88.4(20)

Appendix C

Observed and Calculated Structure Factors,

Anisotropic Temperature Parameters

and Least-Squares Planes for

N,N'-bis[2-(5-t-butyl-3H-1,2-dithiol-3-ylidene)
ethylidene]hydrazine.

H	K	L	Fo	Fc	H	K	L	Fo	Fc	H	K	L	Fo	Fc	H	K	L	Fo	Fc
3	0	0	15	-17	2	6	0	5	4	-2	-6	1	16	-14	5	0	1	3	-2
5	0	0	4	-4	3	6	0	14	-12	-1	-6	1	8	-6	6	0	1	5	6
6	0	0	2	-3	4	6	0	6	-5	0	-6	1	4	4	-6	1	1	2	-3
7	0	0	6	6	-6	7	0	9	-11	1	-6	1	17	18	-5	1	1	8	-11
-6	1	0	3	-4	-4	7	0	8	7	3	-6	1	24	-23	-1	1	1	13	-14
-5	1	0	6	-8	-3	7	0	6	6	4	-6	1	9	8	0	1	1	8	8
-4	1	0	9	-13	0	7	0	8	7	6	-6	1	6	8	1	1	1	26	26
1	1	0	30	-31	1	7	0	24	-22	-1	-5	1	14	16	2	1	1	3	-3
2	1	0	3	-3	2	7	0	6	-6	0	-5	1	11	-11	3	1	1	1	-1
3	1	0	11	-11	4	7	0	8	7	1	-5	1	12	-13	4	1	1	15	15
4	1	0	8	9	-3	8	0	10	9	2	-5	1	7	-7	6	1	1	7	-6
6	1	0	7	6	-2	8	0	12	-11	3	-5	1	27	29	-2	2	1	2	2
7	1	0	6	-6	0	8	0	17	-17	4	-5	1	4	-4	-1	2	1	34	34
-7	2	0	3	-5	1	8	0	7	7	-4	-4	1	7	6	0	2	1	24	25
-6	2	0	2	-3	-3	9	0	17	-17	-2	-4	1	12	-13	1	2	1	4	5
-1	2	0	14	14	-1	9	0	10	11	-1	-4	1	29	-27	3	2	1	13	13
0	2	0	8	-8	1	9	0	6	-6	0	-4	1	13	14	4	2	1	33	-29
1	2	0	15	-14	3	9	0	5	5	1	-4	1	28	28	5	2	1	7	-7
2	2	0	5	5	-5	10	0	7	-5	2	-4	1	1	-2	-7	3	1	2	5
3	2	0	21	21	-3	10	0	8	8	3	-4	1	6	-7	-5	3	1	3	-6
5	2	0	12	-10	-1	10	0	8	-8	4	-4	1	4	5	-2	3	1	6	6
6	2	0	6	-5	0	10	0	5	-5	6	-4	1	5	-8	-1	3	1	26	26
-7	3	0	4	8	-5	11	0	6	5	-6	-3	1	4	4	0	3	1	32	32
-6	3	0	2	4	-3	12	0	5	-6	-4	-3	1	24	-21	1	3	1	32	-32
-5	3	0	6	-10	-2	-11	1	4	5	-3	-3	1	6	-6	2	3	1	25	-23
-3	3	0	7	10	2	-11	1	7	-8	-1	-3	1	19	20	3	3	1	18	-18
-2	3	0	3	2	3	-11	1	7	-8	0	-3	1	13	12	4	3	1	9	8
-1	3	0	6	6	5	-11	1	6	5	1	-3	1	8	-9	5	3	1	6	6
0	3	0	15	17	0	-10	1	6	-7	2	-3	1	4	5	-7	4	1	2	-4
1	3	0	39	39	2	-10	1	3	4	3	-3	1	6	-5	-5	4	1	2	4
2	3	0	22	-22	3	-10	1	5	6	4	-3	1	4	-6	-4	4	1	4	-7
3	3	0	17	-15	4	-10	1	6	-5	5	-3	1	6	8	-3	4	1	17	-19
4	3	0	5	-5	0	-9	1	8	9	6	-3	1	5	7	-2	4	1	22	22
-7	4	0	3	-7	1	-9	1	3	3	-6	-2	1	8	-6	-1	4	1	7	-7
-4	4	0	5	7	2	-9	1	12	-12	-5	-2	1	15	-15	0	4	1	46	-43
-3	4	0	8	10	4	-9	1	4	3	-4	-2	1	15	15	1	4	1	8	-8
-2	4	0	14	15	-2	-8	1	11	11	-3	-2	1	4	5	2	4	1	14	14
-1	4	0	34	34	0	-8	1	17	-17	-1	-2	1	5	5	3	4	1	6	7
0	4	0	21	-22	1	-8	1	6	-5	0	-2	1	26	26	-4	5	1	17	20
1	4	0	37	-35	2	-8	1	5	5	1	-2	1	21	-22	-3	5	1	15	-16
2	4	0	5	-5	3	-8	1	6	-4	2	-2	1	16	-17	-2	5	1	21	-19
3	4	0	13	13	5	-8	1	8	8	5	-2	1	6	-8	0	5	1	15	15
4	4	0	3	-3	7	-8	1	4	-4	6	-2	1	6	-8	2	5	1	5	-5
-2	5	0	17	-16	-4	-7	1	7	6	-5	-1	1	4	5	3	5	1	5	4
-1	5	0	31	-30	-2	-7	1	4	-4	-3	-1	1	8	7	4	5	1	7	-7
0	5	0	11	11	-1	-7	1	22	-21	-2	-1	1	3	-3	5	5	1	10	-8
1	5	0	5	4	0	-7	1	5	5	-1	-1	1	18	-20	-7	6	1	3	5
4	5	0	5	-5	1	-7	1	6	-6	1	-1	1	20	21	-4	6	1	10	-10
-6	6	0	6	9	3	-7	1	11	12	3	-1	1	13	-14	-3	6	1	11	11
-5	6	0	3	4	4	-7	1	5	5	4	-1	1	12	-15	-2	6	1	13	12
-4	6	0	17	-16	5	-7	1	9	-8	5	-1	1	5	-5	-1	6	1	2	-3
-3	6	0	17	-16	6	-7	1	5	-6	-3	0	1	15	-19	1	6	1	14	-12
-2	6	0	14	14	7	-7	1	5	6	1	0	1	9	-9	2	6	1	3	-2
-1	6	0	11	11	-6	-6	1	4	3	2	0	1	25	-24	3	6	1	13	-13
1	6	0	3	-3	-4	-6	1	8	-8	3	0	1	4	4	5	6	1	7	6

Observed and Calculated Structure Factors For
N,N'-Bis[2-(5-t-butyl-3H-1,2-dithiol-3-ylidene)ethylidene]hydrazine

Page 2

H	K	L	Fo	Fc	H	K	L	Fo	Fc	H	K	L	Fo	Fc	H	K	L	Fo	Fc
6	6	1	5	4	-3	-6	2	6	5	2	-1	2	11	11	3	5	2	6	-6
-7	7	1	4	-6	0	-6	2	12	13	3	-1	2	15	-15	4	5	2	7	-7
-5	7	1	10	10	2	-6	2	17	-19	6	-1	2	3	-4	-7	6	2	3	5
-4	7	1	10	9	3	-6	2	13	-14	-6	0	2	4	-5	-6	6	2	4	-6
-3	7	1	8	-8	4	-6	2	15	15	-5	0	2	2	-3	-5	6	2	6	-8
-1	7	1	6	6	5	-6	2	8	8	-4	0	2	13	-14	-4	6	2	3	-4
0	7	1	27	-25	-3	-5	2	8	9	-3	0	2	3	4	-3	6	2	16	15
1	7	1	6	-6	-1	-5	2	12	-13	-2	0	2	12	16	-2	6	2	4	4
2	7	1	5	5	0	-5	2	30	-31	0	0	2	25	-26	-1	6	2	7	-7
3	7	1	11	10	1	-5	2	2	1	1	0	2	31	-31	1	6	2	7	-7
-2	8	1	13	-11	2	-5	2	12	12	2	0	2	7	6	2	6	2	11	-11
-1	8	1	11	-11	3	-5	2	22	21	4	0	2	3	-3	4	6	2	12	10
0	8	1	11	11	7	-5	2	3	-4	5	0	2	4	-5	-7	7	2	3	-5
1	8	1	10	11	-5	-4	2	2	2	6	0	2	11	10	-5	7	2	8	7
3	8	1	5	-6	-3	-4	2	9	-9	7	0	2	3	-3	-3	7	2	6	6
-4	9	1	11	-9	-2	-4	2	41	-40	8	0	2	4	-3	-2	7	2	6	-5
-3	9	1	5	-5	-1	-4	2	3	3	-7	1	2	3	-4	-1	7	2	4	4
-2	9	1	12	12	0	-4	2	39	36	-6	1	2	6	-8	0	7	2	31	-29
-1	9	1	9	9	1	-4	2	13	15	-2	1	2	8	-8	1	7	2	5	4
0	9	1	6	-7	2	-4	2	8	7	-1	1	2	15	-17	2	7	2	11	11
1	9	1	6	-7	3	-4	2	11	11	0	1	2	12	-11	5	7	2	3	-3
-4	10	1	10	8	5	-4	2	11	-12	1	1	2	5	-5	-5	8	2	3	3
-2	10	1	7	-8	6	-4	2	4	-5	2	1	2	10	-9	-4	8	2	10	8
0	10	1	3	-4	7	-4	2	6	8	3	1	2	16	17	-3	8	2	17	-15
1	10	1	4	-6	-5	-3	2	8	-8	6	1	2	11	-10	-2	8	2	9	-8
2	10	1	4	5	-4	-3	2	12	-11	-8	2	2	2	-3	0	8	2	8	8
-4	11	1	8	-7	-3	-3	2	5	-5	-3	2	2	3	-5	2	8	2	6	-6
-3	11	1	4	-4	-2	-3	2	18	18	-2	2	2	8	-9	4	8	2	4	-5
-2	11	1	3	4	-1	-3	2	18	18	0	2	2	13	-13	5	8	2	5	5
1	11	1	6	8	0	-3	2	13	12	1	2	2	38	37	-6	9	2	3	3
-3	13	1	4	5	1	-3	2	23	21	2	2	2	10	11	-4	9	2	11	-9
4	-12	2	4	-4	2	-3	2	8	-9	3	2	2	17	-15	-2	9	2	10	10
-1	-10	2	5	-6	3	-3	2	21	-21	4	2	2	17	-16	-1	9	2	7	-7
0	-10	2	3	-4	4	-3	2	4	-4	6	2	2	6	5	0	9	2	8	-9
1	-10	2	7	9	5	-3	2	12	13	-5	3	2	2	-5	2	9	2	4	5
2	-10	2	8	8	6	-3	2	6	7	-4	3	2	3	6	3	9	2	4	-4
3	-10	2	7	-7	7	-3	2	5	-6	-3	3	2	4	-6	4	9	2	5	5
4	-10	2	7	-6	-7	-2	2	6	-5	-2	3	2	7	-7	-5	10	2	5	4
-1	-9	2	5	6	-5	-2	2	2	-2	-1	3	2	49	46	-3	10	2	6	-6
0	-9	2	3	3	-4	-2	2	13	13	0	3	2	27	28	-5	11	2	5	-4
2	-9	2	18	-19	-3	-2	2	5	-4	2	3	2	24	-23	0	11	2	4	5
4	-9	2	4	3	-2	-2	2	6	5	3	3	2	7	7	-4	12	2	7	-7
-2	-8	2	4	4	-1	-2	2	10	10	4	3	2	2	2	3	-12	3	4	-5
-1	-8	2	16	-17	0	-2	2	8	-9	-2	4	2	23	21	1	-11	3	5	-6
1	-8	2	7	-7	1	-2	2	30	-30	-1	4	2	28	-29	2	-11	3	3	-4
4	-8	2	11	9	2	-2	2	5	-5	0	4	2	16	-14	3	-11	3	7	8
5	-8	2	12	9	3	-2	2	31	32	1	4	2	2	-2	-1	-10	3	6	-7
6	-8	2	4	-5	4	-2	2	3	5	2	4	2	5	6	1	-10	3	4	5
-3	-7	2	8	-8	5	-2	2	8	-8	3	4	2	4	-3	3	-10	3	4	-5
-2	-7	2	6	-7	6	-2	2	5	-6	-6	5	2	2	4	1	-9	3	8	-8
0	-7	2	4	-4	-7	-1	2	7	6	-4	5	2	6	-7	2	-9	3	3	3
2	-7	2	16	14	-3	-1	2	3	-4	-3	5	2	19	-21	-1	-8	3	14	-15
3	-7	2	6	7	-2	-1	2	5	-7	-1	5	2	14	14	0	-8	3	5	6
4	-7	2	7	-7	-1	-1	2	45	-47	1	5	2	13	-16	2	-8	3	4	-4
5	-7	2	11	-11	1	-1	2	8	9	2	5	2	10	8	4	-8	3	12	10

H	K	L	Fo	Fc	H	K	L	Fo	Fc	H	K	L	Fo	Fc	H	K	L	Fo	Fc
5	-8	3	4	-2	1	-2	3	3	-2	0	3	3	40	-36	-1	-9	4	4	-5
6	-8	3	8	-8	2	-2	3	59	58	1	3	3	29	-30	1	-9	4	11	-13
-2	-7	3	14	-14	3	-2	3	8	9	3	3	3	8	8	5	-9	4	6	5
-1	-7	3	5	5	4	-2	3	14	-15	4	3	3	3	3	-5	-8	4	3	2
1	-7	3	7	6	5	-2	3	11	-12	6	3	3	5	3	-2	-8	4	12	-13
2	-7	3	9	8	-3	-1	3	10	-11	-3	4	3	6	5	0	-8	4	7	-7
3	-7	3	13	-11	-2	-1	3	17	-17	-2	4	3	27	-28	2	-8	4	5	5
4	-7	3	3	-4	-1	-1	3	50	51	-1	4	3	27	-25	3	-8	4	14	12
6	-7	3	8	11	0	-1	3	35	37	0	4	3	8	8	5	-8	4	13	-10
-5	-6	3	5	-5	1	-1	3	28	29	1	4	3	16	17	-1	-7	4	6	-5
-3	-6	3	8	-7	2	-1	3	34	-33	5	4	3	7	-6	0	-7	4	9	9
-1	-6	3	16	14	3	-1	3	15	-16	-7	5	3	2	3	1	-7	4	16	15
0	-6	3	4	3	4	-1	3	2	-2	-5	5	3	7	8	3	-7	4	14	-13
1	-6	3	7	-9	5	-1	3	4	-4	-4	5	3	16	-20	4	-7	4	7	-5
2	-6	3	23	-25	7	-1	3	3	3	-3	5	3	10	-9	5	-7	4	12	9
3	-6	3	21	23	-5	0	3	7	-7	-2	5	3	9	9	-1	-6	4	10	8
4	-6	3	6	7	-4	0	3	8	-9	-1	5	3	18	18	0	-6	4	5	-4
5	-6	3	5	5	-3	0	3	16	19	1	5	3	5	-4	1	-6	4	16	-14
-5	-5	3	4	-3	-2	0	3	26	27	3	5	3	14	-14	2	-6	4	6	-6
-3	-5	3	3	3	-1	0	3	25	26	4	5	3	11	-9	3	-6	4	14	16
-2	-5	3	6	6	0	0	3	36	-37	6	5	3	7	6	4	-6	4	3	3
-1	-5	3	16	-18	1	0	3	13	-15	-4	6	3	11	11	5	-6	4	3	-3
0	-5	3	9	-10	2	0	3	7	-7	-1	6	3	13	12	6	-6	4	3	3
1	-5	3	10	12	3	0	3	2	-2	0	6	3	23	-21	-4	-5	4	5	4
2	-5	3	20	21	4	0	3	4	4	1	6	3	12	-10	-2	-5	4	16	-18
5	-5	3	3	3	5	0	3	12	10	2	6	3	14	-14	-1	-5	4	10	-11
6	-5	3	7	-8	7	0	3	6	-5	3	6	3	9	9	0	-5	4	12	14
-5	-4	3	3	2	-7	1	3	2	-2	4	6	3	6	6	1	-5	4	4	6
-4	-4	3	4	-4	-6	1	3	3	-5	-6	7	3	6	7	2	-5	4	8	8
-3	-4	3	7	-8	-5	1	3	4	5	-1	7	3	31	-29	4	-5	4	4	5
-2	-4	3	10	-10	-4	1	3	18	22	1	7	3	11	11	6	-5	4	6	-7
-1	-4	3	7	7	-3	1	3	16	-17	2	7	3	9	10	-4	-4	4	9	-10
0	-4	3	20	20	-2	1	3	3	-4	-4	8	3	5	-5	-3	-4	4	16	-17
1	-4	3	6	-7	-1	1	3	8	8	-3	8	3	13	-12	-2	-4	4	11	11
3	-4	3	7	7	0	1	3	6	5	-1	8	3	10	10	-1	-4	4	23	24
4	-4	3	12	-10	1	1	3	8	-8	0	8	3	5	5	1	-4	4	4	5
5	-4	3	8	-7	2	1	3	3	4	1	8	3	6	-6	2	-4	4	10	10
6	-4	3	5	5	3	1	3	35	33	-5	9	3	6	-5	3	-4	4	7	-6
7	-4	3	7	7	4	1	3	15	-15	-3	9	3	13	12	4	-4	4	10	-10
-6	-3	3	3	-2	5	1	3	12	-11	-1	9	3	9	-10	6	-4	4	11	12
-5	-3	3	14	-12	6	1	3	6	-6	-6	10	3	4	4	-7	-3	4	3	-2
-4	-3	3	8	7	-5	2	3	2	-2	-5	10	3	9	7	-6	-3	4	5	-5
-3	-3	3	3	3	-4	2	3	5	-8	-3	10	3	8	-8	-5	-3	4	7	-8
-1	-3	3	8	-8	-2	2	3	23	22	-1	10	3	2	-3	-4	-3	4	6	5
0	-3	3	14	15	0	2	3	28	28	0	10	3	5	-7	-3	-3	4	9	9
1	-3	3	5	-5	1	2	3	5	-4	1	10	3	6	8	-2	-3	4	10	9
2	-3	3	11	-11	2	2	3	6	5	-2	11	3	4	-4	-1	-3	4	7	7
3	-3	3	2	2	3	2	3	36	-36	0	11	3	5	8	0	-3	4	2	2
4	-3	3	17	19	4	2	3	5	-5	3	-12	4	3	-3	1	-3	4	14	-14
5	-3	3	5	6	5	2	3	6	6	5	-12	4	6	5	2	-3	4	16	-16
6	-3	3	3	-3	-6	3	3	2	-4	0	-10	4	5	6	3	-3	4	16	16
-6	-2	3	5	-6	-5	3	3	4	7	1	-10	4	3	4	4	-3	4	15	15
-5	-2	3	11	10	-3	3	3	9	10	2	-10	4	9	-11	6	-3	4	10	-10
-2	-2	3	7	-7	-2	3	3	29	28	4	-10	4	4	4	-5	-2	4	4	5
-1	-2	3	11	10	-1	3	3	10	10	-2	-9	4	5	6	-3	-2	4	3	3

Observed and Calculated Structure Factors For
N,N'-Bis[2-(5-t-butyl-3H-1,2-dithiol-3-ylidene)ethylidene]hydrazine

Page 4

H	K	L	Fo	Fc	H	K	L	Fo	Fc	H	K	L	Fo	Fc	H	K	L	Fo	Fc
-1	-2	4	31	-33	-4	3	4	3	4	2-12	5	3	-4	-4	-3	-1	5	3	3
0	-2	4	2	1	-2	3	4	36	-35	2-11	5	3	3	3	-2	-1	5	26	28
1	-2	4	11	13	-1	3	4	7	-6	0-10	5	3	4	4	-1	-1	5	27	25
2	-2	4	30	27	0	3	4	39	-38	1-10	5	5	-6	-6	0	-1	5	10	-10
3	-2	4	6	-5	1	3	4	10	-10	-1	-9	5	4	-5	1	-1	5	20	-21
4	-2	4	14	-13	2	3	4	15	16	4	-9	5	8	7	2	-1	5	8	-8
-8	-1	4	3	2	3	3	4	4	4	5	-9	5	4	4	4	-1	5	7	-7
-5	-1	4	3	3	4	3	4	4	-3	-2	-8	5	9	-10	5	-1	5	6	6
-4	-1	4	5	-4	7	3	4	7	-5	2	-8	5	6	6	6	-1	5	5	5
-3	-1	4	11	-10	-5	4	4	11	14	3	-8	5	5	5	-6	0	5	5	-4
-2	-1	4	25	-24	-4	4	4	4	5	5	-8	5	11	-9	-4	0	5	25	24
-1	-1	4	62	64	-2	4	4	15	-14	-3	-7	5	5	-4	-3	0	5	3	4
0	-1	4	7	8	-1	4	4	4	-4	2	-7	5	19	-17	-1	0	5	24	-22
1	-1	4	7	-8	0	4	4	6	7	3	-7	5	6	5	0	0	5	6	-5
2	-1	4	6	-5	4	4	4	7	-6	5	-7	5	11	9	1	0	5	4	-4
3	-1	4	4	4	-7	5	4	3	4	-2	-6	5	6	5	2	0	5	5	-5
4	-1	4	4	-4	-4	5	4	10	-10	-1	-6	5	9	-9	3	0	5	18	20
5	-1	4	6	-6	-3	5	4	11	10	0	-6	5	11	-11	4	0	5	4	4
6	-1	4	7	7	-2	5	4	10	10	1	-6	5	8	-6	5	0	5	3	-4
-7	0	4	2	-3	-1	5	4	9	-11	2	-6	5	28	25	6	0	5	12	-9
-6	0	4	5	-4	0	5	4	8	-7	3	-6	5	7	6	-6	1	5	5	4
-5	0	4	5	-5	1	5	4	7	6	-3	-5	5	7	-6	-5	1	5	9	10
-4	0	4	6	6	2	5	4	9	-9	-2	-5	5	15	-13	-4	1	5	9	-8
-3	0	4	11	11	3	5	4	12	-12	0	-5	5	24	21	-3	1	5	12	-13
-2	0	4	26	26	4	5	4	6	5	1	-5	5	15	13	-2	1	5	9	8
-1	0	4	12	-12	5	5	4	8	8	3	-5	5	3	3	-1	1	5	8	-8
1	0	4	8	9	-7	6	4	3	-4	4	-5	5	3	-3	0	1	5	11	11
2	0	4	3	-3	-5	6	4	6	6	5	-5	5	11	-11	1	1	5	8	9
3	0	4	2	-2	-4	6	4	4	4	-5	-4	5	6	-5	2	1	5	29	31
5	0	4	10	10	-2	6	4	9	-10	-4	-4	5	2	-2	3	1	5	25	-28
6	0	4	9	-9	-1	6	4	10	8	-3	-4	5	4	-5	4	1	5	14	-15
-8	1	4	2	-3	0	6	4	18	-17	-2	-4	5	8	9	-6	2	5	3	-3
-7	1	4	2	-3	1	6	4	7	-8	-1	-4	5	9	10	-4	2	5	4	-4
-6	1	4	5	5	2	6	4	6	6	0	-4	5	7	7	-2	2	5	12	12
-5	1	4	11	13	3	6	4	11	12	2	-4	5	4	-4	-1	2	5	27	27
-3	1	4	8	-8	-4	7	4	4	4	3	-4	5	15	-16	0	2	5	2	-2
-2	1	4	2	-1	-3	7	4	8	-8	5	-4	5	10	11	1	2	5	16	-18
-1	1	4	19	18	-2	7	4	5	-4	6	-4	5	5	6	2	2	5	22	-25
0	1	4	9	-9	-1	7	4	14	-14	7	-4	5	3	-3	4	2	5	9	7
1	1	4	4	-3	0	7	4	11	10	-6	-3	5	7	-7	-6	3	5	2	4
2	1	4	18	18	1	7	4	11	12	-5	-3	5	8	8	-4	3	5	5	5
3	1	4	7	-7	-4	8	4	16	-13	-1	-3	5	15	15	-3	3	5	19	20
4	1	4	12	-12	-2	8	4	13	12	0	-3	5	7	-8	-1	3	5	25	-26
5	1	4	10	-10	-1	8	4	4	4	1	-3	5	23	-24	0	3	5	18	-19
6	1	4	5	5	0	8	4	9	-9	2	-3	5	18	19	1	3	5	6	7
-8	2	4	3	3	1	8	4	6	-7	3	-3	5	18	20	4	3	5	5	4
-5	2	4	6	-7	3	8	4	5	-6	4	-3	5	3	3	6	3	5	6	-4
-2	2	4	3	-3	4	8	4	6	6	5	-3	5	8	-8	-5	4	5	10	11
-1	2	4	15	15	-6	9	4	3	-3	-2	-2	5	6	-6	-4	4	5	9	-9
0	2	4	26	24	-4	9	4	8	6	-1	-2	5	14	13	-3	4	5	15	-14
1	2	4	11	-11	-1	9	4	9	-9	1	-2	5	42	42	-2	4	5	10	-9
2	2	4	27	-28	3	9	4	7	8	3	-2	5	15	-16	-1	4	5	16	16
4	2	4	7	6	-4	10	4	5	-5	4	-2	5	5	-6	4	4	5	10	-9
5	2	4	8	6	-4	11	4	4	-3	-5	-1	5	5	-4	-8	5	5	3	3
-5	3	4	2	-2	-1	11	4	4	6	-4	-1	5	6	-5	-5	5	5	13	-13

Observed and Calculated Structure Factors For
N,N'-Bis[2-(5-t-butyl-3H-1,2-dithiol-3-ylidene)ethylidene]hydrazine

Page 5

H	K	L	Fo	Fc	H	K	L	Fo	Fc	H	K	L	Fo	Fc	H	K	L	Fo	Fc
-3	5	5	9	9	5	-5	6	10	-8	4	1	6	5	-4	-2	-9	7	6	-7
-2	5	5	7	6	6	-5	6	9	8	5	1	6	9	7	2	-9	7	3	4
-1	5	5	3	3	-5	-4	6	5	-4	6	1	6	4	4	3	-9	7	7	7
0	5	5	11	-11	-3	-4	6	5	5	-6	2	6	2	-1	5	-9	7	7	-7
2	5	5	18	-19	-2	-4	6	7	5	-4	2	6	5	6	-3	-8	7	6	-6
4	5	5	7	7	0	-4	6	5	4	-3	2	6	3	-3	1	-8	7	6	7
5	5	5	7	6	1	-4	6	11	10	-2	2	6	17	15	3	-8	7	3	-4
-2	6	5	16	14	2	-4	6	10	-9	-1	2	6	10	10	4	-8	7	7	-7
-1	6	5	31	-28	4	-4	6	9	8	0	2	6	23	-25	5	-8	7	6	6
0	6	5	11	-11	5	-4	6	13	10	1	2	6	22	-19	1	-7	7	12	-13
2	6	5	13	14	6	-4	6	9	-7	3	2	6	12	10	2	-7	7	9	8
-3	7	5	9	-6	-4	-3	6	3	4	-5	3	6	8	7	4	-7	7	5	5
-2	7	5	19	-18	-2	-3	6	5	5	-4	3	6	5	4	-2	-6	7	6	-6
0	7	5	15	16	-1	-3	6	3	-3	-3	3	6	8	7	-1	-6	7	4	-5
4	7	5	4	4	0	-3	6	4	-5	-2	3	6	14	-14	0	-6	7	3	3
-5	8	5	5	-4	2	-3	6	17	19	-1	3	6	19	-21	1	-6	7	15	15
-4	8	5	11	-9	3	-3	6	6	7	0	3	6	7	6	-4	-5	7	5	-4
-3	8	5	7	6	4	-3	6	15	-12	1	3	6	17	15	-2	-5	7	7	7
-2	8	5	7	6	5	-3	6	10	-8	-6	4	6	6	8	-1	-5	7	12	13
-2	9	5	6	-6	-5	-2	6	3	3	-4	4	6	10	-10	0	-5	7	7	6
0	9	5	5	-5	-3	-2	6	6	-6	-3	4	6	6	-5	2	-5	7	3	3
-6	10	5	4	3	-2	-2	6	15	-15	-2	4	6	10	10	3	-5	7	7	-6
-5	10	5	7	-5	-1	-2	6	22	23	0	4	6	3	-3	4	-5	7	10	-9
-4	10	5	5	-5	0	-2	6	15	17	2	4	6	5	-6	-6	-4	7	9	-6
-3	10	5	3	3	1	-2	6	7	6	3	4	6	14	-13	-3	-4	7	8	8
0	10	5	4	7	2	-2	6	13	-15	5	4	6	5	4	-2	-4	7	4	4
1	10	5	4	7	3	-2	6	8	-8	-6	5	6	3	-3	-1	-4	7	5	5
1	-10	6	5	-7	7	-2	6	5	4	-4	5	6	5	4	0	-4	7	6	-6
-2	-9	6	6	-7	-5	-1	6	5	-4	-3	5	6	7	7	1	-4	7	15	-15
0	-9	6	5	-6	-4	-1	6	6	-6	-2	5	6	9	-7	2	-4	7	4	-4
4	-9	6	4	5	-3	-1	6	2	-3	0	5	6	3	-3	3	-4	7	9	9
-3	-8	6	7	-8	-2	-1	6	40	39	1	5	6	16	-17	4	-4	7	11	9
-1	-8	6	4	-4	-1	-1	6	3	-3	2	5	6	7	-8	-2	-3	7	4	-3
1	-8	6	5	6	0	-1	6	10	-11	3	5	6	10	10	-1	-3	7	7	-6
2	-8	6	6	5	1	-1	6	6	-6	4	5	6	10	10	0	-3	7	18	-16
4	-8	6	10	-9	2	-1	6	4	4	-3	6	6	3	-3	1	-3	7	30	27
5	-8	6	5	5	3	-1	6	4	-4	-1	6	6	19	-19	2	-3	7	18	16
-1	-7	6	7	8	5	-1	6	17	13	0	6	6	4	-4	3	-3	7	6	-5
0	-7	6	7	8	7	-1	6	8	-6	1	6	6	12	13	4	-3	7	9	-8
1	-7	6	9	-9	-5	0	6	7	6	2	6	6	8	9	-4	-2	7	3	-2
2	-7	6	9	-9	-3	0	6	10	10	-4	7	6	9	-8	-3	-2	7	7	-7
3	-7	6	4	5	-2	0	6	5	-5	-1	7	6	11	11	-2	-2	7	7	7
4	-7	6	10	9	-1	0	6	3	4	1	7	6	5	-6	-1	-2	7	10	11
-3	-6	6	5	4	1	0	6	7	-8	3	7	6	4	-5	0	-2	7	23	20
-1	-6	6	7	-7	2	0	6	11	12	-5	8	6	9	-7	1	-2	7	3	-3
0	-6	6	5	-5	5	0	6	20	-16	-4	8	6	6	5	2	-2	7	12	-10
1	-6	6	3	-3	-6	1	6	4	4	-3	8	6	10	9	3	-2	7	3	-2
2	-6	6	15	14	-5	1	6	4	-3	-1	8	6	12	-12	4	-2	7	6	-6
7	-6	6	4	-3	-3	1	6	8	8	1	8	6	4	5	6	-2	7	4	2
-5	-5	6	3	2	-2	1	6	2	2	2	8	6	6	-7	-5	-1	7	4	-3
-3	-5	6	12	-10	-1	1	6	2	-3	3	8	6	6	7	-4	-1	7	10	9
-2	-5	6	5	-5	0	1	6	4	5	-3	9	6	7	-7	-3	-1	7	8	8
-1	-5	6	13	11	1	1	6	13	14	2	9	6	6	8	-2	-1	7	11	12
0	-5	6	3	-3	2	1	6	19	-16	0	10	6	5	8	-1	-1	7	7	-7
2	-5	6	9	8	3	1	6	20	-17	0	-10	7	4	-6	0	-1	7	6	-6

H	K	L	Fo	Fc	H	K	L	Fo	Fc	H	K	L	Fo	Fc	H	K	L	Fo	Fc
2	-1	7	9	-8	-1	7	7	7	7	-3	2	8	8	7	-2	-2	9	11	10
3	-1	7	3	-2	1	7	7	5	-6	-1	2	8	24	-22	-1	-2	9	7	7
4	-1	7	8	7	-6	9	7	4	3	0	2	8	10	-10	0	-2	9	5	-6
-5	0	7	12	11	1	9	7	4	6	1	2	8	8	8	1	-2	9	4	-4
-4	0	7	3	-2	-1	10	8	3	4	2	2	8	4	4	3	-2	9	4	-4
-3	0	7	8	-8	2	-9	8	3	3	-6	3	8	5	5	-5	-1	9	7	4
-1	0	7	2	-3	3	-8	8	3	-4	-3	3	8	12	-8	-4	-1	9	5	4
1	0	7	5	-5	4	-8	8	7	7	-1	3	8	3	3	-3	-1	9	3	4
2	0	7	25	23	0	-7	8	3	-4	0	3	8	8	7	-1	-1	9	4	-4
3	0	7	6	-5	2	-7	8	9	10	3	3	8	5	-4	1	-1	9	7	-8
4	0	7	11	-10	4	-7	8	3	-3	-3	4	8	14	11	2	-1	9	5	6
5	0	7	6	-6	-5	-6	8	3	2	-1	4	8	4	-4	3	-1	9	5	5
-5	1	7	4	-3	-3	-6	8	4	-4	0	4	8	4	4	5	-1	9	7	-7
-4	1	7	8	-8	-2	-6	8	6	-6	1	4	8	10	-11	-3	0	9	4	3
-3	1	7	4	3	-1	-6	8	5	5	2	4	8	11	-12	1	0	9	16	16
-2	1	7	3	2	1	-6	8	8	8	4	4	8	9	9	2	0	9	10	-11
-1	1	7	10	11	5	-6	8	7	-6	-1	5	8	10	-10	3	0	9	10	-10
0	1	7	7	6	-4	-5	8	7	-6	0	5	8	13	-14	-3	1	9	7	5
1	1	7	10	9	1	-5	8	7	8	2	5	8	12	13	-2	1	9	8	6
2	1	7	28	-26	2	-5	8	5	-5	3	5	8	5	5	1	1	9	15	-15
3	1	7	11	-9	3	-5	8	7	-6	-2	6	8	15	-15	3	1	9	6	6
4	1	7	8	7	5	-5	8	14	12	-1	6	8	5	5	-4	2	9	10	7
-3	2	7	18	18	-2	-4	8	6	5	0	6	8	9	11	-2	2	9	15	-14
-2	2	7	13	13	1	-4	8	6	-6	1	6	8	5	5	-1	2	9	8	-7
-1	2	7	10	-10	2	-4	8	3	3	-5	7	8	11	-8	1	2	9	5	5
0	2	7	23	-20	3	-4	8	11	12	-2	7	8	7	6	-6	3	9	6	6
1	2	7	11	-9	4	-4	8	3	2	2	7	8	7	-8	-4	3	9	5	-3
2	2	7	6	5	5	-4	8	9	-8	-4	8	8	5	4	-3	3	9	9	-8
-5	3	7	10	7	0	-3	8	7	7	-2	8	8	5	-6	-1	3	9	4	3
-4	3	7	7	7	1	-3	8	12	11	1	8	8	5	-6	3	3	9	5	-6
-3	3	7	2	-2	3	-3	8	11	-10	0	9	8	4	6	4	3	9	4	-4
-2	3	7	18	-20	4	-3	8	6	-5	-2	10	8	5	5	-1	4	9	6	-6
3	3	7	4	4	-3	-2	8	5	-4	1	-8	9	5	-7	0	4	9	4	4
5	3	7	7	-6	-2	-2	8	26	22	0	-7	9	7	-9	1	4	9	9	-11
-6	4	7	6	6	0	-2	8	4	-4	1	-7	9	7	8	2	4	9	4	-5
-5	4	7	9	-8	1	-2	8	13	-13	0	-6	9	6	7	3	4	9	6	7
-4	4	7	3	-3	-5	-1	8	4	3	2	-6	9	4	5	-3	5	9	8	7
-2	4	7	7	6	-3	-1	8	15	17	4	-6	9	6	-6	-2	5	9	9	-10
0	4	7	5	-5	-2	-1	8	11	-10	-3	-5	9	3	3	-1	5	9	6	-6
1	4	7	9	10	-1	-1	8	9	-8	-2	-5	9	3	4	1	5	9	6	8
2	4	7	7	-8	2	-1	8	5	5	-1	-5	9	3	3	-3	6	9	8	-7
3	4	7	8	-9	4	-1	8	15	14	2	-5	9	4	-5	1	-7	10	5	7
5	4	7	8	8	5	-1	8	9	-8	3	-5	9	5	-5	-2	-6	10	5	6
-4	5	7	4	5	6	-1	8	8	-7	5	-5	9	5	4	4	-6	10	5	-6
-2	5	7	11	10	-6	0	8	5	4	-7	-4	9	4	-3	-3	-5	10	3	4
-1	5	7	14	-13	1	0	8	20	19	0	-4	9	9	-10	1	-5	10	4	-5
1	5	7	11	-13	2	0	8	4	-3	1	-4	9	5	5	3	-5	10	3	4
2	5	7	4	5	3	0	8	9	-8	2	-4	9	9	9	4	-5	10	9	9
3	5	7	7	8	4	0	8	16	-15	-3	-3	9	5	-4	-1	-4	10	3	-4
-2	6	7	19	-18	-4	1	8	3	4	0	-3	9	17	18	1	-4	10	7	8
-1	6	7	8	-8	-2	1	8	6	4	1	-3	9	6	5	2	-4	10	6	8
0	6	7	9	10	-1	1	8	15	13	2	-3	9	8	-8	4	-4	10	7	-7
3	6	7	5	-5	1	1	8	18	-18	3	-3	9	5	-4	-3	-3	10	4	-4
-4	7	7	12	-9	2	1	8	16	-15	-5	-2	9	7	-4	-2	-3	10	7	7
-2	7	7	5	4	4	1	8	6	6	-3	-2	9	8	6	-1	-3	10	3	3

Observed and Calculated Structure Factors For
N,N'-Bis[2-(5-t-butyl-3H-1,2-dithiol-3-ylidene)ethylidene]hydrazine

Page 7

H	K	L	Fo	Fc	H	K	L	Fo	Fc	H	K	L	Fo	Fc	H	K	L	Fo	Fc
0	-3	10	7	8	0	1	10	13	-14	3	-6	11	4	-5	0	6	11	3	-4
1	-3	10	4	-5	1	1	10	5	-5	0	-4	11	4	5	0	-4	12	5	7
2	-3	10	5	-5	3	1	10	4	4	1	-4	11	4	5	-3	-3	12	7	8
3	-3	10	5	-5	-4	2	10	6	5	-1	-3	11	6	7	2	-3	12	3	-3
-3	-2	10	14	13	-3	2	10	4	-3	1	-3	11	3	-4	-4	-2	12	6	6
-1	-2	10	3	-4	-2	2	10	10	-10	-4	-2	11	5	5	3	-2	12	7	9
0	-2	10	4	-4	-1	2	10	6	-7	-1	-2	11	3	-4	0	-1	12	5	6
4	-2	10	10	11	0	2	10	7	8	3	-2	11	3	4	3	-1	12	5	-7
-6	-1	10	4	3	0	3	10	5	6	1	-1	11	7	8	0	0	12	5	-6
-2	-1	10	4	-5	-4	4	10	4	3	0	0	11	7	8	1	0	12	5	-6
1	-1	10	7	9	0	4	10	8	-10	1	0	11	11	-13	-2	1	12	6	-6
3	-1	10	6	7	1	4	10	7	-8	2	0	11	5	-6	-1	1	12	7	-8
4	-1	10	9	-10	3	4	10	6	7	4	0	11	4	4	-3	2	12	3	-4
-5	0	10	3	-3	-2	5	10	11	-11	-3	1	11	5	4	-1	3	12	4	5
-1	0	10	6	6	1	5	10	7	9	-2	1	11	5	-5	-2	4	12	3	-2
0	0	10	9	9	-5	6	10	8	-6	0	1	11	5	-6	0	4	12	3	-4
1	0	10	6	-6	-2	6	10	6	6	-3	2	11	6	-6	-3	5	12	5	-6
2	0	10	11	-12	-1	6	10	4	5	-2	4	11	6	-7	-1	-4	13	4	5
3	0	10	6	-7	-6	7	10	4	-4	0	4	11	5	-6	-3	0	13	4	3
-3	1	10	7	5	-4	7	10	5	5	2	4	11	5	7	0	0	13	6	-8
-2	1	10	8	9	0	7	10	3	5	-3	5	11	8	-8	-3	4	13	6	-6
-1	1	10	9	-9	0	-7	11	5	7	0	5	11	6	8					

TABLE B. Anisotropic temperature parameters (\AA^2 , $\times 10^3$)

Atom	U_{11}	U_{22}	U_{33}	U_{23}	U_{13}	U_{12}
S(1)	43(1)	41(1)	38(1)	-6(1)	-12(1)	9(1)
S(2)	57(1)	39(1)	57(1)	-11(1)	-21(1)	23(1)
N(1)	47(4)	20(3)	29(3)	-5(2)	4(3)	-3(3)
C(1)	45(4)	27(3)	21(3)	1(3)	1(3)	8(3)
C(2)	37(4)	28(3)	31(4)	-1(3)	-5(3)	4(3)
C(3)	39(4)	24(3)	27(3)	-1(3)	0(3)	5(3)
C(4)	53(5)	26(4)	41(4)	-2(3)	-4(4)	8(3)
C(5)	53(5)	24(4)	39(4)	-8(3)	6(4)	3(3)
C(6)	43(4)	23(3)	23(3)	2(3)	5(3)	4(3)
C(7)	46(5)	35(4)	33(4)	3(3)	-5(3)	5(3)
C(8)	63(6)	45(5)	42(5)	-9(4)	13(4)	14(4)
C(9)	70(7)	33(4)	47(5)	14(4)	25(5)	8(4)

Least-squares plane through the molecule (excluding the t-butyl groups & H's) and distances of atoms from the plane (\AA , $\times 10^2$)

The plane is defined in orthogonal Angstrom coordinates by the equation: $\underline{A}x + \underline{B}y + \underline{C}z + \underline{D} = 0$

\underline{A} : 0.469(13), \underline{B} : 0.336(8), \underline{C} : -0.817(12), \underline{D} : 0.000(23)

Distances

S(1)	2(2)	S(2)	-1(2)	C(1)	-6(2)	C(2)	-2(2)
C(3)	3(2)	C(4)	4(2)	C(5)	2(2)	N(1)	1(2)
C(6)	-9(2)	C(7)	-67(2)	C(8)	-94(3)	C(9)	134(3)
H(1)	5(9)	H(2)	2(9)	H(3)	18(8)		

Perpendicular distance between the above plane and the equivalent plane through the molecule translated 1 unit cell in x and y : 4.61(2) \AA .

Appendix C

Observed and Calculated Structure Factors,

Anisotropic Temperature Parameters

and Least-Squares Planes for

N,N-dimethyl-N'-[2-(5-t-butyl-3H-1,2-dithiol-3-ylidene)
ethylidene]hydrazine.

N,N-Dimethyl-N'-[2-(5-tert-butyl-3H-1,2-dithiol-3-ylidene)-ethylidene]hydrazine

H	K	L	Fo	Fc	H	K	L	Fo	Fc	H	K	L	Fo	Fc	H	K	L	Fo	Fc
3	0	0	31	33	-1	6	0	14	-12	-7	-6	1	5	5	-8	-1	1	2	2
4	0	0	13	-15	0	6	0	12	15	-6	-6	1	4	-5	-7	-1	1	6	-8
5	0	0	4	-4	1	6	0	2	-2	-4	-6	1	18	18	-5	-1	1	9	13
6	0	0	3	4	2	6	0	16	-17	-3	-6	1	8	-9	-1	-1	1	24	-24
-6	1	0	2	-2	3	6	0	22	22	-2	-6	1	5	-6	0	-1	1	16	17
-3	1	0	12	-12	4	6	0	21	-20	-1	-6	1	9	12	1	-1	1	27	27
-2	1	0	9	-9	6	6	0	10	12	0	-6	1	7	-7	3	-1	1	8	9
-1	1	0	5	-4	7	6	0	6	-5	1	-6	1	9	-8	4	-1	1	4	3
5	1	0	8	11	1	7	0	7	-6	2	-6	1	7	6	-7	0	1	2	2
6	1	0	7	-10	2	7	0	22	19	4	-6	1	4	-3	-6	0	1	4	-5
8	1	0	2	2	3	7	0	3	-3	-6	-5	1	2	-2	-5	0	1	7	-7
-8	2	0	4	-4	4	7	0	8	-8	-3	-5	1	10	9	-4	0	1	8	8
-7	2	0	6	5	5	7	0	11	11	-2	-5	1	17	17	-3	0	1	8	-8
-5	2	0	8	-8	6	7	0	7	-7	-1	-5	1	6	-6	-2	0	1	11	-12
-4	2	0	9	9	-2	8	0	3	-3	0	-5	1	2	-2	2	0	1	28	32
-2	2	0	5	3	0	8	0	6	-6	1	-5	1	20	22	3	0	1	5	6
-1	2	0	22	-21	4	8	0	12	10	2	-5	1	21	-24	4	0	1	16	-16
0	2	0	38	-38	5	8	0	8	-9	3	-5	1	7	6	5	0	1	14	15
1	2	0	34	35	7	8	0	6	5	4	-5	1	8	6	6	0	1	4	-5
2	2	0	31	-33	8	8	0	5	-4	5	-5	1	7	-6	7	0	1	4	-4
7	2	0	2	4	-3	9	0	4	-4	-8	-4	1	1	2	8	0	1	3	2
8	2	0	4	-6	-2	9	0	6	7	-6	-4	1	3	-4	-5	1	1	3	-3
-6	3	0	3	-4	-1	9	0	4	-4	-5	-4	1	2	-3	-3	1	1	12	-12
-5	3	0	9	9	2	9	0	7	-7	-4	-4	1	3	-4	-2	1	1	16	16
-4	3	0	14	-12	8	9	0	3	2	-1	-4	1	16	17	-1	1	1	8	-9
-2	3	0	23	24	0	10	0	4	6	0	-4	1	12	12	0	1	1	15	-16
-1	3	0	6	6	2	10	0	5	-5	1	-4	1	13	-13	5	1	1	7	-9
0	3	0	6	-5	4	10	0	5	-5	2	-4	1	16	16	7	1	1	2	2
2	3	0	9	9	7	10	0	4	-3	3	-4	1	4	-4	8	1	1	4	-4
3	3	0	11	12	3	11	0	5	-7	4	-4	1	9	-9	-4	2	1	5	5
4	3	0	11	-14	5	11	0	3	3	5	-4	1	7	7	-3	2	1	14	-14
5	3	0	4	6	5	12	0	5	-5	7	-4	1	4	-3	-2	2	1	2	-2
8	3	0	3	6	-2	10	1	9	-10	-7	-3	1	3	-4	0	2	1	8	8
-5	4	0	9	-9	-6	-9	1	5	3	-6	-3	1	9	12	1	2	1	11	-11
-2	4	0	18	-18	-3	-9	1	4	3	-5	-3	1	7	-9	2	2	1	3	-4
-1	4	0	8	8	-2	-9	1	6	6	-4	-3	1	6	-8	7	2	1	4	-6
0	4	0	35	32	-1	-9	1	6	-7	-3	-3	1	7	7	-7	3	1	5	-4
1	4	0	22	-23	1	-9	1	5	6	-2	-3	1	16	-16	-6	3	1	2	2
2	4	0	8	8	2	-9	1	8	-9	-1	-3	1	2	2	-5	3	1	8	8
3	4	0	15	16	-7	-8	1	4	3	0	-3	1	17	16	-4	3	1	15	-14
4	4	0	7	7	-6	-8	1	7	-8	1	-3	1	6	7	-3	3	1	4	4
7	4	0	2	2	-5	-8	1	7	8	3	-3	1	6	-5	-1	3	1	19	-19
-5	5	0	5	4	-3	-8	1	9	-8	4	-3	1	7	7	0	3	1	1	-1
-3	5	0	22	-17	-2	-8	1	7	7	5	-3	1	7	-8	1	3	1	3	3
-1	5	0	6	7	-1	-8	1	6	7	-8	-2	1	2	-3	2	3	1	7	-7
0	5	0	34	-34	0	-8	1	4	-4	-7	-2	1	4	5	3	3	1	2	-1
1	5	0	21	20	2	-8	1	5	6	-6	-2	1	3	-5	-7	4	1	3	3
2	5	0	10	9	3	-8	1	6	-6	-4	-2	1	14	17	-5	4	1	6	-6
3	5	0	35	-37	-7	-7	1	9	-8	-3	-2	1	17	-19	-4	4	1	17	17
4	5	0	27	28	-6	-7	1	8	9	-2	-2	1	6	7	-3	4	1	4	-4
5	5	0	2	2	-4	-7	1	6	-7	-1	-2	1	5	5	-2	4	1	32	-31
6	5	0	4	-5	-3	-7	1	7	8	0	-2	1	2	1	-1	4	1	37	34
7	5	0	3	4	-2	-7	1	5	-5	1	-2	1	18	18	0	4	1	23	-25
-3	6	0	8	6	-1	-7	1	8	-7	2	-2	1	12	11	1	4	1	5	-5
-2	6	0	5	-5	0	-7	1	11	11	3	-2	1	4	-3	2	4	1	14	14

N,N-Dimethyl-N'-[2-(5-tert-butyl-3H-1,2-dithiol-3-ylidene)-ethylidene]hydrazine

H	K	L	Fo	Fc	H	K	L	Fo	Fc	H	K	L	Fo	Fc	H	K	L	Fo	Fc
3	4	1	3	-3	-7	-9	2	7	5	-2	-3	2	5	-5	5	1	2	2	-2
-4	5	1	6	-5	-4	-9	2	6	5	-1	-3	2	33	31	6	1	2	8	12
-3	5	1	6	7	-8	-8	2	4	3	0	-3	2	19	-19	8	1	2	2	-2
-2	5	1	9	10	-7	-8	2	4	-4	1	-3	2	10	7	-8	2	2	4	3
-1	5	1	26	-28	-5	-8	2	10	8	2	-3	2	13	12	-7	2	2	7	-5
0	5	1	6	6	-4	-8	2	13	-12	3	-3	2	11	11	-6	2	2	5	5
1	5	1	8	9	-3	-8	2	8	8	4	-3	2	7	6	-5	2	2	8	9
2	5	1	15	-15	-2	-8	2	8	8	5	-3	2	9	-9	-4	2	2	14	-14
3	5	1	4	4	-8	-7	2	4	-3	8	-3	2	3	-3	-3	2	2	16	15
4	5	1	19	19	-6	-7	2	7	8	-8	-2	2	5	6	-2	2	2	7	7
5	5	1	7	-8	-5	-7	2	10	-11	-7	-2	2	3	-3	-1	2	2	29	-27
7	5	1	2	3	-3	-7	2	14	12	-6	-2	2	4	-5	1	2	2	35	-37
-3	6	1	5	4	-2	-7	2	12	-11	-5	-2	2	14	17	2	2	2	5	-4
-1	6	1	4	-3	-1	-7	2	15	15	-4	-2	2	11	-12	6	2	2	2	-5
0	6	1	5	6	0	-7	2	8	8	-3	-2	2	34	-32	8	2	2	5	6
1	6	1	18	-20	1	-7	2	5	-5	-2	-2	2	19	20	-8	3	2	3	-2
2	6	1	3	3	-6	-6	2	9	-10	-1	-2	2	24	-23	-6	3	2	4	4
3	6	1	5	5	-5	-6	2	7	7	0	-2	2	21	-20	-5	3	2	12	-11
4	6	1	12	-11	-4	-6	2	9	9	1	-2	2	16	-14	-4	3	2	15	14
5	6	1	9	10	-3	-6	2	32	-34	2	-2	2	2	-2	-2	3	2	3	-4
6	6	1	5	6	-2	-6	2	21	24	3	-2	2	5	4	-1	3	2	35	34
7	6	1	6	-7	0	-6	2	11	-10	4	-2	2	5	6	0	3	2	3	4
8	6	1	4	4	1	-6	2	21	19	5	-2	2	6	6	2	3	2	8	-7
-4	7	1	3	-4	3	-6	2	6	-5	-6	-1	2	6	8	3	3	2	3	-4
-2	7	1	9	9	4	-6	2	7	6	-5	-1	2	8	-10	4	3	2	6	8
0	7	1	8	-7	-5	-5	2	3	-3	-3	-1	2	35	36	-5	4	2	8	8
1	7	1	9	8	-3	-5	2	18	17	-2	-1	2	60	-61	-4	4	2	5	-5
2	7	1	3	-3	-2	-5	2	20	-20	-1	-1	2	7	-7	-3	4	2	14	-15
3	7	1	15	-17	-1	-5	2	14	-16	1	-1	2	102	-106	-2	4	2	17	17
4	7	1	7	7	0	-5	2	24	26	2	-1	2	2	2	-1	4	2	3	-4
6	7	1	9	-10	1	-5	2	9	-9	3	-1	2	12	13	0	4	2	24	-25
7	7	1	9	9	2	-5	2	7	-6	4	-1	2	13	-11	1	4	2	53	53
8	7	1	3	-2	3	-5	2	8	6	5	-1	2	4	4	2	4	2	18	-16
-4	8	1	5	5	4	-5	2	6	-5	6	-1	2	2	3	3	4	2	23	-24
-2	8	1	6	-7	6	-5	2	4	4	-5	0	2	2	2	4	4	2	25	27
-1	8	1	12	13	-8	-4	2	3	3	-4	0	2	4	3	5	4	2	3	-4
0	8	1	5	-5	-7	-4	2	9	-9	-3	0	2	19	-19	6	4	2	1	-2
1	8	1	3	-2	-6	-4	2	4	5	-2	0	2	22	22	-3	5	2	9	9
2	8	1	4	4	-4	-4	2	8	-8	-1	0	2	2	1	-2	5	2	15	-17
4	8	1	7	-7	-3	-4	2	12	12	2	0	2	10	-10	-1	5	2	7	-8
6	8	1	5	5	-2	-4	2	8	8	3	0	2	25	-28	0	5	2	19	19
-2	9	1	4	5	-1	-4	2	7	7	4	0	2	19	20	1	5	2	33	-32
-1	9	1	10	-12	0	-4	2	18	-18	6	0	2	5	-6	2	5	2	2	2
0	9	1	5	6	1	-4	2	18	18	7	0	2	3	3	3	5	2	16	17
1	9	1	5	6	2	-4	2	16	17	-8	1	2	2	-2	4	5	2	32	-31
2	9	1	12	-12	3	-4	2	10	-10	-7	1	2	7	7	5	5	2	14	16
3	9	1	8	8	4	-4	2	4	-4	-6	1	2	4	-4	6	5	2	5	6
1	10	1	6	-8	5	-4	2	6	4	-5	1	2	3	-3	7	5	2	5	-6
2	10	1	8	10	6	-4	2	6	-5	-4	1	2	4	4	-3	6	2	7	6
3	10	1	7	-7	-8	-3	2	5	-6	-3	1	2	6	-6	-2	6	2	3	2
4	11	1	4	5	-7	-3	2	8	9	-2	1	2	11	-11	-1	6	2	8	7
5	11	1	4	-4	-6	-3	2	3	-4	0	1	2	8	-8	0	6	2	8	-9
-5	12	2	5	4	-5	-3	2	12	-14	1	1	2	9	9	2	6	2	18	18
-3	11	2	4	4	-4	-3	2	8	8	2	1	2	10	-12	3	6	2	25	-25
-4	10	2	5	5	-3	-3	2	9	-9	4	1	2	10	-13	6	6	2	7	-8

N,N-Dimethyl-N'-[2-(5-tert-butyl-3H-1,2-dithiol-3-ylidene)-ethylidene]hydrazine

H	K	L	Fo	Fc	H	K	L	Fo	Fc	H	K	L	Fo	Fc	H	K	L	Fo	Fc
7	6	2	6	7	-1	-7	3	4	4	4	-1	3	4	-4	0	4	3	38	40
-5	7	2	5	-5	0	-7	3	5	-5	5	-1	3	10	10	1	4	3	8	-9
-4	7	2	4	4	1	-7	3	5	5	6	-1	3	3	-4	2	4	3	16	-16
-2	7	2	6	6	-3	-6	3	6	7	-7	0	3	2	3	3	4	3	7	8
1	7	2	3	3	-1	-6	3	15	-14	-4	0	3	5	-5	4	4	3	2	2
2	7	2	4	-5	1	-6	3	8	6	-3	0	3	5	-5	5	4	3	10	-12
3	7	2	10	11	2	-6	3	11	-10	-2	0	3	25	24	-3	5	3	4	5
5	7	2	16	-15	3	-6	3	9	9	-1	0	3	32	-32	-1	5	3	10	10
6	7	2	6	6	-5	-5	3	2	-3	0	0	3	18	-18	1	5	3	16	-16
8	7	2	3	-3	-4	-5	3	3	2	2	0	3	18	-20	2	5	3	20	19
-4	8	2	4	-4	-1	-5	3	11	13	4	0	3	11	11	3	5	3	4	-4
-2	8	2	6	7	0	-5	3	3	-3	5	0	3	10	-11	4	5	3	9	-9
-1	8	2	6	-7	1	-5	3	13	-11	6	0	3	5	6	5	5	3	11	13
0	8	2	6	6	2	-5	3	19	16	8	0	3	2	-2	6	5	3	3	-5
2	8	2	6	-5	3	-5	3	8	-7	-5	1	3	4	4	7	5	3	3	-4
3	8	2	7	6	5	-5	3	7	6	-3	1	3	7	-7	8	5	3	2	3
5	8	2	3	4	-6	-4	3	6	7	-2	1	3	5	5	-4	6	3	6	-5
6	8	2	2	-2	-5	-4	3	13	-13	-1	1	3	9	9	-2	6	3	11	10
8	8	2	4	4	-3	-4	3	3	-3	1	1	3	29	-31	0	6	3	3	-3
-2	9	2	6	-7	-2	-4	3	7	-7	2	1	3	3	-3	1	6	3	15	16
1	9	2	4	-5	-1	-4	3	5	5	3	1	3	8	9	2	6	3	13	-13
4	9	2	6	-5	0	-4	3	5	6	4	1	3	16	-19	3	6	3	8	-8
5	9	2	5	4	2	-4	3	6	-7	5	1	3	11	12	4	6	3	16	15
1	10	2	9	10	3	-4	3	5	5	7	1	3	4	-4	5	6	3	7	-7
3	10	2	9	-9	4	-4	3	6	4	8	1	3	3	2	6	6	3	3	-4
4	10	2	7	6	5	-4	3	6	-5	-6	2	3	5	5	7	6	3	8	9
5	10	2	4	-3	6	-4	3	5	4	-5	2	3	5	5	8	6	3	5	-6
7	10	2	5	3	-7	-3	3	5	5	-4	2	3	8	-8	-3	7	3	9	-9
8	10	2	4	-3	-6	-3	3	6	-6	-3	2	3	15	14	-1	7	3	14	14
3	11	2	4	5	-5	-3	3	9	10	-2	2	3	10	-10	4	7	3	13	-13
5	11	2	4	-4	-3	-3	3	22	-21	-1	2	3	13	13	6	7	3	3	4
6	11	2	6	5	-2	-3	3	5	-4	0	2	3	5	-5	7	7	3	8	-7
7	11	2	5	-3	-1	-3	3	11	-12	1	2	3	7	7	8	7	3	3	3
2	12	2	4	5	0	-3	3	7	-6	2	2	3	13	-12	-3	8	3	4	4
-1	-11	3	4	6	1	-3	3	2	3	3	2	3	6	-8	-1	8	3	15	-16
-1	-10	3	5	-7	-7	-2	3	7	-7	4	2	3	5	6	0	8	3	19	20
2	-10	3	4	-4	-6	-2	3	8	8	5	2	3	2	-3	2	8	3	6	-6
-5	-9	3	7	6	-5	-2	3	7	8	7	2	3	4	5	3	8	3	10	9
-3	-9	3	4	-3	-4	-2	3	17	-17	-7	3	3	3	2	-3	9	3	4	-3
-2	-9	3	5	5	-3	-2	3	35	34	-6	3	3	6	-7	0	9	3	11	-13
-1	-9	3	3	4	-2	-2	3	22	-22	-5	3	3	3	-3	2	9	3	16	16
0	-9	3	3	-4	0	-2	3	3	5	-4	3	3	25	23	3	9	3	13	-13
2	-9	3	4	5	2	-2	3	8	-7	-3	3	3	21	-19	4	9	3	7	6
3	-9	3	4	-5	3	-2	3	4	4	-2	3	3	13	-13	5	9	3	4	3
-8	-8	3	3	-3	-7	-1	3	3	3	-1	3	3	48	46	1	10	3	4	5
-7	-8	3	4	-4	-6	-1	3	6	-7	0	3	3	36	-35	2	10	3	7	-8
-6	-8	3	8	7	-5	-1	3	4	-4	3	3	3	9	-10	3	10	3	5	6
-5	-8	3	9	-8	-4	-1	3	17	19	4	3	3	3	-3	1	11	3	4	-5
-3	-8	3	4	5	-3	-1	3	14	-15	5	3	3	3	-4	2	11	3	4	4
-2	-8	3	5	-5	-2	-1	3	10	9	6	3	3	1	3	4	11	3	7	-7
0	-8	3	8	9	-1	-1	3	5	5	-6	4	3	2	3	5	11	3	6	5
-7	-7	3	5	4	0	-1	3	20	-20	-4	4	3	9	-8	7	11	3	6	-4
-6	-7	3	9	-10	1	-1	3	16	-15	-3	4	3	20	21	4	12	3	5	4
-5	-7	3	3	4	2	-1	3	18	19	-2	4	3	6	6	-7	-9	4	6	-4
-3	-7	3	15	-14	3	-1	3	12	-12	-1	4	3	42	-38	-6	-9	4	4	3

N,N-Dimethyl-N'-[2-(5-tert-butyl-3H-1,2-dithiol-3-ylidene)-ethylidene]hydrazine

H	K	L	Fo	Fc	H	K	L	Fo	Fc	H	K	L	Fo	Fc	H	K	L	Fo	Fc
-4	-9	4	9	-8	6	-3	4	3	-5	0	2	4	25	-26	3	7	4	7	7
-3	-9	4	5	6	-8	-2	4	2	-2	1	2	4	9	-10	5	7	4	6	7
-7	-8	4	5	4	-7	-2	4	5	5	2	2	4	22	-21	6	7	4	8	-8
-5	-8	4	9	-8	-6	-2	4	3	4	3	2	4	1	1	-4	8	4	4	3
-4	-8	4	8	8	-5	-2	4	13	-13	4	2	4	7	7	-3	8	4	4	-4
-3	-8	4	4	-3	-4	-2	4	14	14	5	2	4	10	-12	-2	8	4	11	-11
-1	-8	4	6	7	-3	-2	4	11	10	6	2	4	3	4	0	8	4	6	-7
1	-8	4	4	-4	-2	-2	4	59	-57	-7	3	4	4	-4	5	8	4	4	4
-6	-7	4	5	-7	-1	-2	4	27	28	-5	3	4	10	10	-1	9	4	6	-7
-5	-7	4	14	11	0	-2	4	14	13	-4	3	4	17	-16	1	9	4	8	9
-4	-7	4	6	-4	2	-2	4	9	8	-3	3	4	5	5	2	9	4	9	-9
-3	-7	4	16	-15	4	-2	4	5	-4	-2	3	4	27	25	3	9	4	7	-6
-2	-7	4	20	20	5	-2	4	5	5	0	3	4	14	14	4	9	4	11	9
-1	-7	4	11	-12	-6	-1	4	3	-3	2	3	4	40	-42	5	9	4	7	-5
1	-7	4	9	9	-5	-1	4	12	12	3	3	4	13	-13	6	9	4	3	4
4	-7	4	4	4	-3	-1	4	9	-9	4	3	4	10	11	8	9	4	3	-2
-6	-6	4	4	5	-2	-1	4	38	39	5	3	4	4	-4	0	10	4	5	7
-5	-6	4	7	-8	-1	-1	4	32	-29	6	3	4	3	-5	3	10	4	4	4
-3	-6	4	16	13	0	-1	4	27	-26	-5	4	4	4	-4	4	10	4	8	-7
-2	-6	4	32	-29	1	-1	4	68	67	-2	4	4	26	-26	6	10	4	4	4
-1	-6	4	5	3	2	-1	4	53	-54	-1	4	4	17	17	0	11	4	4	-6
0	-6	4	11	10	3	-1	4	13	-14	0	4	4	24	22	2	11	4	5	7
1	-6	4	10	-10	4	-1	4	9	8	1	4	4	22	-22	3	11	4	4	-5
2	-6	4	4	4	5	-1	4	6	-5	2	4	4	45	44	5	11	4	3	3
3	-6	4	4	4	-6	0	4	6	-7	3	4	4	3	-2	7	11	4	6	4
-6	-5	4	6	7	-4	0	4	3	3	4	4	4	23	-24	0	10	5	3	-5
-4	-5	4	2	-2	-3	0	4	9	9	5	4	4	18	20	-6	-9	5	4	4
-2	-5	4	4	4	-1	0	4	4	4	6	4	4	2	-3	-4	-9	5	5	4
-1	-5	4	10	-11	1	0	4	18	-18	7	4	4	4	-5	-2	-9	5	4	-5
0	-5	4	26	-23	2	0	4	17	16	-3	5	4	5	-5	-5	-8	5	10	9
1	-5	4	17	15	3	0	4	13	14	-1	5	4	5	-5	-5	-7	5	6	-4
3	-5	4	10	-9	4	0	4	27	-26	0	5	4	19	-19	-3	-7	5	4	5
4	-5	4	4	3	5	0	4	3	3	1	5	4	16	15	-2	-7	5	5	-6
-7	-4	4	9	9	6	0	4	4	4	2	5	4	13	11	-1	-7	5	7	-7
-6	-4	4	8	-10	7	0	4	5	-4	3	5	4	19	-20	0	-7	5	3	4
-4	-4	4	13	12	-7	1	4	9	-7	4	5	4	17	17	3	-7	5	3	4
-3	-4	4	10	-9	-6	1	4	8	10	5	5	4	8	-9	-4	-6	5	5	5
-2	-4	4	11	11	-5	1	4	5	-4	7	5	4	6	6	-3	-6	5	4	-3
-1	-4	4	7	7	-4	1	4	10	-10	8	5	4	3	-4	-1	-6	5	4	4
0	-4	4	12	-12	-3	1	4	13	12	-4	6	4	6	5	0	-6	5	12	-13
1	-4	4	3	-4	-2	1	4	7	-6	-3	6	4	3	-3	1	-6	5	6	-6
3	-4	4	5	4	-1	1	4	11	-11	-2	6	4	10	9	2	-6	5	8	8
4	-4	4	4	-3	0	1	4	8	-7	-1	6	4	6	-6	3	-6	5	8	-8
5	-4	4	7	-6	2	1	4	14	13	0	6	4	5	7	-7	-5	5	4	3
6	-4	4	5	4	3	1	4	3	-4	1	6	4	4	-4	-6	-5	5	2	3
-8	-3	4	6	5	4	1	4	7	8	2	6	4	5	-6	-5	-5	5	4	-4
-7	-3	4	10	-9	6	1	4	4	-6	3	6	4	19	18	-4	-5	5	6	6
-6	-3	4	4	5	7	1	4	3	3	4	6	4	14	-12	-2	-5	5	5	5
-5	-3	4	10	10	-8	2	4	3	-3	5	6	4	7	-8	-1	-5	5	5	4
-4	-3	4	19	-19	-7	2	4	6	5	6	6	4	6	7	1	-5	5	3	-3
-2	-3	4	18	16	-5	2	4	8	-7	7	6	4	4	-4	2	-5	5	11	-11
-1	-3	4	10	-11	-4	2	4	23	20	-4	7	4	9	-8	3	-5	5	6	6
0	-3	4	9	10	-3	2	4	12	-12	0	7	4	10	9	-6	-4	5	6	-6
1	-3	4	13	-14	-2	2	4	12	11	1	7	4	5	-5	-5	-4	5	11	10
2	-3	4	5	5	-1	2	4	20	17	2	7	4	3	4	-3	-4	5	3	-3

N,N-Dimethyl-N'-[2-(5-tert-butyl-3H-1,2-dithiol-3-ylidene)-ethylidene]hydrazine

H	K	L	Fo	Fc	H	K	L	Fo	Fc	H	K	L	Fo	Fc	H	K	L	Fo	Fc
-2	-4	5	3	3	8	1	5	3	-2	3	7	5	2	2	-5	-4	6	3	-3
-1	-4	5	3	3	-6	2	5	9	-10	7	7	5	4	3	-4	-4	6	8	-9
0	-4	5	4	6	-5	2	5	5	5	-3	8	5	7	-6	-3	-4	6	13	15
3	-4	5	4	-3	-4	2	5	20	18	-2	8	5	4	4	-2	-4	6	3	4
-7	-3	5	5	-5	-3	2	5	32	-28	-1	8	5	5	5	-1	-4	6	4	3
-6	-3	5	9	11	-2	2	5	8	9	0	8	5	25	-25	0	-4	6	11	10
-5	-3	5	6	-4	-1	2	5	26	25	1	8	5	18	18	1	-4	6	8	-7
-4	-3	5	5	-5	0	2	5	22	-21	2	8	5	7	7	2	-4	6	5	4
-3	-3	5	21	20	1	2	5	20	20	3	8	5	18	-15	3	-4	6	3	-4
-2	-3	5	28	-28	2	2	5	10	11	4	8	5	9	11	-7	-3	6	8	7
0	-3	5	10	11	3	2	5	3	-4	-3	9	5	4	4	-6	-3	6	6	-7
2	-3	5	3	-3	7	2	5	3	-3	-1	9	5	4	-4	-5	-3	6	7	-8
-7	-2	5	4	4	-7	3	5	3	-2	2	9	5	8	-8	-4	-3	6	15	15
-6	-2	5	8	-9	-5	3	5	8	-8	3	9	5	15	14	-3	-3	6	8	-8
-5	-2	5	5	5	-4	3	5	11	-10	4	9	5	7	-6	-2	-3	6	16	-16
-4	-2	5	18	19	-3	3	5	30	28	6	9	5	5	5	-1	-3	6	33	34
-3	-2	5	14	-15	-2	3	5	23	-22	-1	10	5	4	5	1	-3	6	6	-6
-2	-2	5	25	23	0	3	5	55	56	2	10	5	7	8	2	-3	6	14	11
-1	-2	5	5	-4	1	3	5	24	-24	3	10	5	5	-4	-5	-2	6	11	10
0	-2	5	13	-13	2	3	5	7	6	4	10	5	5	-5	-4	-2	6	16	-15
1	-2	5	3	3	3	3	5	11	13	5	10	5	8	7	-3	-2	6	4	-4
2	-2	5	10	9	4	3	5	3	-4	6	10	5	4	-3	-2	-2	6	23	23
3	-2	5	13	-13	5	3	5	5	-6	4	11	5	5	6	-1	-2	6	39	-38
5	-2	5	3	3	-3	4	5	4	-4	5	11	5	8	-6	0	-2	6	10	9
6	-2	5	2	-3	-1	4	5	8	9	4	13	5	5	-6	1	-2	6	31	31
-8	-1	5	2	-2	0	4	5	27	-25	-4	-9	6	5	6	2	-2	6	33	-34
-5	-1	5	5	-5	2	4	5	21	22	-3	-9	6	5	-6	3	-2	6	8	8
-4	-1	5	8	-7	3	4	5	10	-11	-5	-8	6	8	8	4	-2	6	5	4
-3	-1	5	16	16	5	4	5	8	9	-4	-8	6	8	-7	5	-2	6	3	-2
-2	-1	5	21	21	6	4	5	6	-8	-2	-8	6	7	8	-4	-1	6	7	6
-1	-1	5	13	-15	-4	5	5	6	-5	-1	-8	6	7	-9	-3	-1	6	8	7
0	-1	5	17	17	-2	5	5	6	7	0	-8	6	4	5	-2	-1	6	13	-13
1	-1	5	9	10	-1	5	5	8	-8	2	-8	6	4	-5	-1	-1	6	17	17
2	-1	5	14	-13	1	5	5	9	9	-5	-7	6	9	-8	0	-1	6	9	8
3	-1	5	12	10	2	5	5	20	-19	-4	-7	6	9	8	1	-1	6	26	-25
5	-1	5	9	-8	3	5	5	12	12	-3	-7	6	5	6	2	-1	6	33	31
6	-1	5	4	4	4	5	5	13	13	-2	-7	6	15	-16	3	-1	6	7	-6
-4	0	5	8	-8	5	5	5	11	-11	-1	-7	6	14	15	4	-1	6	18	-17
-3	0	5	7	-7	6	5	5	3	4	-8	-6	6	3	-3	5	-1	6	7	7
-2	0	5	5	5	7	5	5	4	4	-4	-6	6	4	-3	7	-1	6	3	-2
-1	0	5	22	20	8	5	5	5	-6	-2	-6	6	11	10	-7	0	6	5	-4
1	0	5	5	-6	-3	6	5	10	-10	-1	-6	6	13	-13	-6	0	6	8	9
2	0	5	14	13	-1	6	5	5	5	1	-6	6	13	14	-5	0	6	14	-13
4	0	5	11	-12	1	6	5	6	-6	2	-6	6	6	-6	-3	0	6	5	5
5	0	5	10	11	2	6	5	5	5	-8	-5	6	3	3	-2	0	6	2	2
6	0	5	5	-7	4	6	5	10	-10	-6	-5	6	7	-9	-1	0	6	6	5
-8	1	5	3	-3	5	6	5	13	13	-5	-5	6	7	7	0	0	6	5	3
-6	1	5	6	6	7	6	5	6	-5	-4	-5	6	4	3	1	0	6	20	19
-2	1	5	14	-14	8	6	5	6	6	-3	-5	6	7	-5	2	0	6	5	5
-1	1	5	21	19	-3	7	5	6	6	-2	-5	6	8	8	3	0	6	4	5
0	1	5	6	-5	-2	7	5	9	-9	0	-5	6	7	-6	4	0	6	9	9
1	1	5	21	19	-1	7	5	14	-14	1	-5	6	6	-7	5	0	6	10	-10
2	1	5	12	-10	0	7	5	23	21	4	-5	6	5	-4	7	0	6	3	2
4	1	5	8	8	1	7	5	9	-8	-7	-4	6	10	-9	-7	1	6	7	6
5	1	5	9	-9	2	7	5	4	-4	-6	-4	6	9	10	-6	1	6	9	-9

N,N-Dimethyl-N'-[2-(5-tert-butyl-3H-1,2-dithiol-3-ylidene)-ethylidene]hydrazine

H	K	L	Fo	Fc	H	K	L	Fo	Fc	H	K	L	Fo	Fc	H	K	L	Fo	Fc
-4	1	6	7	6	5	6	6	4	3	-3	-3	7	15	-17	0	2	7	33	31
-3	1	6	25	-23	6	6	6	7	-8	-2	-3	7	13	15	1	2	7	34	-33
-2	1	6	8	7	7	6	6	5	4	-1	-3	7	20	-18	2	2	7	13	12
-1	1	6	9	-9	8	6	6	2	2	0	-3	7	6	-5	4	2	7	4	-3
0	1	6	10	-10	-5	7	6	4	-4	1	-3	7	11	10	-6	3	7	3	-3
1	1	6	9	9	-4	7	6	9	8	2	-3	7	6	5	-3	3	7	8	-8
2	1	6	6	-5	-3	7	6	8	-8	-6	-2	7	4	4	-2	3	7	14	14
3	1	6	18	18	-1	7	6	14	14	-5	-2	7	5	-5	0	3	7	36	-36
4	1	6	6	7	0	7	6	8	-8	-4	-2	7	4	-4	1	3	7	21	20
5	1	6	4	-4	2	7	6	5	-5	-3	-2	7	19	20	2	3	7	5	4
6	1	6	4	4	7	7	6	3	-2	-2	-2	7	6	-6	3	3	7	12	-10
7	1	6	3	-3	-1	8	6	12	-13	-1	-2	7	9	-11	4	3	7	6	6
-7	2	6	5	-4	2	8	6	12	-11	0	-2	7	8	10	6	3	7	4	-4
-5	2	6	6	6	4	8	6	5	6	1	-2	7	4	-5	7	3	7	3	3
-4	2	6	21	-20	5	8	6	4	-4	2	-2	7	4	-4	-3	4	7	3	4
-3	2	6	21	20	6	8	6	5	6	3	-2	7	11	12	-2	4	7	3	2
-1	2	6	17	-17	-2	9	6	4	-5	4	-2	7	5	-3	-1	4	7	10	-10
1	2	6	5	5	1	9	6	9	-9	-4	-1	7	7	-7	0	4	7	10	10
2	2	6	27	-27	2	9	6	5	5	-3	-1	7	4	-4	1	4	7	14	-15
4	2	6	11	11	4	9	6	11	-9	-2	-1	7	10	10	2	4	7	17	-17
6	2	6	3	-4	-2	10	6	4	5	-1	-1	7	15	15	3	4	7	20	19
-5	3	6	5	-5	0	10	6	5	-6	0	-1	7	13	-14	5	4	7	8	-8
-4	3	6	8	8	3	10	6	7	-7	2	-1	7	10	10	6	4	7	6	7
-2	3	6	15	-14	4	10	6	7	6	3	-1	7	5	-5	8	4	7	3	-2
-1	3	6	33	32	5	10	6	5	-4	5	-1	7	7	7	-2	5	7	7	6
1	3	6	16	-15	6	10	6	5	-4	6	-1	7	5	-5	0	5	7	3	3
2	3	6	35	36	7	10	6	6	5	-7	0	7	4	3	1	5	7	11	-13
3	3	6	26	-26	8	10	6	3	-2	-5	0	7	4	-4	2	5	7	5	5
4	3	6	8	-8	-1	11	6	3	3	-3	0	7	12	-12	3	5	7	8	-7
5	3	6	15	15	5	12	6	3	3	-2	0	7	8	-8	4	5	7	4	-4
6	3	6	4	-5	-5	-9	7	7	7	-1	0	7	6	6	5	5	7	15	13
-4	4	6	3	-3	-5	-8	7	6	-5	0	0	7	3	-4	6	5	7	6	-6
-3	4	6	10	-11	-4	-8	7	5	4	1	0	7	8	9	8	5	7	5	5
-2	4	6	7	8	-3	-7	7	3	-4	2	0	7	12	-13	-5	6	7	5	-5
-1	4	6	20	-20	0	-7	7	5	-6	3	0	7	8	9	-4	6	7	6	5
0	4	6	7	-6	2	-7	7	5	5	4	0	7	6	6	-3	6	7	5	5
1	4	6	30	29	3	-7	7	4	-4	5	0	7	6	-6	-2	6	7	11	-10
2	4	6	4	-4	1	-6	7	3	-4	6	0	7	5	5	0	6	7	19	18
4	4	6	15	15	2	-6	7	4	-4	-8	1	7	4	4	1	6	7	5	-6
5	4	6	13	-12	3	-6	7	6	6	-6	1	7	4	-5	2	6	7	8	-8
6	4	6	5	8	-5	-5	7	9	7	-5	1	7	13	13	4	6	7	3	3
7	4	6	3	2	-4	-5	7	8	-7	-4	1	7	7	7	5	6	7	7	-6
-1	5	6	13	-15	-3	-5	7	5	4	-3	1	7	24	-24	6	6	7	3	3
1	5	6	21	-22	-1	-5	7	7	7	-2	1	7	11	11	7	6	7	3	3
2	5	6	7	6	0	-5	7	4	4	-1	1	7	9	-9	8	6	7	3	-2
3	5	6	19	18	-7	-4	7	3	-2	0	1	7	13	-12	-3	7	7	7	-7
4	5	6	15	-16	-6	-4	7	4	5	1	1	7	5	5	-2	7	7	12	12
5	5	6	8	8	-5	-4	7	11	-12	2	1	7	4	4	-1	7	7	3	-4
7	5	6	2	-2	-3	-4	7	5	4	3	1	7	7	-6	0	7	7	24	-23
-4	6	6	4	-4	-2	-4	7	18	-16	5	1	7	6	6	1	7	7	35	33
-3	6	6	10	10	-1	-4	7	9	8	-6	2	7	5	6	2	7	7	12	-11
-1	6	6	7	6	0	-4	7	12	11	-5	2	7	10	-11	3	7	7	9	-11
0	6	6	5	-5	-8	-3	7	4	3	-4	2	7	3	3	4	7	7	6	6
1	6	6	9	-10	-6	-3	7	9	-10	-3	2	7	33	31	5	7	7	3	-4
3	6	6	5	-5	-5	-3	7	9	9	-2	2	7	38	-37	-3	8	7	7	7

N,N-Dimethyl-N'-[2-(5-tert-butyl-3H-1,2-dithiol-3-ylidene)-ethylidene]hydrazine

H	K	L	Fo	Fc	H	K	L	Fo	Fc	H	K	L	Fo	Fc	H	K	L	Fo	Fc
2	8	7	6	5	-1	-2	8	19	15	5	3	8	12	-11	-5	-5	9	5	-5
3	8	7	12	11	0	-2	8	20	-17	6	3	8	7	7	-4	-5	9	10	9
4	8	7	18	-15	1	-2	8	15	-13	8	3	8	2	-1	-2	-5	9	5	-5
5	8	7	3	4	2	-2	8	27	24	-2	4	8	7	-6	0	-5	9	3	3
7	8	7	3	-2	3	-2	8	15	-13	0	4	8	4	6	-6	-4	9	8	-7
0	9	7	6	-7	5	-2	8	10	7	1	4	8	11	-12	-5	-4	9	11	9
1	9	7	4	-4	-8	-1	8	3	-3	2	4	8	20	21	-4	-4	9	8	-7
2	9	7	11	11	-6	-1	8	4	5	4	4	8	15	-14	-3	-4	9	4	-4
3	9	7	11	-11	-5	-1	8	6	-6	5	4	8	11	10	-2	-4	9	10	9
4	9	7	6	5	-4	-1	8	9	9	6	4	8	5	-5	-1	-4	9	14	-14
6	9	7	4	-5	-2	-1	8	2	3	8	4	8	2	2	1	-4	9	6	6
5	10	7	10	-8	-1	-1	8	8	-8	-3	5	8	6	5	-5	-3	9	10	-8
5	11	7	3	3	1	-1	8	4	5	-1	5	8	5	5	-3	-3	9	12	11
3	12	7	4	3	2	-1	8	13	-15	0	5	8	17	-14	-2	-3	9	18	-17
4	12	7	6	-6	3	-1	8	7	8	3	5	8	4	-4	1	-3	9	8	-8
5	12	7	4	4	5	-1	8	10	-7	4	5	8	7	7	3	-3	9	7	6
4	13	7	4	4	6	-1	8	4	3	6	5	8	4	-4	4	-3	9	5	-4
-5	-8	8	5	-5	7	-1	8	4	2	7	5	8	4	4	-5	-2	9	5	4
-4	-8	8	7	8	-6	0	8	8	-10	-6	6	8	4	-4	-2	-2	9	15	13
-2	-8	8	4	-6	-5	0	8	9	10	-4	6	8	10	9	0	-2	9	18	-17
-1	-8	8	8	10	-4	0	8	3	-3	-3	6	8	10	-10	3	-2	9	8	-7
-4	-7	8	6	-6	-3	0	8	5	-5	-2	6	8	11	12	4	-2	9	5	4
-2	-7	8	6	7	-2	0	8	10	10	-1	6	8	10	8	-7	-1	9	2	2
-1	-7	8	9	-11	-1	0	8	4	-4	0	6	8	3	-3	-3	-1	9	6	-6
0	-7	8	6	7	2	0	8	4	-4	2	6	8	8	-10	-2	-1	9	7	6
1	-7	8	5	6	3	0	8	9	10	3	6	8	2	3	-1	-1	9	6	5
-5	-6	8	5	5	-7	1	8	5	-4	4	6	8	5	-4	0	-1	9	7	6
-3	-6	8	5	-4	-6	1	8	9	10	6	6	8	3	3	2	-1	9	12	-11
0	-6	8	4	-4	-5	1	8	5	-6	7	6	8	6	-5	3	-1	9	8	6
2	-6	8	7	7	-4	1	8	10	-10	-4	7	8	5	-6	6	-1	9	5	4
-8	-5	8	4	-3	-3	1	8	19	20	-3	7	8	6	6	-8	0	9	3	3
-6	-5	8	9	8	-2	1	8	18	-18	-1	7	8	5	-5	-7	0	9	5	-5
-5	-5	8	10	-9	-1	1	8	3	-4	0	7	8	19	19	-5	0	9	7	8
-3	-5	8	7	6	1	1	8	3	-4	3	7	8	5	3	-4	0	9	5	-5
-2	-5	8	7	-7	2	1	8	9	-8	5	7	8	3	-3	-3	0	9	10	-11
1	-5	8	4	-4	4	1	8	10	10	7	7	8	3	-2	-2	0	9	6	7
4	-5	8	4	3	-7	2	8	3	3	-2	8	8	7	-8	-1	0	9	6	-7
-7	-4	8	6	5	-4	2	8	12	13	-1	8	8	6	7	1	0	9	3	4
-6	-4	8	12	-10	-3	2	8	10	-11	2	8	8	11	10	3	0	9	9	-10
-5	-4	8	5	4	-1	2	8	15	16	3	8	8	5	-5	5	0	9	4	3
-4	-4	8	7	6	0	2	8	19	-21	5	8	8	5	5	-7	1	9	4	3
-3	-4	8	13	-11	1	2	8	6	-6	-2	9	8	3	4	-6	1	9	5	4
-1	-4	8	13	12	2	2	8	13	13	1	9	8	9	11	-5	1	9	13	-10
0	-4	8	7	-7	3	2	8	27	-27	4	9	8	8	7	-4	1	9	17	14
-4	-3	8	20	-16	4	2	8	3	2	5	9	8	11	-8	-3	1	9	15	17
-3	-3	8	9	8	5	2	8	8	7	7	9	8	4	4	-2	1	9	31	-34
-2	-3	8	6	6	-5	3	8	5	4	8	9	8	3	-3	-1	1	9	15	17
-1	-3	8	29	-26	-4	3	8	7	-5	3	10	8	5	6	0	1	9	3	3
0	-3	8	22	-20	-2	3	8	16	17	4	10	8	7	-6	1	1	9	15	-17
1	-3	8	7	6	-1	3	8	15	-16	8	10	8	3	2	2	1	9	9	10
2	-3	8	14	-12	0	3	8	15	16	0	11	8	4	5	3	1	9	3	-4
3	-3	8	10	9	1	3	8	12	13	4	11	8	5	4	4	1	9	5	-5
-4	-2	8	7	8	2	3	8	21	-22	-4	-9	9	4	5	-5	2	9	9	7
-3	-2	8	8	-8	3	3	8	6	6	3	-7	9	4	5	-4	2	9	4	-4
-2	-2	8	13	-15	4	3	8	3	-3	-4	-6	9	4	-4	-2	2	9	25	28

H	K	L	Fo	Fc	H	K	L	Fo	Fc	H	K	L	Fo	Fc	H	K	L	Fo	Fc
-1	2	9	10	-11	5	9	9	3	-3	4	1	10	7	5	0	11	10	5	-6
0	2	9	16	-17	6	9	9	7	5	-4	2	10	10	-8	1	11	10	4	5
1	2	9	25	27	3	10	9	3	-3	-3	2	10	12	10	-4	-6	11	5	6
2	2	9	9	-9	5	10	9	7	7	-1	2	10	16	-14	-5	-5	11	7	7
3	2	9	4	-5	6	10	9	6	-5	0	2	10	20	19	-4	-5	11	6	-5
5	2	9	3	-3	5	12	9	6	-5	1	2	10	4	-4	-3	-5	11	6	6
-4	3	9	4	-4	-3	-8	10	4	4	2	2	10	14	-11	-2	-5	11	4	4
-3	3	9	6	5	-1	-8	10	5	-7	3	2	10	9	10	-1	-5	11	4	-5
0	3	9	15	17	0	-7	10	4	-5	4	2	10	7	-8	-5	-4	11	10	-9
1	3	9	20	-22	-5	-6	10	5	-5	5	2	10	3	-3	-4	-4	11	7	6
2	3	9	5	6	-5	-5	10	9	8	-2	3	10	4	-4	-2	-4	11	7	-8
3	3	9	13	14	-2	-5	10	5	5	-1	3	10	16	14	-1	-4	11	7	8
4	3	9	11	-10	0	-5	10	4	-5	0	3	10	4	-4	4	-4	11	4	-4
7	3	9	3	-2	-6	-4	10	5	5	2	3	10	21	18	-4	-3	11	6	-6
-6	4	9	5	5	-5	-4	10	4	-3	3	3	10	9	-10	-2	-3	11	9	9
-3	4	9	4	-4	-4	-4	10	5	-5	4	3	10	3	-4	0	-3	11	4	-5
-1	4	9	5	4	-3	-4	10	11	11	5	3	10	5	5	1	-3	11	4	5
1	4	9	5	-6	-1	-4	10	7	-8	6	3	10	7	-7	4	-3	11	4	3
2	4	9	5	5	0	-4	10	12	13	0	4	10	6	-6	-1	-2	11	4	3
3	4	9	9	-9	1	-4	10	5	-4	1	4	10	15	14	0	-2	11	4	5
4	4	9	5	5	2	-4	10	5	-4	3	4	10	6	7	1	-2	11	6	-7
5	4	9	5	5	-4	-3	10	8	8	4	4	10	6	6	3	-2	11	5	5
6	4	9	9	-9	-3	-3	10	12	-12	5	4	10	5	-5	-4	-1	11	6	-6
-4	5	9	10	9	-1	-3	10	13	13	-6	5	10	4	-5	-2	-1	11	3	3
-2	5	9	6	-7	0	-3	10	15	-16	-5	5	10	3	3	0	-1	11	5	6
-1	5	9	5	4	2	-3	10	10	11	-4	5	10	5	4	1	-1	11	6	6
0	5	9	12	12	3	-3	10	12	-11	-3	5	10	12	-11	3	-1	11	7	-7
2	5	9	9	-10	-4	-2	10	3	3	-2	5	10	9	10	4	-1	11	5	4
3	5	9	6	6	-1	-2	10	9	-9	-1	5	10	6	-7	-7	0	11	6	4
5	5	9	6	-6	0	-2	10	7	7	0	5	10	4	-3	-5	0	11	10	-9
6	5	9	5	5	2	-2	10	10	-10	1	5	10	5	-5	-4	0	11	12	11
8	5	9	3	-2	3	-2	10	11	11	3	5	10	8	7	-2	0	11	23	-22
-4	6	9	6	-6	4	-2	10	6	-6	4	5	10	3	-3	-1	0	11	18	16
-2	6	9	13	13	5	-2	10	4	-3	5	5	10	4	4	0	0	11	5	-5
-1	6	9	14	-15	-6	-1	10	5	-4	-4	6	10	3	-3	2	0	11	9	9
0	6	9	7	-6	-5	-1	10	11	9	-3	6	10	11	11	-5	1	11	10	9
1	6	9	36	33	-4	-1	10	6	-5	-2	6	10	7	-8	-4	1	11	12	-10
2	6	9	18	-16	-3	-1	10	7	6	0	6	10	10	9	-2	1	11	19	18
4	6	9	3	3	-2	-1	10	3	3	-1	7	10	10	10	-1	1	11	28	-26
-3	7	9	5	4	4	-1	10	3	-2	0	7	10	8	-9	1	1	11	16	14
-2	7	9	10	-10	-6	0	10	8	7	1	7	10	6	7	2	1	11	10	-8
-1	7	9	5	5	-5	0	10	16	-13	3	7	10	5	-5	-2	2	11	8	-7
1	7	9	16	-16	-3	0	10	12	11	1	8	10	4	5	0	2	11	3	3
2	7	9	23	21	-2	0	10	12	-11	2	8	10	9	-10	1	2	11	23	-22
4	7	9	13	-11	-1	0	10	11	10	3	8	10	7	7	2	2	11	20	18
5	7	9	6	6	0	0	10	3	3	4	8	10	5	4	4	2	11	9	-6
0	8	9	10	-12	4	0	10	6	5	5	8	10	8	-6	-6	3	11	4	4
1	8	9	5	5	5	0	10	4	-3	6	8	10	6	5	-4	3	11	3	-3
2	8	9	4	5	-6	1	10	5	-5	4	9	10	5	-5	-3	3	11	5	-5
3	8	9	8	-7	-3	1	10	18	-15	5	9	10	7	5	1	3	11	3	2
4	8	9	15	13	-2	1	10	14	13	8	9	10	4	3	4	3	11	12	9
5	8	9	7	-6	0	1	10	10	-9	-3	10	10	4	4	6	3	11	4	-5
7	8	9	3	2	1	1	10	6	6	-1	10	10	3	-4	7	3	11	3	3
-3	9	9	3	-4	2	1	10	8	7	0	10	10	4	5	-4	4	11	5	5
3	9	9	10	10	3	1	10	13	-11	4	10	10	5	5	-3	4	11	8	-7

N,N-Dimethyl-N'-[2-(5-tert-butyl-3H-1,2-dithiol-3-ylidene)-ethylidene]hydrazine

H	K	L	Fo	Fc	H	K	L	Fo	Fc	H	K	L	Fo	Fc	H	K	L	Fo	Fc
-2	4	11	6	-7	-5	0	12	7	6	-4	-6	13	4	-3	5	7	13	4	4
0	4	11	6	6	-4	0	12	6	-6	-3	-6	13	3	4	6	7	13	4	-4
2	4	11	11	-10	-2	0	12	11	11	-4	-5	13	7	7	3	8	13	6	-6
3	4	11	13	11	1	0	12	4	4	-1	-5	13	4	5	4	8	13	7	6
6	4	11	5	5	4	0	12	4	3	-4	-4	13	6	-7	6	8	13	4	-3
7	4	11	4	-3	-6	1	12	4	5	-2	-4	13	4	5	4	9	13	3	-4
-4	5	11	6	-6	-4	1	12	6	-5	-1	-4	13	5	-6	3	10	13	4	5
-3	5	11	7	7	-3	1	12	9	9	1	-3	13	4	-5	4	12	13	4	4
-2	5	11	5	5	-2	1	12	12	-11	2	-2	13	3	-4	-2	-5	14	3	5
-1	5	11	17	-18	0	1	12	9	10	4	-2	13	4	5	-2	-4	14	4	-5
1	5	11	16	15	1	1	12	8	-9	-6	-1	13	5	-5	1	-4	14	4	-6
2	5	11	16	-14	3	1	12	10	9	-4	-1	13	8	7	1	-3	14	3	3
-4	6	11	5	6	4	1	12	4	-4	-3	-1	13	5	-5	-5	-2	14	4	-3
-2	6	11	8	-8	-3	2	12	5	-5	-2	-1	13	5	-5	-4	-2	14	7	7
-1	6	11	12	12	0	2	12	13	-13	-1	-1	13	9	9	-5	-1	14	5	4
0	6	11	8	-9	2	2	12	5	5	0	-1	13	4	-5	-4	-1	14	7	-7
1	6	11	9	-10	3	2	12	12	-11	1	-1	13	3	4	-3	-1	14	4	4
2	6	11	23	22	4	2	12	6	5	-4	0	13	13	-12	-2	-1	14	4	5
3	6	11	11	-10	6	2	12	4	-3	-3	0	13	7	7	-1	0	14	5	6
5	6	11	6	4	7	2	12	6	4	-2	0	13	4	4	1	0	14	4	-5
-2	7	11	7	8	-1	3	12	7	-7	-1	0	13	20	-21	-5	1	14	4	3
1	7	11	8	9	0	3	12	4	4	0	0	13	8	8	-2	1	14	4	5
2	7	11	8	-8	1	3	12	5	5	-4	1	13	8	8	1	1	14	5	6
4	7	11	10	9	2	3	12	8	-8	-2	1	13	5	-5	3	1	14	5	-5
5	7	11	11	-9	3	3	12	8	7	0	1	13	13	-13	4	1	14	5	5
1	8	11	10	-11	-3	4	12	6	-5	1	1	13	11	-12	-1	2	14	6	-6
3	8	11	6	6	-2	4	12	6	7	2	1	13	14	14	1	2	14	3	-4
4	8	11	6	-6	-1	4	12	6	-7	3	1	13	5	-5	3	2	14	4	4
5	8	11	4	3	1	4	12	4	-4	-2	2	13	6	6	4	2	14	5	-5
-1	9	11	3	4	2	4	12	6	6	2	2	13	9	-9	2	3	14	4	5
3	9	11	7	-7	5	4	12	7	5	4	2	13	4	3	3	3	14	5	-5
4	9	11	3	3	-3	5	12	8	7	5	2	13	3	-2	-5	4	14	6	-7
5	9	11	5	5	-2	5	12	11	-11	-3	3	13	4	-4	-2	4	14	6	-7
6	9	11	6	-5	1	5	12	7	-7	0	3	13	6	7	-1	4	14	8	9
7	9	11	4	3	-3	6	12	5	-6	2	3	13	4	-5	0	4	14	4	-6
3	11	11	3	4	-2	6	12	7	8	3	3	13	6	6	-2	5	14	8	9
5	11	11	5	-5	0	6	12	8	-9	4	3	13	6	-5	1	5	14	3	4
-5	-6	12	4	4	1	6	12	6	7	5	3	13	3	3	0	6	14	8	9
-5	-5	12	6	-6	3	6	12	5	-5	7	3	13	5	-3	1	6	14	7	-8
0	-5	12	4	5	3	7	12	7	7	-3	4	13	7	7	-3	7	14	4	-4
-3	-4	12	7	-9	4	7	12	3	-2	-2	4	13	4	-4	3	7	14	6	-7
-2	-4	12	6	7	5	7	12	6	-5	-1	4	13	9	-11	4	7	14	4	4
-1	-4	12	4	5	6	7	12	5	4	0	4	13	5	6	6	7	14	4	-4
0	-4	12	7	-8	2	8	12	9	10	2	4	13	8	-8	0	8	14	3	4
1	-4	12	6	8	3	8	12	6	-7	-4	5	13	8	8	5	9	14	3	3
3	-4	12	4	-5	5	8	12	5	4	0	5	13	12	-13	-4	-1	15	5	-6
0	-3	12	8	10	6	8	12	5	-4	2	5	13	12	13	-3	-1	15	8	9
1	-3	12	4	-5	-3	9	12	5	6	3	5	13	13	-12	-1	-1	15	6	-7
3	-3	12	8	8	0	9	12	4	4	-2	6	13	7	8	0	-1	15	7	9
4	-3	12	5	-5	4	9	12	3	3	-1	6	13	7	-9	-4	0	15	3	4
0	-2	12	3	-4	5	9	12	5	-5	1	6	13	5	6	-3	0	15	8	-9
-5	-1	12	11	-10	-2	10	12	5	7	2	6	13	10	-10	-1	0	15	7	9
-4	-1	12	10	10	1	10	12	6	7	3	6	13	9	9	0	0	15	10	-13
4	-1	12	3	3	2	10	12	3	-4	5	6	13	9	-7	2	0	15	7	8
-6	0	12	5	-4	3	12	12	3	-4	2	7	13	6	7	3	0	15	4	-4

H	K	L	Fo	Fc	H	K	L	Fo	Fc	H	K	L	Fo	Fc	H	K	L	Fo	Fc
-1	1	15	4	-4	3	4	15	5	-5	-1	-1	16	4	6	0	0	17	4	5
0	1	15	4	5	-3	5	15	6	7	-1	3	16	4	5	1	0	17	4	-5
2	1	15	5	-6	-1	5	15	6	-7	-4	4	16	6	-7	3	0	17	4	5
3	1	15	5	5	0	5	15	7	8	-2	4	16	4	6	-4	2	17	4	4
-5	2	15	4	4	2	5	15	5	-5	-1	4	16	5	-6	1	3	17	4	5
-5	3	15	6	-6	3	5	15	10	10	-2	5	16	5	-6	-2	4	17	5	-6
-2	3	15	4	-4	4	5	15	3	-4	1	5	16	6	-7	1	4	17	5	-6
0	3	15	5	6	6	6	15	4	-4	3	6	16	4	-4	3	4	17	5	6
1	3	15	4	5	4	7	15	5	5	4	6	16	4	4	0	5	17	5	-7
-3	4	15	7	-8	4	8	15	4	-3	0	7	16	3	5	4	5	17	5	5
0	4	15	8	-10	5	8	15	4	4	3	7	16	5	6	-1	4	18	5	6
1	4	15	5	6	3	11	15	4	4	4	7	16	4	-4	4	6	18	4	-4
2	4	15	5	6	-3	-2	16	4	6	-1	8	16	5	-6					

Anisotropic Temperature parameters (\AA^2 , $\times 10^3$)

	U_{11}	U_{22}	U_{33}	U_{23}	U_{13}	U_{12}
S(1)	53(1)	52(1)	48(1)	-22(1)	15(1)	-30(1)
S(2)	43(1)	45(1)	37(1)	-13(1)	10(1)	-15(1)
N(1)	56(3)	32(3)	38(3)	-12(2)	3(2)	-7(2)
N(2)	56(3)	34(3)	39(3)	-17(2)	3(2)	-6(2)
C(1)	42(3)	33(3)	35(3)	-9(2)	4(2)	-10(2)
C(2)	41(3)	36(3)	42(3)	-11(3)	11(3)	-12(3)
C(3)	40(3)	37(3)	27(3)	-5(2)	1(2)	-11(2)
C(4)	59(4)	36(3)	50(4)	-20(3)	17(3)	-22(3)
C(5)	62(4)	34(3)	47(4)	-16(3)	7(3)	-17(3)
C(6)	75(6)	49(4)	60(5)	-14(4)	25(4)	-19(4)
C(7)	74(5)	55(4)	58(5)	-31(4)	2(4)	-12(4)
C(8)	43(3)	33(3)	31(3)	-8(2)	-1(2)	-9(2)
C(9)	58(4)	62(5)	57(5)	-32(4)	-1(3)	-14(4)
C(10)	59(4)	49(4)	37(4)	-9(3)	11(3)	-7(3)
C(11)	55(4)	42(4)	53(4)	-8(3)	-10(3)	-6(3)

Least-squares planes

The planes are defined in orthogonal Ångstrom coordinates by the equation: $Ax + By + Cz + D = 0$

Plane	<u>A</u>	<u>B</u>	<u>C</u>	<u>D</u>
1. S(1),S(2),C(1),C(2),C(3)	-0.447(3)	0.390(4)	-0.804(7)	2.397(8)
2. S(2),C(1),C(4),C(5),N(1)	-0.452(2)	0.438(1)	-0.777(2)	2.051(10)

distances of atoms from the plane (\AA , $\times 10^2$)

plane	S(1)	S(2)	N(1)	N(2)	C(1)	C(2)	C(3)	C(4)	C(5)	C(8)
1.	0(1)	0(1)	-12(1)	-25(1)	1(1)	1(1)	-2(1)	-3(1)	-14(1)	-15(1)
2.	-11(1)	0(1)	1(1)	-5(1)	0(1)	-8(1)	-17(1)	2(1)	-2(1)	-38(1)

dihedral angle between the planes: $3.2(3)^\circ$